INFORMATION TO USERS

This manuscript has been reproduced from the microfilm master. UMI films the text directly from the original or copy submitted. Thus, some thesis and dissertation copies are in typewriter face, while others may be from any type of computer printer.

The quality of this reproduction is dependent upon the quality of the copy submitted. Broken or indistinct print, colored or poor quality illustrations and photographs, print bleedthrough, substandard margins, and improper alignment can adversely affect reproduction.

In the unlikely event that the author did not send UMI a complete manuscript and there are missing pages, these will be noted. Also, if unauthorized copyright material had to be removed, a note will indicate the deletion.

Oversize materials (e.g., maps, drawings, charts) are reproduced by sectioning the original, beginning at the upper left-hand corner and continuing from left to right in equal sections with small overlaps.

ProQuest Information and Learning
300 North Zeeb Road, Ann Arbor, MI 48106-1346 USA
800-521-0600

THE ROLE OF FIBROBLAST GROWTH FACTOR-2 (FGF2) IN VASCULAR REMODELING AND ADAPTATION

by

Chris J. Sullivan

A Dissertation Submitted to the Faculty of the

GRADUATE INTERDISCIPLINARY PROGRAM IN PHYSIOLOGICAL SCIENCES

In Partial Fulfillment of the Requirements
For the Degree of

Doctor of Philosophy

In the Graduate College

THE UNIVERSITY OF ARIZONA

2002

ProQuest Information and Learning Company
300 North Zeeb Road
P.O. Box 1346
Ann Arbor, MI 48106-1346

THE UNIVERSITY OF ARIZONA ®
GRADUATE COLLEGE

As members of the Final Examination Committee, we certify that we have read the dissertation prepared by Chris J. Sullivan

entitled The Role of Fibroblast Growth Factor-2 (FGF2) in Vascular Remodeling and Adaptation

and recommend that it be accepted as fulfilling the dissertation requirement for the Degree of Doctor of Philosophy

David J. Hartshorne — Date 11/20/02

Alex Simon — Date 11/20/02

Ronald M. Lynch — Date 11/20/02

Stuart K. Williams — Date 11/20/02

James B. Hoying — Date 11/20/02

Final approval and acceptance of this dissertation is contingent upon the candidate's submission of the final copy of the dissertation to the Graduate College.

I hereby certify that I have read this dissertation prepared under my direction and recommend that it be accepted as fulfilling the dissertation requirement.

Dissertation Director James B. Hoying — Date 11/20/02

STATEMENT BY AUTHOR

This dissertation has been submitted in partial fulfillment of requirements for an advanced degree at The University of Arizona and is deposited in the University Library to be made available to borrowers under rules of the Library.

Brief quotations from this dissertation are allowable without special permission, provided that accurate acknowledgment of source is made. Requests for permission for extended quotation from or reproduction of this manuscript in whole or in part may be granted by the head of the major department or the Dean of the Graduate College when in his or her judgment the proposed use of the material is in the interests of scholarship. In all other instances, however, permission must be obtained from the author.

SIGNED: 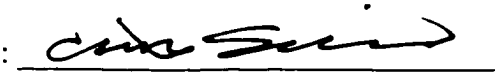

ACKNOWLEDGEMENTS

First, I would like to thank my Dissertation Committee, Dave Hartshorne, Alex Simon, Ron Lynch, Stu Williams, and Jay Hoying. Thank you for your insight, guidance, and for being an important part of my graduate career.

Stu, you deserve particular thanks for introducing me to Jay and, of course, thank you for giving me free run of your lab.

To my mentor, Jay Hoying, thank you for making this a great experience. I can't thank you enough.

I would like to thank my original office mates and fellow graduate students, Donny Dal Ponte, Robbie Kellar, Ben Shepherd and Kameha Kidd. It would not have been this much fun without you guys.

Thanks to everyone in our lab (Hoying Group), Gabi Gruionu, Mark Schwartz, Kevin Greer, and Helen Chen. Also, I can't forget to thank all the original members of the Hoying Lab, Tushara Gunatilaka, Alicia Newkirk, and Adam Budoff.

I would like to thank everyone in the Williams Lab, in particular Vangie Patula, Leigh Kleinert, and Charlotte Todd. Your help was always appreciated.

I would like to thank everyone in the Physiological Sciences Graduate Program and, of course, Holly Lopez.

I would like to thank my family for all their help over the years. None of this would have been possible without all of you.

Last, I would like to thank my wife, Stefanie, for her patience and support. The sweet is never as sweet without the sour.

DEDICATION

For my family.

Events consistent with our expectations are perceived and processed easily, while events that contradict prevailing expectations tend to be ignored or distorted in perception.

-Richards J. Heuer, Jr.

TABLE OF CONTENTS

TABLE OF CONTENTS – *Continued*

LIST OF FIGURES

LIST OF FIGURES – *Continued*

LIST OF FIGURES – *Continued*

LIST OF FIGURES – *Continued*

LIST OF TABLES

LIST OF TABLES – *Continued*

ABSTRACT

The goal of this dissertation was to test the hypothesis that fibroblast growth factor-2 (FGF2) is required during diseased-related vascular growth and remodeling in the adult organism. Given previous research, it is generally assumed that FGF2 is an important regulator of vessel growth during various pathophysiological processes (e.g. tissue ischemia, vessel injury, and flow-dependent remodeling). However, such studies only indirectly implicate FGF2 in vascular adaptation and remodeling. In contrast, experiments using mice with a targeted disruption of the *Fgf2* gene have allowed direct determination of the biological roles of endogenous FGF2. Thus, experimental models of flow-dependent remodeling and ischemic revascularization were used to compare the responses of $Fgf2^{-/-}$ and $Fgf2^{+/+}$ mice to directly identify the function of FGF2 during vascular adaptation in the adult animal. Surprisingly, the lack of FGF2 did not appear to affect vascular growth in these models. First, using a novel model of flow-dependent remodeling, $Fgf2^{-/-}$ mice had equivalent carotid artery adaptation in response to both high-flow and low-flow was as wildtype counterparts. Second, angiogenesis and arteriogenesis were not different between the ischemic limbs $Fgf2^{+/+}$ and $Fgf2^{-/-}$ mice, demonstrating that FGF2 is not required for vascular adaptation in response to ischemia. However, these experiments led to the observation that reactive hyperemia was impaired in ischemic limb of $Fgf2^{-/-}$ mice. These results indicate that vessel responsiveness is altered in the collateral circulation of the ischemic $Fgf2^{-/-}$ limb. This possible identification of FGF2 as a "functional" factor in the collateral circulation suggests a novel, non-mitogenic role for endogenous growth factors. Finally, $Fgf2^{-/-}$ mice had

altered gene expression in the ischemic limb as evaluated using cDNA microarrays. The significance of differential gene expression in the absence of FGF2 is unknown. It is unclear whether such changes in gene expression are related to the FGF2 hyperemia phenotype or whether they are related to an unknown phenotype present in the ischemic limb of *Fgf2*$^{-/-}$ mice. Overall, this dissertation provides new evidence that endogenous FGF2 has important actions in the remodeling vasculature during ischemic revascularization. Specifically, endogenous FGF2 appears to modulate vascular reactivity of the collateral circulation of the hindlimb.

1. INTRODUCTION

Vascular growth and remodeling are critical to various physiological and pathological processes in the adult animal. Vessel adaptation, including expansion and regression of the existing vascular network, is part of the female reproductive cycle, wound healing, and occurs in response to chronic exercise training. Pathological conditions, such as atherosclerosis, chronic ischemia, and hypertension, induce wide-ranging changes in the vascular tree. Vascular endothelial growth factor (VEGF), angiopoietin, and platelet-derived growth factor are examples of peptides definitively identified as critical regulators of blood vessel formation and maturation during embryogenesis (Ferrara et al., 1996; Leveen et al., 1994; Lindahl et al., 1997; Suri et al., 1996). However, it is unclear whether these same endogenous molecules direct vascular growth in the adult animal. Gene knockout studies in mice suggest that regulation of post-natal vascular adaptation is not simply a recapitulation of developmental gene programs. For example, endothelial nitric oxide synthase (eNOS) deficient mice are viable and fertile, with a primary phenotype of hypertension (Shesely et al., 1996). Adult eNOS knockout mice have significantly impaired ischemia-induced vascular adaptation, wound healing, and retinal revascularization (Ando et al., 2002; Lee et al., 1999; Murohara et al., 1998; Rudic et al., 1998; Tamarat et al., 2002). Disruption of the placental growth factor (PlGF) gene had no effect on embryonic angiogenesis, but adult PlGF knockout mice had impaired tumor angiogenesis and ischemia-induced collateral artery growth (Carmeliet et al., 2001). Finally, tumor necrosis factor-alpha (TNF-α) deficient mice had significantly reduced collateral artery formation following arterial

occlusion, but there was no evidence of altered embryonic vascular development in these knockout mice (Hoefer et al., 2002). These studies show that molecules essential for disease-related vessel growth and remodeling may in some cases be distinct from those molecules controlling embryonic vascular growth.

Historically, fibroblast growth factor-2 (FGF2 or bFGF) and VEGF have been the most widely studied of all the peptide growth factors in the field of angiogenesis and vascular growth (Pepper, 1997; Ribatti et al., 2000). In vitro, these proteins positively regulate the various cell functions required during angiogenesis, including proliferation, migration, and matrix degradation (Papetti et al., 2002). FGF2, identified initially as basic FGF based on its isoelectric point, was first isolated from bovine pituitary and was found to stimulate the proliferation of cultured fibroblasts (Gospodarowicz, 1974; Westall et al., 1978). Later, FGF2 was identified as a potent mitogen for both endothelial cells and smooth muscle cells *in vitro* (Davis et al., 1997; Gospodarowicz et al., 1988; Sato et al., 1988; Shing et al., 1984; Shing et al., 1985). Since the mid-1980s there has been a tremendous amount of research examining FGF2 in the context of inducing angiogenesis, as well as in a variety of other areas ranging from neurogenesis to tumor progression (Bikfalvi et al., 1997; Folkman et al., 1987). Nevertheless, despite almost two decades of *in vitro* and *in vivo* research focused on exogenous FGF2, very little is known in regard to the specific actions of endogenously produced FGF2 during vascular growth and remodeling in the adult animal.

Fibroblast Growth Factor-2

FGF2 is the prototypical member of a family of at least 22 structurally related protein growth factors. The FGF proteins have diverse roles ranging from the regulation of embryonic development to the promotion of tissue repair in the adult (Ornitz et al., 2001) Many of the *Fgf* genes have been deleted or disrupted by homologous recombination in mice. The outcome of these gene deletions varies from no identifiable phenotype as observed in the FGF1 knockout mice to embryonic lethality (Table 1.1) (Ornitz et al., 2001).

LMW and HMW FGF2

In the mouse, FGF2 exists in three different molecular weight isoforms; 18-kDa or low molecular weight (LMW) FGF2 and 21-kDa and 22-kDa or high molecular weight (HMW) FGF2 (Zhou et al., 1998). These isoforms arise from alternative translation sites within a single *Fgf2* mRNA species (Florkiewicz et al., 1989; Prats et al., 1989). LMW FGF2 is secreted from cells, but this FGF2 isoform lacks a signal sequence for secretion (Mignatti et al., 1992). Thus, it is thought that LMW FGF2 is secreted via a mechanism of exocytosis that is distinct from the classical endoplasmic reticulum-Golgi pathway (Mignatti et al., 1992; Yu et al., 1993). The HMW isoforms contain a nuclear localization signal in the NH2-terminal which causes transportation of HMW FGF2 to the nucleus (Bugler et al., 1991; Quarto et al., 1991; Renko et al., 1990). Although there is no nuclear accumulation of endogenous LMW FGF2, exogenously added LMW FGF2 is transported into the nucleus of endothelial cells grown in culture (Baldin et al., 1990). Studies show

Table 1.1: FGF knockout mice

Gene	Survival	Phenotype
Fgf1	Viable	None identified
Fgf2	Viable	Mild neural, skeletal, cardiovascular
Fgf3	Viable	Mild inner ear, skeletal
Fgf4	Lethal, E4	Inner cell mass proliferation
Fgf5	Viable	Long hair, angora mutation
Fgf6	Viable	Muscle regeneration (strain dependent)
Fgf7	Viable	Hair follicle growth, ureteric bud growth
Fgf8	Lethal, E7	Gastrulation defect, CNS and limb development
Fgf9	Lethal, P0	Lung mesenchyme, XY sex reversal
Fgf10	Lethal, P0	Multiple organ development
Fgf11	No mouse reported	——
Fgf12	Viable	Neuromuscular phenotype
Fgf13	No mouse reported	——
Fgf14	Viable	Neurological phenotypes
Fgf15	Lethal, E9.5	Not clear
Fgf16	No mouse reported	——
Fgf17	Viable	Cerebellar development
Fgf18	Lethal, P0	Skeletal development

Modified from Ornitz and Itoh, 2001.

that nuclear targeted HMW FGF2 promotes a growth phenotype in cells through an intracrine pathway (Arese et al., 1999; Davis et al., 1997). Using cultured cells from transgenic mice, overexpression of HMW FGF2 enhanced proliferation of vascular smooth muscle cells whereas overexpression of the LMW isoform did not (Davis et al., 1997). These authors suggest that the intracrine action of HMW FGF2 may act synergistically with the autocrine actions of LMW FGF2 or other growth inducers. However, the specific functions of nuclear-targeted HMW FGF2 *in vivo* are unknown. Although FGF2 is considered the prototypical FGF member, this characteristic of nuclear accumulation is shared by only two other FGF proteins, FGF1 and FGF3/Int-2 (Acland et al., 1990; Cao et al., 1993). Also, of all the identified FGF family members, only FGF1 and FGF2 are secreted via a non-classical secretory pathway (Powers et al., 2000).

FGF Receptors and Signaling

The biological actions of LMW FGF2 are mediated through a receptor system consisting of high-affinity (Kd = 10^{-9} to 10^{-12} M) transmembrane receptors and low-affinity (Kd = 10^{-8} to 10^{-9} M) heparan sulfate proteoglycans (Bikfalvi et al., 1997; Brown et al., 1995; Moscatelli, 1987). Heparan sulfate and heparan sulfate proteoglycans (HSPGs) bind FGF2 and assist in the binding of FGF2 to the extracellular domain of the high-affinity FGF receptors (Kan et al., 1999; Kato et al., 1998a; Yayon et al., 1991). HSPGs are also thought to serve as a storage site for secreted FGFs, binding them to the extracellular matrix and protecting the FGFs from degradation (Powers et al., 2000). The amount and type of HSPGs expressed in a cellular environment may help regulate FGF

activity and function (Nugent et al., 2000). In addition, FGF2 binds to extracellular chaperones or binding proteins (FGF-BPs), which act to present FGF2 to its high-affinity receptors (Aigner et al., 2002). FGF-BPs, like the HSPGs, are thought to regulate the bioavailability of secreted FGF2 (Tassi et al., 2001). To date, a total of five high-affinity FGF receptors (FGFR) have been identified and each of the FGFs binds these receptors with different affinities (Ornitz et al., 1996; Sleeman et al., 2001). These receptors arise from distinct genes, though each gene produces multiple receptors isoforms by alternative mRNA splicing (Ornitz et al., 2001; Orr-Urtreger et al., 1993; Sleeman et al., 2001). The nomenclature for the isoforms of FGFRs 1-3 (termed IIIa, IIIb, and IIIc) is based on the fact that mRNA splicing results in differences in the third extracellular Ig-like domain of these receptors (Ornitz et al., 2001). Importantly, these receptor variants have differential ligand binding specificities (Table 1.2) (Ornitz et al., 1996; Werner et al., 1992). This extracellular region is not alternatively spliced in FGFR4, and FGFR5 does not even contain this third Ig-like domain (Sleeman et al., 2001; Vainikka et al., 1992). All of the membrane bound FGFRs have an extracellular ligand binding domain and a single transmembrane domain. Interestingly, the IIIa splice form of the FGFR is secreted and binds FGF2 with high affinity (Duan et al., 1992). The significance of this soluble FGFR variant *in vivo* is unknown, although it may function to regulate the activity of FGFs. FGFRs 1-4 have an intracellular tyrosine kinase domain, whereas the recently identified FGFR5 lacks any identifiable tyrosine kinase domain (Ornitz et al., 2001; Sleeman et al., 2001). LMW FGF2 is capable of binding all of the FGFRs, but FGF2 appears to have a high specificity for only certain receptors and their isoforms (Table 1.2). It is believed

that the specificity and diversity of FGF signaling is partly achieved through spatial and temporal expression of the assorted FGFRs and the ligand specificity of each of the receptor splice variants.

Table 1.2: Functional specificity of FGFs 1-9 for the various FGF receptor isoforms relative to FGF1. Engineered BaF3 cells expressing only one of the major splice variants of all the known FGF receptors were used to assay the relative mitogenic activity of the nine known FGF ligands. Using FGF1 as an internal standard, they determined the relative activity of all the other members of the FGF family. Relative mitogenic activity does not necessarily reflect previously described FGF receptor/ligand affinities.

FGFR	FGF1	FGF2	FGF4	FGF5	FGF6	FGF7	FGF8	FGF9
1, IIIb	100	60	16	4	5	6	4	4
1, IIIc	100	104	102	59	55	0	1	21
2, IIIb	100	9	15	5	5	81	4	7
2, IIIc	100	64	94	25	61	3	16	89
3, IIIb	100	1	1	1	1	1	1	42
3, IIIc	100	107	69	12	9	1	41	96
4	100	113	108	7	79	2	76	75

Modified from Ornitz et al. 1996

Ligand binding to FGFRs, like other receptor tyrosine kinases, leads to receptor dimerization and autophosphorylation of tyrosine residues within the cytoplasmic domains of the receptor (Fantl et al., 1993). FGF2 induced FGFR activation leads to a variety of cell signaling events (Powers et al., 2000). For example, phosphotyrosines on the FGFR are binding sites for src homology domain-containing proteins such as phospholipase Cγ, which activates the protein kinase C pathway (Figure 1.1) (Nugent et al., 2000). Also, the phosphorylated tyrosines bind the adapter protein Shc, leading to activations of the Ras-MAPK signaling pathway (Boilly et al., 2000). The specific intracellular signaling pathway activated appears to be dependent on the FGFR type activated and the different pathways are each associated with distinct biological responses (LaVallee et al., 1998; Powers et al., 2000). The various transduction pathways may be differentially activated depending on the duration of FGF ligand exposure. For example, transient exposure of FGF1 caused cell migration via the Src pathway, while longer duration FGF1 exposure stimulated proliferation via MAPK signaling (LaVallee et al., 1998). Still, very little is known regarding how FGF-FGFR binding can induce such diverse biological end-points (e.g., proliferation, migration, and differentiation) through seemingly common signaling pathways and molecules.

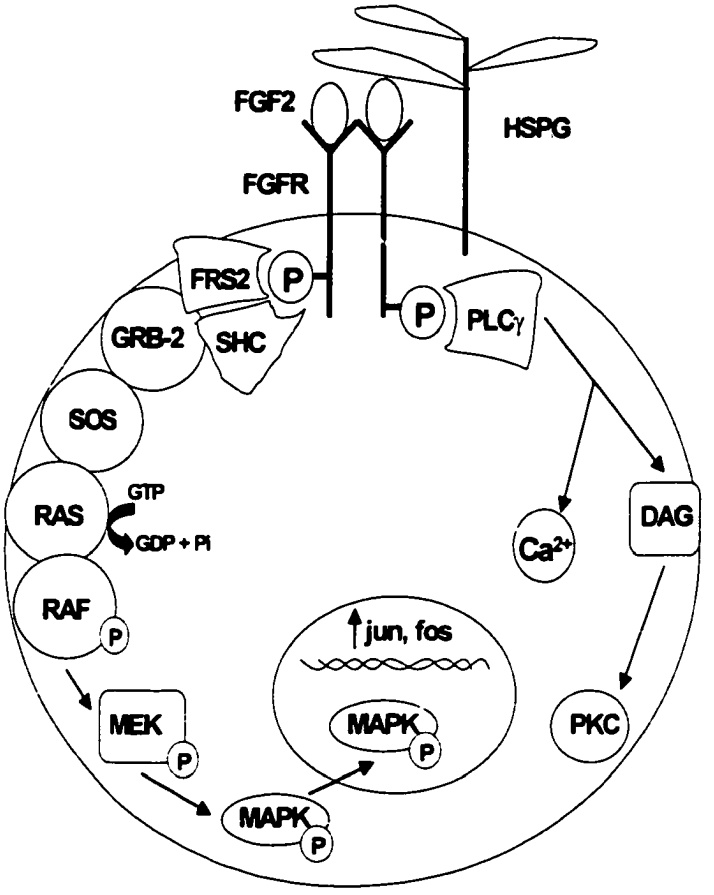

Figure 1.1 Ligand binding to FGFRs, like other receptor tyrosine kinases, leads to receptor dimerization and autophosphorylation of tyrosine residues within the cytoplasmic domains of the receptor. FGF2 induced FGFR activation leads to a variety of cell signaling events. Two pathways activated by FGF2-FGFR binding are the MAPK and PKC signaling cascades, which are diagrammed above. Modified from (Nugent & Iozzo 2000).

Traditionally, the functions of FGF2 have been based largely on studies examining the pattern and location of FGF2 expression as well as studies applying exogenous FGF2 *in vitro* and *in vivo*. These studies implicate FGF2 in a wide variety of signaling processes ranging from embryonic growth and differentiation to adult physiology and pathology (Bikfalvi et al., 1997). However, numerous regulatory steps may be absent *in vitro*, such as FGF binding proteins and HSPGs that are important in regulating bioavailability and ligand-receptor binding (Tassi et al., 2001; Whitelock et al., 1996; Yayon et al., 1991). Further, exogenous delivery of FGF protein eliminates transcriptional, translational, and secretory control over its bioavailability. Thus, these types of experiments must be interpreted with some degree of caution, as they do not necessarily identify the biological functions of endogenously produced FGF2.

FGF2 Knockout Mice

The recent creation of mice lacking FGF2 (*Fgf2*$^{-/-}$ mice; Figure 1.2) has helped to clarify the specific roles of endogenous FGF2 during development and normal physiological function. Knockout mice have the advantage of allowing evaluation of the importance of a specific molecule in the context of the intact animal. To date, three independently generated lines of *Fgf2*$^{-/-}$ mice have been generated and all are fertile and grow to maturity (Dono et al., 1998; Ortega et al., 1998; Zhou et al., 1998). It was surprising that FGF2 disruption was non-lethal, given that FGF2 was considered to be critical for embryonic development of numerous organ systems including the brain, heart, blood vessels, muscles and bones (Bikfalvi et al., 1997). For example, FGF2 was thought

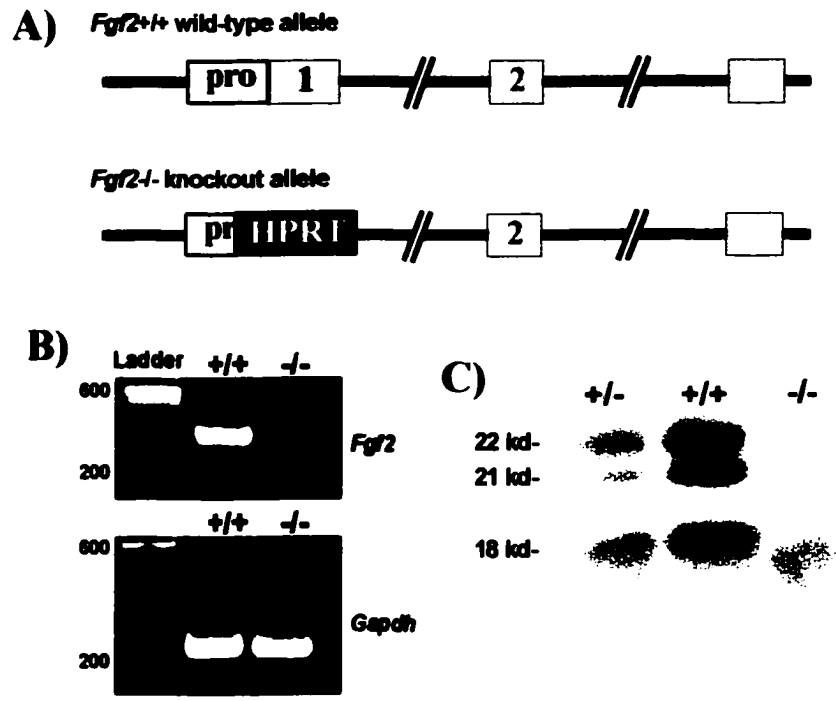

Figure 1.2 A) Scheme for generation of *Fgf2* null allele. The *Fgf2* gene was disrupted by replacing the proximal promoter region and the entire first exon with an *Hprt* minigene. B) RT-PCR was used to detect *Fgf2* mRNA in skeletal muscle isolated from wildtype (+/+) and knockout (-/-) mice. *Gapdh* serves as a control for cDNA template. C) Western blot analysis of FGF2 protein in the brain. In mice, FGF2 protein exists in three different molecular weight isoforms; 18-kDa or low molecular weight (LMW) and 21-kDa and 22-kDa or high molecular weight (HMW). Panels A and C were modified from (Zhou, Sutliff, et al. 1998).

Table 1.3: Summary of phenotypes identified in *Fgf2* knockout mice

Phenotype	Reference
Decreased portal vein contractility	Zhou et al. 1998
Low blood pressure	Zhou et al. 1998; Dono et al. 1998
Thrombocytosis	Zhou et al. 1998
Delayed wound healing	Ortega et al. 1998
Impaired baroreceptor response	Dono et al. 1998
Reduced neuronal density in motor cortex	Ortega et al. 1998
Decreased neuronal density in cerebral cortex	Dono et al. 1998; Raballo et al. 2000; Korada et al. 2002
Decreased bone mass and formation	Montero et al. 2000
Reduced pressure-induced cardiac hypertrophy	Schultz et al. 1999
Attenuated neurogenesis in adult hippocampus after brain injury	Yoshimura et al. 2001
Impaired development of neural circuitry regulating blood pressure	Dono et al. 2002

to be a key molecule during vascular development in the embryo, but there is no evidence of structural abnormalities in the vascular system of FGF2 knockout mice (Dono et al., 1998; Ortega et al., 1998; Zhou et al., 1998). However, *Fgf2*$^{-/-}$ mice have numerous phenotypes (Table 1.3), with various functional or anatomical disorders identified in the cardiovascular, skeletal, and nervous systems (Dono et al., 1998; Montero et al., 2000; Schultz et al., 1999; Zhou et al., 1998). In addition, pathologically induced cardiac hypertrophy and brain neurogenesis are impaired in adult FGF2 knockout mice. Also, adult FGF2 knockouts have delayed healing of full-thickness excisional skin wounds (Ortega et al., 1998). These studies imply that FGF2, in addition to its developmental roles, functions in situations of tissue injury, stress, and repair in the adult organism. However, others have shown that FGF2 is not essential during several disease-related responses previously believed to require endogenous FGF2 signaling (Table 1.4) (Foletti et al., 2002; Ozaki et al., 1998; Tobe et al., 1998; Zhou et al., 1998).

Further studies with FGF2 knockout mice will help to advance our understanding of the importance of FGF2 in both physiological and pathophysiological processes. There remains much to be learned regarding the role of FGF2 during vascular remodeling in the adult, particularly during disease-related processes. Specifically, the role of endogenous FGF2 in angiogenesis related to the progression of ischemic disease in the heart and limbs has not been determined. Also, the importance of FGF2 during remodeling of arteries and arterioles, relevant to both ischemia and atherosclerosis, has not been directly studied in adult animals. These areas will be the focus of this dissertation and the research described in subsequent chapters.

Table 1.4: Lack of phenotype in studies using *Fgf2* knockout mice. The following papers reported no difference between wildtype and knockout mice.

Observation	Reference
Hyperplastic response following vessel injury	Zhou et al. 1998
Neovascularization related to ischemic retinopathy	Ozaki et al. 1998
Injury-induced choroidal neovascularization	Tobe et al. 1998
Growth and formation of vascularized tumors	Foletti et al. 2002

Arterial Remodeling

Vascular remodeling is the structural reorganization of a vessel involving a variety of cell activities including proliferation, apoptosis, migration, and extracellular matrix restructuring (Gibbons et al., 1994; Langille, 1993; Ward et al., 2000b). Remodeling of the arterial wall occurs following chronic changes in blood pressure and blood flow and in response to vessel injury (Figure 1.3) (Guyton et al., 1985; Kakuta et al., 1994; Korsgaard et al., 1993; Langille et al., 1986). The term "arterial remodeling" has been recently used to describe changes in artery size based on changes in the outer vessel diameter or cross-sectional area within the external elastic lamina (Ward et al., 2000b). Thus, lumen narrowing due to intimal hyperplasia without a concomitant change in the outer vessel diameter is not by definition considered to be arterial remodeling. Typically, a reduction in vessel size is referred to as inward remodeling whereas an increase in vessel size is referred to as outward remodeling. The various terms used to describe arterial remodeling are shown below.

Table 1.5: Terminology used to describe arterial remodeling.

Change in Vessel Size	
Increase	*Decrease*
Outward remodeling	Inward remodeling
Compensatory enlargement	Paradoxical shrinkage
Expansive remodeling	Constrictive remodeling
Positive remodeling	Negative remodeling

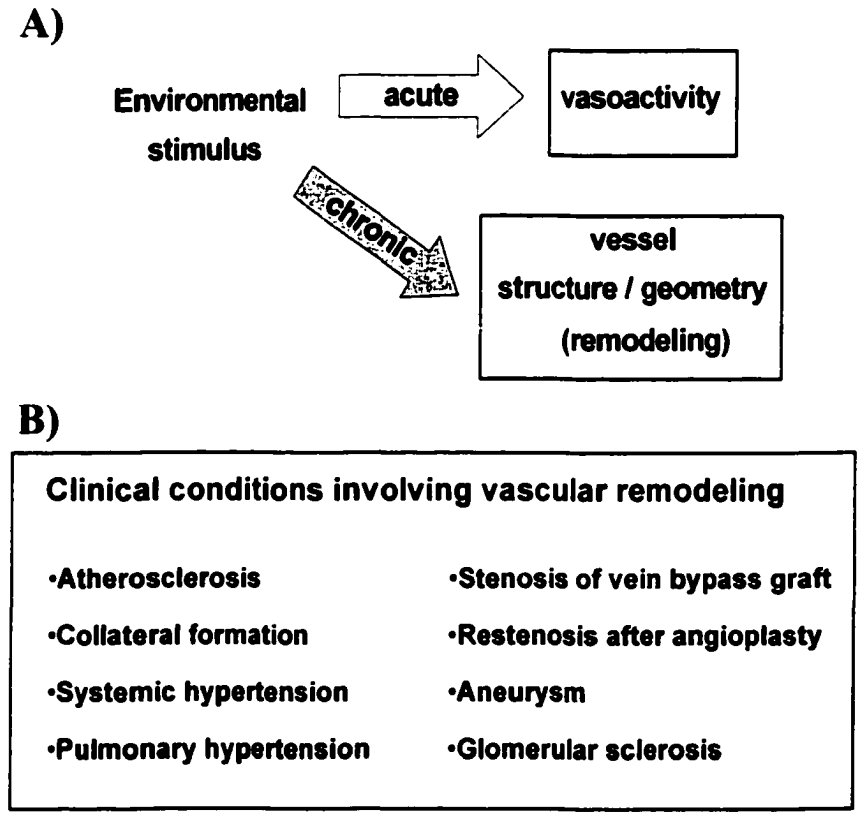

Figure 1.3 A) Environmental stimuli (e.g., hemodynamic forces) acutely alter vessel tone whereas chronic stimuli cause actual structural remodeling of the vessel wall. B) Examples of clinical conditions involving vascular remodeling.

Flow-Dependent Remodeling

Artery remodeling due to changes in blood flow (flow-dependent remodeling) occurs in both physiological (Langille, 1993; Miyachi et al., 2001) and pathological situations (Krams et al., 1998; Ward et al., 2000a; Ward et al., 2001; Wentzel et al., 2001). For example, studies show that endurance training can stimulate enlargement (outward remodeling) of the femoral artery in the trained legs, presumably due to flow-dependent remodeling (Dinenno et al., 2001; Miyachi et al., 2001). In pathological settings, such as atherosclerosis and angioplasty, artery remodeling plays a critical role in the degree of vessel narrowing during plaque or lesion progression (Glagov et al., 1987; Kakuta et al., 1994; Mintz et al., 1996; Pasterkamp et al., 1995; Pasterkamp et al., 2000). It is thought that a chronic change in blood flow through the affected artery is a significant stimulus for the remodeling events in atherosclerotic vessels and post-angioplasty restenosis (Krams et al., 1998; Ward et al., 2000a; Ward et al., 2001; Wentzel et al., 2001). Studies in humans show that atherosclerotic peripheral and coronary arteries can undergo both compensatory vessel enlargement and vessel shrinkage (inward remodeling) at or near the site of plaque formation (Glagov et al., 1987; Pasterkamp et al., 1995; Pasterkamp et al., 2000; Smits et al., 1998). In addition to local remodeling at the lesion site, it is recognized that remote parts of the circulation affected by the progressing plaque may undergo remodeling due to altered hemodynamics (Kakuta et al., 1998; Langille, 1991). For example, with advanced obstructions or restenosis, adjacent arteries may shrink as flow becomes compromised (Kakuta et al., 1998; Langille, 1991). Conversely, lesion progression in one artery segment may cause compensatory

A)

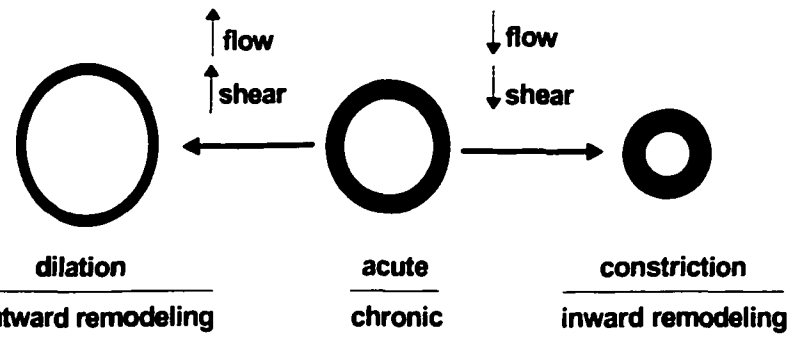

B)

• Vasoactive molecules	• Growth regulators	• Matrix modulators
Nitric oxide	FGF2 (bFGF)	Collagen
Bradykinin	PDGF-B	MMPs
Prostaglandin	TGF-β	tPA
Prostacyclin	Nitric oxide	
Angiotensin II	Angiotensin II	
Endothelin-1	Endothelin-1	

Figure 1.4 A) Blood flow and subsequent changes in shear stress in arterial vessels leads to outward remodeling or inward remodeling in response to high flow or low flow, respectively. B) Partial list of vasoactive molecules, growth regulators, and matrix-related molecules typically believed to be important in flow-dependent remodeling.

enlargement of collateral arteries as flow increases in the collateral segment (Langille, 1991; Shircore et al., 1995). Along these lines, a recent study reported that patients with unilateral internal carotid artery occlusion had reduced common carotid artery blood flow, which was associated with reduced common carotid artery diameter on the occluded side (Kubis et al., 2001). In contrast, the contralateral common carotid artery had increased blood flow and a larger diameter than control carotid arteries. Generally, increased blood flow leads to artery enlargement whereas blood flow reduction results in artery diameter reduction (Ben Driss et al., 1997; Kamiya et al., 1980; Kubis et al., 2001; Langille et al., 1986; Langille et al., 1989; Miyashiro et al., 1997; Tuttle et al., 2001).

Acutely, changes in blood flow are sensed by the endothelium, which releases vasoactive factors to adjust lumen diameter thereby normalizing wall shear stress (Figure 1.4) (Davies, 1995; Rubanyi et al., 1986). However, acute changes in blood flow result in only transient adjustments in vessel tone and diameter. Only sustained changes in flow, typically 7 days or longer, result in permanent structural remodeling of arteries (Langille et al., 1989; Rudic et al., 2000) and this process is endothelium-dependent (Langille et al., 1986; Rudic et al., 1998; Tohda et al., 1992). The endothelium is viewed as the critical transducer of hemodynamic stimuli into arterial restructuring (Lehoux et al., 2002).

Shear and the Endothelium

Numerous gene products, vasoactive substances and growth factors, are differentially expressed in endothelial cells following alterations in blood flow and shear stress (Figure 1.5) (Malek et al., 1995). Many of these genes, such as PDGF-B, have a

putative shear stress response element (GAGACC) in their promoter region (Resnick et al., 1993). FGF2 production is clearly shear responsive, but a mechanism for this shear regulation has yet to be identified within the promoter region of the *Fgf2* gene (Malek et al., 1995; Malek et al., 1993). Shear responsive transcription factors, such as activator protein-1 (AP-1) and nuclear factor kappa B (NFκB), may regulate the expression of certain shear activated genes (Lan et al., 1994; Malek et al., 1995; Nagel et al., 1999). Relatively little is known in regard to how sustained hemodynamic stimuli lead to permanent changes in artery size. It is clear that endothelial-derived vasoactive substances, like nitric oxide (NO) and endothelin-1, are capable of regulating vascular cell proliferation and extracellular matrix remodeling (Salani et al., 2000; Tronc et al., 2000; Vernon et al., 1997; Ziche et al., 1997). Thus, the same molecules controlling vessel tone may be responsible for initiation of the various events required for structural modification of the vessel wall. In fact, pharmacological inhibition of NO production attenuates flow-dependent arterial remodeling (Guzman et al., 1997; Tronc et al., 1996; Tronc et al., 2000). Examining endothelial cells *in vitro*, it has been demonstrated that different gene expression patterns are initiated depending on the duration of shear exposure (Figure 1.6) (Malek et al., 1995). It is possible that those genes that are highly expressed only after sustained shear changes (e.g., eNOS, TGFβ, and FGF2) are the same genes required for permanent structural adaptation in the vessel. Consistent with *in vitro* studies, FGF2 protein and mRNA levels are increased in carotid arteries exposed to chronically increased blood flow (Singh et al., 1998). It was not clear from this study which aspect(s) of arterial remodeling that might be affected by the upregulation of

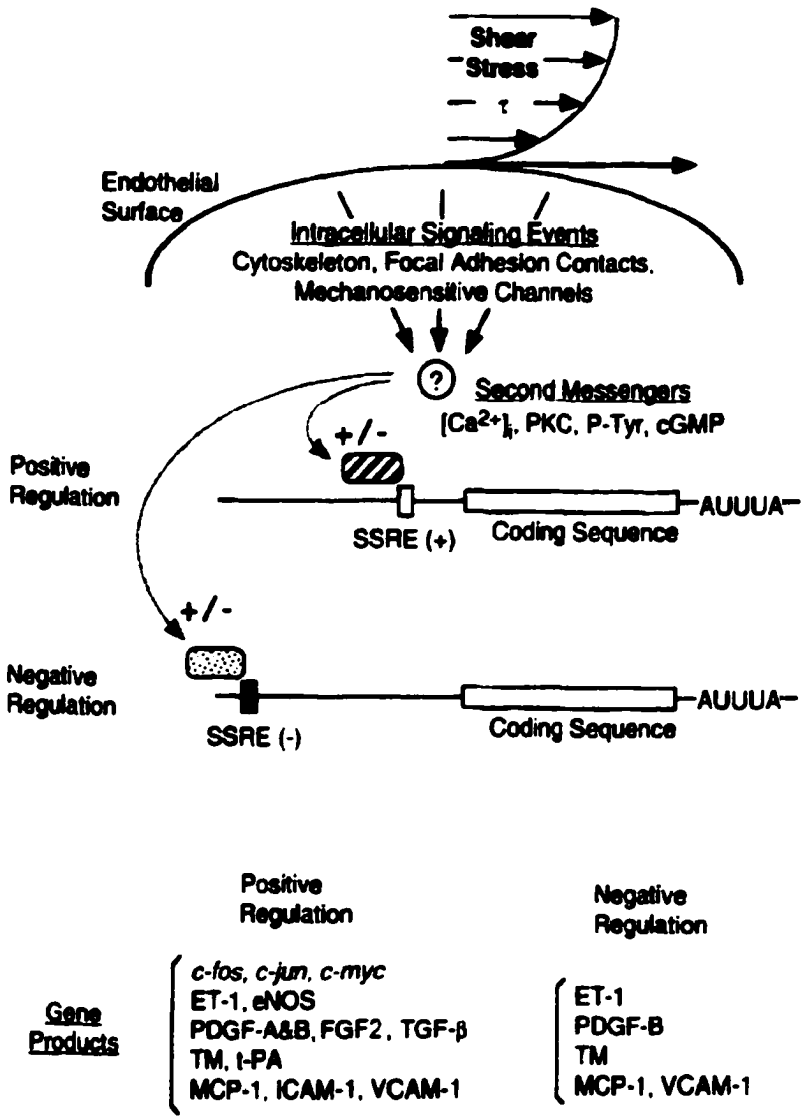

Figure 1.5 Schematic of the steps in shear stress regulation of endothelial cell gene expression. Shear stress on the surface of the endothelial cells activates mechanosensitive signals, possibly involving the cytoskeleton, adhesion contacts, and/or ion channels. Next, various second messenger systems are turned on, which then activate various DNA binding factors. These transcription factors bind to shear stress response elements (SSRE), which either positively or negatively regulate gene transcription of various genes. Reprinted from Journal of Biomechanics , Vol 28, No 12, Malek and Izumo, Control of endothelial cell gene expression by shear, pages 1515-1528,1995, with permission from Elsevier Science.

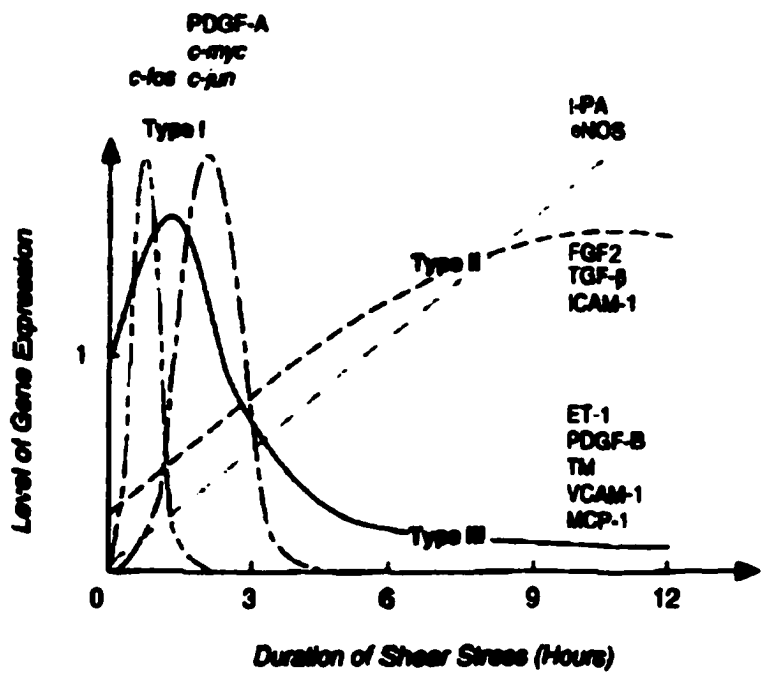

Figure 1.6 Studying endothelial cells *in vitro*, it has been demonstrated that different gene expression patterns are initiated depending on the duration of shear exposure. Malek et al. categorized flow-stimulated genes into three types based on their expression patterns: type I genes increase early and transiently, type II genes show a steady and continued increase, and type III increase for a period and then are down regulated by sustained shear. Reprinted from Journal of Biomechanics , Vol 28, No 12, Malek and Izumo, Control of endothelial cell gene expression by shear, pages 1515-1528,1995, with permission from Elsevier Science.

endogenous FGF2. Interestingly, antibody neutralization of endogenous FGF2 reduced inward remodeling in the mouse carotid artery following flow cessation (Bryant et al., 1999). This suggests that FGF2 may also be important during inward remodeling following flow reduction, although flow interruption may trigger a different remodeling response as compared to reduced shear stress. PDGF and transforming growth factor beta-1 (TGFβ1) are both upregulated in response to shear *in vitro*, but their functions during remodeling have not been directly examined *in vivo* (Malek et al., 1995; Mitsumata et al., 1993; Ohno et al., 1995; Resnick et al., 1993). PDGF appears to be important during inward remodeling given that arteries exposed to chronically reduced flow show increased levels of PDGF-A and PDGF-B, while high flow arteries had no change in PDGF (Mondy et al., 1997). In contrast, TGFβ1 and the TGFβ1-activating endoprotease furin are both upregulated in carotid arteries exposed to high shear, suggesting that TGFβ1 may be playing a role during outward remodeling (Negishi et al., 2001).

Arterial remodeling is characterized by increased vascular cell turnover. Both high-flow and low-flow remodeling are associated with concurrent increases in apoptosis and proliferation rates of endothelial and smooth muscle cells in the affected arteries (Buus et al., 2001; Mondy et al., 1997; Rudic et al., 2000). Interestingly, elevated rates of cell death are observed even in remodeling events that lead to net growth in the artery (Buus et al., 2001; Jackson et al., 2002). Overall, it appears that increased cell cycling (simultaneous proliferation and apoptosis) is present in most remodeling responses regardless of whether vessel size is increasing or decreasing. The specific molecules

regulating vascular cell growth or apoptosis during flow-dependent remodeling are largely unknown. Carotid arteries of *eNOS*$^{-/-}$ mice subjected to chronically reduced flow showed increased vascular cell proliferation and cell number versus *eNOS*$^{+/+}$ mice (Rudic et al., 1998). Thus, endothelial derived NO may be an essential controller of vascular cell turnover during flow-dependent carotid remodeling. Previous studies show that FGF2 can mediate endothelial cell and smooth muscle cell proliferation (Gospodarowicz et al., 1988; Itoh et al., 1992; Lindner et al., 1990; Lindner et al., 1991) and apoptosis (Fox et al., 1996; Karsan et al., 1997; Kondo et al., 1994). Interestingly, FGF2 has been shown to stimulate *eNOS* mRNA expression and eNOS protein production in cultured endothelial cells (Babaei et al., 1998; Kostyk et al., 1995). Also, it has been shown that NO promotes proliferation of *in vitro* endothelial cells through endogenous FGF2 (Ziche et al., 1997). Further, NO has been shown to selectively augment the mitogenic action of FGF2 in cultured aortic smooth muscle cells (Hassid et al., 1994). Thus, FGF2 may regulate vascular cell turnover during remodeling, possibly in conjunction with endothelial-derived NO.

Extracellular Matrix Remodeling

Breakdown and rebuilding of the extracellular matrix (ECM) scaffolding in the vessel wall is considered to be an essential process in arterial remodeling (Galis et al., 2002; Godin et al., 2000; Masuda et al., 1999). MMPs are believed to be the primary molecules responsible for ECM degradation during arterial remodeling (Lehoux et al., 2002). Carotid artery remodeling in the mouse is associated with temporal changes in the

expression of MMP-2 and MMP-9 (Godin et al., 2000). Similarly, remodeled sections of atherosclerotic arteries in humans express high levels of MMP-2 and MMP-9 (Pasterkamp et al., 2000). Flow-loaded arteries contain increased levels of membrane type-1 MMP (MT1-MMP), which is a protein shown to regulate MMP-2 activity *in vivo* (de Kleijn et al., 2001; Shankavaram et al., 2001; Zhou et al., 2000). Most importantly, inhibition of MMPs causes significant attenuation of both outward and inward remodeling (Abbruzzese et al., 1998; de Smet et al., 2000; Margolin et al., 2002; Tronc et al., 2000). Flow-induced vessel enlargement results in localized disruptions in the internal elastic lamina (IEL) as well as enlargement of pre-existing fenestrae within the IEL (Masuda et al., 1999; Wong et al., 1996). These gaps in the IEL, often occurring in close proximity to proliferating endothelial cells, are thought to permit eventual expansion of the artery wall (Lehoux et al., 2002; Masuda et al., 1999). Similarly, inward remodeling may require ECM degradation in order to reorganize the intimal and medial layers into a smaller artery. Importantly, FGF2 has been shown to regulate expression of molecules involved in extracellular matrix remodeling such as urokinase-type plasminogen activator (uPA) and matrix metalloproteinases (MMPs) (Odekon et al., 1992; Pickering et al., 1997; Ziche et al., 1997). uPA expression indirectly increases MMP activity through plasmin-dependent activation of MMP zymogens (pro-MMPs) (Carmeliet et al., 2001).Vascular smooth muscle cells treated with FGF-2 increase their expression of MMP-1 and decrease expression of tissue inhibitor of matrix metalloproteinases (TIMPs) (Pickering et al., 1997). Thus, FGF2 may act in a paracrine and/or autocrine manner to promote the production of molecules required for degradation of collagen and elastin in

the vessel wall. MMPs, in addition to their restructuring of the ECM, may also liberate growth factors and vasoactive peptides from the ECM (Fernandez-Patron et al., 2000; Whitelock et al., 1996). Certain MMPs are capable of releasing matrix-bound FGF2, however MMP-2 and MMP-9 did not affect the bioavailability of FGF2 *in vitro* (Whitelock et al., 1996).

While roles of growth factors in intimal hyperplasia and neoitimal formation have been widely studied, the specific roles of growth factors such as FGF2, TGFβ, and PDGF during arterial remodeling are relatively unexplored (Schwartz et al., 1995). Further studies are required to directly identify the processes involved in arterial remodeling (e.g., proliferation, apoptosis, and matrix degradation) that are regulated by these endogenous peptides.

Ischemic Revascularization

Arterial occlusive disease of the heart and limbs leads to inadequate blood supply to these tissues at rest and/or during exercise (i.e., ischemia). Of course, this can have harmful consequences in terms of the function of the under-perfused organ or tissues. The body adapts to impaired perfusion in many ways, including the growth of vascular elements in order to functionally resupply blood flow downstream of blocked or severely narrowed vessels (referred to here as revascularization). In animal models and in humans, endogenous revascularization is often unable to adequately replace the blocked arteries and so tissue perfusion remains impaired (Brevetti et al., 2001; Hoefer et al., 2001; Ito et al., 1997a; Niebauer et al., 1995). Understandably, there is a tremendous interest in the

mechanisms of revascularization in order to enable manipulation of these processes to improve the blood supply in conditions such as coronary artery disease and peripheral vascular disease (Waltenberger, 1997).

Revascularization in the adult is typically categorized into two distinct vascular growth processes termed angiogenesis and arteriogenesis (Figure 1.7) (Hershey et al., 2001; Ito et al., 1997b). Angiogenesis refers to the growth of capillaries from preexisting microvessels whereas arteriogenesis refers to the growth and remodeling of preexistent arterial vessels into functional collateral arteries (Ito et al., 1997a; Risau, 1997). The endogenous mediators of revascularization are for the most part unknown. VEGF appears to be a major regulator of ischemia-induced angiogenesis (Couffinhal et al., 1998) while a host of other molecules have been implicated in both angiogenesis and arteriogenesis (Table 1.6), including FGF2, tumor necrosis factor-α (TNF-α), and monocyte chemoattractant protein-1 (MCP-1) (Arras et al., 1998; Hoefer et al., 2001; Walgenbach et al., 1995; Yang et al., 1996). Many of these studies are based on exogenous delivery of the molecule or protein *in vivo* and *in vitro*. Consequently, such experiments may not reflect the endogenous activity of these molecules. Recent studies using knockout mice have identified several genes that either positively or negatively modulate revascularization in the setting of hindlimb ischemia (Table 1.7).

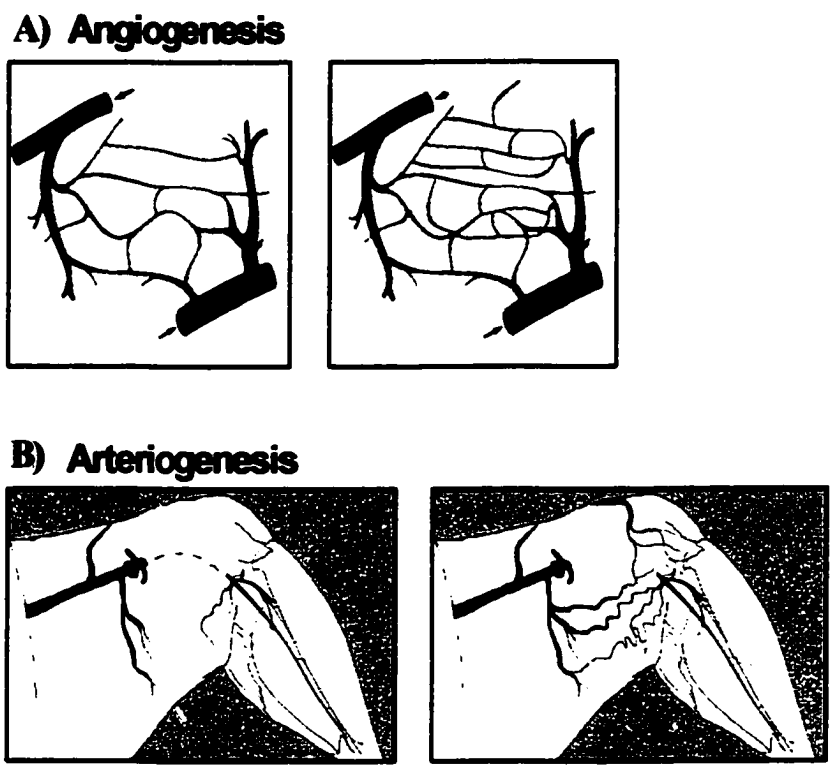

Figure 1.7 There are at least two types of vessel growth commonly examined during ischemic revascularization. A) Angiogenesis refers to the growth of capillaries from preexisting microvessels. The left panel represents the typical microvascular network including an arteriole (red), terminal arterioles, capillaries, and venules (blue). Angiogenesis increases the number of capillaries in the network, represented in the right panel. B) Arteriogenesis refers to the growth and remodeling of preexistent arterial vessels into functional collateral arteries. For example, arterial occlusion of a major feed artery (left panel) leads to growth, in both length and diameter, of preexisting arterioles and small arteries (right panel) that exist in arcades, functionally linking two or more feed arteries.

Table 1.6: Examples of stimulators of angiogenesis and arteriogenesis.

Stimulate angiogenesis			Stimulate arteriogenesis		
FGF-2	FGF-1	FGF-5	FGF-2	FGF-4	PDGF
VEGF	PDGF	MCP-1	MCP-1	GM-CSF	NO
PlGF	IGF-1	TNFα	TNFα	TGFβ	
HGF	ANG-1	TGFβ			
NO					

Modified from Carmeliet et al. 2000.

Table 1.7: Knockout mice showing altered revascularization in hindlimb ischemia model. Some knockout mice had decreased revascularization, while others had increased revascularization

Knockout		Revascularization response	Ref
eNOS -/-	Endothelial nitric oxide synthase	Decreased	(Murohara et al. 1998)
TNFα -/-	Tumor necrosis factor-α	Decreased	(Hoefer et al. 2002)
ApoE-/-	Apolipoprotein E	Decreased	(Couffinhal et al. 1998)
AT1a -/-	Angiotensin II type 1 receptor	Decreased	(Sasaki et al. 2002)
PlGF -/-	Placental growth factor	Decreased	(Carmeliet et al. 2001)
Klotho +/-	Aging-suppressor gene	Decreased	(Fukino et al. 2002)
Agtr2 -/Y	Angiotensin II type 2 receptor	Increased	(Silvestre et al. 2002)
IL-10 -/-	Interleukin-10	Increased	(Silvestre et al. 2000)
Ror alpha sg/sg	Staggerer mutant with Ror alpha gene deletion	Increased	(Besnard et al. 2001)

Arteriogenesis

Arteriogenesis (also referred to as collateralization and collateral development) is essential during revascularization since this is the only known process in the adult that leads to the formation of conductance arteries, which then function to bridge the blocked arterial segments. These collateral vessels develop from preexisting arteries and arterioles that exist in networks, functionally linking two or more feed arteries (Engelson et al., 1985; Hill et al., 1992; Scholz et al., 2001; Scholz et al., 2002). During arteriogenesis collateral arteries undergo extensive remodeling, such that growing arteries can double in length and increase their diameter up to several-fold (Scholz et al., 2001; Scholz et al., 2002). The characteristic tortuosity and corkscrew appearance of collaterals is due to this large amount of longitudinal growth. Flow and pressure within the collateral circuits are thought to be the guiding forces driving arteriogenesis (Scholz et al., 2001). Upon occlusion of a large artery, blood flow is redirected into neighboring collateral vessels, which causes shear stress to increases. Thus, many of the mechanisms discussed in regard to flow-dependent remodeling may be at work during arteriogenesis. In fact, arteriogenesis may simply reflect flow-induced remodeling in smaller arteries or arterioles. Flow-dependent remodeling in very large arteries (e.g., carotid artery) is not associated with longitudinal growth. This could be due to different factors, such as metabolic stimuli, present in ischemic revascularization as compared to situations of pure flow-dependent remodeling. The size of the arterial vessel that is undergoing remodeling may determine whether shear forces induce diameter and/or length changes. Similar to

the carotid artery, relatively large femoral artery branches outward remodel, but do not appear to grow in length during hindlimb revascularization (Scholz et al., 2002).

Schaper and colleagues suggest that during arteriogenesis shear activation of the endothelium lining the collaterals causes recruitment of circulating monocytes (Buschmann et al., 2000; Scholz et al., 2001). Shear stress has been shown to upregulate the expression of MCP-1 in endothelial cells (Bao et al., 1999; Shyy et al., 1995; Shyy et al., 1994). MCP-1 expression attracts circulating monocytes, which adhere to growing collaterals and migrate into the perivascular space (Arras et al., 1998). Activated monocytes/macrophages are capable of releasing numerous vascular growth factors including FGF2, TNFα, TGFβ, and PDGF (Sunderkotter et al., 1991). In particular, monocytes in the tissue surrounding arteriogenic collateral vessels stain strongly for FGF2 and TNFα (Arras et al., 1998; Scholz et al., 2002). Presumably, these growth factors then stimulate endothelial cell and smooth muscle cell proliferation in the collateral artery. In fact, TNFα knockout mice were shown to have significantly impaired collateral artery development during hindlimb revascularization (Hoefer et al., 2002). Macrophages also produce molecules that directly or indirectly modulate the ECM (Shankavaram et al., 2001; Sunderkotter et al., 1991). As mentioned earlier, ECM remodeling is important during arterial remodeling and MMP-2 and MMP-9 are upregulated in developing collaterals (Cai et al., 2000). eNOS knockout mice have severely impaired collateral development following arterial occlusion in the hindlimb, which supports that shear stress is a critical stimulus in arteriogenesis (Tamarat et al., 2002). Interestingly, shear-induced NO production caused upregulation of MCP-1 in

human endothelial cells *in vitro* (Bao et al., 1999). Overall, the above studies suggest a possible model of shear-induced artery growth that begins with eNOS activation and leads to growth factors release, which in turn regulates vascular cell proliferation and ECM remodeling (Figure 1.8).

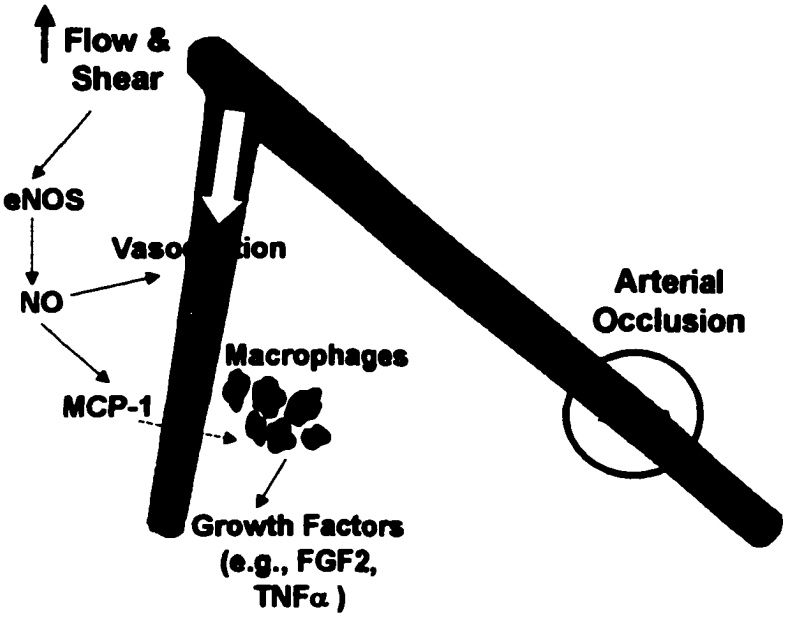

Figure 1.8 One possible model of shear-induced artery growth (arteriogenesis). Increased shear in the collateral vessel stimulates NO production via eNOS activation. NO acts to dilate the collateral vessel and NO causes upregulation of MCP-1 in endothelial cells. MCP-1 expression attracts circulating monocytes that adhere to growing collaterals and migrate into the perivascular space. Activated monocytes/macrophages are capable of releasing numerous vascular growth factors including FGF2 and TNFα. Presumably, these growth factors then stimulate endothelial cell and smooth muscle cell proliferation in the collateral artery. Macrophages also produce molecules that directly or indirectly modulate the ECM.

Angiogenesis

Angiogenesis is the other vascular growth process that is typically examined during revascularization. Angiogenesis, strictly defined, refers to the formation of new capillaries from preexisting microvessels (Buschmann et al., 1999; Pepper, 1997). The initial steps of angiogenesis involve ECM degradation and endothelial cell proliferation and migration (Carmeliet, 2000). These steps are followed by tube formation and endothelial cell redifferentiation. During revascularization, the end result of these events is the growth of new capillaries and the expansion of existing capillary networks in the ischemic tissue.

Many of the inflammatory and mitogenic molecules discussed above in regard to arteriogenesis have been previously identified in the regulation of angiogenesis (Table 1.6). Inflammatory cells, such as macrophages and T lymphocytes, may be a critical source of growth factors during ischemia-induced angiogenesis (Couffinhal et al., 1999; Kuwabara et al., 1995). As mentioned earlier, macrophages can produced various growth factors and metalloproteinases that are required during vascular growth. Studies in athymic nude mice and ApoE knockout mice show a strong association between impaired T lymphocyte infiltration and reduced angiogenesis (Couffinhal et al., 1999). T lymphocytes appear to be an important source of VEGF in the ischemic tissue(Couffinhal et al., 1999). Chronically elevated shear stress has been shown to cause capillary growth (Dawson et al., 1989; Egginton et al., 2001; Milkiewicz et al., 2001). Thus, shear stress may be an initiating stimulus of both angiogenesis and arteriogenesis following arterial occlusion. Along these lines, eNOS is a common molecular pathway in both types of

vessel growth given that angiogenesis and collateral development are diminished in adult eNOS knockout mice (Lee et al., 1999; Murohara et al., 1998; Tamarat et al., 2002). However, differences exist between the regulation of arteriogenesis and angiogenesis. For example, localized hypoxia and ischemia (i.e., metabolic stimuli) potently stimulate angiogenesis whereas arteriogenesis occurs in tissue sites with normal high-energy phosphate and oxygen levels (Carmeliet, 2000; Deindl et al., 2001; Ito et al., 1997a). Also, arteriogenesis occurs without upregulation of VEGF and hypoxia-inducible genes (e.g., HIF-1α) that are thought essential for angiogenesis (Deindl et al., 2001; Hershey et al., 2001).

FGF2 and Revascularization

FGF2, with the possible exception of VEGF, has been the most widely studied angiogenic growth factor in the area of ischemic revascularization. Numerous studies have established that exogenous FGF2 stimulates angiogenesis in models of ischemia (Baffour et al., 1992; Battler et al., 1993; Bush et al., 1998; Chleboun et al., 1994; Masaki et al., 2002). More importantly, endogenous FGF2 expression increases within and around ischemic cardiac and skeletal muscle (Breen et al., 1996; Bush et al., 1998; Chleboun et al., 1994; Lefaucheur et al., 1995; Xie et al., 1997). Specifically, in a rat model of hindlimb ischemia, permanent ligation of the femoral artery caused a ten-fold increase in FGF2 levels in the ischemic hindlimb (Chleboun et al., 1994). The increased FGF2 levels persisted for 3 weeks post-ligation and closely correlated with improved blood flow to the ischemic hindlimb. In a rabbit model of hindlimb ischemia, areas of

FGF2 immunostaining were localized to clusters of newly formed vessels in the ischemic muscle (Bush et al., 1998). Similarly, studies using a mouse model of denervation and devascularization have shown that FGF2 increases in injured and ischemic muscle (Anderson et al., 1995; Lefaucheur et al., 1995). Finally, FGF2 has been localized to sprouting capillaries in ischemic myocardium (Chiba et al., 1989; Xie et al., 1997). Two recent studies have utilized neutralizing antibody to FGF2 to determine whether the increase in FGF2 levels is responsible for the ischemia-induced angiogenesis (Lefaucheur et al., 1996; Walgenbach et al., 1995). Walgenbach et al. demonstrated that transposing a well-perfused muscle flap onto an ischemic hindlimb in the rabbit results in angiogenesis and vessel growth within the ischemic skeletal muscle (Walgenbach et al., 1995). FGF2 mRNA and FGF2 protein levels were increased early at the interface between the well-perfused muscle flap and the ischemic region and later within the ischemic muscle. In contrast, *Fgf2* mRNA levels and protein were not increased when a well-perfused muscle flap was transposed onto healthy muscle. Anti-FGF-2 antibody therapy significantly reduced angiogenesis in the ischemic muscle and the newly formed muscle interface. In another study, antibody neutralization of endogenous FGF2 significantly reduced the capillary density measured in chronically ischemic muscles of the mouse hindlimb (Lefaucheur et al., 1996). However, given that at least 7 FGFs can be expressed in the cardiovascular system, and since there are 22 different FGF family members, potential cross-reactivity of anti-FGF2 antibodies to other FGFs cannot be ruled out in these studies (Schultz et al., 2002; Yamashita et al., 2000). The specificity of neutralizing

antibodies is never certain, thus antibody studies could be overestimating the role of FGF2 if the antibody cross-reacts with other proteins or other FGF molecules.

Interestingly, studies suggest that FGF2 may mediate the angiogenic activity of VEGF (Jonca et al., 1997; Mandriota et al., 1998). Antibody neutralization of endogenous FGF2 inhibited VEGF-induced in vitro tube formation in cultured microvascular endothelial cells (Mandriota et al., 1998) and angiogenesis in a corneal pocket assay induced by the 189 amino acid isoform of VEGF (Jonca et al., 1997). Also, a recent study showed that FGF2 increases the expression of VEGFR-2 (Flk-1/KDR) *in vitro* (Pepper et al., 1998). Similarly, ischemia increases VEGFR-2 expression in vascular cells in the mouse retina (Suzuma et al., 1998). Likewise, it has been shown that hypoxic myoblasts can increase VEGFR-2 expression in cultured endothelial cells via a paracrine mechanism (Brogi et al., 1996). It is interesting to speculate that FGF2, in addition to increasing VEGF expression, might make endothelial cells more responsive to VEGF by increasing their expression of VEGFR2. Collectively, these studies suggest that FGF2 may act to support the angiogenic activity of VEGF.

It is important to note that angiogenesis in response to ischemic retinopathy and ocular choroidal injury was unaltered in the absence of FGF2 (Ozaki et al., 1998; Tobe et al., 1998). These results can be broadly interpreted to mean that FGF2 is not a critical mediator of all disease-related angiogenesis in the adult. However, the mechanisms of retinal and choroidal neovascularization may be specific to angiogenesis within avascular regions of the eye and may not be readily extrapolated to angiogenic mechanisms in muscle or other pathological conditions (Campochiaro, 2000). Also, experiments in the

eye reflect the role of FGF2 during capillary formation only, since neovascularization in the eye is not typically associated with arteriole and artery formation (Campochiaro, 2000). Lastly, vascular growth related to female reproduction is apparently unaffected by the lack of FGF2 as female FGF2 knockout mice are fertile (Zhou et al., 1998). This implies that FGF2 is not regulating physiological angiogenesis, though other types of physiological vessel growth (e.g., due to exercise training) have not been studied in adult FGF2 mice.

Arterialization of Capillaries

In addition to angiogenesis and arteriogenesis, vascular adaptation during revascularization may include a third and distinct growth process. Numerous studies have documented the growth and formation of terminal and preterminal arterioles in adult skeletal muscle in response to chronic stimuli such as vasodilation, electrical stimulation, stretch, or hypoxia (Hansen-Smith et al., 1998; Hansen-Smith et al., 2001; Price et al., 1998a; Price et al., 1998b). For example, the number of terminal arterioles (<10μm) more than doubled in adult skeletal muscle exposed to 20 days of hypoxia (Price et al., 1998b). Electrical stimulation of skeletal muscle for 7 days caused the density of both terminal and preterminal (≥10μm) arterioles to increase by approximately two-fold (Hansen-Smith et al., 1998). Although capillary growth and collateral formation have been studied rather extensively in ischemic models, the formation of arterioles has received very little attention. The formation of new arterioles in the adult is thought to occur through the arterialization of preexisting capillaries (also referred to as "arteriolarization") in

response to both physical and biochemical stimuli (Hansen-Smith et al., 1998; Skalak et al., 1996). It is thought that the conversion of capillaries into arterioles occurs through one of three likely mechanisms (Skalak et al., 1996). First, smooth muscle cells from an upstream arteriole may migrate downstream to the remodeling capillary. Second, pericytes located on the abluminal surface of remodeling capillaries may differentiate into smooth muscle. Finally, perivascular fibroblasts may migrate to the arterializing capillary and then differentiate into smooth muscle cells. Chronic vasodilation in skeletal muscle induced selective proliferation of adventitial cells in close proximity to terminal arterioles (Price et al., 1998a). This study demonstrated increased arteriole formation in response to a chronic hemodynamic stress, but the identity of the proliferating cells, presumed to be fibroblasts, could only be inferred from the data. Fibroblasts injected into the gracilis muscle of young rats showed significant recruitment into the walls of microvessels (Skalak et al., 1998). Hansen-Smith et al. provide evidence that the growth of arterioles is associated with differentiation of both pericytes and adventitial fibroblasts, while proliferation was only observed in perivascular fibroblasts (Hansen-Smith et al., 2001). However, pericyte proliferation may have been missed simply due to the low density of pericytes cell bodies adjacent to capillaries in this study. During revascularization, the formation of new arterioles in response to hypoxia or shear stress may be important to regulate flow within the newly remodeled microvascular beds of ischemic tissue. Factors such as TGFβ, FGFs, and PDGF may be involved in arterialization of capillaries. Specifically, TGFβ is a potent inducer of smooth muscle phenotype in non-smooth muscle cells, including fibroblasts (Hautmann et al., 1999;

Peehl et al., 1998). FGF2 can affect the migration, proliferation, and differentiation of both smooth muscle cells and fibroblasts (Bikfalvi et al., 1997; Swinscoe et al., 1992). Overexpression of FGF1 in the hearts of mice increased arteriole density but not capillary density (Fernandez et al., 2000). Thus, FGF1 may be involved in arteriole formation in adult cardiac or skeletal muscle. Interestingly, mice overexpressing FGF2 in the heart had normal arteriole density but increased capillary density. Evidence from angiopoietin-1 (Ang1) knockout mice suggests a role for Ang1 in the interaction of endothelial cells with surrounding mesenchymal cells during vascular development (Suri et al., 1996). Thus, Ang1 signaling may be involved in the arterialization of preexisting capillaries. Similarly, PDGF-B may be important in the recruitment of pericytes and perivascular cells to remodeling capillaries in the adult, given that PDGF-B knockout mice lack microvascular pericytes (Lindahl et al., 1997). Although very little is know about the formation of arterioles during ischemia-induced vascular adaptation, it is reasonable to assume that coordinated growth of arterioles, along with capillaries and arteries, is required for successful revascularization of ischemic regions.

Overall, the studies outlined in the above sections identify FGF2 as a primary candidate to control vascular growth during ischemic revascularization. The temporal upregulation and localized expression of FGF2 following arterial occlusion and its various affects on vascular cells, give FGF2 the potential to regulate angiogenesis, arteriogenesis, and arterialization of capillaries.

Vascular Reactivity and Ischemic Revascularization

Despite a rather remarkable amount of vascular adaptation and remodeling, maximal blood flow in many ischemia models reaches only 30-60 percent of normal weeks after occlusion of a major feed artery (Hoefer et al., 2001; Ito et al., 1997a). This may be due to insufficient collateral formation and vascular growth. However, altered vascular reactivity may also contribute to flow limitations in arterial occlusive disease. In this discussion, vascular reactivity refers to the functional responsiveness of arterial vessels in terms of vasoconstriction and vasodilation due to a stimulus (e.g., drug application or muscle stimulation). Numerous studies have demonstrated reduced vascular reactivity in response to vasodilator stimuli in collateral arteries and the collateral-dependent microcirculation using models of coronary artery occlusion or peripheral artery ligation (Bauters et al., 1995; Kelsall et al., 2001; Laham et al., 1998; Sellke et al., 1994). Similarly, studies of the heart and hindlimb have shown increased agonist-induced vasoconstriction (hyperreactivity) in collateral-dependent vessels during chronic ischemia (Nelissen-Vrancken et al., 1992; Peters et al., 1989; Rapps et al., 1997a; Rapps et al., 1997b). Overall, it appears that the recovery of blood flow during revascularization of ischemic tissue depends on at least two factors: (1) collateral development (including arteries, arterioles, and capillaries) and (2) proper responsiveness of the collateral vessels and collateral-dependent microcirculation to vasomotor stimuli.

Altered reactivity has been demonstrated in arterial vessels of various sizes, ranging from the small arterioles to large conductance arteries, using animal models of arterial occlusion (Heaps et al., 2000; Kelsall et al., 2001; Sellke et al., 1992). Figure 1.9

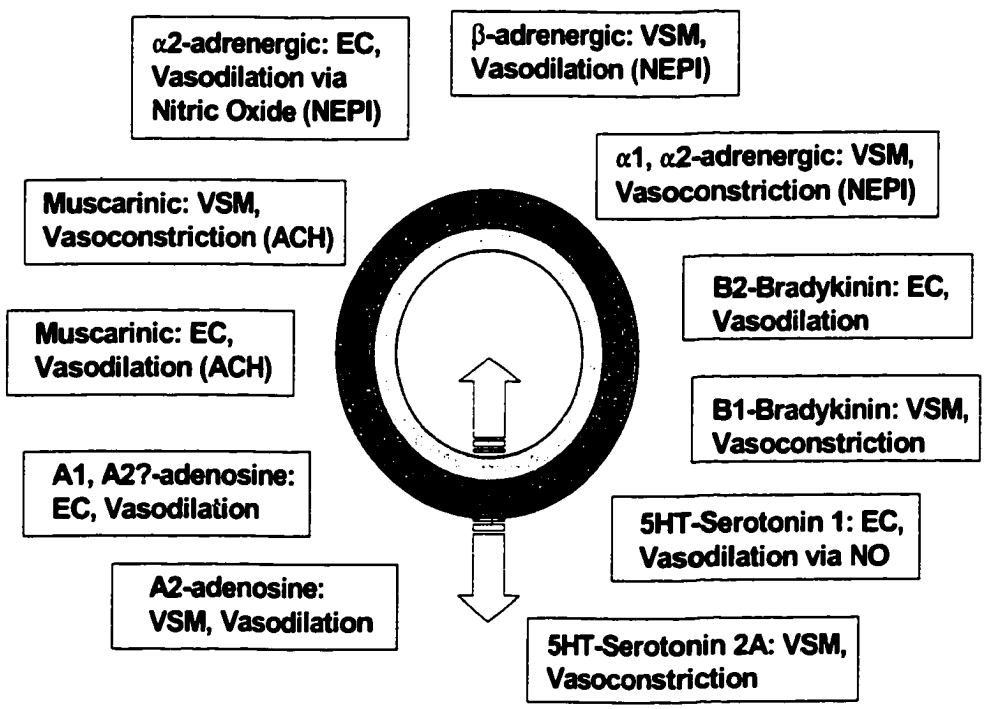

Figure 1.9 Partial list of agonists, with their respective receptors on endothelial cells (EC) and vascular smooth muscle cells (VSM), used to test vasomotor function and vascular reactivity. The receptor is listed first followed by the cell type and action (vasodilation or vasoconstriction) upon activation of the receptor by agonist. Agonist is abbreviated in parentheses if not implied in the receptor name. Abbreviations: NEPI, norepinephrine; ACH, acetylcholine; NO, nitric oxide.

displays a sampling of the various agonists, with their respective receptors, used to study vascular responsiveness. A recent study examined vascular reactivity using intravital microscopy to visualize preterminal (A3) and terminal (A4) arterioles (vessels ≤10μm) in chronically ischemic skeletal muscle (Kelsall et al., 2001). After 5 weeks of ischemia, they found that A3 and A4 arterioles had reduced vasodilation to bradykinin (endothelium-dependent) and sodium nitroprusside (SNP; endothelium-independent). Interestingly, the response to acetylcholine was reversed from vasodilation to vasoconstriction. In this study, ischemia had no effect on resting diameters of arterioles. This study directly demonstrates vascular dysfunction in the resistance arteries of ischemic tissue. Although resting diameters of arterioles were unaltered, the impaired vascular response to agonists suggests that hyperemia may be impaired in situations requiring flow beyond that of rest (e.g., exercise). In fact, Hudlicka et al. showed that terminal arterioles in ischemic muscle did not dilate during electrically stimulated muscle contractions (Hudlicka et al., 1994). It is unclear whether changes in the endothelium or smooth muscle or both cause this observed vascular dysfunction.

Similarly, endothelium-dependent responses are altered in small arteries (60-220μm diameter) from collateral-perfused regions of the ischemic myocardium (Laham et al., 1998; Sellke et al., 1990; Sellke et al., 1992). For example, several weeks after placement of an ameroid constrictor, arterial microvessels were isolated from collateral-dependent regions (ischemic) and non-ischemic regions of the myocardium, and then the responsiveness of isolated vessels was examined *in vitro* (Laham et al., 1998). Arteries from the collateral-dependent territories had significantly reduced relaxation to

endothelium-dependent agonists, but not endothelium-independent agonists. The responses of relatively large collateral arteries (>1000μm diameter) are similarly impaired in the models of myocardial ischemia (Heaps et al., 2000).

In addition to altered relaxation to agonists, collateral-dependent vessels have been shown to be hyperreactive to various vasoconstrictor substances. Increased reactivity (vasoconstriction) to angiotensin II and phenylephrine was observed in the ischemic hindlimbs of rats (Nelissen-Vrancken et al., 1992). Likewise, isolated vessels from collateral-dependent regions in ischemic myocardium showed increased vasoconstriction in response to vasopressin and norepinephrine (Rapps et al., 1997a; Rapps et al., 1997b). Enhanced responsiveness to vasopressin was associated with increased agonist-induced intracellular calcium release, while the increased norepinephrine response may have resulted from impaired α2-adrenergic stimulation of NO synthesis. In contrast, studies have shown reduced vasoconstriction to epinephrine in arterioles within the ischemic rat hindlimb as well as impaired constriction to endothelin in coronary collateral vessels (Kelsall et al., 2001; Rapps et al., 1997a). Thus, altered responsiveness is agonist specific and probably does not reflect a general hyperreactivity to all vasoconstrictor stimuli.

Importantly, this phenomenon is not limited to animal models of ischemic revascularization. For example, resistance arteries from human patients with chronic limb ischemia were isolated from ischemic (distal) and non-ischemic (proximal) regions of the same limb and then studied *in vitro* (Jarajapu et al., 2001). Arteries isolated from ischemic skeletal muscle had increased vasoconstriction to α-adrenergic agonists

norepinephrine and phenylephrine when compared to arteries from non-ischemic muscle. In contrast, others reported reduced responsiveness to norepinephrine in vessels from ischemic regions of patients with critical limb ischemia (Hillier et al., 1999). Arteries in the latter study were isolated from subcutaneous fat and so the conflicting results between these studies may be due to the tissue source (fat versus skeletal muscle) of the isolated arteries. In the study by Hillier et al. artery dilations to bradykinin and acetylcholine were significantly impaired in vessels from ischemic tissue. Overall, the findings of these human studies mirror fairly well the experiments examining vascular reactivity in animal models of hindlimb ischemia (Bauters et al., 1995; Kelsall et al., 2001; Nelissen-Vrancken et al., 1992).

The underlying cause of disturbed endothelial cell and smooth muscle cell function in collateral-dependent vessels is unclear. Several hypotheses have been proposed including: (1) ischemia-induced vascular cell damage in distal segments of the collateral and collateral-dependent circulation, (2) endothelial cell dysfunction due to altered hemodynamic forces (e.g., reduced shear and/or pressure) in distal portions of the collateral circulation, and (3) altered function due to proliferation/differentiation state of vascular cells during growth of collateral circulation (Bauters et al., 1995; Bauters, 1997; Rapps et al., 1997b).

Exogenous Growth Factors Improve Vessel Reactivity

It is well recognized that delivery of exogenous growth factors, such as FGF2 and VEGF, can improve or maintain vascular reactivity in models of chronic ischemia

(Bauters et al., 1995; Laham et al., 1998; Sellke et al., 1994; Takeshita et al., 1998). Specifically, sustained FGF2 delivery in the ischemic myocardium enhanced the responses of collateral-perfused coronary microvessels to endothelium-dependent vasodilators (Sellke et al., 1994). Similarly, a single intrapericardial injection of FGF2 into chronically ischemic hearts improved the responses of resistance arteries isolated from ischemic collateral-dependent regions of the myocardium (Laham et al., 1998). VEGF has been shown to have similar effects on endothelium-dependent responses in the rabbit ischemic hindlimb (Bauters et al., 1995). In this study, the iliac artery was ligated and 10 days later a bolus of either VEGF or saline was administered to the ischemic limb. A total of 40 days after iliac occlusion, vessel responses were evaluated in ischemic collateral-dependent regions of the hindlimb. Vessels from saline-treated ischemic limbs constricted in response to serotonin and had reduced acetylcholine-induced vasodilation. In contrast, the vasculature from VEGF-treated ischemic limbs vasodilated after serotonin administration and had increased relaxation to acetylcholine. Similarly, intramuscular gene transfer of VEGF in the rat ischemic hindlimb improved vascular responses to acetylcholine (Figure 1.10). Reversal of the vascular response to serotonin (vasoconstriction instead of vasodilation) has been observed in other studies of hindlimb revascularization (Orlandi et al., 1986; Verheyen et al., 1989; Verheyen et al., 1991). The vascular response to serotonin is a balance between vasoconstriction mediated by serotonin type 2 receptors located on smooth muscle cells and vasodilation mediated by serotonin type 1 receptors located on endothelial cells (Van Nueten et al., 1985). Thus, the augmented vasoconstrictor response to serotonin in the ischemic limb may be due to

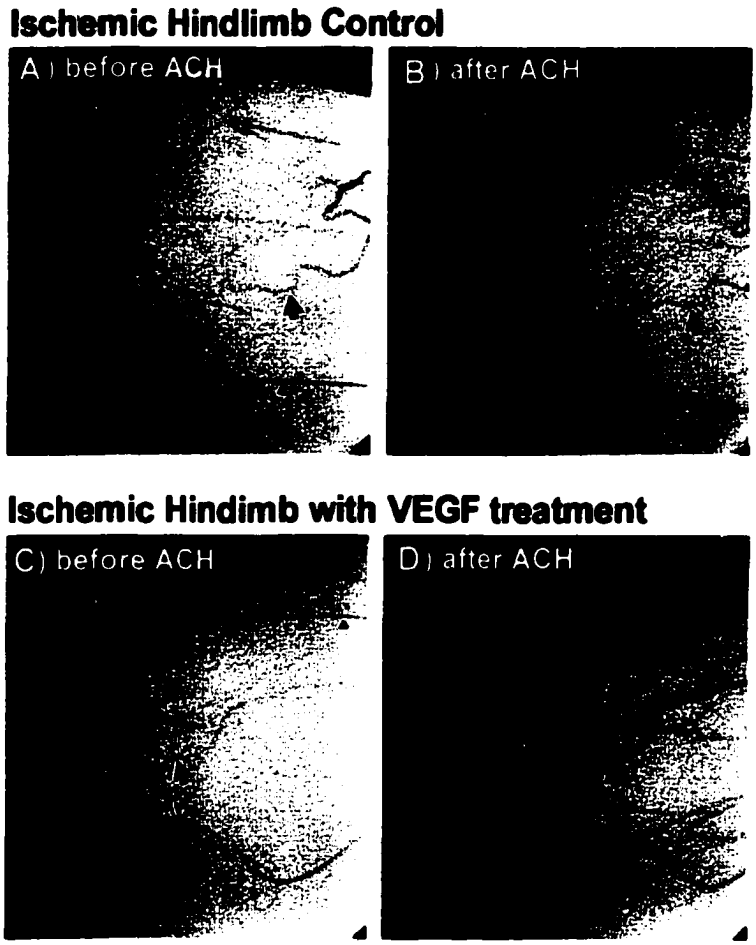

Figure 1.10 Hindlimb angiograms demonstrate the improved endothelium-dependent responses of the ischemic limb vasculature treated with VEGF. B) Vessels from saline-treated (Control) ischemic limbs had little or no vasodilation upon acetylcholine (ACH) administration. D) In contrast, the collateral vessel in VEGF-treated ischemic limbs showed extensive vasodilation in response to ACH. Small arrowheads identify a 100μm reference wire. Large black and open arrows indicate collateral vessels supplying the ischemic limb. Adapted from (Takeshita, Isshiki, et al. 1998)

loss of endothelium-dependent signaling and/or increased smooth muscle serotonin receptor sensitivity. Also, altered acetylcholine responsiveness most likely reflects endothelium-dependent mechanisms.

The basis for improved vasomotor responsiveness caused by FGF2 or VEGF treatment in these models of ischemia remains to be determined. A number of mechanisms could explain the ability of exogenous growth factors to increase vascular reactivity of the collateral-dependent circulation (Figure 1.11). The first possible mechanism is related to the ability of exogenous growth factors to enhance vascular collateral growth and vascular adaptation during ischemia (Laham et al., 2000; Takeshita et al., 1994). Increased growth in the collateral circulation promotes faster recovery of blood flow, which helps restore perfusion pressure and presumably shear stress in the distal collateral-dependent vessels (Takeshita et al., 1994; Tsurumi et al., 1996). It has been suggested that improved pressure and flow might positively affect endothelium-dependent function in the collateral vessels (Takeshita et al., 1998). Alternatively, improved perfusion recovery, secondary to improved vascular growth, may simply reduce the ischemic damage to distal portions of the hindlimb vasculature. The second possibility is that FGF2 and VEGF have direct actions on endothelium and smooth muscle that are independent of their growth promoting effects. For instance, FGF2 administered to hypercholesterolemic rabbits significantly improved endothelium-dependent responses of atherosclerotic vessels (Meurice et al., 1997). There was no evidence that FGF2 administration altered plaque formation or reendothelialization of the atherosclerotic vessels. The lack of structural differences between FGF2-treated and

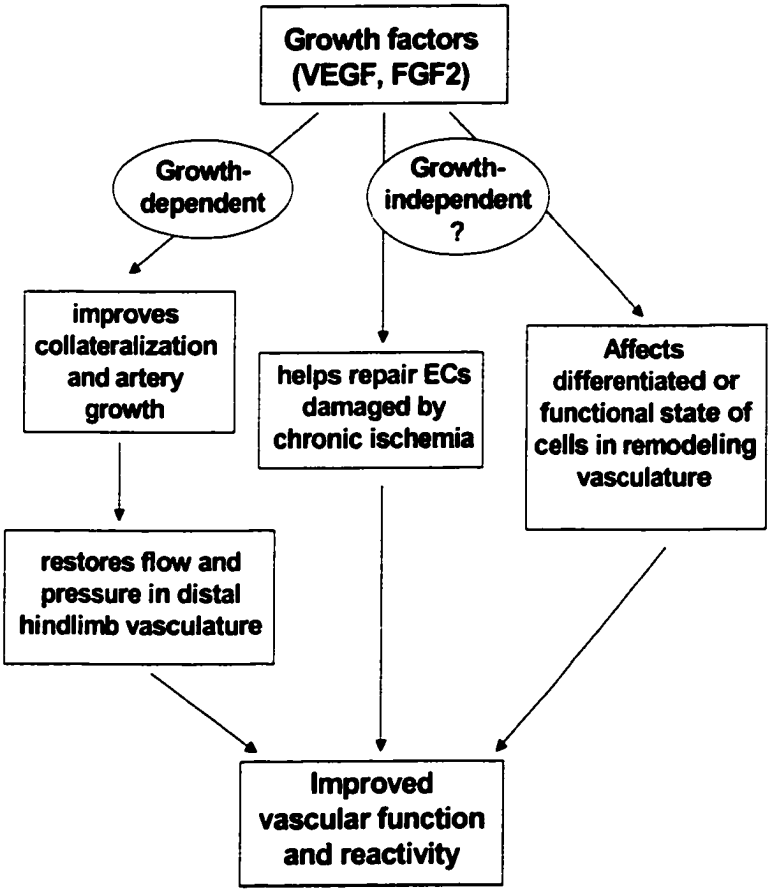

Figure 1.11 A number of mechanisms could explain the ability of exogenous growth factors to increase vascular reactivity of the collateral-dependent circulation. The first possible mechanism is related to the ability of exogenous growth factors to enhance vascular collateral growth during ischemia. The second possibility is that FGF2 and VEGF have direct actions on endothelium and smooth muscle that are independent of their growth promoting effects. Some suggest that VEGF or FGF2 may help to protect or repair vascular cells in the ischemic regions. Also, growth factors may act to regulate gene expression in the vasculature, thus altering vasomotor responses. In addition, it is conceivable that growth factors supplied to the ischemic limb modulate the phenotypic state of smooth muscle cells and/or endothelial cells

control-treated vessels suggests that improved endothelial function by FGF2 was not simply due to increased endothelial cell growth. Meurice et al. reported that FGF2 treatment of balloon-injured arteries improved relaxation to acetylcholine (Meurice et al., 1996). FGF2 enhanced reendothelialization in this model, which suggests that the improved endothelium-dependent responses may be due to the promotion of endothelial growth. However, others have shown that endothelium-dependent relaxation remains impaired despite reendothelialization of the artery (Weidinger et al., 1990). Again, this suggests that the affect of FGF2 on vascular function is not simply due to regulation of cell growth. Growth factors may act to regulate gene expression in the vasculature, thus altering vasomotor responses. For example, addition of exogenous FGF2 to vascular cells increases eNOS and cyclooxygenase-2 (COX-2) expression (Kage et al., 1999; Karim et al., 1997; Kostyk et al., 1995). Thus, FGF2 levels could possibly modulate vascular reactivty indirectly via the regulation of enzymes (e.g., eNOS, COX) involved in the production of vasoactive substances (e.g., NO, prostacyclin). Also, exogenous FGF2 is capable of regulating the contractile phenotype of vascular smooth muscle (Kato et al., 1998b). It is conceivable that FGF2 supplied to the ischemic limb modulates the phenotypic state of smooth muscle cells (or even endothelial cells) by regulating the shift to or from the quiescent state, perhaps independent of its mitogenic activity.

The results from studies using exogenous growth factors to improve vasomotor function raise the question of whether endogenously produced FGF2 or VEGF act to modulate the responsiveness of the vasculature in conditions such as chronic ischemia. This possible function of endogenous growth factors has yet to be determined. Along

with vascular growth, the vasomotor responsiveness of collateral and collateral-dependent vessels may be a critical factor determining blood flow to ischemic tissues.

Significance and Research Plan

The overall goal of this project was to test the **hypothesis that fibroblast growth factor-2 (FGF2) is required during disease-related vascular growth and remodeling in the adult organism.** From previous research, it is clear that FGF2 is a potent vascular cell mitogen *in vitro* and that exogenous FGF2 stimulates angiogenesis and vessel growth *in vivo*. Additionally, the expression of FGF2 is upregulated during a variety of pathological conditions (e.g. tissue ischemia, vessel injury, and flow-dependent remodeling) associated with extensive remodeling of the existing vascular tree. Given these observations, it is generally assumed that FGF2 is an important regulator of vessel growth during these pathophysiological processes. However, such studies only indirectly implicate FGF2 in vascular adaptation and remodeling. In contrast, experiments using mice with a targeted disruption of the *Fgf2* gene allow direct determination of the biological roles of endogenous FGF2. Experimental models of flow-dependent remodeling and ischemic revascularization were used to compare the responses of $Fgf2^{-/-}$ and $Fgf2^{+/+}$ mice to directly identify the function of FGF2 during vascular adaptation in the adult animal. This work has contributed to the understanding of FGF2 in vascular physiology and pathophysiology.

Specific Aim 1. Determine the role of FGF2 during flow-dependent arterial remodeling. FGF2 has been implicated as a mediator of flow-dependent vascular remodeling. In particular, FGF2 is upregulated in vascular cells following changes in blood flow (shear stress) and FGF2 upregulation precedes flow-induced artery

enlargement. Additionally, antibody neutralization of FGF2 reduced structural remodeling following chronic flow cessation. Based on this, experiments were designed to test the hypothesis that the absence of FGF2 would result in altered flow-dependent arterial remodeling. Chronically altered blood flow was used to study outward remodeling (high-flow induced) and inward remodeling (low-flow induced) in the carotid arteries of mice in the absence of FGF2. Vessel geometry and vascular cell turnover (proliferation and apoptosis) were analyzed during the remodeling response.

Specific Aim 2. Determine the role of FGF2 during ischemic revascularization. Endogenous FGF2 levels increase during ischemic revascularization and exogenous FGF2 is a potent stimulator of vascular growth and improves collateral flow in ischemic tissue. The ability of exogenous FGF2 to improve collateral-dependent flow may be due to increased collateral artery growth and/or improved vascular function given that vascular reactivity is enhanced in the collateral circulation of animals treated with FGF2. Given this, experiments were designed to test the hypothesis that FGF2 is essential during ischemic revascularization. A mouse model of hindlimb ischemia was used to evaluate revascularization. Hindlimb perfusion and vascular growth (angiogenesis, arteriogenesis and arteriole formation) were examined serially to define the role of FGF2 in these processes. This same model was used to evaluate vascular reactivity (by way of reactive hyperemia) during the revascularization process.

Specific Aim 3. Examine differential gene expression in the revascularizing hindlimb in the absence of FGF2. Gene expression in the ischemic hindlimb was examined in $Fgf2^{+/+}$ and $Fgf2^{-/-}$ using a cDNA microarray consisting of 15,000 clones. This was done in order to identify distinct gene expression patterns during revascularization in the presence and absence of endogenous FGF2. The overall goal of this comparison was to: (1) identify genes or pathways regulated by FGF2 during ischemic revascularization, (2) identify potential candidate molecules that may act to compensate for the absence of FGF2, and (3) identify the mechanism(s) of altered vascular reactivity in the FGF2 knockout hindlimb vasculature (observed in specific aim 2).

2. FLOW-DEPENDENT REMODELING IN THE CAROTID ARTERY OF FGF2 KNOCKOUT MICE*

*Portions of this chapter were published in Arteriosclerosis, Thrombosis, and Vascular Biology (Sullivan et al., 2002).

C.J. Sullivan, J.B. Hoying. Flow-Dependent Remodeling in the Carotid Artery of Fibroblast Growth Fatcor-2 Knockout Mice. *Arterioscler Thromb Vasc Biol.* 2002; 22(7): 1100-1105.

Introduction

Vascular remodeling is the structural reorganization of a vessel involving a variety of cell activities including proliferation, apoptosis, migration, and extracellular matrix restructuring (Gibbons et al., 1994; Langille, 1993; Ward et al., 2000b). Remodeling of the arterial wall occurs following chronic changes in blood pressure, blood flow and in response to vessel injury (Guyton et al., 1985; Kakuta et al., 1994; Korsgaard et al., 1993; Langille et al., 1986). Artery remodeling due to changes in blood flow (flow-dependent remodeling) occurs in both physiological (Langille, 1993; Miyachi et al., 2001) and pathological situations (Krams et al., 1998; Ward et al., 2000a; Ward et al., 2001; Wentzel et al., 2001). For example, studies show that endurance training can stimulate enlargement (outward remodeling) of the femoral artery in the trained legs, presumably due to flow-dependent remodeling (Dinenno et al., 2001; Miyachi et al.,

2001). In pathological settings, such as atherosclerosis and angioplasty, artery remodeling plays a critical role in the degree of vessel narrowing during plaque or lesion progression (Glagov et al., 1987; Kakuta et al., 1994; Mintz et al., 1996; Pasterkamp et al., 1995; Pasterkamp et al., 2000). It is thought that a chronic change in blood flow through the affected artery is a significant stimulus for the remodeling events in atherosclerotic vessels and post-angioplasty restenosis (Krams et al., 1998; Ward et al., 2000a; Ward et al., 2001; Wentzel et al., 2001). Studies in humans show that atherosclerotic peripheral and coronary arteries can undergo both compensatory vessel enlargement and vessel shrinkage (inward remodeling) at or near the site of plaque formation (Glagov et al., 1987; Pasterkamp et al., 1995; Pasterkamp et al., 2000; Smits et al., 1998). In addition to local remodeling at the lesion site, it is recognized that remote parts of the circulation affected by the progressing plaque may undergo remodeling due to altered hemodynamics (Kakuta et al., 1998; Langille, 1991). For example, with advanced obstructions or restenosis, adjacent arteries may shrink as flow becomes compromised (Kakuta et al., 1998; Langille, 1991). Conversely, lesion progression in one artery segment may cause compensatory enlargement of collaterals arteries as flow increases in the collateral segment (Langille, 1991; Shircore et al., 1995). Along these lines, a recent study reported that patients with unilateral internal carotid artery occlusion had reduced common carotid artery blood flow, which was associated with reduced common carotid artery diameter on the occluded side (Kubis et al., 2001). In contrast, the contralateral common carotid artery had increased blood flow and a larger diameter than control carotid arteries.

Acutely, changes in blood flow are sensed by the endothelium, which releases vasoactive factors to adjust lumen diameter thereby normalizing wall shear stress (Davies, 1995; Rubanyi et al., 1986). However, acute changes in blood flow result in only transient adjustments in vessel tone and diameter. Chronic changes in flow result in permanent structural remodeling of the vessel (Langille et al., 1989; Rudic et al., 2000) and this process is believed to be endothelium-dependent (Langille et al., 1986; Rudic et al., 1998; Tohda et al., 1992). Generally, increased blood flow leads to artery enlargement whereas blood flow reduction results in artery diameter reduction (Ben Driss et al., 1997; Kamiya et al., 1980; Kubis et al., 2001; Langille et al., 1986; Langille et al., 1989; Miyashiro et al., 1997; Tuttle et al., 2001).

The molecular mediators of vessel remodeling are still unclear. Fibroblast Growth Factor-2 (FGF2) is one molecule strongly implicated in flow-dependent remodeling. *Fgf2* mRNA expression is sensitive to alterations in fluid flow and shear stress (Malek et al., 1993) and FGF2 protein expression increases in the vascular wall during flow-induced arterial enlargement (Singh et al., 1998). In addition, antibody neutralization of endogenous FGF2 reduced inward remodeling in a mouse model of carotid artery flow cessation (Bryant et al., 1999). The specific function of FGF2 during these remodeling events is not clear. Previous studies suggest that FGF2 could possibly be affecting vascular cell turnover, gene expression, or matrix restructuring in the adapting vessel (Cai et al., 2000; Fox et al., 1996; Karsan et al., 1997; Kostyk et al., 1995; Lindner et al., 1991; Ziche et al., 1997).

A novel mouse model of vessel remodeling was used with *Fgf2* knockout mice (*Fgf2*$^{-/-}$) in order to test the hypothesis that FGF2 is required during flow-dependent, artery remodeling. This procedure induces both inward (low-flow induced) and outward remodeling (high-flow induced) in the left and right carotid arteries, respectively.

Methods

Experimental animals

Male *Fgf2*$^{+/+}$ and *Fgf2*$^{-/-}$ mice (Zhou et al., 1998), 50% Black Swiss and 50% 129 SV, were used for all experiments according to the University of Arizona IACUC approved procedures. All mice were genotyped by PCR using primers specific for the *Fgf2* wildtype allele (forward, 5'– GCTGTACACTCAAGGGGCTC –3'; reverse, 5'– CGCCGTTCTTGCAGTAGAG –3') and the *Fgf2* knockout allele (forward, 5'– TCCAAAGCCTGACTTGATCC –3'; reverse, 5'– CTGACTAGGGGAGGAGTAGAAGG –3'), following collection of genomic DNA from tail clips. Procedures were timed so that all mice were 8 weeks of age (± 4 days) at the time of sacrifice. Mice were anesthetized with 2.5% Avertin (2.5% 2,2,2-tribromoethanol, 2.5% tert-amyl alcohol in PBS: Aldrich) at a dose of 0.15 ml per 10 gram body weight injected intraperitoneally.

Surgery to induce flow-dependent carotid remodeling

The mouse model presented is a modification of procedures previously published for use in the rat (Miyashiro et al., 1997; Mondy et al., 1997). Mice were anesthetized and a midline incision was made along the neck. All branches originating from the left common carotid artery (LCCA), except for the left thyroid artery, were ligated (6.0 silk) in order to reduce flow in the LCCA and increase flow in the contralateral right common carotid artery (RCCA). Specifically, the distal portion of the left external carotid was

ligated where it bifurcates while the internal carotid and occipital arteries were ligated with a single suture at their origin (Figure 2.1). Mice were sacrificed at day 4, 7, and 28 following surgical ligation. Age- and sex-matched control animals were sacrificed without having undergone ligation.

Carotid artery blood flow

Carotid artery (RCCA and LCCA) blood flow was measured using an ultrasonic transit-time flowmeter (Transonic Systems, Inc.) with a 0.5 V-series probe as described previously (Rudic et al., 2000). Blood flow was evaluated in mice (n=3 per genotype) before ligation, immediately after ligation (day 0), and again at day 14 after ligation. Average volume flow (ml/min) was recorded for 5 min in each artery. The values presented are the average for the 5 min data acquisition period. After ligation of the LCCA branches, blood flow measurements were repeated after a stabilization period of at least 15 min. The incision was closed and mice were allowed to recover. After 14 days, the mice were reanesthetized and blood flow was evaluated for a final time.

Morphometry

Control (n=4 per genotype), day 7 (n=6 per genotype), and day 28 (+/+ n=7; -/- n=6) animals were perfusion-fixed through a polyethylene catheter placed in the left ventricle. Animals were perfused at constant pressure (90-100 mmHg) with 20 ml of heparinized PBS, followed by 10 ml of 10% phosphate buffered formalin. The neck, between the clavicle and mandible, was isolated and placed in fixative overnight. Neck

sections were then decalcified using Decalcifier I and II (Surgipath) for 24 hours each. Decalcified necks were processed, paraffin embedded, and serial sections cut (8 μm) for morphometric analysis. Cross sections of the entire neck were stained using hematoxylin. Morphometric analysis was carried out on the RCCA and LCCA of each animal from 2 whole-neck sections approximately 160-200 μm apart, cut at approximately the mid-portion of the common carotid artery. Digitized images were analyzed using image analysis software (Scionimage 4.0). The perimeter (length) of the lumen, internal elastic lamina (IEL), and external elastic lamina (EEL) were measured and these values were used to calculate various vessel dimensions, assuming the artery was a perfect circle (Kumar et al., 1997b; Rudic et al., 1998).

Angiography

Mice were anesthetized and subsequently overdosed with 2.5% Avertin following exposure of the thoracic cavity and heart. The arterial circulation was perfused (constant pressure of 90-100 mmHg) with PBS containing $1x10^{-5}$ mol/L sodium nitroprusside, followed by filling with contrast agent (barium sulfate 210% w/v, Liqui-Coat, Lafayette Pharmaceuticals, Inc) through a tapered polyethylene catheter (PE-90) inserted into the left ventricle. Angiograms of the head and neck region were obtained using a high-definition x-ray cabinet system (Faxitron).

Vascular cell proliferation and apoptosis

To examine proliferation, animals (n=3 per genotype) were injected with bromodeoxyuridine (BrdU: 30mg/kg body weight: Sigma Chemical Co., St.Louis, MO) i.p. at 24 hours and 12 hours prior to sacrifice on day 4 following LCCA surgery. Decalcification interfered with BrdU and TUNEL staining. So, mice were perfusion-fixed and the vertebrae along with all other bones were removed by careful dissection prior to paraffin embedding. BrdU incorporation into the nuclei of proliferating cells was identified on 6-μm sections(Couffinhal et al., 1998) using a peroxidase-conjugated sheep anti-BrdU antibody (Biodesign International, Kennebunk, ME). BrdU-positive nuclei were counted per two whole vessel transverse sections from each artery. Proliferation is expressed as the percentage of the total nuclei counted in the vessel cross-section that stain positive for BrdU. Apoptotic cells were identified using Boehringer-Mannheim's In Situ Cell Death Detection Kit. Apoptosis in each vessel was expressed as a percentage of total nuclei per vessel cross-section that are labeled as apoptotic. Calculations (e.g., proliferation index) were performed for the media (between the IEL and EEL), intima (lumen side of the IEL), and the whole vessel (intima + media).

Statistical analysis

Values are presented as the mean±SEM. Comparison between two means was done using Student's unpaired t-Test. Multiple groups were compared by One-Way ANOVA with a Student-Newman-Keuls Test (Sigma Stat 2.0, Jandel Scientific). Comparison of carotid artery blood flow, within a genotype, before and after ligation was

done using a One-Way Repeated Measures ANOVA with a Student-Newman-Keuls Test. Statistical significance was set at $P < 0.05$. Not significantly different, P=NS

Results

Carotid artery blood flow

Carotid artery blood flow was evaluated in the LCCA and the RCCA (Figure 2.2; Table 2.1). Acutely, the procedure significantly reduced flow in the LCCA (decreased by >80%) and significantly increased flow in the contralateral right common carotid artery (RCCA, increased by >40%). These changes persisted by day 14 following the LCCA surgery. Blood flow values were not significantly different between $Fgf2^{+/+}$ and $Fgf2^{-/-}$ mice. Similar to previously published data (Rudic et al., 2000), ligation of just the left external carotid artery caused only a modest decrease in LCCA blood flow (≈30% reduction versus 80% in our study) and resulted in no change in blood flow within the contralateral RCCA (data not shown).

Flow-dependent arterial remodeling

At day 7 and day 28 following surgery, in both $Fgf2^{+/+}$ and $Fgf2^{-/-}$ mice, the low-flow LCCA inward remodeled whereas the high-flow RCCA outward remodeled (Figure 2.3; Tables 2.2 & 2.3). Photography and angiograms of the carotid circulation at day 28 after LCCA surgery show that remodeling appears to take place along the entire length of the common carotid artery (Figure 2.4). In $Fgf2^{+/+}$ mice the diameter changes observed at day 28 corresponded to a 47% decrease in LCCA lumen area and an increase of 33% in RCCA lumen area (Table 2.2). Equivalent changes were observed in the day 28 remodeled arteries of $Fgf2^{-/-}$ mice, showing a 50% decrease in LCCA lumen area and an

increase of 42% in RCCA lumen area (Table 2.3). There were no statistically significant differences in the various vessel dimensions examined between the remodeled arteries of $Fgf2^{+/+}$ and $Fgf2^{-/-}$ mice at any of the time points examined. Medial cross-sectional area (CSA) and medial thickness were not different between $Fgf2^{+/+}$ and $Fgf2^{-/-}$ mice (Tables 2.2 & 2.3). No significant changes in lumen diameter were observed at day 4 in high-flow or low-flow arteries versus control. However, there was a noticeable trend towards a reduced diameter in the LCCA and an increased diameter in the RCCA even at this early time point (Tables 2.2 & 2.3). Perfusion with PBS containing $1x10^{-5}$ mol/L sodium nitroprusside to maximally dilate the carotid vessels prior to fixation demonstrated no diameter differences versus perfusion with PBS without vasodilator at both day 7 and day 28 (data not shown). This suggests that the changes in diameter are structural rather than simply alterations in vascular tone. Examination of serial sections showed no intimal lesion formation (neointima) in day 28 mice (Figure 2.3). A single $Fgf2^{+/+}$ mouse (and no $Fgf2^{-/-}$ mice) examined at day 7 (out of 6 total) had a small intimal lesion. Serials sections showed that the intimal lesion in this mouse was not present along the entire length of the vessel.

Vascular cell turnover

Examining the TUNEL index in the medial layer of day 4 remodeled vessels showed increased apoptosis in both the RCCA and LCCA. Concomitantly, changes in the BrdU index showed an increased rate of cell proliferation in both remodeled arteries at day 4 (Figure 2.5). The single intimal cell layer displayed similar changes in cell turnover

(data not shown) and positive BrdU and TUNEL staining can be seen on the lumen side of the IEL at day 4 (Figure 2.5). To determine the net change in smooth muscle cell number we counted the total nuclei per medial cross section at day 28. This showed a significantly reduced medial cell count at day 28 in the low flow LCCA of both genotypes (Figure 2.6). However, medial cell density did not change in the day 28 remodeled arteries. The RCCA showed a trend of increased medial cell number at day 28 in both genotypes, but this difference was not significant. No differences were observed between *Fgf2*$^{+/+}$ and *Fgf2*$^{-/-}$ mice.

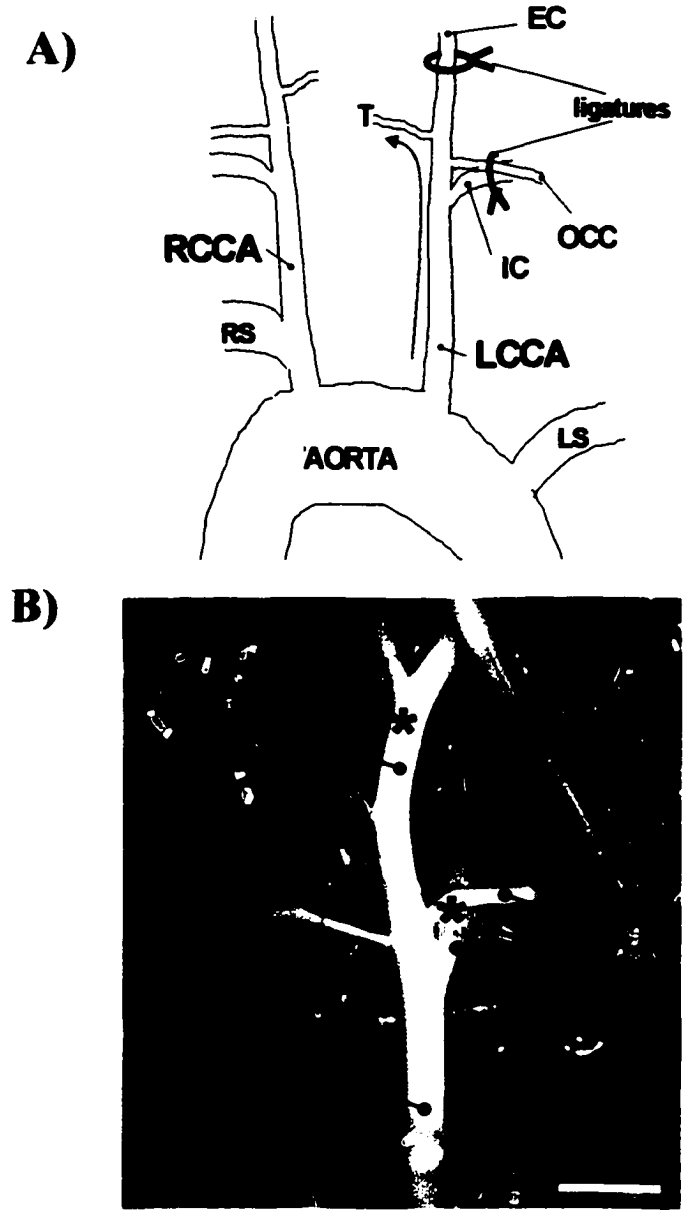

Figure 2.1 A) Diagram of left common carotid artery (LCCA) and its branches including the external carotid artery (EC), internal carotid artery (IC), occipital artery (OCC), and left thyroid artery (T). To alter flow, the EC, IC, and OCC were permanently. A single ligature was used to occlude both the IC and OCC. B) Photograph of LCCA and its branches. To alter flow, the EC, IC, and OCC were permanently ligated at positions indicated by an asterisk (*). The arterial circulation was filled with a white contrast agent (barium sulfate) to improve visualization for this photo.

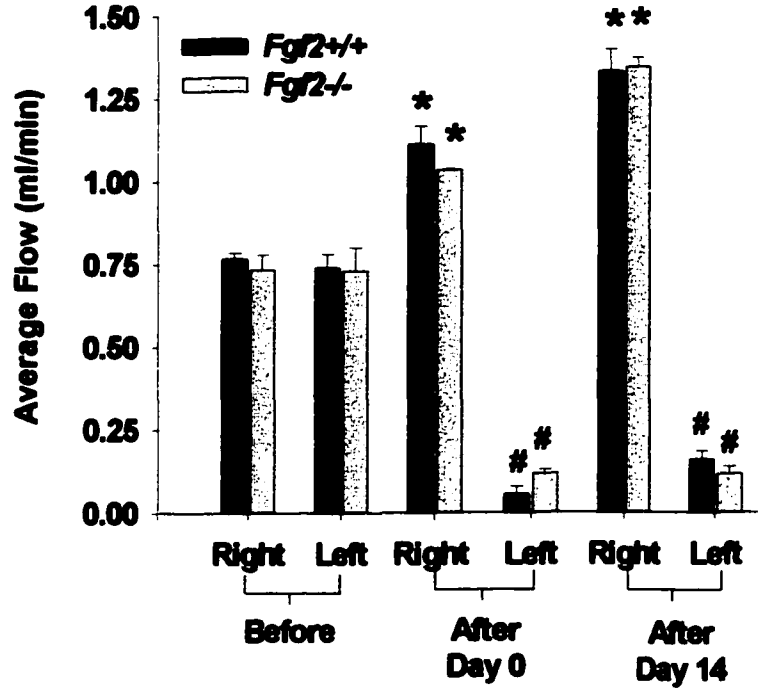

Figure 2.2 Average blood flow (ml/min) in the LCCA and RCCA of *Fgf2*+/+ (n=3) and *Fgf2*-/- (n=3) mice before ligation of LCCA branches, immediately after the ligations (day 0), and again at 14 days after the ligations (day 14). **P*<0.05 vs respective control (before) values. *P*=NS for *Fgf2*+/+ vs *Fgf2*-/-.

Table 2.1 Blood flow changes before and after ligation of LCCA branches in *Fgf2*+/+ and *Fgf2*-/- mice.

	Control		Day 0		Day 14	
	Right	**Left**	**Right**	**Left**	**Right**	**Left**
Fgf2+/+ (n)	0.77 ± 0.02 (3)	0.74 ± 0.04 (3)	1.11 ± 0.05* (3)	0.06 ± 0.02* (3)	1.33 ± 0.07* (3)	0.16 ± 0.03* (3)
Fgf2-/- (n)	0.73 ± 0.05 (3)	0.73 ± 0.07 (3)	1.03 ± 0.01* (3)	0.12 ± 0.01* (3)	1.34 ± 0.03* (3)	0.12 ± 0.02* (3)

*$P<0.05$ vs respective control (before) values. *Fgf2*+/+ vs *Fgf2*-/-, P=NS. Average blood flow (ml/min) in the LCCA (left) and RCCA (right) of *Fgf2*+/+ and *Fgf2*-/- mice before ligation of LCCA branches, immediately after the ligations (day 0), and again at 14 days after the ligations (day 14). Values are mean ± SEM.

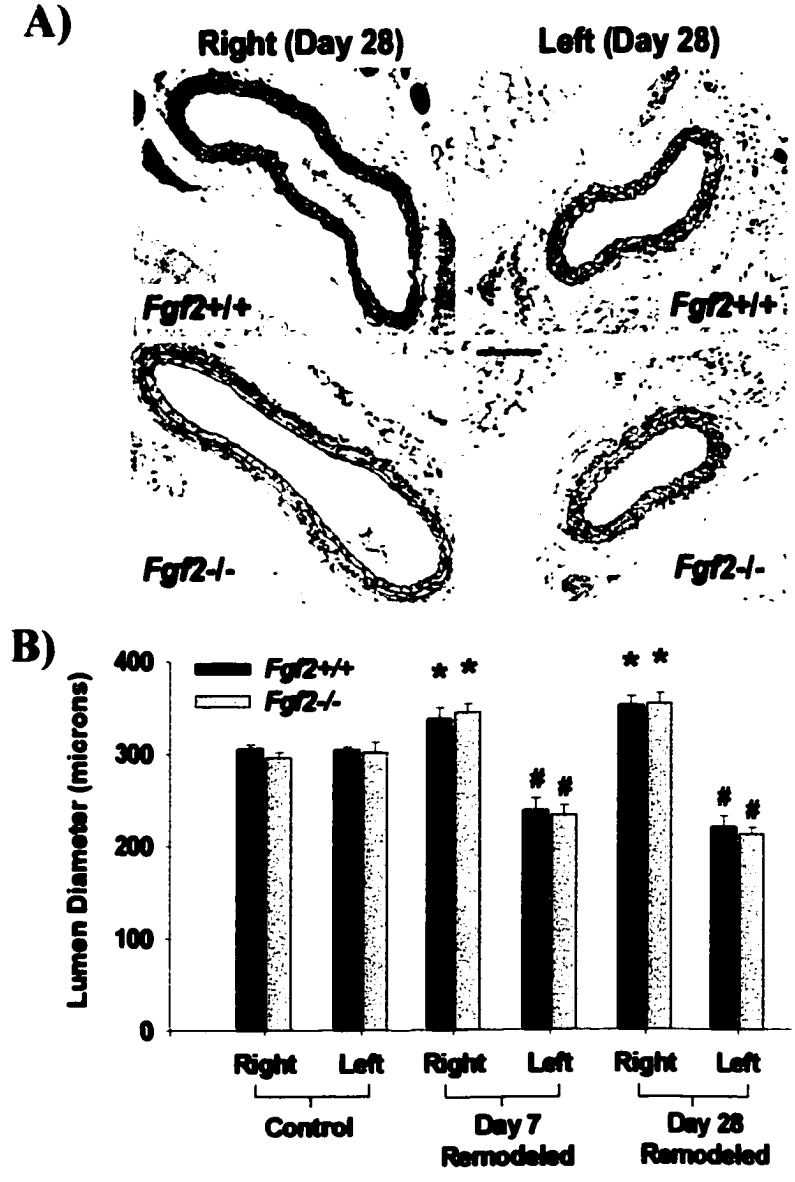

Figure 2.3 A) Representative photomicrographs of carotid artery cross-sections from *Fgf2*+/+ and *Fgf2*-/- mice showing day 28 flow remodeled arteries stained with hematoxylin. RCCA and LCCA images are from the same histology section (i.e., a single cross-section from an individual animal). Scale bar equals 100μm. B) Lumen diameter (μm) of control, day 7, and day 28 arteries. Lumen diameter was calculated using the measured lumen perimeter and assuming the artery was a circle. **P*<0.05 and #*P*<0.01 vs respective control. *P*=NS for *Fgf2*+/+ vs *Fgf2*-/-.

Table 2.2 Time course of arterial remodeling in *Fgf2*+/+ mice following ligation of the left common carotid artery (LCCA) branches.

Fgf2+/+	**Control**		**Day 4**		**Day 7**		**Day 28**	
	Right	**Left**	**Right**	**Left**	**Right**	**Left**	**Right**	**Left**
(n)	(4)	(4)	(8)	(8)	(6)	(6)	(7)	(7)
IEL Perimeter (μm)	961 ± 14	957 ± 8	990 ± 28	855 ± 35	1061 ± 39	775 ± 40	1106 ± 28	691 ± 37
EEL Perimeter (μm)	1073 ± 21	1069 ± 15	1099 ± 26	1018 ± 38	1200 ± 39	941 ± 42	1211 ± 34	821 ± 33
Lumen Diameter (μm)	306 ± 4	305 ± 3	315 ± 9	270 ± 11	338 ± 12	238 ± 13	352 ± 9	220 ± 12
Vessel Diameter (μm)	342 ± 7	340 ± 5	350 ± 8	324 ± 12	382 ± 13	299 ± 13	385 ± 11	262 ± 11
Lumen Area (μm^2)	73460 ± 2150	72870 ± 1258	78384 ± 4460	58879 ± 4605	90186 ± 6478	45193 ± 5332	97796 ± 4979	38665 ± 3912
Vessel Area (μm^2)	91789 ± 3517	90959 ± 2627	96554 ± 4728	83217 ± 6012	115195 ± 7430	71100 ± 6283	117251 ± 6590	54238 ± 4266
Medial Area (μm^2)	18328 ± 1371	18089 ± 1454	18170 ± 621	24339 ± 3118	25010 ± 3820	22675 ± 2159	19455 ± 1855	15573 ± 763
Medial Thickness (μm)	18 ± 1	18 ± 1	17 ± 1	26 ± 3	22 ± 3	26 ± 2	17 ± 1	21 ± 1

Table 2.3 Time course of arterial remodeling in *Fgf2-/-* mice following ligation of the left common carotid artery (LCCA) branches.

Fgf2-/-	**Control**		**Day 4**		**Day 7**		**Day 28**	
(n)	**Right** (4)	**Left** (4)	**Right** (8)	**Left** (8)	**Right** (6)	**Left** (6)	**Right** (6)	**Left** (6)
IEL Perimeter (μm)	931 ± 19	949 ± 35	985 ± 19	847 ± 28	1084 ± 29	732 ± 31	1113 ± 32	667 ± 22
EEL Perimeter (μm)	1033 ± 18	1052 ± 34	1091 ± 17	1022 ± 37	1191 ± 37	874 ± 18	1225 ± 33	812 ± 19
Lumen Diameter (μm)	296 ± 6	302 ± 11	314 ± 6	269 ± 9	345 ± 9	233 ± 10	354 ± 10	212 ± 7
Vessel Diameter (μm)	329 ± 6	334 ± 11	347 ± 6	325 ± 12	379 ± 12	278 ± 6	390 ± 11	258 ± 6
Lumen Area (μm^2)	68979 ± 2737	71870 ± 5201	77372 ± 2917	57441 ± 3628	93813 ± 5070	43025 ± 3683	98952 ± 5795	35604 ± 2261
Vessel Area (μm^2)	85004 ± 3022	88325 ± 5642	94794 ± 3010	83883 ± 6288	113492 ± 7202	60872 ± 2541	119796 ± 6432	52548 ± 2415
Medial Area (μm^2)	16025 ± 342	16545 ± 696	17422 ± 573	23602 ± 2258	19679 ± 2336	17848 ± 1620	20844 ± 1994	16945 ± 1520
Medial Thickness (μm)	16 ± 1	17 ± 1	17 ± 1	25 ± 2	17 ± 2	23 ± 3	18 ± 2	23 ± 2

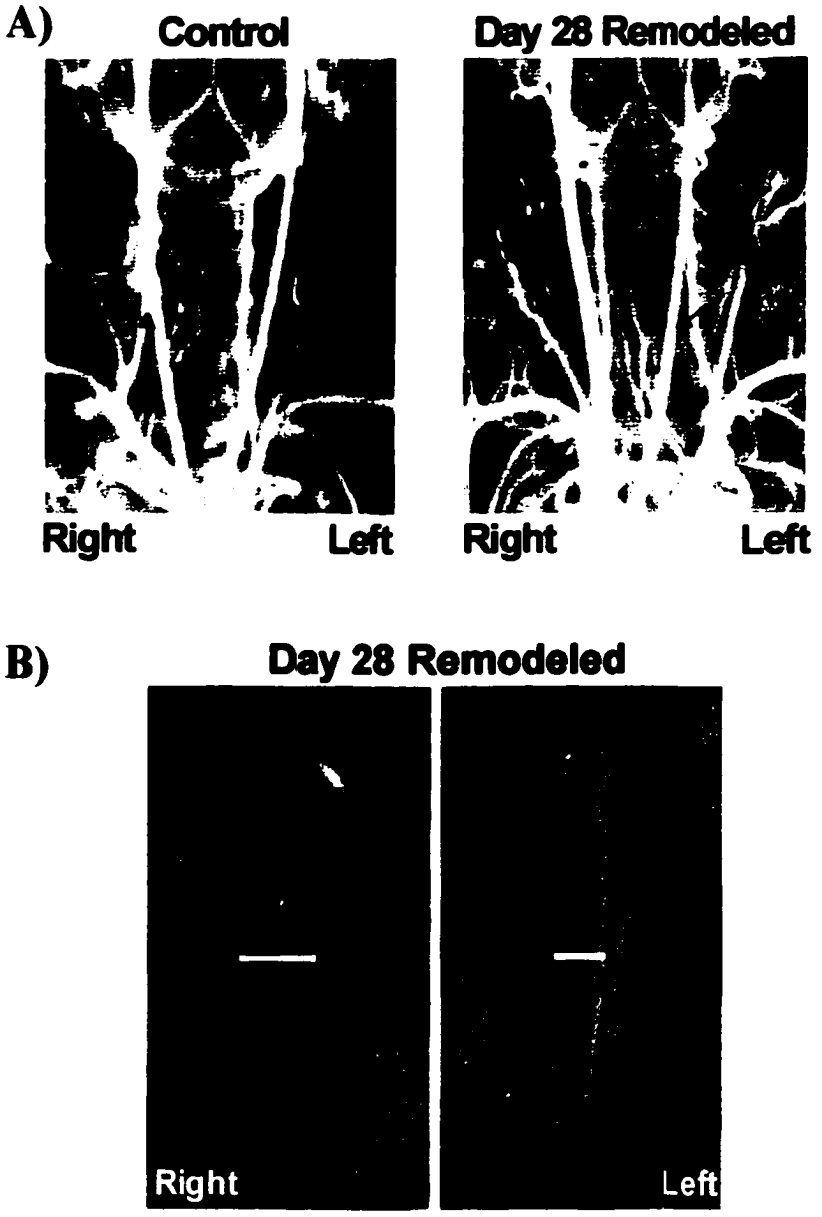

Figure 2.4 A) Representative angiograms of neck circulation from control and day 28 remodeled wildtype mice. The arrows indicate the common carotid artery. B) Photograph of the RCCA and LCCA from a day 28 remodeled wildtype mouse.

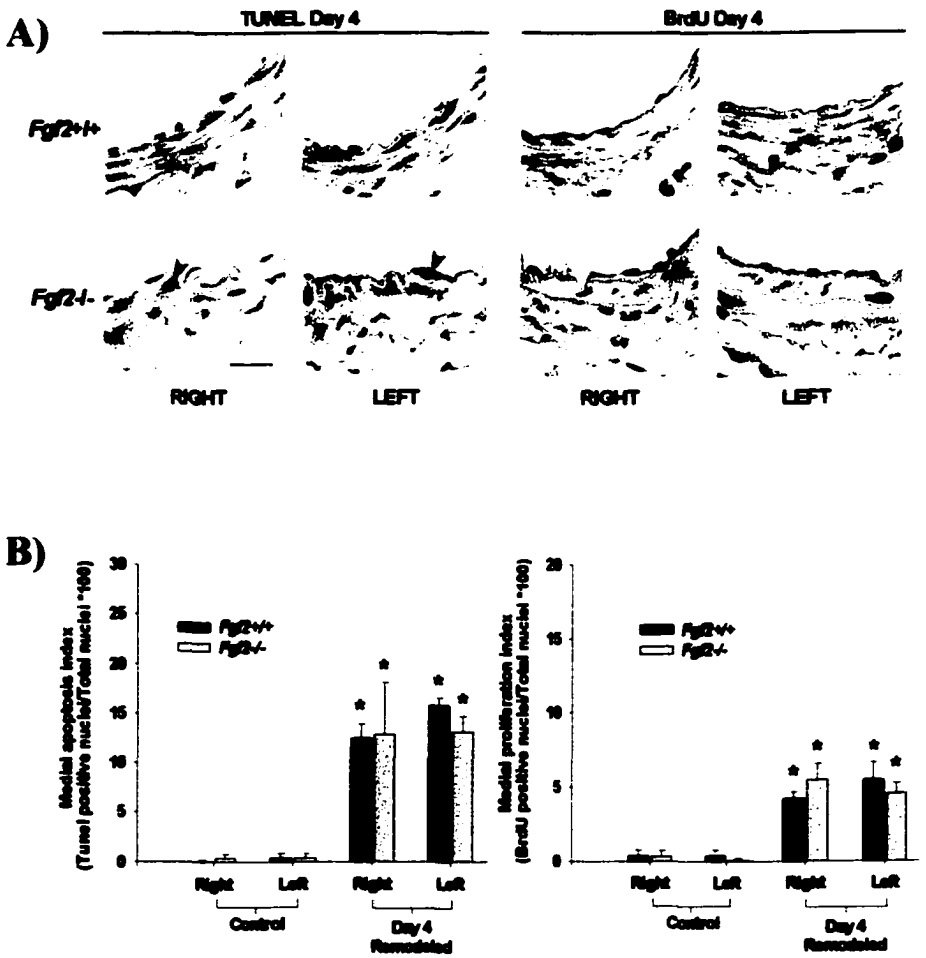

Figure 2.5 A, Representative photomicrographs of carotid artery cross-sections at day 4 after ligation of LCCA branches stained for TUNEL (apoptosis) or BrdU (proliferation) and counterstained with hematoxylin. Scale bar equals 25μm. B, Quantification of medial cell apoptosis and proliferation for control and day 4 remodeled vessels. **P*<0.05 vs respective control. *P*=NS for *Fgf2*+/+ vs *Fgf2*-/-.

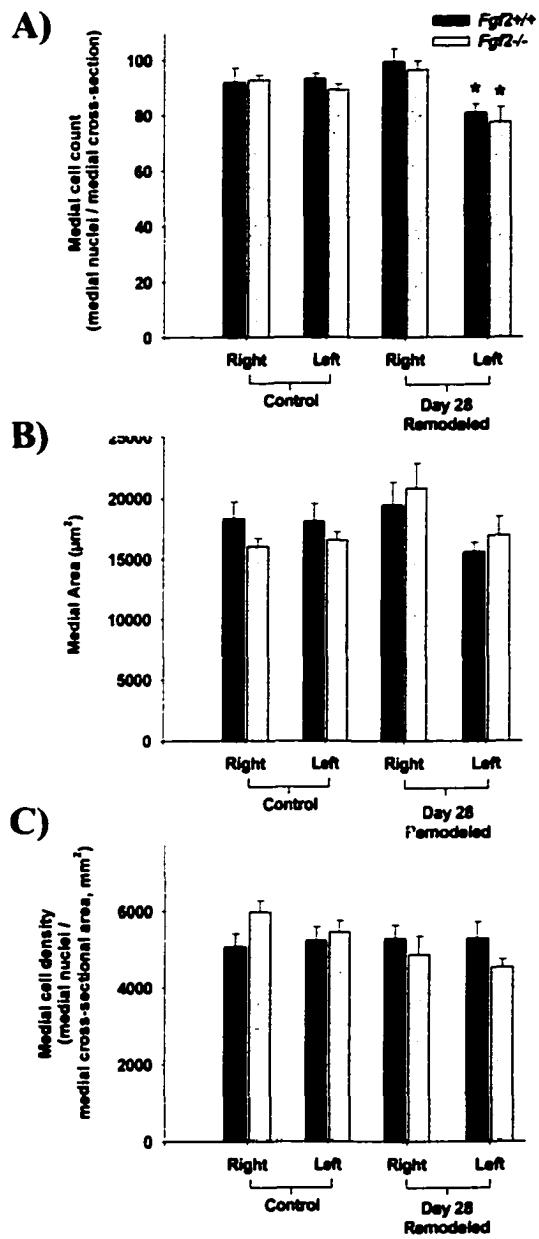

Figure 2.6. A) Medial cell count, equal to number of nuclei per medial cross section, for control and day 28 remodeled LCCA and RCCA. B) Medial area (cross-sectional) calculated for control and day 28 remodeled arteries. C) Medial cell density for control and day 28 remodeled arteries. Medial cell density was expressed as number of medial cells per medial cross-sectional area (mm^2) *$P<0.05$ vs respective control. P=NS for *Fgf2*+/+ vs *Fgf2*-/-.

Discussion

Previous studies have implicated FGF2 in a wide variety of vascular cell signaling processes, including proliferation, differentiation, and migration (Bikfalvi et al., 1997). Specific to flow-dependent remodeling, arterial endothelial cells upregulate *Fgf2* mRNA levels in response to fluid shear stress (Malek et al., 1993) and FGF2 expression increases in the vascular wall during flow-induced arterial enlargement (Singh et al., 1998). In addition, FGF2 regulates the expression of molecules involved in extracellular matrix remodeling (Ziche et al., 1997), which is an important component of arterial wall reorganization (Gibbons et al., 1994; Langille, 1993). Furthermore, FGF2 is also thought to be an important regulator of endothelial cell and smooth muscle cell proliferation (Gospodarowicz et al., 1988; Itoh et al., 1992; Lindner et al., 1990; Lindner et al., 1991) and apoptosis (Fox et al., 1996; Karsan et al., 1997; Kondo et al., 1994). The most direct evidence to date supporting a role for FGF2 in arterial remodeling is the attenuation of inward remodeling by antibody neutralization of endogenous FGF2 in a mouse model of carotid artery flow cessation (Bryant et al., 1999). Despite this large body of evidence, we did not to observe an essential role of FGF2 in flow-dependent carotid artery remodeling given the equivalent remodeling responses of $Fgf2^{+/+}$ and $Fgf2^{-/-}$ mice. Thus, the results of the present study do not support the hypothesis that FGF2 is required for large artery restructuring in response to chronically decreased or increased blood flow.

The apparent contradiction between our results and the previous study in which antibodies to FGF2 attenuated inward remodeling following complete LCCA ligation in mice (Bryant et al., 1999) may simply be due to the differences between the two models

(flow cessation versus low-flow remodeling) and the distinct stimuli present in each model. In the flow cessation model, originally published by Kumar and Lindner, net forward blood flows is completely interrupted resulting in blood stasis in the LCCA (Kumar et al., 1997b). By contrast, our procedures cause substantial blood flow reduction, but forward flow is maintained within the LCCA via the patent thyroid artery. Following complete ligation, a gradient of increased intimal lesion formation is observed towards the clotted ligation site (Kumar et al., 1997b). Depending on the strain used, varying amounts of neointimal lesion formation and/or inward remodeling are observed in the ligated artery (Harmon et al., 2000). Also, it was reported that the endothelial layer, although intact, detaches from the IEL in the ligated LCCA (Kumar et al., 1997b). This exposes the highly thromobogenic extracellular matrix and may increase activation of blood components such as platelets (Harmon et al., 2000). The possibility exists that additional factors, not present in the low-flow situation, contribute to the carotid artery responses induced by complete flow cessation. Platelet activation, hypoxia, metabolite accumulation, and/or inflammation could potentially influence the remodeling response in the completely ligated artery (Harmon et al., 2000; Kawasaki et al., 2001; Kumar et al., 1997a). Such a stimulus, possibly unique to the no-flow condition, may require FGF2 signaling to induce inward remodeling. Alternatively, animals with a chronic gene ablation (e.g., knockout mice) and animals with an acute loss of a gene product (e.g., antibody neutralization) may simply have different responses to a given stimulus. Lastly, it is possible that FGF2 neutralizing antibodies are cross-reacting with other fibroblast

growth factors (FGF) given that there are at least 22 known FGF family members (Yamashita et al., 2000).

The changes in flow and the resulting carotid remodeling observed in our studies are comparable to prior studies in the rat (Miyashiro et al., 1997; Mondy et al., 1997), but different than a previous study in the mouse in which blood flow was only moderately reduced and the LCCA diameter decreased by just 8-10% (Rudic et al., 1998; Rudic et al., 2000). The LCCA branch ligations, performed in our study, reduced flow in the LCCA by approximately 80% while increasing the contralateral RCCA flow by 40%. The comparable procedures in the rat reduced LCCA flow by 90% and increased RCCA flow by 45% (Miyashiro et al., 1997). These flow changes in the rat caused a 16% reduction in LCCA outer diameter and an 11% increase in RCCA outer diameter after 4 weeks of remodeling. In comparison, wildtype mice in our study showed an approximately 23% reduction in LCCA vessel diameter and a 13% increase in RCCA vessel diameter at day 28. In rabbits, ligation of the left external carotid (EC) artery decreased LCCA blood flow by 70% causing a 21% reduction of LCCA lumen diameter after 2 weeks (Langille et al., 1986). Overall, our results in the mouse are consistent with previous studies of flow-dependent remodeling in other species demonstrating that chronically increased blood flow leads to artery enlargement (outward remodeling) whereas blood flow reduction results in artery narrowing (inward remodeling) (Buus et al., 2001; Kamiya et al., 1980; Langille et al., 1989; Miyashiro et al., 1997).

Associated with structural remodeling in this model is increased vascular cell turnover as indicated by increased apoptosis and proliferation in both the low-flow LCCA

and the high-flow RCCA early in the remodeling process. Previous investigators have observed increased BrdU labeling and increased apoptosis in vessels following chronic flow reduction (Buus et al., 2001; Mondy et al., 1997; Rudic et al., 2000). Similar to others, we demonstrate a net loss of vascular cells after chronic flow reduction in the mouse (Rudic et al., 1998). Specifically, we observed a reduced medial smooth muscle cell count in the low-flow LCCA at day 28. However, medial smooth muscle density remained unchanged due to the noticeable trend towards reduced medial CSA in the LCCA. In the high-flow RCCA both apoptosis and proliferation increased but there was not a significant change in medial cell count, density, or CSA versus control. A study of flow remodeling in the rat mesentery showed increased apoptosis and proliferation occurred simultaneously in high-flow exposed resistance arteries, and this was coupled to an increase in medial CSA of high-flow arteries (Buus et al., 2001). Miyashiro et al. showed no change in medial CSA in the low-flow carotid artery of juvenile rats while the high-flow carotid artery had increased medial CSA (Miyashiro et al., 1997). Taken as a whole, our results are in agreement with the concept that chronic changes in blood flow result in dynamic changes in vascular cell turnover (Langille, 1993; Miyashiro et al., 1997), though we observed a constancy in medial cell density in both flow conditions.

The specific molecules regulating vascular cell growth or apoptosis during flow remodeling are largely unknown. Carotid arteries of *eNOS*$^{-/-}$ mice subjected to chronically reduced flow showed increased vascular cell proliferation and cell number versus *eNOS*$^{+/+}$ mice (Rudic et al., 1998). Thus, endothelial derived nitric oxide (NO) may be an essential controller of vascular cell turnover during flow-dependent carotid

remodeling. Previous studies show that FGF2 can mediate endothelial cell and smooth muscle cell proliferation (Gospodarowicz et al., 1988; Itoh et al., 1992; Lindner et al., 1990; Lindner et al., 1991) and apoptosis (Fox et al., 1996; Karsan et al., 1997; Kondo et al., 1994). Interestingly, FGF2 has been shown to stimulate *eNOS* mRNA expression and eNOS protein production in cultured endothelial cells (Babaei et al., 1998; Kostyk et al., 1995). Also, it has been shown that NO promotes proliferation of *in vitro* endothelial cells through endogenous FGF2 (Ziche et al., 1997). However, there was no difference between $Fgf2^{+/+}$ and $Fgf2^{-/-}$ mice in our study that would indicate that vascular cell turnover was affected by lack of FGF2. Thus, FGF2 does not appear to be an essential mediator acting upstream or downstream of NO signaling in this model. In terms of vascular cell proliferation, it was previously shown that the carotid arteries of $Fgf2^{-/-}$ mice undergo a normal hyperplastic response following intra-arterial mechanical injury (Zhou et al., 1998). Also, intimal area and cellularity were not affected by FGF-2 antibody in the ligated mouse carotid artery, suggesting that smooth muscle proliferation was not altered by FGF2 neutralization (Bryant et al., 1999).

Overall, the apparently normal remodeling responses observed in $Fgf2^{-/-}$ mice may reflect compensation for the loss of FGF2 by another gene product. There are numerous FGF family members and these proteins bind to a common group of receptors, although with differing affinities (Bikfalvi et al., 1997). Thus, it is possible that one or more FGF proteins could be compensating for the disruption of the *Fgf2* gene. Recently, a double knockout of FGF1 and FGF2 was shown to have the same phenotype as $Fgf2^{-/-}$ mice (Miller et al., 2000). This suggests that FGF1, the most closely related FGF family

member to FGF2, is not compensating for the loss of FGF2 in situations such as development and wound healing (Miller et al., 2000). On the other hand, it is possible that there is not compensation and other growth factors or molecules may be the actual endogenous mediators of processes currently ascribed to FGF2 (e.g., flow-dependent remodeling). In this regard, changes in FGF2 expression may be mediating some other event during arterial remodeling which is either unrelated or not critical for structural changes in the artery.

It is important to note that considerable strain variability in the vascular responses of mice to various challenges has been described (Harmon et al., 2000; Rohan et al., 2000). Investigators using the LCCA flow cessation model in mice, demonstrated a large degree of strain-dependent variability in carotid remodeling of the ligated LCCA (Harmon et al., 2000). Additionally, they showed that not all strains displayed significant outward remodeling of the contralateral RCCA. Others using the flow cessation model observed no RCCA enlargement despite measuring a near doubling of RCCA blood flow in 129 SV mice (Schiffers et al., 2000). Thus, it is reasonable to expect that there might be strain-specific differences in the extent and character of vessel remodeling using the model presented in our study. In preliminary experiments, we noted that the LCCA and RCCA carotid arteries of FVB/NJ and C57BL/6J mice remodeled to a similar extent as observed in the *Fgf2*$^{+/+}$ and *Fgf2*$^{-/-}$ mice, which are on a mixed background of 50% Black Swiss and 50% 129 SV (data not shown). These other strains showed inward remodeling with minimal neointimal lesion formation in the LCCA. When a neointima was observed in these mice, it was typically only 2-3 cell layers thick (data not shown). We also noticed

strain-dependent variations in the carotid artery architecture (i.e., position of branching vessels).

Conclusion

This study describes a model of bi-lateral carotid remodeling in the mouse. In a single mouse, the simultaneous reduction in blood flow in the LCCA and increase in blood flow in the RCCA provides a powerful research tool to effectively examine the molecular mechanisms of artery remodeling. With this model, we show that lack of FGF2 does not affect structural remodeling of large arteries in response to chronically altered blood flow. FGF2 appears dispensable during flow-dependent remodeling of the artery wall and does not significantly regulate vascular cell turnover in this model.

3. TARGETED DISRUPTION OF THE FGF2 GENE DOES NOT AFFECT VASCULAR GROWTH IN THE MOUSE ISCHEMIC HINDLIMB*

*Portions of this chapter have been submitted for publication in the Journal of Applied Physiology (Sullivan et al., 2002).

C.J. Sullivan, T. Doetschman, J.B. Hoying. Targeted Disruption of the *Fgf2* Gene Does Not Affect Vascular Growth in the Mouse Ischemic Hindlimb. *J Appl Physiol.* In press.

Introduction

The prevalence of ischemic disease in the heart and limbs has lead to extensive investigation in the area of therapeutic blood vessel growth (Isner et al., 1998). Much of the research in this area has focused on the use of growth factors to induce or augment the body's naturally occurring revascularization process (Simons et al., 2000). Despite the recent work in this field, much remains unanswered in regard to the basic biological events of vessel growth in the adult organism. Importantly, the specific roles of endogenously produced growth factors in ischemic revascularization, the very same molecules used therapeutically, remain largely unknown.

Spontaneously occurring revascularization, as a consequence of arterial occlusion, is characterized by significant vascular adaptation including both angiogenesis and arteriogenesis (Hershey et al., 2001; Ito et al., 1997). Angiogenesis refers to the growth of capillaries via endothelial cell sprouting whereas arteriogenesis refers to the growth and

remodeling of preexistent arterial vessels into functional collateral arteries (Ito et al., 1997). The endogenous mediators of these processes are only beginning to be identified. Vascular endothelial growth factor (VEGF) appears to be a major regulator of ischemia-induced angiogenesis (Couffinhal et al., 1998) and endothelial nitric oxide synthase (eNOS) may be required for both angiogenesis and arteriogenesis during peripheral revascularization (Murohara et al., 1998; Tamarat et al., 2002). In addition, a host of other molecules have been implicated in angiogenesis and arteriogenesis, including fibroblast growth factor-2 (FGF2 or bFGF), tumor necrosis factor-α (TNF-α), monocyte chemocattractant protein-1 (MCP-1), and transforming growth factor-β1 (TGF-β1) (Arras et al., 1998; Hoefer et al., 2001; van Royen et al., 2002; Walgenbach et al., 1995; Yang et al., 1996).

In particular, FGF2 upregulation parallels vessel growth and improved blood flow in models of hindlimb arterial occlusion (Arras et al., 1998; Chleboun et al., 1994) and myocardial ischemia (Cohen et al., 1994). Increased expression of FGF2 colocalizes to growing and newly formed microvascular segments in or around ischemic tissues (Bush et al., 1998; Walgenbach et al., 1995). Additionally, exogenous FGF2, a potent vascular cell mitogen, enhances angiogenesis and arteriogenesis in animal models of peripheral arterial occlusion (Baffour et al., 1992; Bush et al., 1998; Yang et al., 1996). Lastly, in experimental models of angiogenesis, addition of FGF2 upregulated VEGF expression in capillary vascular cells (Seghezzi et al., 1998) and modulated remodeling of the microvascular tree (Parsons-Wingerter et al., 2000).

Given these observations, it is often assumed that endogenous FGF2 is a required mediator of vascular growth and adaptation during ischemic revascularization. However, these studies do not definitively identify FGF2 as the natural mediator of these processes in vivo because they are based largely on application of exogenous FGF2 or monitoring of endogenous FGF2 expression. Thus, a model of hindlimb ischemia was used to compare the responses of mice lacking FGF2 ($Fgf2^{-/-}$) and wildtype mice ($Fgf2^{+/+}$) to directly examine the importance of FGF2 during revascularization. Angiogenesis, arteriogenesis, and the recovery of hindlimb perfusion were evaluated to determine the specific role of endogenous FGF2 in this model.

Methods

Experimental animals

Male and female *Fgf2*$^{+/+}$ and *Fgf2*$^{-/-}$ mice (Zhou et al., 1998) (8-12 weeks of age, 50% Black Swiss and 50% 129 SV) were used for all experiments according to the University of Arizona IACUC approved procedures. All mice were genotyped by PCR using primers specific for the *Fgf2* wildtype allele (forward, 5'– GCTGTACACTCAAGGGGCTC –3'; reverse, 5'– CGCCGTTCTTGCAGTAGAG –3') and the *Fgf2* knockout allele (forward, 5'– TCCAAAGCCTGACTTGATCC –3'; reverse, 5'– CTGACTAGGGGAGGAGTAGAAGG –3'), following collection of genomic DNA from tail clips. Note that equal numbers of male and female mice were included in each experimental group. Mice were anesthetized with 2.5% Avertin (2.5% 2,2,2-tribromoethanol, 2.5% tert-amyl alcohol in PBS: Aldrich) at a dose of 0.15 ml per 10 gram body weight injected intraperitoneally.

Hindlimb ischemia

The model used to produce hindlimb ischemia has been described previously (Murohara et al., 1998). To reduce flow to the left hindlimb, we ligated and and excised a portion of the left femoral circulation (both artery and vein). The proximal femoral ligation was made upstream to the medial circumflex femoral artery and the popliteal artery branches. The distal ligation was made in the saphenous artery and vein midway between the ankle and knee. Care was taken to leave the femoral nerve undamaged. Skin

incisions were closed with 7.5 mm Michel suture clips and 7.0 prolene non-absorbable suture (Ethicon). See Appendix X for detailed description of the hindlimb surgery.

Fgf2 transcript levels in ischemic hindlimb (RT-PCR)

Tissue (≈100 mg) from the calf of ischemic and contralateral (non-ischemic) hindlimbs of $Fgf2^{+/+}$ and $Fgf2^{-/-}$ mice was harvested at days 3, 7, and 14 following surgery (n=2 for each time point). The tissue was immediately homogenized in RNAzol B (Tel-Test Inc) for RNA extraction per manufacturer's instructions. Equal amounts (1 μg) of total RNA from each sample were reverse transcribed into first strand cDNA using Superscript Reverse Transcriptase (Gibco BRL). *Fgf2* and *Gapdh* transcripts were amplified by PCR in separate 100 μl reactions (Zhou et al., 1998). Aliquots of 20 μl were withdrawn at sequential cycles during the PCR reaction for evaluation.

Laser Doppler perfusion imaging (LDPI)

Hindlimb perfusion was measured using a laser Doppler perfusion imager (PIM II, Lisca AB/ Perimed) (Couffinhal et al., 1998; Wardell et al., 1993). Laser Doppler perfusion imaging (LDPI) extends early laser Doppler flowmetry technology to two-dimensional mapping of blood flow in tissues and organs. With this method, relative perfusion values are given through detection of blood cell movement in the tissue by analyzing the Doppler shift of backscattered light originating from a laser light source. More specifically, the LDPI system utilizes a low power 670 nm solid-state laser to non-invasively scan the tissue surface in a stepwise manner. At each sequential measurement

site (up to 4,096 measurement sites per scan) the laser light covers a 1 mm^2 surface area and penetrates the tissue to an approximate depth of 1 mm, thus giving a tissue volume of 1 mm^3. The system senses both the average Doppler frequency (average velocity of red blood cells) and the magnitude of the Doppler signal (which relates to the number of red blood cells) within the tissue volume. The output signal scales linearly with the product of this velocity and number of red blood cells within the scanned tissue, thus providing a unit-less perfusion value. The developers of this technology used a flow simulator to verify the linear relationship between LDPI perfusion values and the product of red cell velocity and concentration (Wardell et al., 1993). Since the optical properties of biological tissue differ from those of the flow model tested, no absolute calibration (e.g., in terms of ml blood / 100 g tissue / min) can be made using the LDPI system.

Perfusion was evaluated before (control) and immediately after surgery (day 0) as well as serially at days 3, 7, 14, 21, 28 and 35 following induction of ischemia ($Fgf2^{+/+}$, n=4: $Fgf2^{-/-}$, n=4). For LDPI measurements, mice were kept on a heating pad maintained at 37°C for 10 min prior to scanning, as well as during scanning, to minimize temperature variations during perfusion scans. A perfusion ratio was calculated by dividing the mean perfusion value of the ischemic hindlimb (dorsal side of calf and foot) by the mean perfusion value of an identical region in the non-ischemic hindlimb from the same scan. As a positive control, male *eNOS* knockout mice ($eNOS^{-/-}$; n=4) and *eNOS* wildtype mice ($eNOS^{+/+}$; n=4) were evaluated using LDPI following femoral ligation. $eNOS^{-/-}$ mice have been previously shown to have impaired hindlimb revascularization (Murohara et al.,

1998; Tamarat et al., 2002). *eNOS* mice on a C57BL/6J background were obtained from The Jackson Laboratory (Bar Harbor, Maine).

Histology and vessel densities

Animals were sacrificed without surgery (control) and following hindlimb surgery at days 7, 14, 21, and 35 for histology ($Fgf2^{+/+}$, n=4: $Fgf2^{-/-}$, n=4). Whole animals were perfuse-fixed with Histochoice (Amresco) at constant pressure (90-100 mmHg) and hindlimbs were placed in fixative overnight. The entire hindlimb between the knee and ankle was isolated and the tibia bone was carefully removed. Microvessels were identified on 6-μm paraffin sections cut from the middle portion of the calf using standard histochemistry techniques. Capillaries were identified as GS1 (*Griffonia simplicifolia* I lectin: EY-Labs) positive vessels smaller than 10 μm in outer-diameter. Arterioles were identified as vessels between 10 μm and 30 μm in outer-diameter that were stained positive for α-SMA (monoclonal antibody against α-smooth muscle actin: Sigma) around the entire vessel cross-section. Capillaries and arterioles were counted per twenty randomly selected high-power fields (162 μm x 162 μm field) on two whole limb transverse sections from each hindlimb. Vessel densities are expressed as the number of vessels per mm^2.

Average muscle fiber cross-sectional area

To calculate cross-sectional area (CSA) per muscle fiber, digitized images were captured using a CCD digital camera (Sony DKC-5000) attached to a microscope (Nikon

Optiphot) and then analyzed using image analysis software (Scion Image 4.0). For each animal, at total 3 images (420 μm x 320 μm field) were taken of the same generalized region of the calf (medial gastrocnemius). Perimeters were measured and CSA was calculated for all muscle fibers completely within the image frame. Also, the number of muscle fibers per image were recorded. These measurements were performed on control, day 7, and day 35 animals (n=4 per genotype for each time point).

Cell proliferation

Animals were injected with bromodeoxyuridine (BrdU: 30mg/kg body weight: Sigma Chemical) i.p. at 24 hours and 12 hours prior to sacrifice. BrdU incorporation into the nuclei of proliferating cells was identified on 6-μm sections using a peroxidase conjugated sheep anti-BrdU antibody (Biodesign International) as described previously (Couffinhal et al., 1998). See Appendix X for detailed description of BrdU staining of paraffin-embedded sections. BrdU-positive nuclei were counted per twenty randomly selected high-power fields (162 μm x 162 μm field) on two whole limb transverse sections from each hindlimb. Proliferation is expressed as the number of BrdU-positive nuclei per mm^2. Serially cut sections were used to identify the same microscopic fields to colocalize GS1 stained capillaries and BrdU-positive nuclei in order to determine the identity of the proliferating cells. It has been previously shown that endothelial cells comprise the predominant proliferative cell type in the mouse ischemic hindlimb (Couffinhal et al., 1998). Analysis of cell proliferation in the hindlimb was performed on

control (non-ischemic) and day 7 ischemic limbs based on the previous report of peak proliferation at day 7 in this mouse model (Couffinhal et al., 1998).

Microangiography

Collateral artery growth (arteriogenesis) was evaluated at days 14 and 35 using microangiography (*Fgf2*$^{+/+}$, n=4: *Fgf2*$^{-/-}$, n=4). Animals were anesthetized and subsequently overdosed with 2.5% Avertin following exposure of the abdominal aorta. Hindlimbs were perfused (90-100 mmHg) with PBS containing $1x10^{-5}$ M sodium nitroprusside through a tapered polyethylene catheter (PE-50) inserted into the aorta, above the iliac branches, to induce maximal vasodilation and ensure complete filling with contrast agent (barium sulfate 210% w/v, Liqui-Coat, Lafayette Pharmaceuticals, Inc). In non-ischemic limbs, a ligature was placed around the ankle to occlude arterio-venous shunts present in the foot (data not shown) and limit filling to arteries only. High-definition angiograms (Faxitron Systems) were generated and scanned into a computer for quantitative evaluation using image analysis software (Scion Image). Vessel area was calculated from inverted images for the entire thigh region between the ligation site and the knee and below the femur by thresholding-out non-filled structures. Next, the vessel area, measured from thresholded images, was divided by the total area of the region examined (normalized vessel area). Lastly, an angiographic score was obtained by dividing the normalized vessel area for the left (ischemic) limb by the value obtained for the right (non-ischemic) limb.

Statistical analysis

Values are presented as the mean±SEM. Comparison between two means was done using Student's unpaired t-Test. Multiple groups were compared by One Way ANOVA with a Student-Newman-Keuls Test. Statistical significance was set at $P < 0.05$. Not significantly different, P=NS

Results

Fgf2 expression is increased in ischemic hindlimbs of $Fgf2^{+/+}$ mice

We used semiquantitative RT-PCR (Zhou et al., 1998) to confirm that *Fgf2* mRNA expression is increased in the hindlimb following ischemia in this model. *Fgf2* transcript levels increased in the ischemic hindlimb of $Fgf2^{+/-}$ mice by approximately twofold at day 3 relative to the contralateral, non-ischemic hindlimb. This difference was greater than fourfold by day 7 and returned to control levels by day 14 (Figure 3.1). As expected, no *Fgf2* transcript was detected in hindlimb tissue from $Fgf2^{-/-}$ mice (Figure 3.1).

Recovery of resting hindlimb perfusion

Serial perfusion measurements, by LDPI in the same animal over 5-weeks, were used to evaluate the temporal recovery of resting perfusion in the ischemic hindlimb. In both $Fgf2^{+/+}$ and $Fgf2^{-/-}$ mice, the hindlimb perfusion ratio (ischemic to non-ischemic) was reduced immediately after surgery (Figure 3.2). Perfusion progressively improved following induction of ischemia to near normal by day 35 for both $Fgf2^{+/-}$ and $Fgf2^{-/-}$ mice. No significant differences were observed between the perfusion ratios of $Fgf2^{+/-}$ and $Fgf2^{-/-}$ mice at any of the time points examined. As previously shown,(Murohara et al., 1998; Tamarat et al., 2002) recovery of hindlimb perfusion was significantly impaired in $eNOS^{-/-}$ mice. These mice were studied to confirm that the LDPI methods used to evaluate the *Fgf2* mice would in fact detect any differences if they were present.

Importantly, the lack of revascularization in the *eNOS*$^{-/-}$ mice was associated with a progressive necrosis of the ischemic hindlimb (Figure 3.3). In fact, the majority of *eNOS*$^{-/-}$ mice studied lost some portion the distal hindlimb to necrosis as early as day 7. By contrast, *Fgf2*$^{-/-}$ mice (as well as *Fgf2*$^{+/+}$ and *eNOS*$^{+/+}$) had no signs of necrosis or tissue loss in the hindlimb following femoral ligation (Figure 3.3). It should be noted that LDPI measurements in our study were done under resting conditions and resting perfusion values typically reflect only a small portion of the entire perfusion capacity in the hindlimb (Brevetti et al., 2001). However, others report that warming of the mice during LDPI (as performed in our study) induces some degree of vasodilation in the hindlimb (Scholz et al., 2002). Thus, perfusion measurements performed in this manner may represent a larger fraction of total perfusion capacity than actual resting perfusion values.

Ischemia-induced changes in microvessel density

We measured capillary and arteriole density in the calf skeletal muscle of non-ischemic and revascularized hindlimbs to assess angiogenesis and microvascular remodeling. Capillary density (per mm^2) in the ischemic calves of both *Fgf2*$^{+/+}$ and *Fgf2*$^{-/-}$ mice increased significantly ($P<0.05$) by day 7 to nearly 1.5 times the respective contralateral, non-ischemic hindlimb densities (Figure 3.4). Capillary density remained elevated in the ischemic hindlimb in all mice through day 35. No such changes in capillary density were detected in the thighs of ischemic hindlimbs for either genotype (data not shown). No significant differences in capillary density were observed in

revascularizing hindlimbs between *Fgf2*$^{+/+}$ and *Fgf2*$^{-/-}$ mice. Arteriole density (per mm^2) in day 7 ischemic hindlimbs of both *Fgf2*$^{+/+}$ and *Fgf2*$^{-/-}$ mice was elevated nearly twofold relative to non-ischemic hindlimbs ($P<0.05$ vs control; Figure 3.5). As with capillary density, arteriole density remained elevated in the ischemic hindlimbs at day 35. No significant differences in arteriole density were observed between *Fgf2*$^{+/+}$ and *Fgf2*$^{-/-}$ mice.

Ischemia-induced muscle regeneration and changes in muscle fiber area

Hindlimb ischemia caused extensive muscle fiber degeneration-regeneration as evidenced by the changes in muscle fiber morphology (Figure 3.6). Newly regenerated myofibers were apparent throughout the calf at day 7, each with a centrally located nucleus and relatively small fiber size. Regenerated fibers display numerous centrally aligned nuclei (as seen in longitudinal section) which is due to the fusion of many myoblasts (differentiated satellite cells) to form a single myofiber. The new fibers progressively increase in size, however the central nuclei are evident up to 20 weeks after femoral ligation (Figure 3.6). Due to extensive fiber regeneration, we evaluated muscle fiber cross-sectional area, given that changes in fiber area can affect capillary density independent of angiogenesis (Sarelius et al., 1983). As shown in Figure 3.6, fiber area was not different between the genotypes at the various time point examined. Thus, comparison of vessel density between *Fgf2*$^{+/+}$ and *Fgf2*$^{-/-}$ mice is not being affected by differential changes in fiber area in one particular genotype. However, we did measure a significantly reduced fiber area at day 7 in all mice. This suggests that capillary density

changes measured at this early time point might reflect both changes in fiber area and vascular growth (angiogenesis). Based on previous data (Sarelius et al., 1983), the fiber area decrease observed in our study would not completely explain the increase in capillary density measured at day 7 (approximately 300 capillaries per mm^2). Nevertheless, fiber area returned to control values when measured at day 35. Thus, changes in capillary density in the ischemic limb measured at day 35 appear to be due to angiogenesis rather than changes in muscle fiber area.

Ischemia-induced changes in cell proliferation

Numerous proliferating cells were detected in the ischemic limbs of both genotypes at day 7 in the ischemic limb (Figure 3.7). Very few BrdU-positive cells were seen in the non-ischemic hindlimbs. Staining of serial sections showed rather consistent co-localization of BrdU-positive cells with GS1-labeling. This is consistent with previous data showing that endothelial cells are the predominant cell type undergoing proliferation at day 7 in the ischemic mouse hindlimb (Couffinhal et al., 1998). Finally, there was no difference in cell proliferation between *Fgf2*$^{+/+}$ and *Fgf2*$^{-/-}$ mice in the day 7 ischemic limbs (Figure 3.7).

Arteriogenesis in the ischemic mouse hindlimb

We evaluated arteriogenesis (collateral artery development) in the ischemic hindlimbs using high-resolution microangiography. This technique allowed us to visualize vessels with inner diameters greater than or equal to approximately 50 μm.

Representative angiograms from *Fgf2*$^{+/+}$ and *Fgf2*$^{-/-}$ mice are shown in Figure 3.8. Angiograms of non-ischemic hindlimbs showed no architectural differences in the vasculature between *Fgf2*$^{+/+}$ and *Fgf2*$^{-/-}$ mice. Few angiographically visible collateral vessels were evident immediately following femoral ligation (day 0). At days 14 and 35 post-surgery, collateral arteries (with typical corkscrew patterns) were visible, spanning from the lateral circumflex femoral and deep femoral arteries to the genual arteries (near the knee) and saphenous artery branches (Figure 3.9). The same general pattern of collateral vessel growth was observed for both *Fgf2*$^{+/+}$ and *Fgf2*$^{-/-}$ mice at all time points examined. We used an angiographic score to quantify visible vascular area in the hindlimb (Figure 3.10). This score was expressed as a ratio of normalized vessel area in the affected (left) limb divided by normalized vessel area in the unaffected (right) limb. As expected, the scores were approximately 1.0 for non-ischemic (control) mice. Immediately following ligation (day 0), scores decreased significantly ($P<0.05$) in both the *Fgf2*$^{+/+}$ and *Fgf2*$^{-/-}$ mice. At day 14, scores for *Fgf2*$^{+/+}$ and *Fgf2*$^{-/-}$ mice increased significantly ($P<0.05$) above pre-surgery values and remained elevated in the revascularized hindlimb through day 35 (Figure 3.10). The amount of angiographically visible arteries in the hindlimb did not differ between *Fgf2*$^{+/+}$ and *Fgf2*$^{-/-}$ mice.

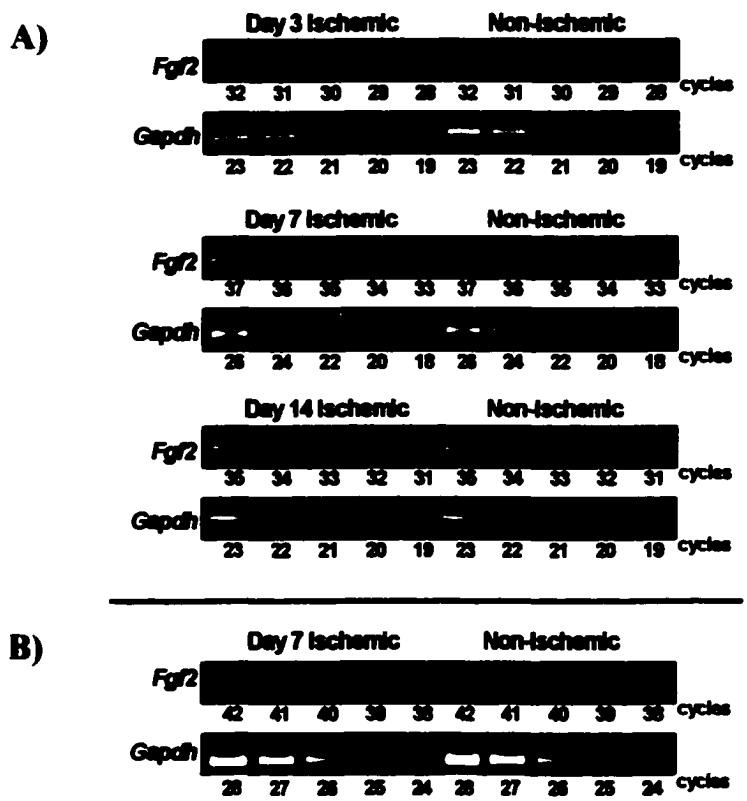

Figure 3.1 A) Relative *Fgf2* mRNA expression by RT-PCR in ischemic and non-ischemic (contralateral) hindlimbs of $Fgf2^{+/+}$ mice. Shown are representative results at 3, 7, and 14 days following left femoral artery ligation. Aliquots of the amplification reaction were removed during sequential cycles and gel electrophoresed. *Gapdh* serves to control for cDNA template quantity and linear amplification. B) No *Fgf2* mRNA was detected in tissues from $Fgf2^{-/-}$ mice using RT-PCR.

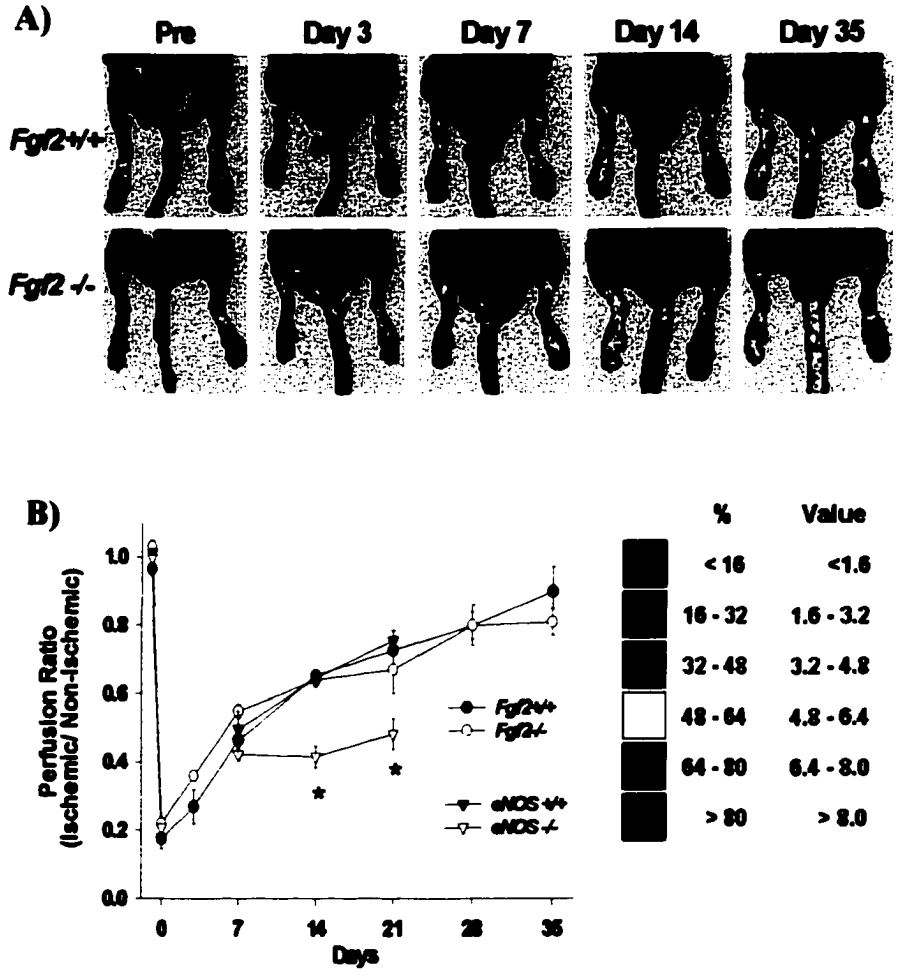

Figure 3.2 A) Representative LDPI scans of *Fgf2*$^{+/+}$ and *Fgf2*$^{-/-}$ mice before (Pre) and serially after left femoral ligation. Red tones represent highest perfusion and blue indicates lowest perfusion. B) The time course of perfusion recovery after femoral ligation measured from LDPI scans. The perfusion ratio is the average left (ischemic) hindlimb perfusion value divided by the average right (non-ischemic) perfusion value. *P*=NS for *Fgf2*+/+ vs *Fgf2*-/-. *eNOS*$^{+/+}$ vs *eNOS*$^{-/-}$ were significantly different from each other as indicated by the asterisk, $P<0.05$.

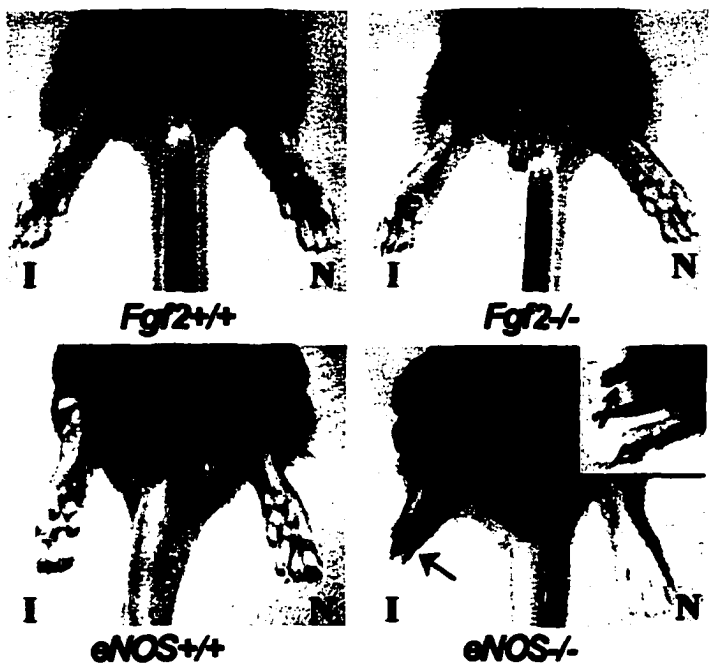

Figure 3.3 Representative photographs of the dorsal aspect of the mouse hindlimbs at 7 days after induction of ischemia. I= ischemic limb; N = non-ischemic limb. The black arrows indicate necrosis and tissue loss, which was typically observed in *eNOS*$^{-/-}$ mice, but not in the other genotypes examined.

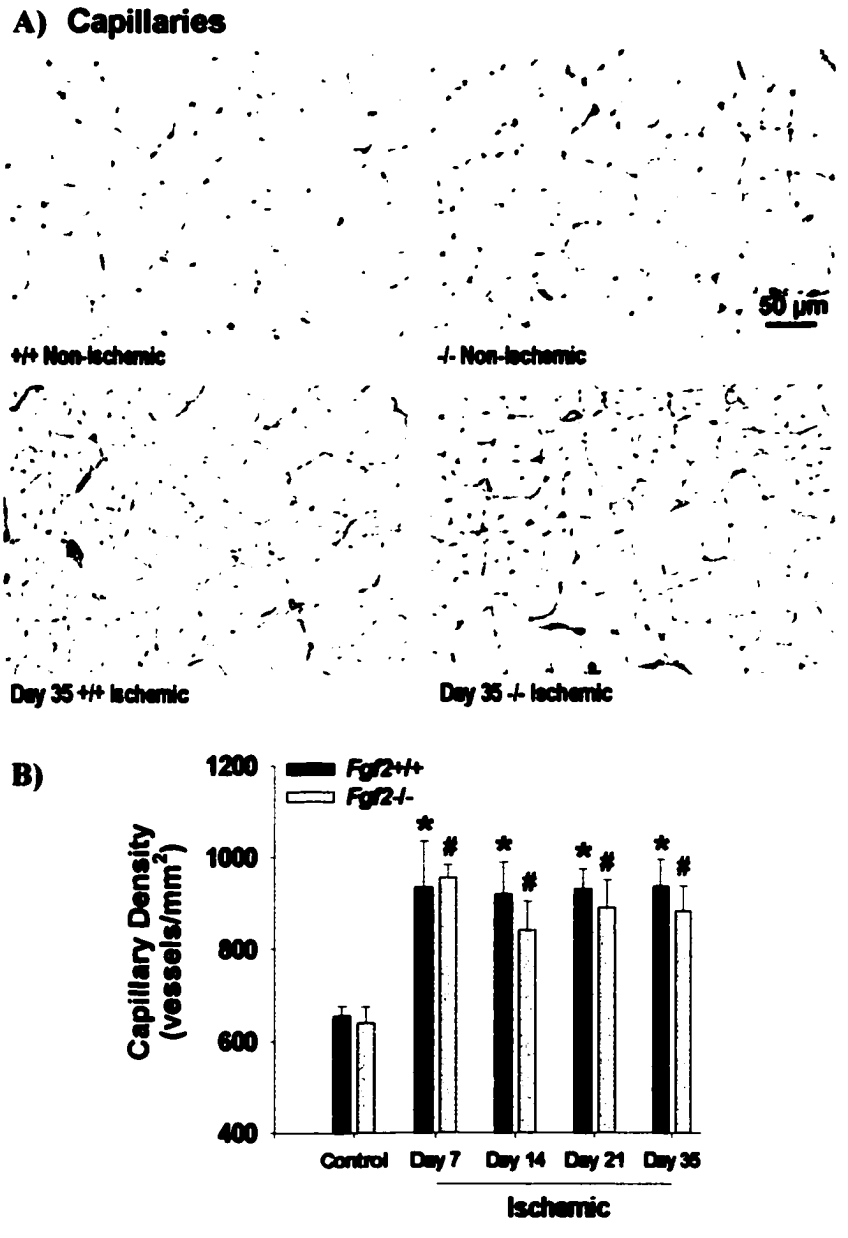

Figure 3.4 A) Representative photomicrographs of muscle cross-sections from non-ischemic (control) and day 35 post-ischemic hindlimbs of *Fgf2*+/+ and *Fgf2*-/-, stained with *Griffonia simplicifolia* I lectin to identify capillaries. Sections are counter-stained with hematoxylin. B) Capillary density in hindlimb muscle without femoral ligation (control) and 7, 14, 21, and 35 days after ligation. **P*<0.05 vs *Fgf2*+/+ Control. # *P*<0.05 vs *Fgf2*-/- Control. *P*=NS for *Fgf2*+/+ vs *Fgf2*-/-.

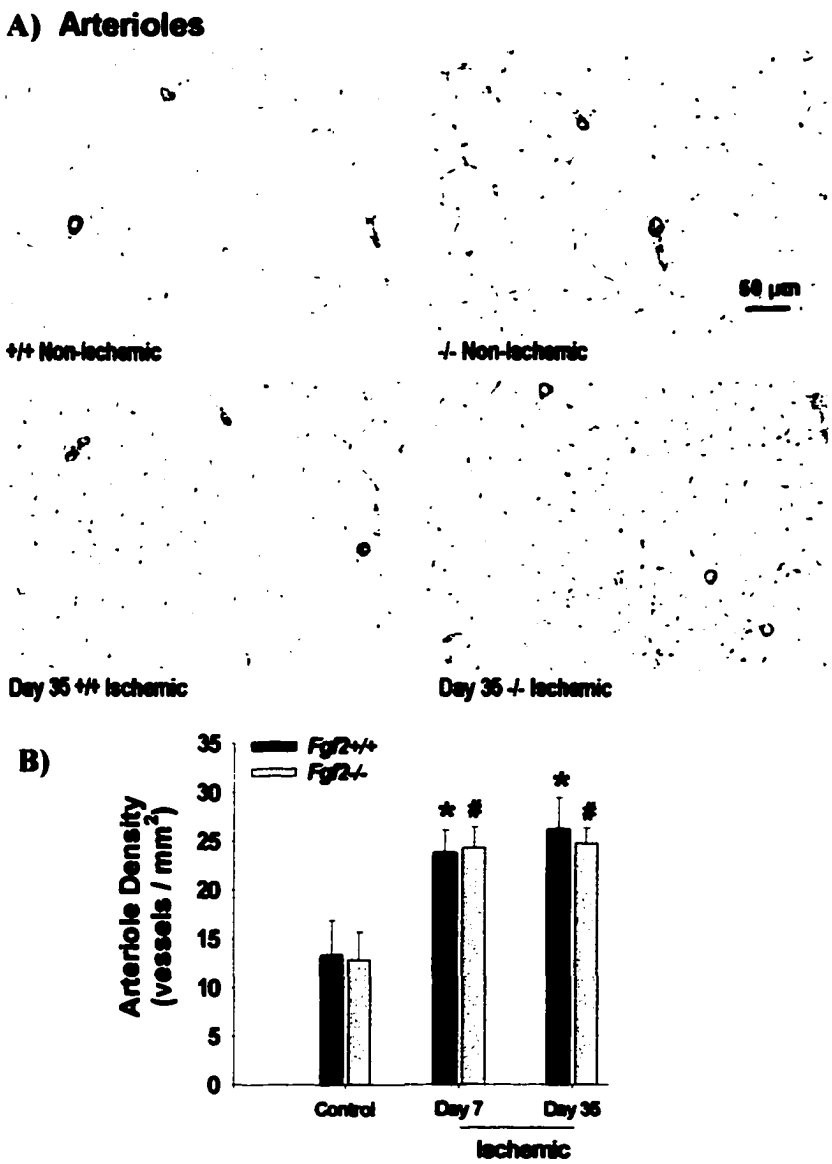

Figure 3.5 A) Representative photomicrographs of muscle cross-sections from non-ischemic and day 35 post-ischemic hindlimbs of *Fgf2*+/+ and *Fgf2*-/-, stained with antibody against α-smooth muscle actin to identify arterioles. Sections are counter-stained with hematoxylin. B) Arteriole density in hindlimb muscle without femoral ligation (control) and 7 and 35 days after ligation. **P*<0.05 vs *Fgf2*+/+ Control. # *P*<0.05 vs *Fgf2*-/- Control. *P*=NS for *Fgf2*+/+ vs *Fgf2*-/-.

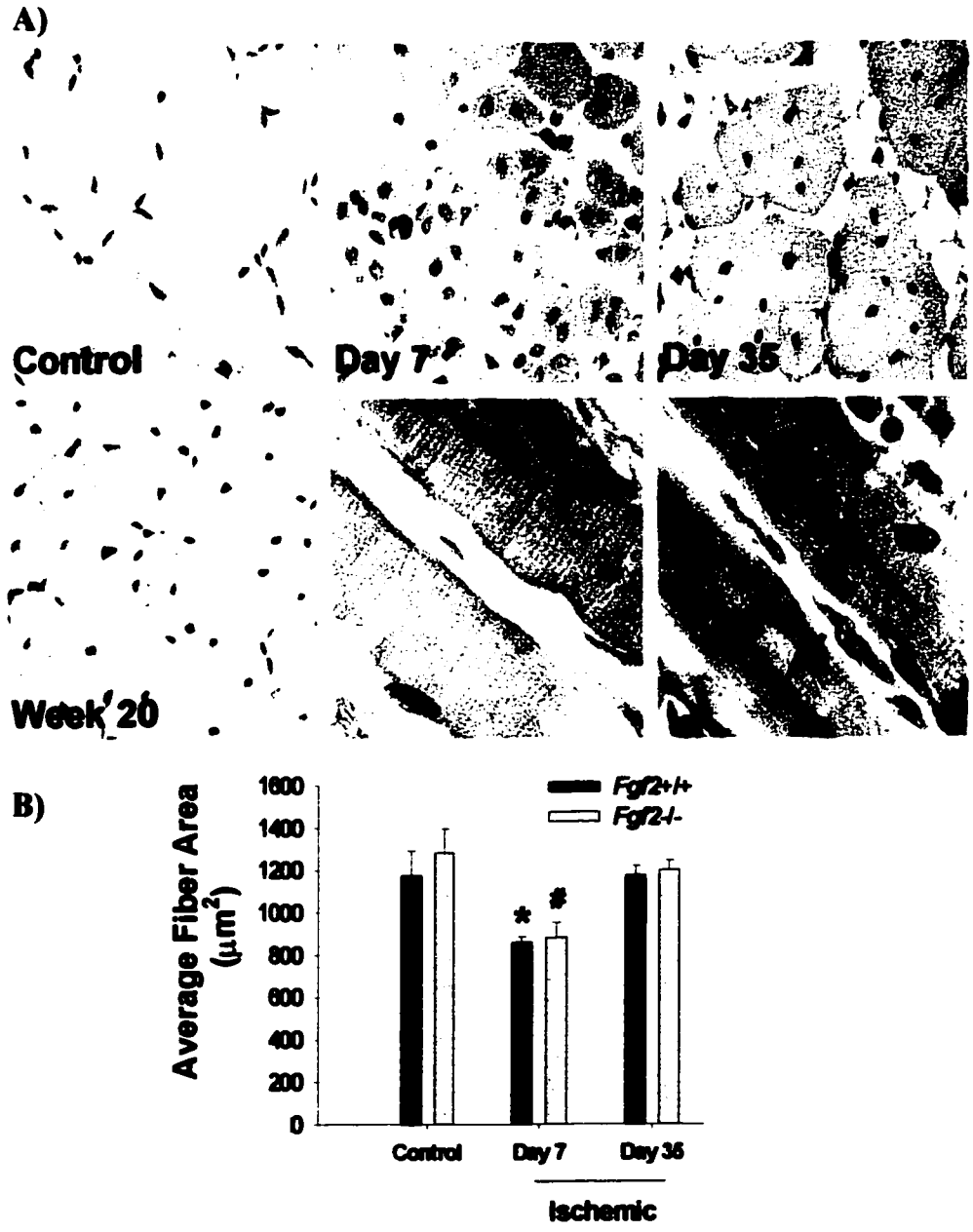

Figure 3.6 A) Photomicrographs of control, day 7, day 35, and week 20 muscle cross-sections showing the progression of myocyte regeneration. Longitudinal sections through a normal fiber (bottom row, middle) and a regenerating myofiber (bottom row, right) with characteristic central nuclei. B) Average muscle fiber area (cross-sectional) in hindlimb muscle without femoral ligation (control) and day 7 and 35 after ligation. **P*<0.05 vs *Fgf2*$^{+/+}$ Control; Day 35. #*P*<0.05 vs *Fgf2*$^{-/-}$ Control; Day 35. *P*=NS for *Fgf2*+/+ vs *Fgf2*-/-.

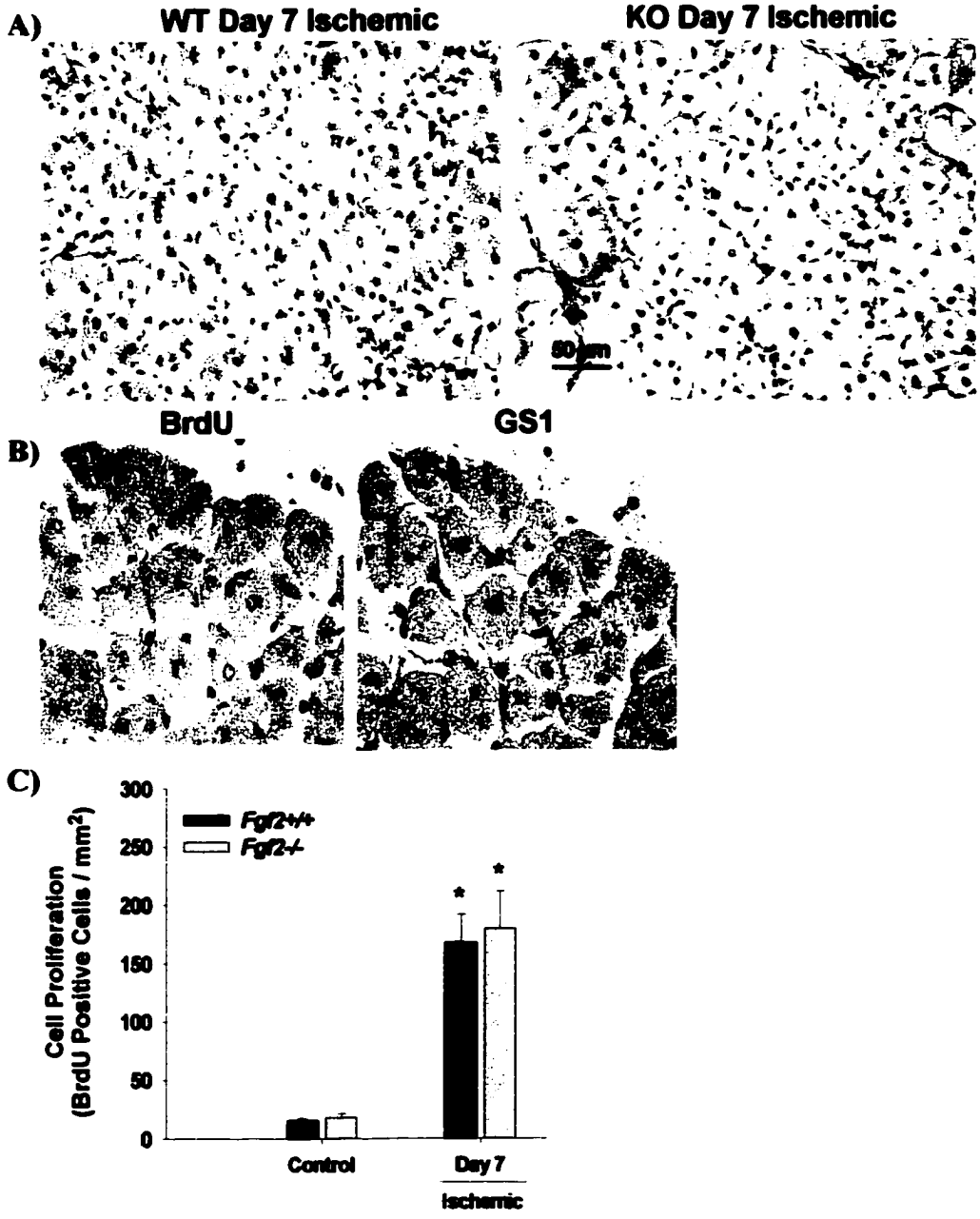

Figure 3.7 A) Representative photomicrographs of muscle cross-sections from day 7 post-ischemic hindlimbs of *Fgf2*$^{+/+}$ (WT) and *Fgf2*$^{-/-}$ (KO), stained with BrdU (blackish-brown stained nuclei) to identify proliferating cells. B) Serial sections (6 μm each) from hindlimb stained with BrdU or GS1 to identify proliferating endothelial cells. C) Quantification of cell proliferation in hindlimb muscle without femoral ligation (control) and 7 days after ligation. *$P<0.05$ vs respective control. P=NS for *Fgf2*+/+ vs *Fgf2*-/-.

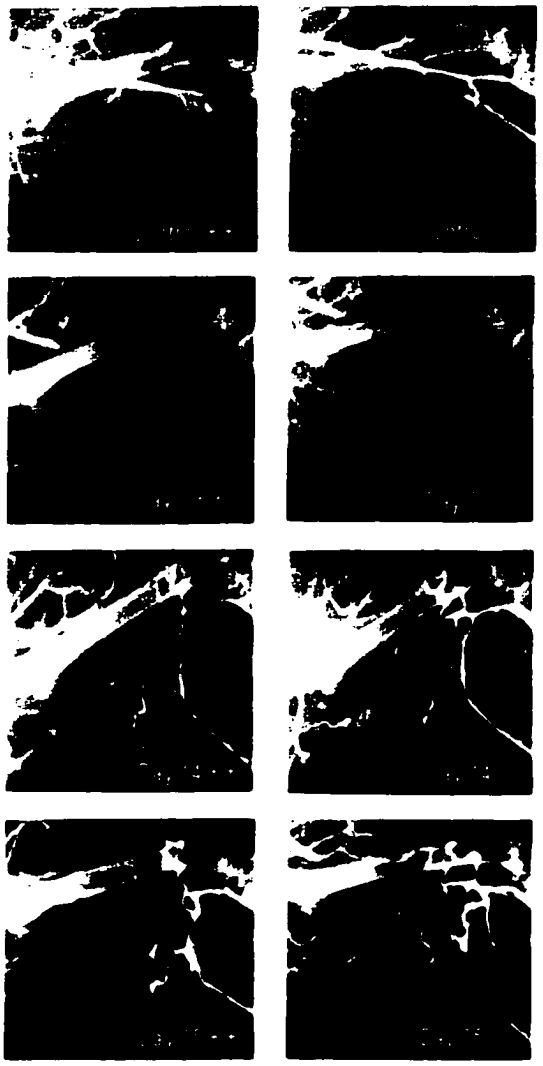

Figure 3.8 Representative angiograms taken of left hindlimbs of *Fgf2*+/+ vs *Fgf2*-/- mice without ligation (control), immediately after ligation (Day 0), 14 days, and 35 days after surgery.

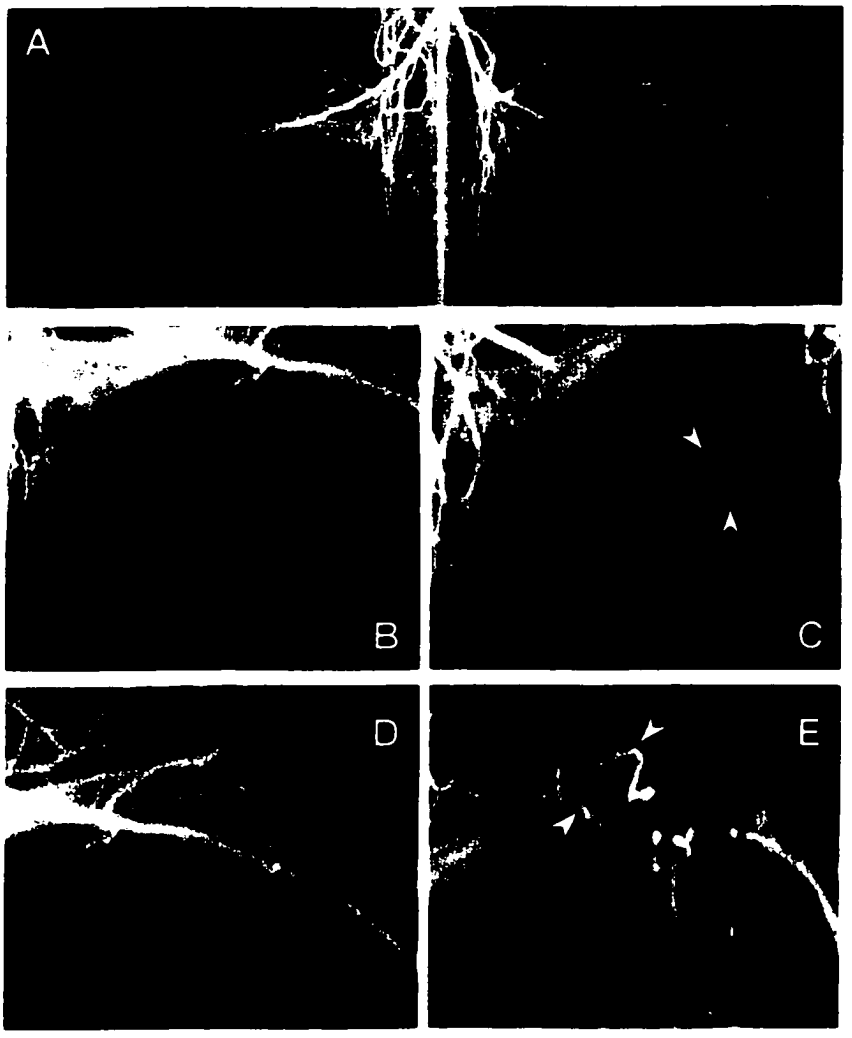

Figure 3.9 A) Angiogram showing ischemic limb at day 14 and non-ischemic contralateral limb. Asterisk marks the proximal femoral ligation. B) Mirror image (i.e., flipped horizontally) of the contralateral limb for comparison to panel C. C) Day 14 post-surgery, collateral arteries spanning from the deep femoral artery (black arrows) to the saphenous artery branches in the calf (white arrows). D) Mirror image of the contralateral limb for comparison to panel E. E). Collateral arteries (with typical corkscrew patterns) spanning from the lateral circumflex femoral artery (black arrows) to the genual arteries near the knee (white arrows).

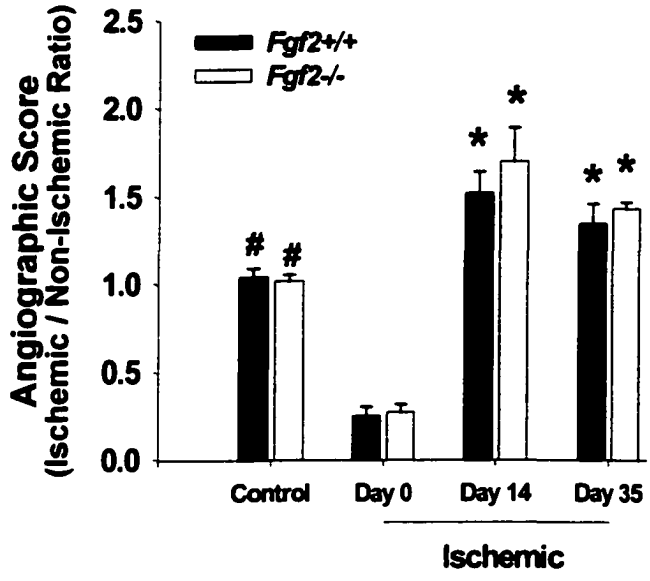

Figure 3.10 Quantification of angiographically visible arteries in hindlimb. Angiographic score is expressed as left hindlimb vessel area divided by right hindlimb vessel area. **P*<0.05 vs Control and vs Day 0. #*P*<0.05 vs Day 0. *P*=NS for *Fgf2*+/+ vs *Fgf2*-/-.

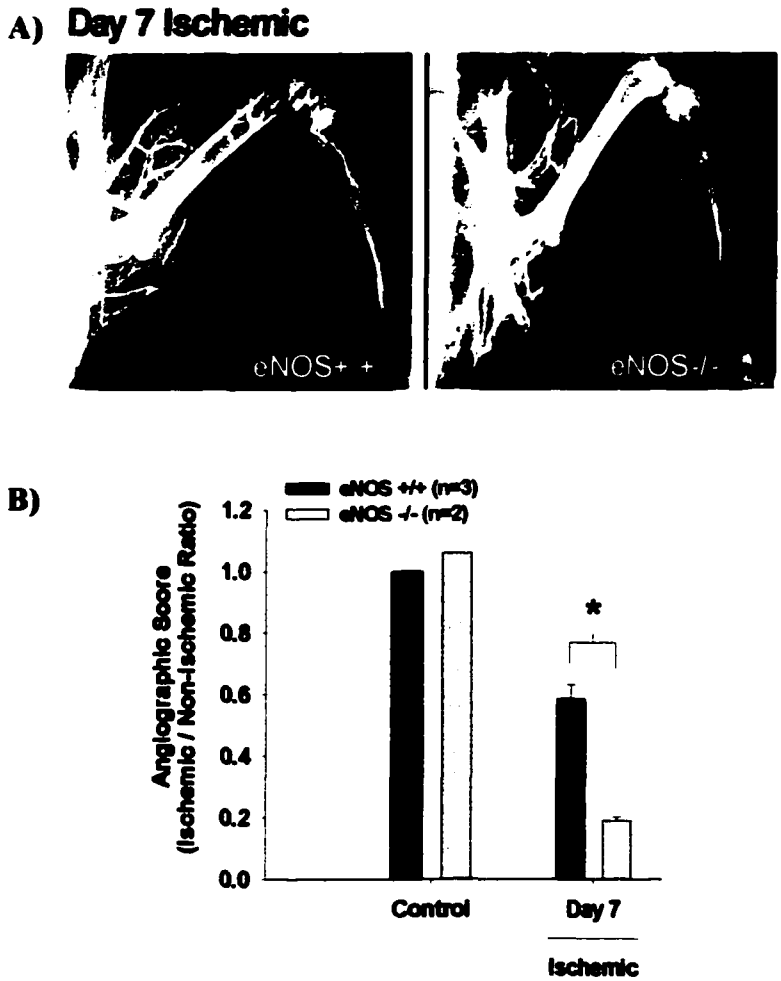

Figure 3.11 A) Representative angiograms in left hindlimbs of *eNOS*$^{+/+}$ and *eNOS*$^{-/-}$ mice at 7 days after femoral ligation. B) Quantification of angiographically visible arteries in hindlimb. Angiographic score is expressed as left hindlimb vessel area divided by right hindlimb vessel area. *$P<0.05$ for *eNOS+/+* vs *eNOS-/-* at day 7

Discussion

To my knowledge, this is the first study to directly examine the importance of endogenous FGF2 during revascularization in the setting of peripheral ischemia. The absence of FGF2 did not appear to affect vascular growth in this model. No differences in vessel density were detected including capillaries, arterioles, and angiographically visible arteries when comparing the ischemic limbs of $Fgf2^{+/+}$ and $Fgf2^{-/-}$ mice. Consistent with the above findings, recovery of resting hindlimb perfusion was similar between the FGF2 wildtype and knockout animals. Furthermore, the absence of any tissue necrosis or gross abnormality in the ischemic limbs of $Fgf2^{-/-}$ mice provides additional evidence that the revascularization process does not require FGF2.

These results are somewhat surprising in view of the extensive collection of research implicating FGF2 in the revascularization of ischemic tissue (Arras et al., 1998; Bush et al., 1998; Chleboun et al., 1994; Walgenbach et al., 1995). In animal models, FGF2 expression has been identified around newly formed microvessels during hindlimb ischemia (Bush et al., 1998) and strong FGF2 staining was detected in monocytes accumulating in growing collateral arteries (Arras et al., 1998). In other studies, FGF2 is upregulated more globally in the revascularizing regions (Chleboun et al., 1994; Cohen et al., 1994; Walgenbach et al., 1995). Similarly, in our study *Fgf2* expression was elevated in the ischemic hindlimb of wildtype mice at days 3 and 7. During ischemia, the temporal change in FGF2 expression and its localization to growing collateral arteries and capillaries strongly implicates FGF2 in the revascularization process. Importantly, Walgenbach et al. (Walgenbach et al., 1995) used anti-FGF2 antibody therapy to

significantly reduced angiogenesis in ischemic skeletal muscle using a rabbit model. In a study examining injury-induced revascularization in mice, antibody neutralization of endogenous FGF2 significantly reduced the capillary density measured in ischemic muscle of the hindlimb (Lefaucheur et al., 1996). In contrast, there was no evidence that angiogenesis was altered in the ischemic limbs of *Fgf2*$^{-/-}$ mice in our study. Even the amount of cell proliferation (presumably endothelial cells) within the ischemic tissues was not different between *Fgf2*$^{+/+}$ and *Fgf2*$^{-/-}$ mice, further indicating that angiogenesis was not affected by the absence of FGF2. Our data are consist with other results using *Fgf2*$^{-/-}$ mice showing that angiogenesis during ischemic retinopathy (Ozaki et al., 1998) and ocular choroidal injury (Tobe et al., 1998) does not require endogenous FGF2. Perhaps the most novel finding in the present study is that arteriogenesis appeared unaffected by the lack of FGF2. The previous studies cited above examined vascular adaptation at the level of the microcirculation rather than adaptation and growth of larger conductance arteries. Our evaluation of angiographically visible arteries, tissue perfusion, and hindlimb viability strongly suggest that collateral artery growth is not impaired in *Fgf2*$^{-/-}$ mice. In contrast to *Fgf2*$^{-/-}$ and wildtype mice, *eNOS*$^{-/-}$ animals had reduced limb perfusion and no angiographically visible collateral vessels (Figure 3.11), which was associated with progressive tissue necrosis.

The conflicting results between our study and the various studies using antibody neutralization of FGF2 could be due to several possibilities. Neutralization studies that identify FGF2 as an essential mediator of angiogenesis may be overestimating the role of FGF2 due to inhibition of other FGF proteins. There are at least 22 FGF family members

and these proteins bind to a common group of receptors, although with differing affinities (Bikfalvi et al., 1997; Yamashita et al., 2000). Alternatively, chronic gene loss (e.g., gene knockout) and acute protein loss (e.g., antibody neutralization) may result in distinct responses to the same stimulus. Lastly, differences in the animal models used to examine ischemia and angiogenesis might also account for the contradictory observations.

The apparently normal revascularization response observed in *Fgf2*$^{-/-}$ mice may reflect compensation for the loss of FGF2 by another gene product. Given the large number of FGF proteins, it possible that there is some degree of redundancy among the FGF family members. Genetic ablation of two or more genes in a single animal (e.g., double knockout) is one approach to directly test for compensation. Recently, a double knockout of FGF1 and FGF2 was shown to have the same phenotype as *Fgf2*$^{-/-}$ mice (Miller et al., 2000). This suggests that FGF1, the most closely related FGF family member to FGF2, is not compensating for the loss of FGF2 in situations of vascular growth. However, we cannot rule out that FGF1 or other proteins are acting to functionally replace FGF2 in our model. Alternatively, it is possible that there is not compensation and that other growth factors or molecules may be the actual mediators of biological events currently ascribed to FGF2. In this regard, increased FGF2 expression observed in ischemic tissue may be mediating some other process during revascularization (e.g., vessel responsiveness) that is either unrelated or not critical for structural adaptation of the vasculature. Of course, we cannot exclude that subtle differences may have been present in the vessels of the ischemic limb of *Fgf2*$^{-/-}$ mice, which were simply not detected in our study.

Although not rigorously examined in the present study, skeletal muscle regeneration did not appear to be altered in the ischemic hindlimbs of *Fgf2*$^{-/-}$ mice. The ischemic limb musculature was indistinguishable between genotypes in terms of muscle fiber size, number of fibers per area of tissue, and extent of myocyte loss. This is important to note considering that FGF2 and various other FGF-family members are considered to be important regulators of satellite cell activation and skeletal muscle regeneration in response to injury (Anderson et al., 1995; Hawke et al., 2001; Lefaucheur et al., 1995; Lefaucheur et al., 1996; Sheehan et al., 1999). Given our results, it appears that FGF2 is not required for skeletal muscle regeneration and presumably satellite cell proliferation caused by chronic ischemia.

To date, three independently generated *Fgf2*$^{-/-}$ mouse lines have all been shown to be fertile and grow to maturity (Dono et al., 1998; Ortega et al., 1998; Zhou et al., 1998). However, numerous phenotypes have been identified in these *Fgf2*$^{-/-}$ mice including thrombocytosis, altered blood pressure regulation, decreased vein vascular smooth muscle activity, impaired cerebral cortex development, and decreased bone mass (Dono et al., 1998; Montero et al., 2000; Ortega et al., 1998; Zhou et al., 1998). Studies of adult *Fgf2*$^{-/-}$ mice in pathological situations have identified an indispensable and uncompensated role for FGF2 in wound healing, pressure-induced cardiac hypertrophy, and neurogenesis after brain injury (Ortega et al., 1998; Schultz et al., 1999; Yoshimura et al., 2001).

Conclusion

Contrary to what was expected, this study demonstrates that endogenous FGF2 is not required for vascular adaptation during ischemic revascularization in the mouse hindlimb. Overall, the lack of a detectable deficit in vascular growth, either developmental or pathological, in *Fgf2*$^{-/-}$ mice suggests that we may have to reconsider the importance of endogenous FGF2 in angiogenesis and arteriogenesis.

Comments on Impaired Arteriogenesis in eNOS knockout mice

As noted above, *eNOS*$^{-/-}$ mice had reduced limb perfusion and this was associated with few if any angiographically visible collateral vessels at day 7. These results suggest that impaired perfusion in the *eNOS*$^{-/-}$ ischemic limb is the result of impaired arteriogenesis. Others have suggested that the impaired perfusion recovery in *eNOS*$^{-/-}$ mice is due to reduced angiogenesis in the ischemic limb (Murohara et al., 1998). This raises the question of which adaptation, arteriogenesis or angiogenesis, is more critical to the reestablishment of blood following arterial occlusion in the hindlimb. A recent study by Scholz et al. evaluated hindlimb ischemia in different strains of mice (Scholz et al., 2002). Balb/C mice had the slowest perfusion recovery in the ischemic limb among the strains tested, yet Balb/C mice had the largest increase in capillary density in the ischemic limb. Importantly, Balb/C mice had significantly reduced collateral vessel size at day 3 and day 21 after femoral ligation as compared to C57Bl/6 mice-the strain to recover hindlimb perfusion the fastest. This study shows a clear disassociation between capillary density in the ischemic limb and recovery of limb perfusion. Thus, compared to

angiogenesis, arteriogenesis appears to be more critical to the recovery of blood flow following arterial occlusion in the hindlimb.

4. REACTIVE HYPEREMIA IS IMPAIRED IN THE ISCHEMIC HINDLIMB OF FGF2 KNOCKOUT MICE

Introduction

Numerous revascularization studies have demonstrated reduced vascular function and reactivity in response to vasodilator stimuli in collateral arteries and the collateral-dependent circulation (Bauters et al., 1995; Hillier et al., 1999; Kelsall et al., 2001; Laham et al., 1998; Sellke et al., 1994; Takeshita et al., 1998). Similarly, studies of the heart and hindlimb have shown increased agonist-induced vasoconstriction (hyperreactivity) in collateral-dependent vessels after chronic ischemia (Nelissen-Vrancken et al., 1992; Peters et al., 1989; Rapps et al., 1997a; Rapps et al., 1997b). These studies clearly show abnormal function in the collateral circulation supplying tissues downstream of an arterial occlusion. Reduced vasodilation and/or enhanced vasoconstriction in the collateral vasculature may limit blood flow in the growing and remodeling collateral circulation. Thus, recovery of blood flow following arterial occlusion depends on not only vascular growth, but also proper functioning of the collateral arteries and resistance vessels supplying the ischemic region. The cause of altered vascular function during revascularization is unknown. Both endothelial dysfunction and vascular smooth muscle impairment have been observed in arterioles and larger conductance arteries in ischemia models (Sellke et al., 1994; Sellke et al., 1996) (Kelsall et al., 2001; Takeshita et al., 1998). Abnormal contractile responsiveness of collateral vessels may be due to altered receptor expression in vascular cells, thus making

vessels more or less sensitive to vasoactive factors (Peters et al., 1989; Rapps et al., 1997b; Rapps et al., 1997a).

It is recognized that delivery of exogenous growth factors, such as FGF2 and VEGF, can improve or maintain vascular reactivity in models of chronic ischemia (Bauters et al., 1995; Laham et al., 1998; Sellke et al., 1994; Takeshita et al., 1998). For example, FGF2 treatment enhanced the responses of collateral-perfused coronary microvessels to endothelium-dependent vasodilators (Sellke et al., 1994). Similarly, administration of VEGF improved the response of the collateral circulation to endothelium-dependent agonists in the rabbit ischemic hindlimb (Bauters et al., 1995; Laham et al., 1998). Interestingly, FGF2 administered to hypercholesterolemic rabbits significantly improved vascular function of atherosclerotic vessels (Meurice et al., 1997) and VEGF treatment accelerated recovery of endothelium-dependent reactivity in balloon-injured arteries (Asahara et al., 1996). The mechanisms underlying the beneficial effects of FGF2 and VEGF in these various models of vascular dysfunction are not clear. Regardless, these studies raise the question of whether endogenously produced growth factors (e.g., FGF2) act to modulate the responsiveness of the vasculature in pathological conditions such as peripheral ischemia.

Using the model of hindlimb ischemia described in the previous chapter, we evaluated reactivity or functional responsiveness of the vasculature in the ischemic limbs of $Fgf2^{+/+}$ and $Fgf2^{-/-}$ mice. This study will allow us to determine the importance of endogenous FGF2 in regulating reactivity of the vasculature during ischemic revascularization.

Methods

Reactive Hyperemia

Vascular reactivity in the ischemic hindlimb was evaluated using reactive hyperemia. Reactive hyperemia refers to the transient increase in blood flow that follows a brief arterial occlusion (Figure 4.1) (Feigl, 1989). Reactive hyperemia reflects localized vasodilation in the vessels subjected to the temporary flow cessation and is therefore a measure of vascular responsiveness or reactivity (Gentry et al., 1972; Johnson, 1989; Roy et al., 1879). When evaluated at the single vessel level, reactive hyperemia is a direct measure of vessel reactivity. When the evaluation of the hyperemia is at the whole organ or tissue level then the hyperemia response depends on both vascular reactivity and the number of vessels supplying the tissue being studied.

In this study, animals were examined at day 14 (post-ischemia) when resting perfusion is typically 60% of normal in the ischemic limb ($Fgf2^{+/+}$, n=6: $Fgf2^{-/-}$, n=7). Temporary (10-min) occlusion of the left iliac artery (feeding the ischemic hindlimb) was used to induce vasodilation and subsequent hyperemia in the ischemic limb only (Figure 4.2). The length of occlusion (10-min) was selected based on pilot experiments using different occlusion durations and previous research showing that longer occlusion times produce a greater hyperemic response (Johnson et al., 1976; Roy et al., 1879). Animals were anesthetized with 2.5% Avertin and a small midline incision was made in the abdomen to expose the left iliac artery. The artery was occluded with a removable vascular clamp (Fine Science Tools, clamp size B-1, recommended for 0.4 – 1.0mm vessel diameter) and the skin incision was partially closed with a 7.5mm Michel suture

clip, leaving the clamp accessible for removal after 10-min. LDPI scanning (see previous chapter for LISCA description) was used to determine perfusion in the feet of the ischemic and contralateral hindlimbs before, during and after the 10-min occlusion. Each LDPI scan, encompassing the left and right limb, requires approximately 1-min. Three scans were performed before the temporary iliac occlusion and averaged for this period. Scans were done repeatedly during the 10-min occlusion period to confirm absence of flow in the occluded limb. Following release of the occlusion, 16 sequential LDPI scans were performed on the limbs (approximately 16-min total time). A comparison of the perfusion ratio (ischemic to contralateral) before left iliac occlusion and after release of the occlusion reflected the hyperemic response in the ischemic hindlimb. Reactive hyperemia was also investigated in non-ischemic limbs (no left femoral artery ligation) of *Fgf2*$^{+/+}$ and *Fgf2*$^{-/-}$ mice (n=4).

Measurement of arterial pressure

In a subset of *Fgf2*$^{+/+}$ and *Fgf2*$^{-/-}$ mice, arterial blood pressure was monitored continuously during the hyperemia procedure using a polyethylene (PE10 tubing) catheter placed in the left common carotid artery and integrated with a pressure transducer and a computer data acquisition system (Notochord). For detailed instructions on the construction of polyethylene catheters refer to the Transonic Systems Inc. handbook titled, *Tools & Techniques for Hemodynamic Studies in Mice*. These experiments showed that arterial pressure was not significantly altered during the iliac occlusion and subsequent hyperemia (Figure 4.3). Decreased blood pressure upon release

of the occlusion might adversely affect flow in the hindlimb. Similarly, autonomic responses, triggered by reductions in pressure, could potentially diminish the hyperemic responses under investigation (Feigl, 1989; Klabunde, 1986; Pawlik et al., 1991). Arterial occlusion and subsequent vasodilation might elicit baroreceptor activity and system-wide cardiovascular adjustments. Since neural regulation of blood pressure by the baroreflex may be diminished in *Fgf2*$^{-/-}$ mice it was important for us to not disturb systemic blood pressure (Dono et al., 1998). Also, given that *Fgf2*$^{-/-}$ mice have been shown to have reduced mean arterial pressure (MAP) (Dono et al., 1998; Zhou et al., 1998), we compared MAP during the hyperemia response between the genotypes and found no difference (Figure 4.3). Others have reported similar blood pressure values between *Fgf2*$^{+/+}$ and *Fgf2*$^{-/-}$ mice during procedures involving anesthesia (Schultz et al., 1999).

Results

Temporary (10-min) occlusion of the left iliac artery induced unilateral vasodilation and subsequent hyperemia in downstream vessels. Reactive hyperemia in non-ischemic hindlimbs of both genotypes responded in a similar manner (with the exception of 1 min post occlusion), reflecting a rapid increase in perfusion followed by a return to baseline (Figure 4.4). The peak hyperemia response in day 14 ischemic hindlimbs of $Fgf2^{+/+}$ mice was noticeably delayed versus the non-ischemic responses (Figure 4.4). However, the percent increase in perfusion ratio during hyperemia (post peak - pre / pre) was not different in ischemic $Fgf2^{+/+}$ mice when compared to the responses of non-ischemic $Fgf2^{+/+}$ and $Fgf2^{-/-}$ mice (Table 4.1). In contrast, the hyperemia response was barely discernible in the day 14 ischemic hindlimb of $Fgf2^{-/-}$ mice (percent increase 8.5±2.9%). Specifically, the hindlimb hyperemia response was significantly reduced ($P<0.05$) in day 14 ischemic $Fgf2^{-/-}$ mice versus day 14 ischemic $Fgf2^{+/+}$ mice at 4 min through 12 min post occlusion. Likewise, the peak hyperemia response (post peak) was significantly reduced ($P<0.05$) in ischemic hindlimb of $Fgf2^{-/-}$ mice (Figure 4.5). The peak hyperemia response was not different between non-ischemic $Fgf2^{+/+}$ and $Fgf2^{-/-}$ mice.

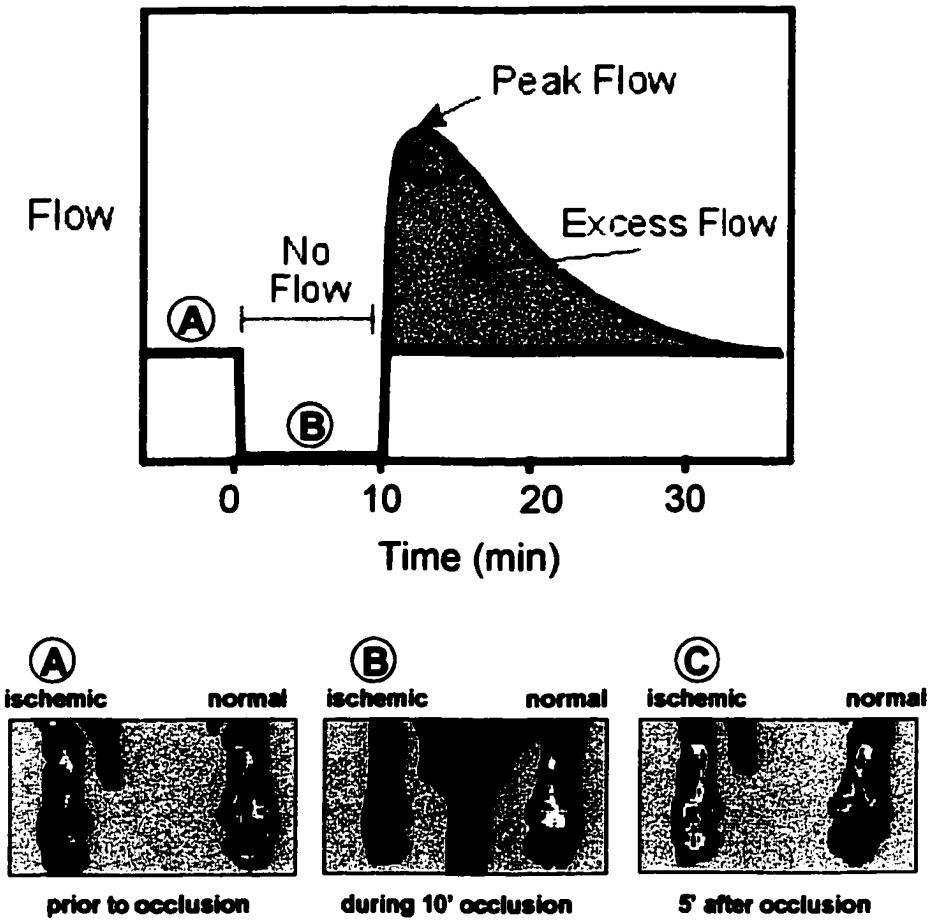

Figure 4.1 Diagram of reactive hyperemia protocol showing expected response of blood flow versus time. Labels A (baseline), B (during occlusion), and C (peak flow) correspond to representative LDPI images taken of the dorsal footpads during hyperemia. The hyperemia response is visible in the left ischemic foot (caused by 10-min occlusion of left iliac artery only), while perfusion in the contralateral (normal) foot remains unchanged.

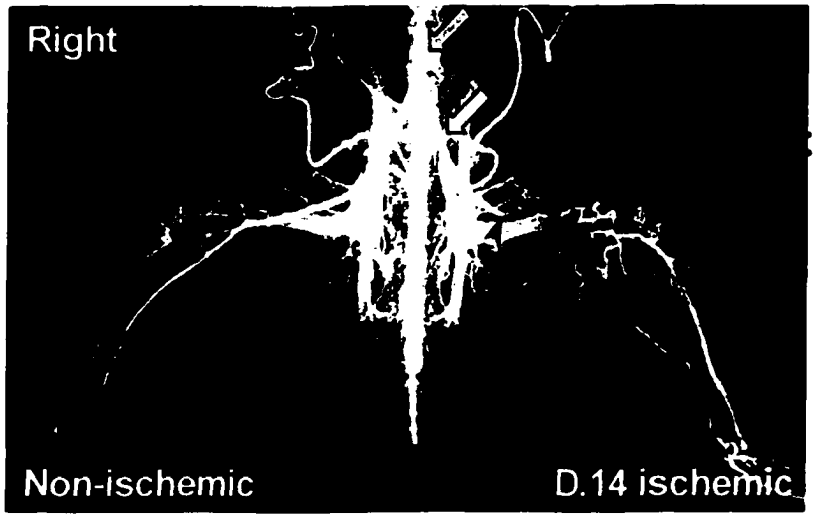

Figure 4.2 Angiogram of mouse hindlimb circulation (ventral view) 14 days following permanent ligation of the left femoral artery (black arrow head). The gray arrow indicates the abdominal aorta and the white arrow indicates the site of temporary occlusion of the left iliac artery. 10-min occlusion at this location was used to induce hyperemia in the left limb without changing perfusion in the contralateral (right) limb. This angiogram shows the extensive collateral network in the ischemic hindlimb, with these arteries stemming from branches downstream of the iliac artery.

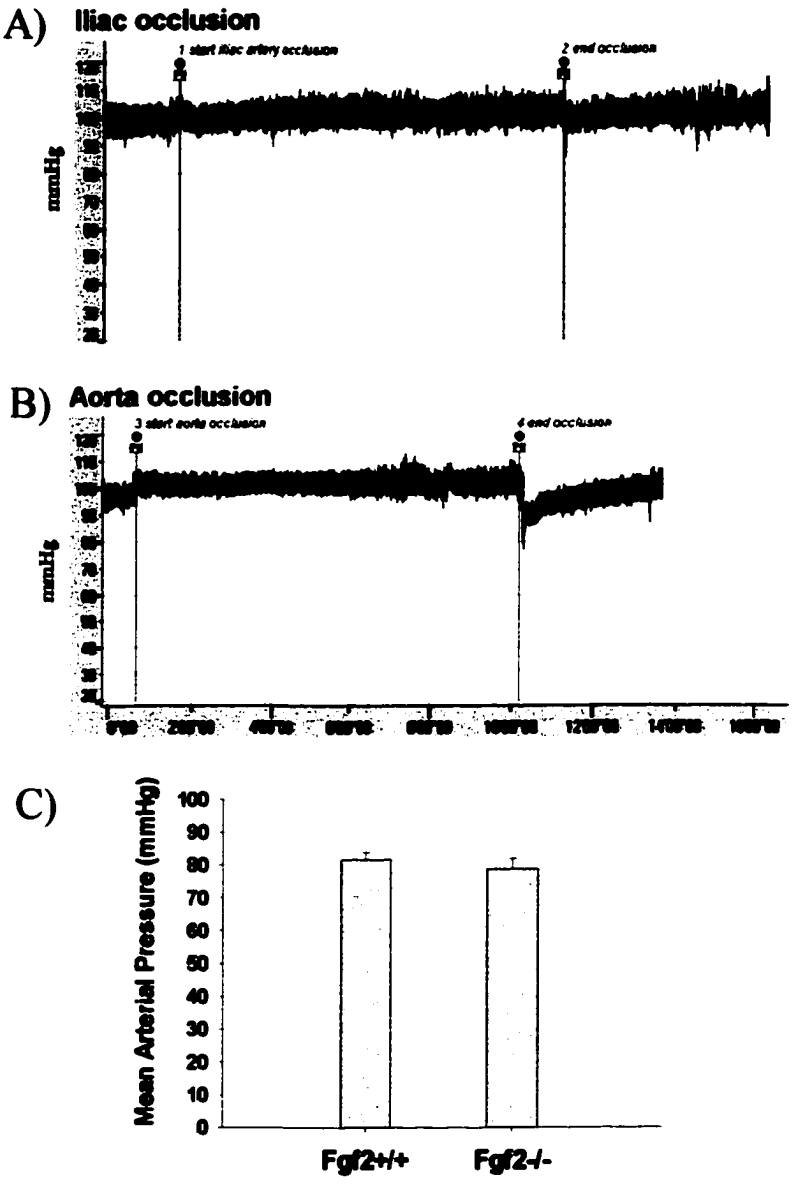

Figure 4.3 Arterial pressure was measured in mice via the left common carotid artery throughout the hyperemia protocol. Representative pressure tracings from a single mouse before and after 10-min occlusion of the left iliac artery (A) and the distal abdominal aorta (B). Mean arterial pressure (MAP) calculated for wildtype and knockout mice, averaged over the period following release of the 10-min iliac occlusion (C).

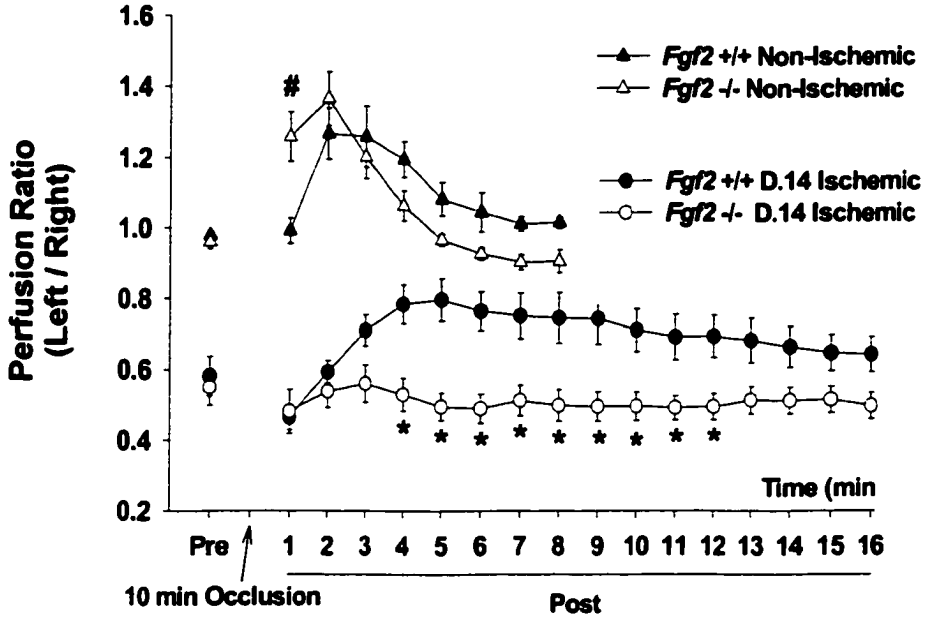

Figure 4.4 Reactive hyperemia response in non-ischemic and day 14 ischemic hindlimbs. Perfusion ratio is equal to perfusion in the left foot relative to the right foot. Pre indicates baseline perfusion ratio before temporary 10-min iliac artery occlusion. Post indicates the perfusion ratio serially following release of the iliac occlusion. Non-Ischemic indicates mice without femoral artery ligation. Day 14 ischemic indicates mice having undergone left femoral artery ligation 14 days prior to analysis. #$P<0.05$, Non-Ischemic *Fgf2*+/+ vs. Non-Ischemic *Fgf2*-/-. *$P<$ 0.05, D.14 Ischemic *Fgf2*+/+ vs D.14 Ischemic *Fgf2*-/-.

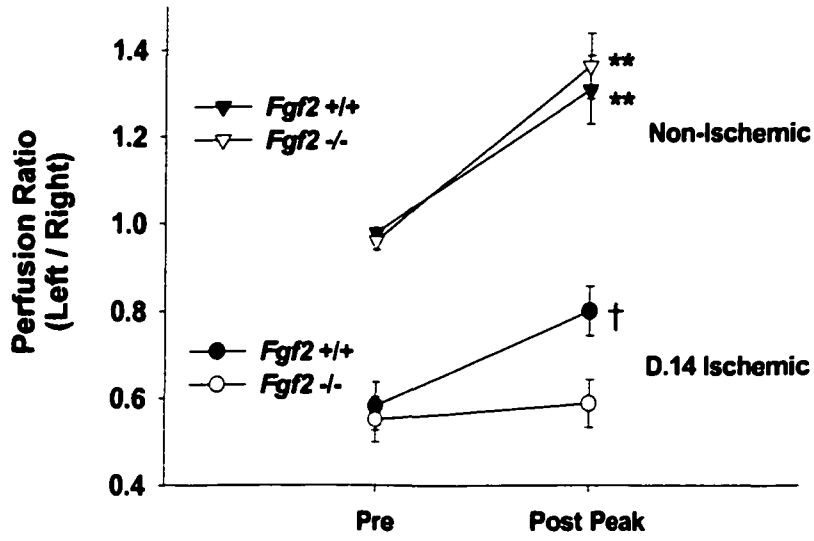

Figure 4.5 Peak hyperemia response (Post Peak) vs Pre for non-ischemic and day 14 ischemic hindlimbs. $^{**}P< 0.05$, Pre vs Post Peak Non-Ischemic *Fgf2*+/+; Pre vs Post Peak Non-Ischemic *Fgf2*-/-. $^{\dagger}P< 0.05$, Pre vs Post Peak D.14 Ischemic *Fgf2*+/+; Post Peak D.14 Ischemic *Fgf2*+/+ vs Post Peak D.14 Ischemic *Fgf2*-/-.

Table 4.1. Reactive hyperemia response in non-ischemic and day 14 ischemic limbs

	Perfusion Ratio (left to right)		
	Pre	Post Peak	% Increase
Non-Ischemic			
Fgf2+/+	0.98±0.01	1.31±0.08	33.5±7.1
Fgf2-/-	0.96±0.03	1.33±0.10	42.3±9.2
Day 14 Ischemic			
Fgf2+/+	0.58±0.06	0.80±0.06*	40.1±7.4*
Fgf2-/-	0.55±0.05	0.59±0.06	8.5±2.9

Perfusion ratio is equal to perfusion in the left hindlimb relative to the right hindlimb. Pre indicates baseline perfusion ratio before temporary 10-min iliac artery occlusion. Post indicates the peak perfusion ratio following release of the iliac occlusion. Non-Ischemic indicates mice without femoral artery ligation. Day 14 ischemic indicates mice having undergone left femoral artery ligation 14 days prior to analysis. Values are mean±SEM. * Statistically different $P<0.05$, D.14 Ischemic Fgf2+/+ vs D.14 Ischemic Fgf2-/-.

Discussion

These results clearly show that the hyperemic response is impaired in the ischemic, but not the non-ischemic, hindlimb of *Fgf2*$^{-/-}$ mice. This suggests that vascular reactivity is altered in the ischemic limb in the absence of endogenous FGF2. Given that the hyperemia-related, *Fgf2*$^{-/-}$ phenotype was limited to the revascularized hindlimb, it appears that FGF2 has an uncompensated activity in the peripheral vasculature of only ischemic or actively repairing tissues. This is consistent with other studies indicating that FGF2 is important during pathology-related situations in the adult (Cuevas et al., 1996; Ortega et al., 1998; Schultz et al., 1999; Yoshimura et al., 2001). Reactive hyperemia in non-ischemic (control) *Fgf2*$^{+/+}$ and *Fgf2*$^{-/-}$ hindlimbs was rapid, reaching a peak within 2 minutes after release of the occlusion. The hyperemic response in the ischemic hindlimb of *Fgf2*$^{+/+}$ mice was noticeably delayed (peaking at 5 min), but similar to the non-ischemic responses in terms of percent increase. The delayed reactive hyperemia in *Fgf2*$^{+/+}$ mice suggests that some degree of vascular dysfunction is associated with the revascularization process, which is in agreement with previous studies examining the reactivity of collateral and collateral-dependent vessels (Bauters et al., 1995; Hillier et al., 1999; Kelsall et al., 2001; Laham et al., 1998; Sellke et al., 1994; Takeshita et al., 1998). Alternatively, peak perfusion could have been delayed in the wildtype mice due to the architecture of the collateral circulation in the ischemic limb (e.g., increased length and tortuosity versus control limbs) (Scholz et al., 2002).

Since reactive hyperemia was used in an attempt to study the reactivity of the hindlimb vasculature, it is necessary to consider each of the many variables affecting

hyperemia in order to analyze the potential mechanism(s) of impaired vascular function in the ischemic *Fgf2*$^{-/-}$ limb. First, hyperemia could have been reduced due to diminished vascular growth in the *Fgf2*$^{-/-}$ hindlimb. In the present study, the hyperemia response reflects both functional and anatomical elements. Meaning that, hyperemia is dependent on both vasodilation (functional component) of the arterial circulation and the number of vessels (anatomical component) supplying the tissue or organ being studied. Thus a reduction in the number of arteries or arterioles supplying the ischemic limb in *Fgf2*$^{-/-}$ mice would lead to an impaired hyperemic response. Since resting perfusion ratios were similar between *Fgf2*$^{+/+}$ and *Fgf2*$^{-/-}$ animals, this would require that the *Fgf2*$^{-/-}$ vasculature (if reduced in number) be dilated to a greater extent at rest compared to *Fgf2*$^{+/+}$ mice. It is known that vessels with low resting tone (i.e., already dilated) show little or no vasodilation during reactive hyperemia (Gentry et al., 1972). Again, if the *Fgf2*$^{-/-}$ vessels were maximally dilated at rest than we would expect an absence of a hyperemic response after the 10-min occlusion. However, there is no evidence that vessel number was altered in the ischemic limbs of *Fgf2*$^{-/-}$ mice as compared to wildtype mice. Results presented in Chapter 3 support that artery, arteriole, and capillary number were not different between the genotypes. Also, based on angiography there did not appear to be any difference in the architecture of the collateral circulation between *Fgf2*$^{+/+}$ and *Fgf2*$^{-/-}$ mice. The architecture of the microcirculation was not directly examined in our study, but histology of the hindlimb showed no evidence that would indicate a difference. Given an equivalent vasculature in the ischemic limbs of both genotypes, maximal resting dilation might still be present in the *Fgf2*$^{-/-}$ mice and again this would result in an absence of hyperemia.

However, this would also cause the measured resting perfusion ratio to be higher in the ischemic hindlimb of *Fgf2*$^{-/-}$ versus *Fgf2*$^{+/+}$ mice. This is clearly not the case (Figure 4.4 and Figure 3.2 previous chapter). If we accept the assumption that the vasculature of the *Fgf2*$^{+/+}$ and *Fgf2*$^{-/-}$ mice is not significantly different in terms of anatomical structure, then the absence of reactive hyperemia in the limbs of *Fgf2*$^{-/-}$ mice must be due to a lack of vasodilation.

Reactive hyperemia appears to be the result of several superimposed mechanisms acting to regulate vascular tone, including metabolic, myogenic, flow-dependent dilation, neurogenic, and conducted responses (Duling et al., 1987; Johnson et al., 1975; Klabunde, 1986). However, the primary components mediating reactive hyperemia are thought to be the myogenic, metabolic, and flow-dependent responses (Johnson et al., 1975; Koller et al., 1990b; Lombard et al., 1981; Pohl et al., 2000). Vasodilation during and immediately after an occlusion of short duration (1 sec to 30 sec) is likely due to the myogenic response of vascular smooth muscle as a result of changes in arterial pressure (Bayliss, 1902; Gentry et al., 1972; Lombard et al., 1981). Reactive hyperemia after a relatively long occlusion (1 min and beyond) is best explained by metabolic and flow-dependent mechanisms. Vasodilation at the onset of flow stoppage occurs because of the decreased intravascular pressure in the vessels down stream of the occlusion (myogenic effect). However, when flow is resumed arterial pressure quickly increases and so the myogenic response rapidly favors increased vessel tone rather than dilation (Bjornberg et al., 1990). Build-up of metabolites (including adenosine, hydrogen ions, and potassium) or reduction in oxygen during the occlusion contribute to vasodilation during hyperemia

(Haddy et al., 1975; Klabunde et al., 1979; Lombard et al., 1981). Vasodilation presumably persists until flow is sufficient to wash away the metabolites and therefore reduce the signals producing vessel relaxation. However, hyperemia following long duration occlusions cannot be adequately explained by metabolic vasodilators alone (Pohl et al., 2000). Flow-dependent vasodilation, via endothelium-dependent production of factors such as nitric oxide (NO) and prostaglandin (PG), is also important during the hyperemic response (Koller et al., 1990a; Koller et al., 1990b; Meredith et al., 1996; Messina et al., 1977). It appears that the flow-stimulated release of NO acts to oppose pressure-induced myogenic vasoconstriction (de Wit et al., 1998; Ekelund et al., 1992; Pohl et al., 1991). During reactive hyperemia, Pohl et al. (2000) suggest that flow-dependent responses coordinate the dilation of downstream and upstream segments of the arterial vasculature. Metabolic dilation of small resistance vessels (downstream) should cause enhanced blood flow through the larger upstream vessels, resulting in flow-dependent vasodilation of these upstream arteries. Thus, there is a matched response in upstream and downstream vessels that allows resistance to fall in the vascular network.

Alterations in any one of these mechanisms could result in the impaired hyperemic response observed in the *Fgf2*$^{-/-}$ mice. Examining the known phenotypes in the *Fgf2*$^{-/-}$ mice does not necessarily help to identify any clear source of this diminished vascular responsiveness (Dono et al., 1998; Ortega et al., 1998; Zhou et al., 1998). These mice have decreased spontaneous vascular smooth muscle contractility in the portal vein, but not the aorta (Zhou et al., 1998). However, vessels (portal vein and aorta) had normal responsiveness to contractile agonists (Zhou et al., 1998). Also, *Fgf2*$^{-/-}$ mice have slightly

reduced MAP due to impaired neural regulation of blood pressure by the baroreceptor reflex (Dono et al., 1998; Dono et al., 2002). This reduced sympathetic nervous activity described in the *Fgf2*$^{-/-}$ mice should not impair hyperemia given that increased (not decreased) sympathetic output reduces reactive hyperemia (Klabunde, 1986; Pawlik et al., 1991). Also, we did not observe any arterial blood pressure changes in *Fgf2*$^{-/-}$ mice during reactive hyperemia, suggesting that changes in systemic hemodynamics are not affecting blood flow responses in the ischemic limb. Additionally, there is no evidence that neural abnormalities in the cerebral cortex and higher motor areas observed in *Fgf2*$^{-/-}$ mice affect the function of the peripheral vasculature (Ortega et al., 1998; Raballo et al., 2000).(Raballo et al., 2000)

The ability of vascular cells to sense and respond to signaling molecules could be altered in revascularized limb in the absence of endogenous FGF2. Exogenous FGF2 altered the capacity of vascular smooth muscle to bind the vasoconstrictor endothelin-1 (Cristiani et al., 1994). As stated previously, abnormal responsiveness of collateral vessels may be due to altered receptor expression in vascular cells, thus making vessels more or less sensitive to vasoactive factors (Peters et al., 1989; Rapps et al., 1997b; Rapps et al., 1997a). Conversely, loss of FGF2 in the repairing hindlimb may result in a failure of the skeletal muscle or vascular cells to produce necessary vasodilators during reactive hyperemia. In fact, exogenous FGF2 has been shown to have direct vasoactive effects (Cuevas et al., 1991). However, it is unlikely that FGF2 is directly mediating vasodilation during hyperemia since the hyperemic response in the non-ischemic hindlimbs of *Fgf2*$^{-/-}$ mice was equal to that measured in *Fgf2*$^{+/+}$ mice. Also, it was shown

that physiological doses of FGF2 have no influence on vasomotor tone of coronary arterioles (Sellke et al., 1994). The largest increase in FGF2 transcription in the hindlimb occurred within the first week of ischemia, during which new vessel elements were forming (arteriogenesis and angiogenesis). However, vascular reactivity was compromised in *Fgf2*$^{-/-}$ mice two weeks after surgery, when *Fgf2* transcript levels had returned to baseline in the wildtype animals. Thus, it seems that FGF2 upregulation precedes whatever effect it is having on vascular reactivity. Others have reported that the delivery of exogenous FGF2 early in or continually during the revascularization process restores vasodilator responsiveness in vessels examined weeks after the actual FGF2 administration (Laham et al., 1998; Sellke et al., 1994). Also, systemic injection of a single dose of FGF1 (aFGF) was able to reduce blood pressure in hypertensive rats for greater than 5 days (Cuevas et al., 1996). The FGF1 delivery increased eNOS expression in the vasculature of the hypertensive animals, which was correlated with blood pressure reduction and lessening of vessel reactivity to vasoconstrictor agonists (Cuevas et al., 1996). Collectively, these studies demonstrate that FGFs are capable of having long lasting effects on vascular cell function. FGF2 may be acting on vascular cells, early during revascularization, to preserve vasoactive capabilities in the remodeling vascular bed, perhaps by affecting vascular cell differentiation or gene expression.

FGF2 has been shown to influence the expression of various proteins important in the regulation vascular tone (Kage et al., 1999; Kostyk et al., 1995; Sasaki et al., 1998). Specifically, addition of exogenous FGF2 to cultured bovine endothelial cells increased *eNOS* mRNA expression as well as eNOS protein content (Kostyk et al., 1995). Also,

FGF2 promoted the expression of cyclooxygenase-2 (COX-2) mRNA and COX-2 protein in bone-derived endothelial cells and aortic smooth muscle cells *in vitro* (Kage et al., 1999; Karim et al., 1997). Interestingly, exogenous FGF2 stimulated the production of prostacyclin (PGI2) in uterine arteries (Krishnamurthy et al., 1999). COX-2 is a key enzyme in the conversion of arachidonic acid to the vasodilator PGI2 (DuBois et al., 1998). Also, FGF2 treatment increased PGI2 release from uterine endothelial cells derived from pregnant but not non-pregnant donor animals (Bird et al., 2000). These studies suggest that FGF2 levels could possibly modulate vascular tone indirectly via the regulation of enzymes (e.g., eNOS, COX) involved in the production of vasoactive substances (e.g., NO, PGI2). Additionally, it possible that this role of FGF2 is limited to certain physiological or pathological states, rather than normal homeostatic control processes.

Exogenous FGF2 has also been shown to regulate the contractile phenotype of vascular smooth muscle (Kato et al., 1998). Smooth muscle cell differentiation has been characterized as either a contractile (quiescent) or a synthetic (proliferative) phenotype (Thyberg et al., 1990). Increased FGF2 levels reduced both contractile protein content (smooth muscle α-actin and myosin heavy chain) and collagen synthesis independent of FGF2-stimulated proliferation (Kato et al., 1998). Loss of contractile protein is associated with the synthetic phenotype, but reduced extracellular matrix synthesis is typical of the contractile phenotype. It is interesting that FGF2 caused these two seemingly opposing changes in smooth muscle cell phenotype. Chronic ischemia and the subsequent remodeling events cause re-entry of quiescent vascular cells into the cell cycle and loss of

their differentiated phenotype (Scholz et al., 2002; Ward et al., 2000). At some point these same cells transition from the synthetic phenotype back to the quiescent, differentiated phenotype. Based on the study by Kato et al. (1998), it is conceivable that increased FGF2 expression in the ischemic limb modulates the phenotypic state of smooth muscle cells (or even endothelial cells) by regulating the shift to or from the quiescent state, perhaps independent of its mitogenic activity.

Future studies

From the present study, no specific mechanism or cause of impaired hyperemia can be determined. Further studies are necessary to determine: 1- The arterial segment(s) that have diminished reactivity during reactive hyperemia (e.g., small arterioles versus small arteries); 2- The vascular cell type that is responsible for the altered function during the hyperemia (endothelial cell versus smooth muscle cell); 3- The maximal flow capacity of vasculature in hindlimb of $Fgf2^{+/+}$ and $Fgf2^{-/-}$ mice, in order to confirm results previously shown using LDPI and angiography (Chapter 3).

Maximal flow capacity in the hindlimb can be measured by injection of fluorescent microspheres, suspended in a vasodilator cocktail solution (sodium nitroprusside/adenosine/papaverine in PBS), into the thoracic aorta via a polyethylene catheter. A recent study injected 100,000 microspheres (15 μm, Molecular Probes) at a constant pressure (100 mmHg) to quantify hindlimb perfusion capacity in mice (Scholz et al., 2002). These authors quantified the number of microspheres in serial cross-sections from each limb using a fluorescent microscope. The number of spheres in the ischemic

hindlimb was presented as a percentage of the non-ischemic (contralateral) limb. This procedure is relatively simple to perform and the measurements would further demonstrate whether or not reduced vascular growth is contributing the hyperemia phenotype observed in the ischemic *Fgf2*$^{-/-}$ hindlimb. I would expect perfusion capacity, as measured with microspheres, to be the same between the genotypes. This is based on the LDPI, angiography, and vessel density data presented in the previous chapter. However, if *Fgf2*$^{-/-}$ mice have reduced perfusion capacity using microspheres, it suggests that some aspect of vascular growth is impaired in the revascularized limb. Perhaps there is a difference in the number of arterial vessels approximately 30-50 μm in diameter (i.e., those arteries not visible from angiography and not quantified via histology) in the knockout ischemic limb. Then again, lack of responsiveness to the vasodilators during the microsphere injection could result in diminished perfusion capacity independent of vascular growth. Use of multiple vasodilators (i.e., vasodilator cocktail) at a high dosage should help to minimize this possibility since any one these vasodilators alone should be able to induce maximal vasodilation in normal vessels.

Intravital microscopy of the hindlimb vasculature (examined *in situ*) will help to identify the specific arterial segments with altered reactivity (Kelsall et al., 2001). Diameter changes in an individual vessel can be measured throughout the reactive hyperemia response (Bjornberg et al., 1990; Meininger, 1987). This technique can be used to evaluate individual vessel segments in the distal calf region (ischemic tissue) and in the proximal thigh musculature (remodeling but non-ischemic). Further, reactivity at all levels of the arterial resistance tree can be measured, ranging from the smallest

arterioles to the large conductance arteries. The most likely cause of impaired reactive hyperemia would tend to be at the level of the small arterioles (<25 μm) since these vessels have been identified as the primary resistance vessels during hyperemia (Bjornberg et al., 1990; Meininger, 1987). However, studies have identified an important resistance component in large arterioles and small arteries during hyperemia in skeletal muscle (Bjornberg et al., 1990). Importantly, this large artery contribution to vascular conductance appears to be more prominent during longer length occlusions (e.g., the 10-min duration used in our study). Finally, using pharmacological agonists to induce vasodilation (endothelium-dependent and independent) and vasoconstriction, it can be determined whether endothelial cell or smooth muscle cell responses are selectively altered in the absence of FGF2.

Comments

Vascular reactivity is commonly overlooked in studies of ischemic revascularization. Some investigators are quick to attribute reduced flow capacity to diminished collateral formation and impaired vascular adaptation. However, the contribution of impaired vascular reactivity must be considered when interpreting blood flow and perfusion measurements related to revascularization. Studies often lack experimental end-points designed to properly evaluate vascular growth (e.g., angiography) and yet authors of these studies interpret blood flow values to be a measure of collateralization (Lloyd et al., 2001; Yang et al., 2001). In fact, results from such studies may be due, at least in part, to altered vascular reactivity of the collateral-

dependent vasculature. Moreover, maximal flow capacity is often evaluated via procedures using either adenosine or SNP without consideration that vasomotor responses to these vasodilators may be altered in the collateral and collateral-dependent circulation (Kelsall et al., 2001; Laham et al., 1998). In studies of revascularization, both anatomical adaptation and functional responsiveness of the collateral circulation must be considered when evaluating the cause impaired flow capacity.

Conclusion

The lack of hyperemia observed in the ischemic limbs of *Fgf2*$^{-/-}$ mice appears to be secondary to altered vascular reactivity rather than impaired vascular growth during revascularization of the knockout hindlimb. Future studies will provide a better understanding of the specific mechanism(s) for the altered vascular responsiveness in the *Fgf2*$^{-/-}$ mice.

5. DIFFERENTIAL GENE EXPRESSION IN THE REVASCULARIZING HINDLIMB IN THE ABSENCE OF FGF2

Introduction

cDNA microarray technology, pioneered by Pat Brown and colleagues (Schena et al., 1995) in the mid 1990's, makes possible the measurement of RNA expression levels for thousands to tens of thousands of unique transcripts simultaneously. Microarray analysis is based upon hybridization between sequences of nucleic acids immobilized on a solid matrix and pools of fluorescently labeled cDNA representing experimental RNA populations (Duggan et al., 1999). Microarrays have been used in recent years to determine the underlying molecular mechanisms of various physiological and pathological processes (Duggan et al., 1999; Henriksen et al., 2002). In cancer research, cDNA microarrays have been used to generate transcription profiles or molecular phenotypes of human tumors in an effort to identify unique patterns of expression that might have prognostic or diagnostic value (Pollack et al., 2002).

Recently, microarrays have become an important tool in the evaluation of knockout mice. Investigators have used microarrays to study gene expression in knockout mice in order to discover previously unknown phenotypes and to identify possible pathways compensating for gene deletion (Chandrasekharan et al., 2002; Monti et al., 2001; Schlake et al., 2001). For example, mice deficient in the Src family kinase *Frk/rak* had no detectable phenotype in various organs and tissues examined (Chandrasekharan et al., 2002). However, microarray analysis identified an unexpected expression difference

in a small subset of genes regulated by thyroid hormone in *Frk/rak*$^{-/-}$ mice. These authors went on to detect significantly reduced levels of T3 (thyroid) hormone in these knockout mice. Also, as determined by array analysis, *Frk/rak*$^{-/-}$ mice had increased c-*src* expression in intestinal tissue. Epithelial organs such as the intestine show the highest level of endogenous *Frk/rak* expression, yet these organs had no overt phenotype in *Frk/rak*$^{-/-}$ mice. The authors suggest that increased expression of c-*src*, a related *Frk/rak* family member, may act to compensate for loss of *Frk/rak*. In other cases, microarrays have been used to examine possible molecular mechanisms of previously identified phenotypes in mutant mice. For example, tissue from mice with a mutation of the *Whn* gene (nude mice) was examined to identify differentially expressed genes related to alopecia in the skin of these mice (Schlake et al., 2001). This study discovered numerous differentially expressed genes that are thought to be involved in hair follicle formation. Several uncharacterized genes were differentially expressed in the skin of nude mice, but their biological functions are unknown.

Given the utility of array analysis in the evaluation of knockout mice, gene expression was examined in the ischemic hindlimb of *Fgf2*$^{+/+}$ and *Fgf2*$^{-/-}$ using a microarray consisting of 15,000 cDNA clones (Figure 5.1). This was done in order to identify distinct gene expression patterns during revascularization in the presence and absence of endogenous FGF2. The overall goal of this comparison was to (1) discover genes or pathways regulated by FGF2 during ischemic revascularization, (2) identify potential candidate molecules that may act to compensate for the absence of FGF2, and (3) possibly identify the mechanism(s) of altered vascular reactivity in the FGF2

knockout hindlimb.

Methods

Experimental Design

The experimental design for the microarray study- in regard to the number of arrays and determining which samples should be paired on arrays- was based on incomplete block designs presented by Kerr et al. (Kerr et al., 2001a). This design allowed for a minimum number of microarrays, which was necessary because of the limited amount of RNA for each sample. Each timepoint (e.g., knockout ischemic day 3) consisted of a pooled RNA sample from 2 individual mice. These pooled samples were used to generate fluorescently labeled cDNA, which was hybridized to microarrays according to the scheme shown in Figure 5.2. In Figure 5.2, each arrow represents one single microarray. For example, the arrow indicated by an asterisk (*) represents hybridization to a single array with the WT day 3 cDNA sample labeled with "green" fluorescent dye and the WT normal cDNA sample labeled with "red" fluorescent dye. A total of 7 microarrays were used in this design, with each sample hybridized to at least two arrays and also each sample was labeled at least once with each of the fluorescent dyes. The microarray hybridizations were as follows: (K=knockout, W=wildtype, N=non-ischemic, 3= day 3 ischemic, 7= day 7 ischemic)

K7 (green) versus KN (red)

KN (green) versus K3 (red)

WN (green) versus KN (red)

W7 (green) versus K7 (red)

K3 (green) versus W3 (red)

W3 (green) versus WN (red)

WN (green) versus W7 (red)

cDNA Microarrays

Microarrays were prepared within the Genomic Research Laboratory at the University of Arizona. Arrays were generated on coated glass slides (2% solution of 3-aminopropyltrimethoxysilane in 95% EtOH) using a Virtek ChipWriter microarray-printing robot. The cDNA clones used to make these arrays are from the National Institute on Aging (NIA) 15K cDNA set, which was derived from embryonic and fetal cells and tissues (Tanaka et al., 2000). DNA elements to be printed onto the microarray slides consisted of purified PCR-amplified inserts (100 µl reaction/clone) utilizing primer pairs specific to the M13 sequences flanking each insert. DNA inserts were suspended in 50% DMSO at approximately 300 ng/ml in 384-well plates. Each clone was printed in duplicate onto the coated slides in a 45% humidified chamber with individual spots averaging 130 µm in diameter and separated by 160 µm center-to-center. Microarrays were stored in a desiccator at room temperature until ready for use.

RNA Isolation

The muscles of the calf were excised, minced, and submerged in RNA*later* (Ambion). Prior to RNA isolation, tissue was removed from RNA*later* by centrifugation. RNA isolation was performed according to the protocol provided with RNA Bee (Tel-Test, Inc.). Briefly, the tissue was placed in a 6 ml round-bottom tube and RNA Bee was

added at 2 ml per 100 mg. Using a tissue homogenizer, tissue was ground in RNA Bee to free RNA from cells. The homogenized mixture was then added to a 2 ml Phase Lock Gel (Eppendorf) tube to provide a stable barrier between the organic phase and the nucleic-acid aqueous phase. Chloroform was added at 200 µl per 2 ml of RNA Bee solution. The tube was shaken for 15 seconds and centrifuged at 12,000 x g for 15 minutes at 4 °C. Upon completion of centrifugation, the aqueous layer was decanted and placed in a fresh tube. An equal volume of 100% isopropanol was added and mixed by inverting the tube several times. The tube was again placed in the centrifuge and spun for 15 minutes to pellet the RNA. The pellet was briefly washed with a 70% EtOH solution. EtOH was removed and the pellet was allowed to air dry during which time any residual EtOH evaporated. The pellets were then resuspended in nuclease-free water to a final concentration of 2-2.5 µg/µl. Following this isolation, RNA samples from 2 animals per timepoint were combined to yield a pooled RNA sample. This was necessary in order to have the required amount of RNA needed for the microarray experiments. Quantity and quality of RNA was determined by spectrophotometry (typically $\geq$ 2 µg/µl concentration and a 260/280 ratio $\geq$ 1.6). Also, approximately 2 µg of RNA from each pooled sample was run on an agarose gel to check for RNA degradation.

DNA Synthesis, Labeling, and Hybridization

Total RNA (15 µg) from each pooled sample was reversed transcribed into cDNA using EndoFree RT (Ambion) during which amino-allyl modified dUTPs were incorporated. To increase signal, reactions were run for 2 hours at 42 °C. After 2 hours,

samples were denatured at 95 °C for 5 minutes and immediately transferred to ice. Base hydrolysis of remaining RNA was performed by addition of 8.6 µl of 1M NaOH and 8.6 µl of 0.5M EDTA, pH 8, and incubated at 65 °C for 15 minutes. The solution was neutralized by adding 8.6 µl of 1M HCl.

Amino-allyl modified cDNA was purified using PCR purification columns (Qiagen). cDNA samples were brought up to 100 µl with Milli-Q H_2O to which 500 µl of Buffer PB was added. The PCR purification protocol was followed exactly, with the exception of substituting 75% EtOH for Buffer PE as a wash solution. cDNA was eluted off the column by using Milli-Q H_2O with a pH of 8.0.

After cDNA purification, samples were dried to 1-2 µl by vacuum centrifugation. Samples were then resuspended in 3 µl of sodium bicarbonate ($NaHCO_3$; 25 mg/ml). Lyophilized Alexa dyes 546 "green" and 647 "red" (Molecular Probes) were diluted in 250 µl of DMSO, of which 5 µl of the appropriate dye were added to the cDNA/$NaHCO_3$ solution. The solution was allowed to sit in the dark for 1 hour. After 1 hour the samples were brought up to 50 µl, after which the samples labeled with 546 and 647 were combined and purified as described above, the only exception being that one extra wash with 75% EtOH was administered. To the eluate, an equal volume of 2X hybridization buffer (8X SSC, 60% Formamide, 0.2% SDS) was added along with 10 µg of Cot-1 DNA and 10 µg of poly dA. This solution was applied to a microarray slide using a GeneTac hybridization station (Genomic Solutions) and hybridized at 47°C overnight. The slides were washed using two wash solutions (1X SSC, 0.1% SDS and 0.1X SSC,

0.01% SDS) by passing the solutions over the slides. Finally, slides were rinsed in 0.1X SSC and dried.

Scanning of Array

Hybridized slides were scanned using a white light/CCD based scanner (ArrayWorX). Random areas of the slide were examined to determine proper exposure for each channel. Once exposure times were established, the printed region was scanned and the data was collected. Using the spot finding analysis software (MolecularWare), signal intensities for each spot were calculated including a correction for background intensity. From that data, location-specific signal intensities across the slide were generated.

Data Analysis

A multivariate statistical approach was used in the analysis of the microarray data. This approach enables analysis of a variety of variables (e.g., time course, treatment, condition, genotype, etc) and takes into account the many sources of experimental variance in the microarray data (e.g., array variation, dye performance, etc). This approach is based on an analysis of variance (ANOVA) statistical model originally presented by Churchill and colleagues with custom modifications to the best-fit algorithm (Kerr et al., 2000; Kerr et al., 2001b). This algorithm permits a robust characterization and classification of the data as well as provides outputs of residuals and other statistical parameters as references for users. Overall, the ANOVA based analysis 1) allows

normalization of the array data, 2) estimates relative changes in gene expression, 3) corrects for confounding effects, 4) allows statistical evaluation of the array data, and 4) provides the framework for the overall experimental design. Once the data was reduced and evaluated using the ANOVA model, expression values were clustered using a hierarchical clustering algorithm developed in the laboratory. Genes were clustered based on their expression pattern across each of the timepoints/samples.

Results

Of the approximately 15,000 genes represented on the mouse array, a total of 1985 genes were detected as determined by the ANOVA analysis. Of those 1985 genes, the ANOVA model selected 184 that were differentially expressed between at least two of the timepoints/samples examined. The selection criteria for the ANOVA model required that 1) the gene show up on a sufficient number of arrays, 2) at least a 2-fold change in intensity was required between at least two of the samples, and 3) this difference had to pass a statistical threshold (95% confidence level). These 184 genes were grouped based on expression patterns across each of the samples using a hierarchical clustering algorithm. Figure 5.4 shows the expression profile for a selected set of genes. Each relative expression value for a sample can be compared to all the other samples/timepoints for an individual gene. In Figure 5.4, the expression values for each gene are relative to the expression for that same gene in the wildtype non-ischemic sample. For example, CINP (panel A) expression is lower in day 3 & 7 ischemic samples versus non-ischemic (both wildtype and knockout). A value of zero is interpreted to mean no difference in expression from the wildtype non-ischemic value. Related to clustering, genes represented in panels A and B (Figure 5.4) have similar profiles and were grouped with 37 other genes showing related expression changes (cluster 2; Figure 5.5). Likewise, genes shown in panels C and D were grouped together based on the likeness of their expression profiles (cluster 5).

Hierarchical clustering generated a total of 12 clusters comprised of the 184 genes, with groups ranging in size from 39 genes to as small as 4 genes. Cluster 2, the

largest group, is characterized by higher expression in the non-ischemic tissue, with lower expression in the day 3 and day 7 ischemic samples. Also, the *Fgf2*$^{+/+}$ and *Fgf2*$^{-/-}$ responses were the same or similar in this cluster of genes. Clusters 1 and 3 show a similar pattern of expression with reduced expression in the ischemic tissues, and the majority of genes behave similarly between wildtype and knockout samples. Within cluster 1, many of genes display reduced expression in the *Fgf2*$^{-/-}$ sample at day 7 as compared to the *Fgf2*$^{+/+}$ day 7 sample. Cluster 4 is made up of genes upregulated specifically at day 7 in both the wildtype and knockout samples, while cluster 5 is comprised of genes with higher expression at day 3 only. Interestingly, the genes in cluster 5 show lower expression in the knockout non-ischemic tissue as compared to the wildtype non-ischemic sample. Several of the other clusters illustrate differential gene expression between the *Fgf2*$^{+/+}$ versus *Fgf2*$^{-/-}$ samples in either the non-ischemic or ischemic tissues (e.g., cluster 6, 10, & 11).

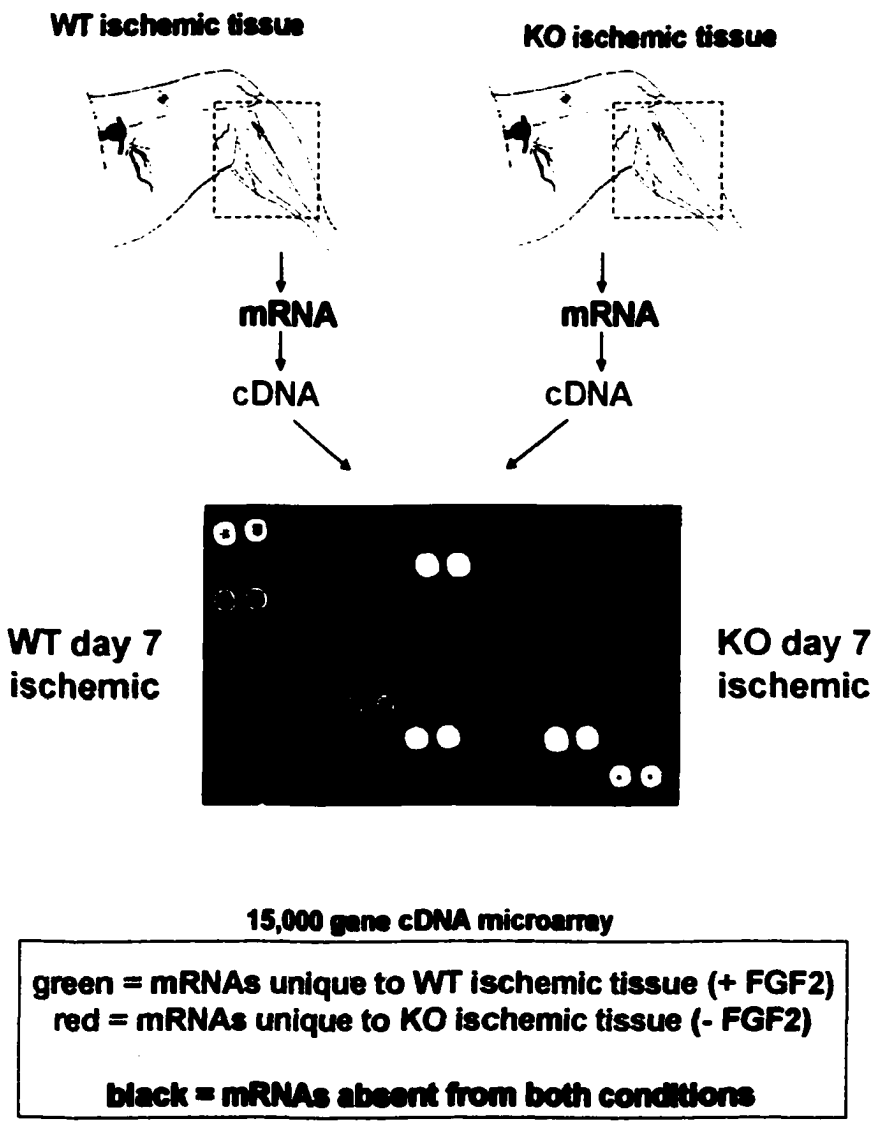

Figure 5.1 Gene expression in the ischemic hindlimb was examined in *Fgf2*$^{+/+}$ and *Fgf2*$^{-/-}$ using a cDNA microarray consisting of 15,000 clones. This was done in order to identify distinct gene expression patterns during revascularization in the presence and absence of endogenous FGF2. RNA from samples was reverse transcribed into cDNA, labeled with fluorescent dye, and then hybridized to cDNA microarrays.

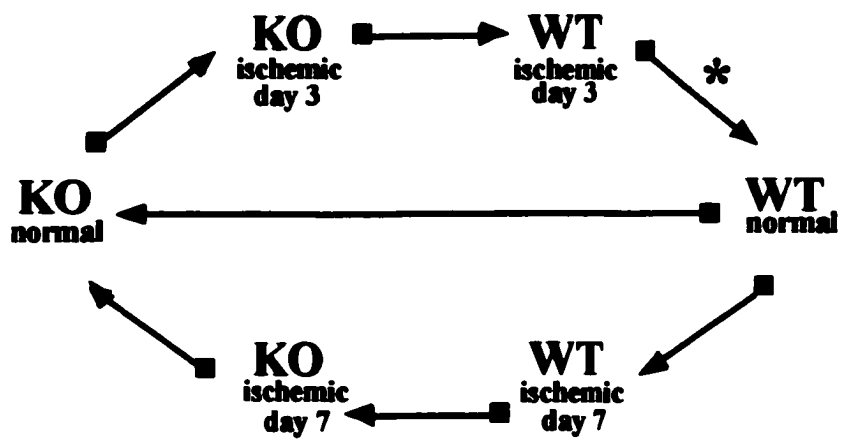

Figure 5.2 Experimental design utilized in this study, based on 6 varieties or samples and minimizing the number of microarrays required due to limited RNA for each sample. This is an incomplete block design and is discussed in detail by Kerr et al. 2001. Each arrow represents one single microarray. For example, the arrow indicated by an asterisk (*) represents a hybridization on a single array with WT day 3 sample labeled with "green" fluorescent dye and WT normal labeled with "red" fluorescent dye. A total of 7 microarrays are used in this incomplete block design, with each sample hybridized to at least two arrays and each sample is labeled at least once with each fluorescent dye.

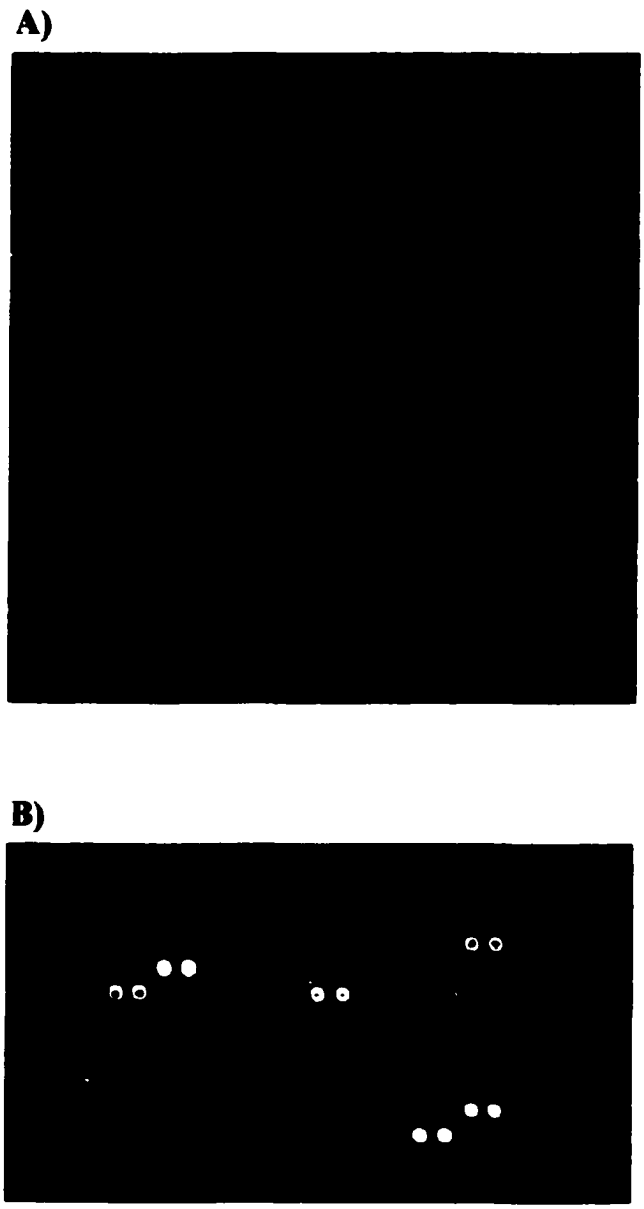

Figure 5.3 A) Example image of scanned microarray showing approximately 1/3 of total slide surface of the 15K mouse array. B) Close-up image of hybridized microarray.

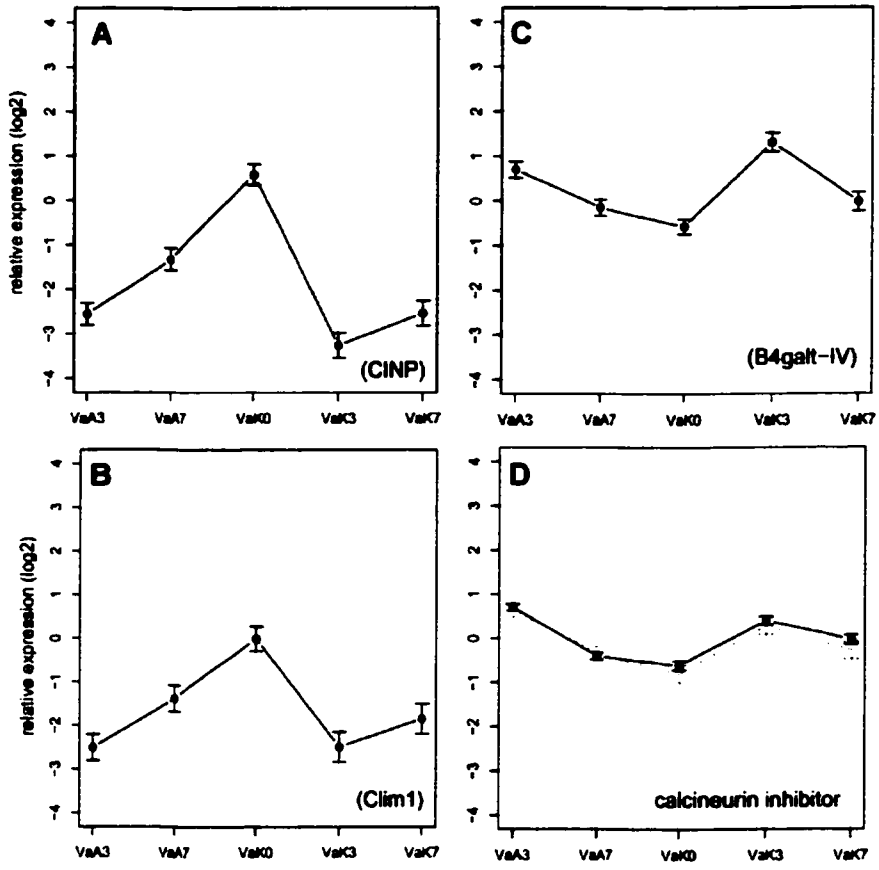

Figure 5.4 Relative expression values (profile) for several example genes as estimated from the ANOVA model. A) Homo sapiens HeLa cyclin-dependent kinase 2 interacting protein (CINP), mRNA; B) Mus musculus carboxyl terminal LIM domain protein 1 (Clim1), mRNA; C) Mus musculus beta-1,4-galactosyltransferase IV (B4galt-IV), mRNA; D) Mus musculus calcineurin inhibitor mRNA. Each expression value for a given sample can be compared to all the other samples/timepoints. Expression values for each gene are relative to the expression for that gene in the wildtype non-ischemic sample. For example, CINP (panel A) expression is lower in day 3 & 7 ischemic samples versus non-ischemic. A value of zero is interpreted to mean no difference in expression from the wildtype non-ischemic value. Abbreviations: wildtype day 3 ischemic (A3), wildtype day 7 ischemic (A7), knockout non-ischemic (K0), knockout day 3 ischemic (K3), knockout day 7 ischemic (K7). Based on similar expression profiles, genes represented in panels A & B were grouped together (cluster 2) using hierarchical clustering. Similarly, genes in panels C & D were grouped together in cluster 5.

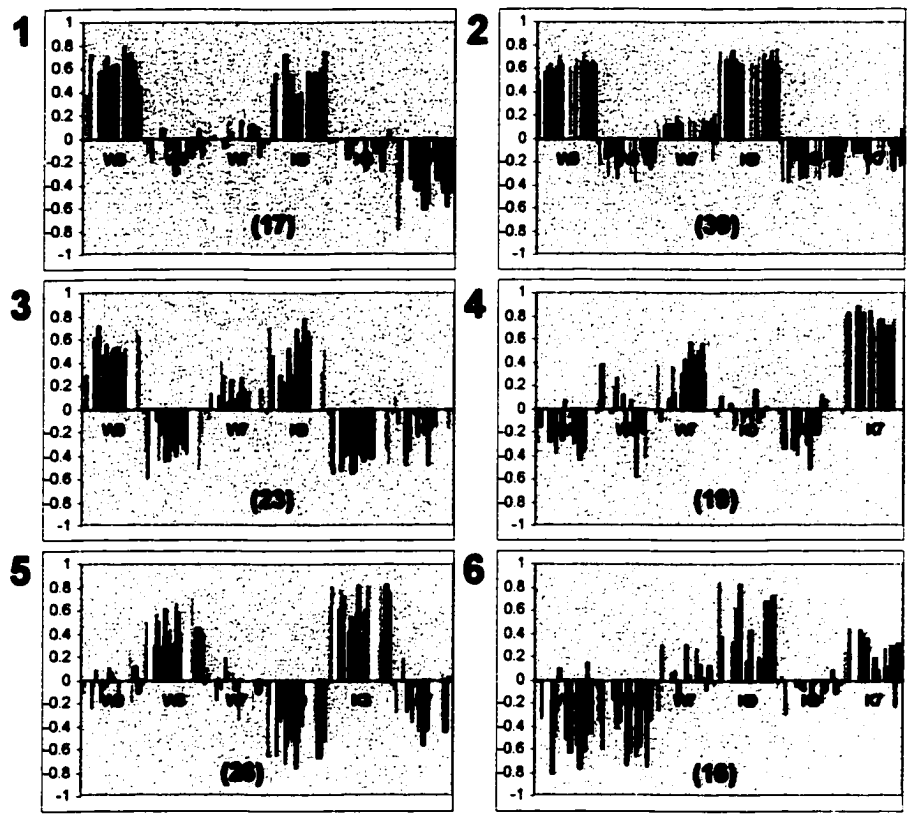

Figure 5.5 Results from hierarchical cluster analysis of the 184 genes identified from the ANOVA modeling. Shown are clusters 1-6. Individual gene names or accession numbers are shown in corresponding tables. Abbreviations: wildtype non-ischemic (W0), wildtype day 3 ischemic (W3), wildtype day 7 ischemic (W7), knockout non-ischemic (K0), knockout day 3 ischemic (K3), knockout day 7 ischemic (K7). Each colored bar represents normalized (mean-centered) expression values for a single gene. The total number of genes in each cluster is shown parentheses.

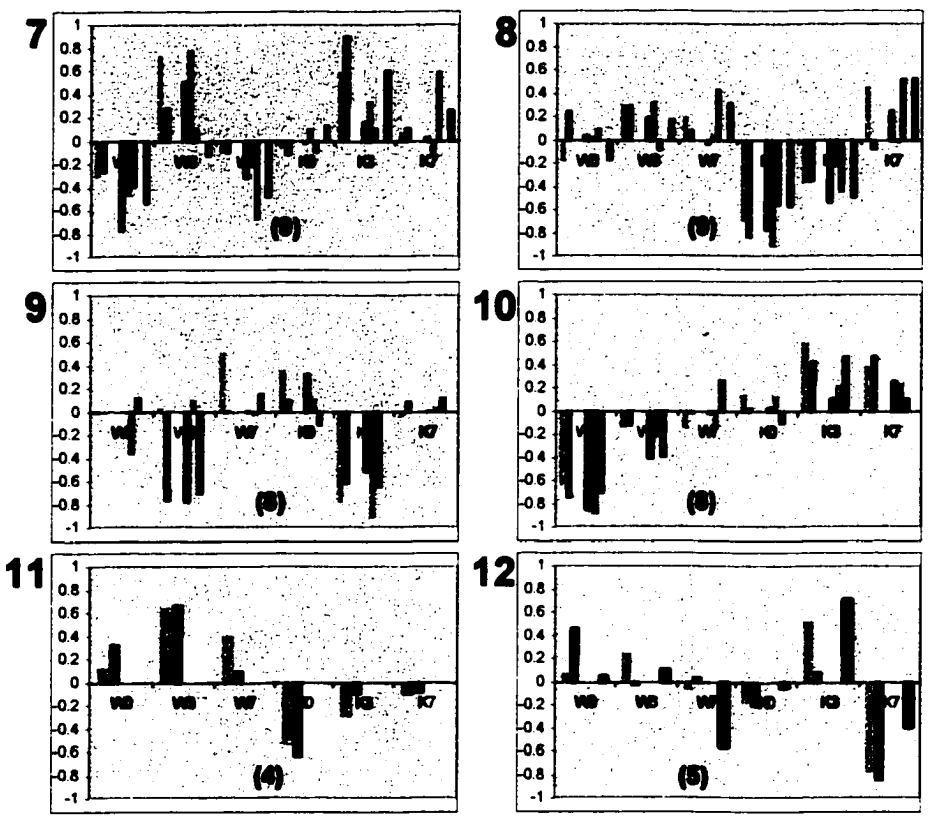

Figure 5.6 Shown are clusters 7-12. Individual gene names or accession numbers are shown in corresponding tables. Abbreviations: wildtype non-ischemic (W0), wildtype day 3 ischemic (W3), wildtype day 7 ischemic (W7), knockout non-ischemic (K0), knockout day 3 ischemic (K3), knockout day 7 ischemic (K7). Each colored bar represents normalized (mean-centered) expression values for a single gene. The total number of genes in each cluster is shown parentheses.

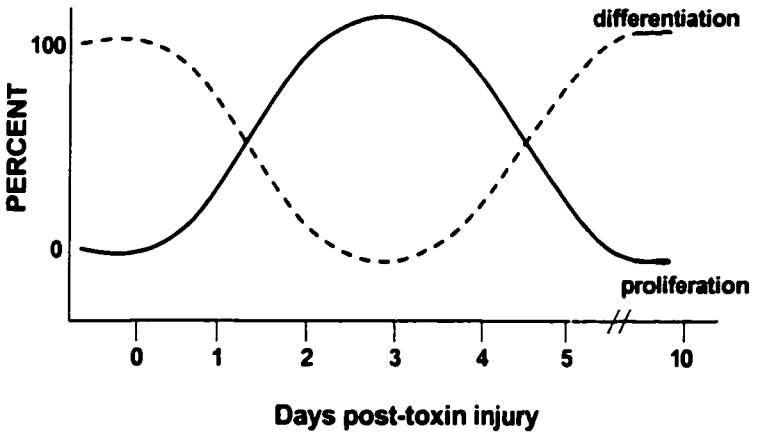

Figure 5.7 Schematic diagram showing the temporal pattern of satellite cell proliferation and myofiber differentiation following toxin induced regeneration of adult mouse skeletal muscle. (Adapted from Hawke & Garry, 2001)

Table 5.1 Cluster 1

Gene name or GenBank accession number
AW556756
BG074202
Mus musculus glyceraldehyde-3-phosphate dehydrogenase (Gapd), mRNA
Z3002B11
Mus musculus glyceraldehyde-3-phosphate dehydrogenase (Gapd), mRNA
AW551176
Mus domesticus strain MilP mitocondrion genome, complete sequence
Mus musculus testis RNA binding protein MSY4 mRNA, complete cds
Mus musculus flap structure specific endonuclease 1 (Fen1), mRNA
Mus domesticus strain MilP mitocondrion genome, complete sequence
BG071910
Mus musculus transcription complex subunit NF-ATc4 (Nfatc4)
Mus domesticus strain MilP mitocondrion genome, complete sequence
Mus domesticus strain MilP mitocondrion genome, complete sequence
Mus musculus glyceraldehyde-3-phosphate dehydrogenase (Gapd), mRNA
Mus musculus microtubule-actin crosslinking factor (Macf) mRNA, complete cds
BG065404

Table 5.2 Cluster 2

Gene name or GenBank accession number
Mus musculus scmh1 mRNA for sex comb on midleg homolog protein, complete cds
Human RNA polymerase II subunit (hsRPB8) mRNA, complete cds
Z3002A02
Mus musculus replication factor C, 140 kDa (Recc1), mRNA
Mus musculus hypothetical protein (Yr29-pending), mRNA
Homo sapiens from HeLa cyclin-dependent kinase 2 interacting protein (CINP), mRNA
Mus domesticus strain MilP mitocondrion genome, complete sequence
BG070783
AU022550
AU016199
BG076049
Mus domesticus strain MilP mitocondrion genome, complete sequence
Mus musculus carboxyl terminal LIM domain protein 1 (Clim1), mRNA
Homo sapiens insulin receptor tyrosine kinase substrate (LOC55971), mRNA
Mus musculus Cdc42 GTPase-inhibiting protein (Cdgip-pending), mRNA
Mus musculus bone morphogenetic protein (Bmp-1) mRNA, complete cds
Mus domesticus strain MilP mitocondrion genome, complete sequence
Mus domesticus strain MilP mitocondrion genome, complete sequence
Mus musculus glyceraldehyde-3-phosphate dehydrogenase (Gapd), mRNA
AU045206
Mus domesticus strain MilP mitocondrion genome, complete sequence
Mouse mRNA for murine CXCR-4, complete cds
Mus domesticus strain MilP mitocondrion genome, complete sequence
Mus domesticus strain MilP mitocondrion genome, complete sequence
Mus domesticus strain MilP mitocondrion genome, complete sequence
BG067190
AU024393
Homo sapiens p45SKP2-like protein mRNA, complete cds
Murine mRNA for integrin beta subunit
BG071256
AW549112
Mus domesticus strain MilP mitocondrion genome, complete sequence
Human ATP synthase beta subunit (ATPSB) gene, complete cds
BG073995
Mouse placental lactogen I (PL-I) mRNA, complete cds
Mus domesticus strain MilP mitocondrion genome, complete sequence
Mus musculus tetratricopeptide repeat domain (Ttc3), mRNA
Mus musculus EIG-1 (Eig1), mRNA
AA410046

Table 5.3 Cluster 3

Gene name or GenBank accession number
Rattus norvegicus MG87 mRNA, complete cds
Mus musculus cytochrome c oxidase, subunit VIIc (Cox7c), mRNA
Mouse skeletal muscle beta tropomyosin mRNA, complete cds
AW558059
Mus musculus aldolase 1, A isoform (Aldo1), mRNA
Mus domesticus strain MilP mitocondrion genome, complete sequence
Mouse beta-tropomyosin 2 mRNA, complete cds
Mus domesticus strain MilP mitocondrion genome, complete sequence
Mus musculus programmed cell death 8 (apoptosis inducing factor) (Pdcd8), mRNA
Mus musculus melanoma X-actin (Actx), mRNA
Mouse tropomyosin isoform 2 mRNA, complete cds
Mus domesticus strain MilP mitocondrion genome, complete sequence
Homo sapiens signal sequence receptor, alpha (translocon-associated protein alpha) (SSR1), mRNA
AW548714
Homo sapiens ubiquinol-cytochrome c reductase binding protein (UQCRB), mRNA
Mus domesticus strain MilP mitocondrion genome, complete sequence
Mus musculus adenylate kinase 4 (Ak4), mRNA
Mus domesticus strain MilP mitocondrion genome, complete sequence
Mus domesticus strain MilP mitocondrion genome, complete sequence
Mus domesticus strain MilP mitocondrion genome, complete sequence
AW554651
Mus musculus Fc receptor, IgG, high affinity I (Fcgr1), mRNA
Homo sapiens mRNA; cDNA DKFZp434E033 (from clone DKFZp434E033)

Table 5.4 Cluster 4

Gene name or GenBank accession number
BG075076
BG068225
Homo sapiens BTB and CNC homology 1, basic leucine zipper transcription factor 1 (BACH1), mRNA
AW538984
C81187
Homo sapiens mRNA for KIAA1098 protein, partial cds
Mus musculus midnolin (Midn-pending), mRNA
BG062937
Mouse metallothionein-I (MT-I) gene, 5` end
Mus musculus toll/interleukin-1 receptor 8 (TIR8) mRNA, complete cds
BG071491
Mus musculus vacuolar adenosine triphosphatase subunit A gene, complete cds
Mus musculus monoclonal non-specific suppressor factor beta mRNA, complete cds
Mus musculus calcium channel, voltage dependent, alpha2/delta subunit 3 (Cacna2d3), mRNA
AW539304
AA410137
BG064969
M.musculus COL3A1 gene for collagen alpha-I
AW544146

Table 5.5 Cluster 5

Gene name or GenBank accession number
AW544238
AW544782
Human thermostable phenol sulfotransferase (STP2) gene, partial cds
AW542467
AW543494
Homo sapiens CGI-96 protein (CGI-96), mRNA
AW537514
BG067494
AW538653
Mus musculus ribosomal protein L23 (Rpl23) gene, complete cds
AW537120
Homo sapiens gene with variants near HD locus on 4p16.3 (RES4-22), mRNA
AW546256
AW558051
Mus musculus calcineurin inhibitor mRNA, complete cds, alternatively spliced
Mus musculus mRNA, complete cds
Mus musculus ribosomal protein S8 (Rps8), mRNA
Homo sapiens cDNA: FLJ23008 fis, clone LNG00455
AW557566
AW556849
Mus musculus hypoxanthine guanine phosphoribosyl transferase (Hprt), mRNA
BG074387
AW557939
Homo sapiens fatty-acid-Coenzyme A ligase, long-chain 3 (FACL3), mRNA
Mus musculus beta-1,4-galactosyltransferase IV (B4galt-IV), mRNA
BI076847

Table 5.6 Cluster 6

Gene name or GenBank accession number
BG076291
AW549180
Homo sapiens ADP-ribosylation factor-like 1 (ARL1), mRNA
AW558996
Mus musculus ribosomal protein S8 (Rps8), mRNA
Mouse beta-globin major gene
Mus musculus Sui1 homolog mRNA, complete cds
C79876
Mouse hexokinase mRNA, complete cds
BG063361
Mus musculus MRP S24 gene
BI076713
M.musculus DNA for alpha globin gene and flanking regions
Human polyadenylate binding protein (TIA-1) mRNA, complete cds
Human ATP synthase beta subunit (ATPSB) gene, complete cds

Table 5.7

Cluster 7
AW555437
M.musculus mRNA for ribosomal protein L5, 3`end
BG076316
Mus musculus synapsin I (Syn1), mRNA
Homo sapiens ephrin-A1 (EFNA1), mRNA
AW555711
AU023385
Mus musculus ribosomal protein S29 (Rps29), mRNA
Mouse ribosomal protein L7 (rpL7) mRNA, 5` end
Cluster 8
Human heparan sulfate-N-deacetylase/N-sulfotransferase mRNA, clone HSST3`, 3`UTR
Homo sapiens fetal Alzheimer antigen (FALZ), mRNA
Homo sapiens mRNA; cDNA DKFZp586J2118 (from clone DKFZp586J2118)
BG067165
Mouse mRNA for KIFC2, complete cds
BG071833
Homo sapiens HSPC015 protein (HSPC015), mRNA
Mus musculus vacuolar protein sorting 45 (yeast) (Vps45), mRNA
Mus musculus CPN10-like protein (Cpn10-rs1) gene, complete cds
Cluster 9
BG077400
AW555035
Mus musculus synapsin I (Syn1), mRNA
Mouse Y box transcription factor (MSY-1) mRNA, complete cds
Mus musculus ubiquitin B (Ubb), mRNA
M.musculus aspartate aminotransferase gene exon 10 and 3`-flank
HSP90=heat shock protein [mice, heart, mRNA Partial, 806 nt]
Mus musculus ribosomal protein S4, X-linked (Rps4x), mRNA

Table 5.8

Cluster 10
BG070422
Mus musculus ferritin light chain 1 (Ftl1), mRNA
Mus musculus elongation factor Tu (eEF-Tu, eEf-1-alpha) mRNA, complete cds
BG073317
Z3002C11
Mus musculus synapsin I (Syn1), mRNA
C78001
AW555492
Cluster 11
BG067252
BG072665
Homo sapiens F-box protein FBX29 (FBX29) mRNA, partial cds
Mus musculus KID1 (Kid1) mRNA, complete cds
Cluster 12
Homo sapiens TFIIB-related factor 2 mRNA, complete cds
AW537151
Z3002D12
Mus domesticus strain MilP mitocondrion genome, complete sequence
Z3002H01

Discussion

One of the primary goals of this study was to identify possible mechanism(s) of altered vascular reactivity in the FGF2 knockout hindlimb vasculature described in chapter 4. What has become evident is that the microarray analysis, as performed here, is probably not capable of examining vascular specific genes. Unfortunately, transcripts derived from skeletal myocytes, not vascular cells, dominate the RNA pools used in the array analysis. Therefore, the data obtained in this study most likely reflect gene expression related to the processes of myocyte regeneration rather than vascular growth and function. Thus, the goal of discovering the molecular mechanism of the *Fgf2*$^{-/-}$ hyperemia phenotype was not achieved in this analysis. Strategies that might improve the ability to measure vascular gene expression and to improve the overall design of this study will be discussed later.

Hindlimb ischemia, used typically to study vascular adaptation, is a model of ischemic-induced muscle injury. Myocyte loss via necrosis, and presumably apoptosis, occurs due to prolonged ischemia in the hindlimb (Carpenter, 1990; Hanzlikova et al., 1979; Jennische, 1986). Myocyte loss is followed by regeneration of myotubes from resident satellite cells (Hawke et al., 2001). Overall, the process of muscle generation proceeds in four phases: 1) proliferation of satellite cells, 2) fusion of myoblasts/satellite cells, 3) elongation of the developing myofiber/myocyte, and 4) circumferential growth of the muscle fiber (Allbrook, 1981; Hawke et al., 2001). The mouse hindlimb ischemia model is characterized by widespread regeneration in the calf musculature. However, histological examination shows small regions of uninjured muscle throughout the calf

(data not shown). The uninjured fibers have peripheral nuclei whereas regenerated fibers have characteristic centrally located nuclei (Figure 3.6; Chapter 3). Also, within some regions of regenerated fibers are small islands of presumably healthy myocytes, showing no histological signs of ischemic injury. The timecourse of regeneration is rapid in ischemic skeletal muscle, but the speed of regeneration may depend on how quickly blood flow is reestablished to the injured tissue (Allbrook, 1981; Jennische, 1986). In a model of hindlimb ischemia/reperfusion, invading macrophages and neutrophils rapidly (within 24-48 hours) phagocytized debris from necrotic myofibers (Jennische, 1986). This was followed by proliferation of satellite cells that remain in the intact basal lamina of the phagocytized fibers at 3 days after injury. Satellite cells also appeared to be derived from uninjured myocytes in and around the necrotic fibers. At 4 days post injury, satellite cells appeared to have fused, forming small immature muscle cells. Finally, by day 21 the regenerating muscle fibers had returned to normal size, but still had centrally positioned nuclei.

Thus, isolated RNA from the ischemic calf at days 3 and 7 after femoral ligation should capture gene expression related to proliferation and differentiation of the regenerating myocytes. Based on these previous studies, satellite cell proliferation and the inflammatory response clearing the debris from injured fibers are the primary events occurring in the calf musculature at day 3. Myocyte proliferation appears to be complete by day 7 since immature muscle fibers are evident throughout the calf (Figure 3.6; Chapter 3). Of course, endothelial cell proliferation is occurring in the ischemic hindlimb at day 7 (Figure 3.7; Chapter 3), but the small number of proliferating EC's- relative to

myocytes- is probably not contributing significantly to the RNA collected from the calf. Thus, gene expression in the calf at day 7 most likely reflects muscle growth (i.e., circumferential and longitudinal) and myocyte differentiation.

Clusters 1, 2, and 3 are all characterized by higher expression in non-ischemic state and lower expression in the ischemic state. These may be genes expressed in highly differentiated muscle (adult, non-ischemic calf) and are therefore not expressed in the regenerating musculature at day 3 and day 7. Genes upregulated selectively at day 3, (e.g., cluster 5) may be related to satellite proliferation or tissue remodeling. In contrast, genes showing higher expression at day 7 (Cluster 4) may be important during myocyte differentiation and/or growth of the existing myofibers. Given the presence of multiple cell types (myocytes, endothelial cells, smooth muscle cells, macrophages, etc.) in the extracted calf tissue, the specific cell type(s) contributing to the observed changes in gene expression cannot be determined.

Regarding FGF2 and gene expression, it is evident that the absence of FGF2 affects gene expression both in non-ischemic tissue and in ischemic tissue. For example, genes in cluster 5 appear to have lower expression in the *Fgf2*$^{-/-}$ non-ischemic group as compared to the wildtype non-ischemic group. In contrast, the genes represented by cluster 4 show similar expression at day 0 (non-ischemic) and day 3 between the genotypes. However, expression appears to be higher for this cluster in the knockout at day 7. The converse to this is cluster 1, which shows lower expression of this gene group selectively at day 7. The physiological significance of altered gene expression in the absence of FGF2 remains to be determined. No obvious defects were found in *Fgf2*$^{-/-}$

muscles examined via histology. No evaluation of skeletal muscle function, either ischemic or non-ischemic, of *Fgf2*$^{-/-}$ mice has been performed. Thus, *Fgf2*$^{-/-}$ mice could possibly have abnormalities in the musculature that are not detected from histological techniques. The question remains whether genes displaying lower gene expression are indicative of some impaired biological process in the knockout or whether higher expression reflects compensatory mechanisms in the absence of FGF2.

Overall, the lack of an obvious phenotype in the hindlimb of *Fgf2*$^{-/-}$ mice is at least partly supported by the array data, given that many of the 184 genes analyzed showed similar changes in the wildtype and knockout groups. Still, certain subsets of genes showed differential expression between the *Fgf2*$^{+/+}$ and *Fgf2*$^{-/-}$ hindlimbs. This suggests that FGF2 (or the absence of FGF2) is affecting certain events in the normal and ischemic calf musculature, since gene expression ultimately determines biological behavior. Also, it is interesting that those genes that are expressed at different levels in the ischemic *Fgf2*$^{-/-}$ limb as compared to ischemic *Fgf2*$^{+/+}$ limb are not necessarily altered in the non-ischemic limb (e.g., cluster 1). This observation may be interpreted to mean that FGF2 is affecting the expression of certain genes only in the ischemic or injured condition. This might be related to why the hyperemia phenotype in the *Fgf2*$^{-/-}$ mice is only observed in the ischemic limb. Nevertheless, future studies are required to determine the biological significance, if any, of these differences in gene expression in mice lacking FGF2.

Future studies

This study was RNA limited, which minimized the number of arrays and hybridizations that could be completed. RNA amplification allows for the generation of large amounts of RNA from a relatively small amount of starting tissue (Pabon et al., 2001). More RNA would allow for a more thorough analysis using another incomplete block design with more arrays and hybridizations. Each sample could be hybridized to at least 4 arrays as compared to the current use of only 2 arrays. Increased replication (i.e., samples hybridized to more arrays) in the experimental design allows improved analysis via the ANOVA model. RNA amplification offers other advantages since amplification apparently increases the likelihood of detecting low abundance or rare transcripts (Puskas et al., 2002). Importantly, this might improve the chances of identifying differences in expression of vascular related genes during hindlimb ischemia. Also, RNA amplification allows for RNA extraction from a single muscle group with a homogeneous response to the ischemic insult. The current method of isolating RNA from the entire calf means that tissues contributing to the pool of RNA vary from very ischemic muscle groups to relatively uninjured, non-ischemic muscle. This increases the likelihood of missing differentially expressed genes since the RNA pool is effectively diluted with non-ischemic muscle and tissue.

Reviewers of the research presented in Chapter 2 and 3 have expressed interest in the expression levels of the various FGF family members in the absence of endogenous FGF2. It is often assumed that increased expression of other *Fgf* genes is compensating for the loss of FGF2. Given the large number of FGFs and related proteins, microarray analysis would be useful to address the possibility of compensation in FGF knockout

mice. Unfortunately, the 15K mouse array used in this study contained sequences for only *Fgf1*, *Fgf2*, *Fgfr1*, and *Fgfr2*. It also contained a few FGF related proteins and FGF binding proteins, such as *Frag1* and *Fgfrp*. Interestingly, none of these genes were among the 1985 genes initially detected in the array analysis. It is possible that these genes were simply not expressed at sufficient levels to be captured in the array analysis.

Conclusion

This microarray study demonstrates that gene expression is affected by the absence of FGF2 in both non-ischemic and ischemic tissue of the hindlimb. FGF2 may have important functions during the ischemic response in the mouse hindlimb.

6. CONCLUSIONS AND DISCUSSION

Three research aims were undertaken in order to identify the function of FGF2 during disease-related vascular growth and adaptation in the adult animal. A summary of the results from these experiments is shown in Table 6.1. Overall, these observations support at least two important conclusions in regard to the role of FGF2 during vascular remodeling. (1) Endogenous FGF2 is not required for growth and adaptation during flow-dependent remodeling or ischemic revascularization. (2) During ischemic revascularization, endogenous FGF2 may regulate vascular reactivity in the collateral and collateral-dependent circulation. The lack of impaired vascular growth in these experiments was somewhat surprising given the amount of previous research establishing FGF2's importance in this area. The identification of FGF2 as a "functional" factor (i.e., affecting vessel responsiveness) in the collateral circulation suggests a novel, non-mitogenic role for endogenous growth factors during ischemic revascularization.

Impaired Hyperemia in the Ischemic Hindlimb of FGF2 Knockout Mice

Reactive hyperemia was significantly impaired in the ischemic, but not the non-ischemic, hindlimb of *Fgf2*$^{-/-}$ mice. This finding taken together with the results from chapter 3, suggest that reduced vascular reactivity is the likely cause of the hyperemia phenotype observed in *Fgf2*$^{-/-}$ mice. Thus, FGF2 appears to have an uncompensated activity in the peripheral vasculature of only ischemic or actively repairing tissues. This is consistent with other studies indicating that FGF2 is important during pathology-related

Table 6.1: Summary of research results comparing *Fgf2*+/+ (WT) and *Fgf2*-/- (KO) mice.

Observation	Chapter
Equivalent remodeling responses in carotid arteries of WT and KO mice (outward remodeling and inward remodeling)	2
Vascular cell proliferation and apoptosis was not different in remodeling carotid arteries of KO mice as compared to WT mice	2
Equal changes in capillary density in the ischemic limbs of WT and KO mice (angiogenesis)	3
Similar changes in cell proliferation in the ischemic hindlimb of WT and KO mice	3
Equal changes in arteriole density in the ischemic limbs of WT and KO mice	3
Equivalent changes in angiographic score in thigh of revascularizing hindlimbs of WT and KO (arteriogenesis)	3
No difference between WT and KO mice in terms of terms of skeletal muscle fiber size within the ischemic calf (muscle regeneration)	3
Impaired hyperemia response in ischemic limb of KO mice. No difference in the hyperemia response between non-ischemic WT and KO mice	4
Differential gene expression in the ischemic hindlimb in the absence of FGF2	5

situations in the adult (Cuevas et al., 1996; Ortega et al., 1998; Schultz et al., 1999; Yoshimura et al., 2001).

As described in Chapters 4, exogenous FGF2 can alter the function of collateral arteries and collateral-dependent microvessels, possibly independent of its mitogenic activity. Although FGFs are primarily thought of as growth regulators or proliferative agents, many studies have demonstrated non-mitogenic activities of these proteins (Bauters, 1997; Cuevas et al., 1991; Cuevas et al., 1996; Cuevas et al., 1997a; Cuevas et al., 1997b; Meurice et al., 1997). A primary example is in the ability of exogenous FGFs to protect the myocardium from ischemia-reperfusion injury (Cuevas et al., 2002). Numerous studies show that FGF1 and FGF2 are able to improve mechanical function of the heart and reduce myocardial injury during brief periods of ischemia and reperfusion (Cuevas et al., 1997b; Padua et al., 1995; Padua et al., 1998). The effects of FGFs during cardioprotection may be mediated by ATP-sensitive K^+ channels or activation of inducible nitric oxide synthase (iNOS or NOS2) (Cuevas et al., 2002; Hampton et al., 2000). In ex-vivo hearts subjected to 30-min of ischemia followed by reperfusion, FGF2-induced cardioprotection was blocked by chelerythrine, a specific protein kinase C (PKC) inhibitor (Jiang et al., 2002). Importantly, myocardial protection in these studies is independent of flow modulation by FGF2 (Padua et al., 1998). This was examined since FGFs have direct vasoactive effects *in vivo* (Cuevas et al., 1991; Kadota et al., 1995). Interestingly, a non-mitogenic form of FGF1 had the same cardioprotective effects as native FGF1 and FGF2 in rat hearts exposed to 10 minutes of ischemia followed by reperfusion (Cuevas et al., 1997b). Further, non-mitogenic FGF1 prevented cardiac

myocyte apoptosis and decreased neutrophil accumulation in a similar model of rat ischemia/reperfusion injury (Cuevas et al., 1997c). These studies show that exogenous FGFs are capable of regulating various cellular activities, other than growth and proliferation, which protect myocytes from ischemic damage. Thus, it is possible that endogenous FGF2 acts in a similar manner to protect vascular cells from ischemic injury during the early phases of ischemic revascularization.

It would be interesting to test the hypothesis that endogenous FGF2 protects vascular cells from ischemic damage, which in turn affects vascular function. Measuring the structural integrity and vascular reactivity of arterial vessels in skeletal muscle exposed to short duration ischemia (minutes to hours), and comparing the responses of $Fgf2^{+/+}$ and $Fgf2^{-/-}$ mice, tests this hypothesis. This hypothesis predicts that the vasculature of $Fgf2^{-/-}$ mice would be less reactive following the ischemic insult. The short duration of ischemia should eliminate the possibility that FGF2 is having a mitogenic or vascular growth effect.

It is possible that revascularization was more rapid during the first few days of ischemia in the wildtype mice. This would lessen the ischemic insult on the endothelium and smooth muscle, perhaps making the wildtype vasculature more responsive during reactive hyperemia at day 14. However, results did not show evidence of a difference in the time course of revascularization when comparing genotypes. $Fgf2^{+/+}$ and $Fgf2^{-/-}$ mice had equal resting perfusion at day 3 after femoral occlusion. Also, the extent of myocyte injury and regeneration did not appear different between $Fgf2^{+/+}$ and $Fgf2^{-/-}$ mice, indicating that recovery of perfusion was similar. Of course, the present studies do not

rule out that perfusion recovery was altered before day 3 in the ischemic limbs of *Fgf2*$^{-/-}$ mice.

As outlined in Chapter 4, further studies are required to eliminate the possibility that the *Fgf2*$^{-/-}$ hyperemia defect reflects an anatomical impairment. Direct measurements of vessel responses in the ischemic hindlimb will provide the best evidence that vascular reactivity is impaired during revascularization in *Fgf2*$^{-/-}$ mice. Nevertheless, this potential non-mitogenic function of endogenous FGF2 may be important in ischemic responses of many tissues, including the brain, heart, skeletal muscle, and kidney.

Remodeling and Revascularization in FGF2 Knockout Mice: Compensation by Other FGFs?

The absence of particular phenotypes in FGF knockout mice is often attributed to compensation by other FGF proteins. Consequently, some might ascribe the lack of detectable growth-related phenotypes in the experiments presented in this dissertation to compensation by FGFs or other vascular growth factors. It is believed that there is some degree of redundancy in the FGF/FGFR system (Ornitz et al., 2001; Powers et al., 2000). This assumption is partly based on the observation that certain sub-groups of FGFs have overlapping expression patterns and similar binding specificities for the FGFRs. Also, there is no one-to-one correspondence between the FGF ligands and the FGF receptors. In mice, there are 22 identified FGF ligands and only 10 or so FGFR isoforms (Ornitz et al., 1996). This is interpreted to indicate that functional redundancy may exist between FGF proteins. Also, the relatively mild phenotype in many of the FGF knockout mice is

taken to mean that there is compensation by related FGF proteins. However, the FGF members are quite varied in terms of expression pattern, receptor specificity, and protein structure (Ornitz et al., 2001). This diversity may limit the functional redundancy between FGFs. In fact, only a portion of the FGFs have a closely related family member, as is the case with FGF1 and FGF2. LMW FGF2 and FGF1 share approximately 55% amino acid sequence identity, and these proteins have several unique characteristics in common (Coulier et al., 1997). For example, similar to LMW FGF2, FGF1 is released from cells despite lacking a signal sequence for secretion (Jackson et al., 1992; Prudovsky et al., 2002). Like HMWFGF2, FGF1 has a nuclear localization signal in the 5' end and is localized in the nucleus (Cao et al., 1993). Unlike many of the other FGF proteins, FGF1 and FGF2 are detected in nearly all tissue in the adult animal, including skeletal muscle (Bikfalvi et al., 1997; Miller et al., 2000). Further, FGF1 has the ability to promote angiogenesis and vascular growth *in vitro* and *in vivo* (Friesel et al., 1995; Nabel et al., 1993; Sellke et al., 1996; Winkles et al., 1987).

The similarities between FGF1 and FGF2 have led to the hypothesis that these two proteins comprise a redundant pair of FGFs. Thus, FGF1 is the most likely molecule acting to compensate for the loss of FGF2 in the studies presented in this dissertation. *Fgf1* mRNA was detected in ischemic and non-ischemic calf tissue, but ischemia did not increase *Fgf1* transcripts in wildtype mice (Figure 6.1).

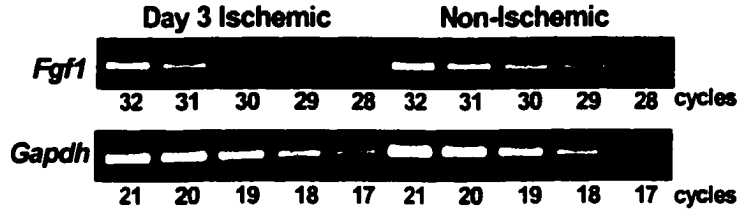

Figure 6.1 Relative *Fgf1* mRNA expression by RT-PCR in ischemic and non-ischemic (contralateral) hindlimbs of *Fgf2*$^{+/+}$ mice. Shown are representative results 3 days following left femoral artery ligation. Aliquots of the amplification reaction were removed during sequential cycles and gel electrophoresed. *Gapdh* serves to control for cDNA template quantity and linear amplification.

It is unknown whether *Fgf1* mRNA levels were upregulated in ischemic skeletal muscle of FGF2 knockout mice. Selective upregulation of FGF1 only in the knockout ischemic limb would imply that FGF1 is compensating for the loss of FGF2. However, the only way to directly test for redundancy between FGF1 and FGF2 in the hindlimb model is to repeat the experiments with *Fgf1-Fgf2* double knockouts. Identification of a phenotype (e.g., impaired arteriogenesis) in the double mutant that is absent in both single knockouts would directly demonstrate redundancy/compensation between these FGFs.

Investigators have generated mice deficient in both FGF1 and FGF2 (Miller et al., 2000). The *Fgf1-Fgf2* double knockouts were made in order to test the hypothesis that the lack of any obvious phenotype in $Fgf1^{-/-}$ mice was due to compensation by FGF2, while the relatively mild phenotype observed in $Fgf2^{-/-}$ mice was due to an overlapping role of FGF1. It was predicted that the double knockouts would have more severe abnormalities than the single knockout animals or that novel defects might be present only in the double knockouts. However, the double mutants had the same phenotype as FGF2 knockout mice when examining wound healing, neural development, and hematopoiesis. This demonstrates that compensation between FGF1 and FGF2 does not explain the unexpected lack of severe phenotypes in the single knockout mice. Of course, this study does not eliminate the possibility that other FGFs or factors are compensating for the loss of either FGF1 or FGF2. Alternatively, these experiments can be interpreted to mean that FGF1 and FGF2 have very specific and limited functions in development and in adult homeostasis. Lack of a knockout phenotype may simply mean that the respective FGF is not an endogenous regulator of a particular biological process.

FGF1 is not the only FGF member that might compensate for the loss of FGF2. Multiple FGFs, in addition to FGF1, have the ability to stimulate angiogenesus, including FGF3 (int-2), FGF4 (hst-1), FGF5, and FGF8 (Costa et al., 1994; Giordano et al., 1996; Mattila et al., 2001; Yoshida et al., 1994). Of these, only FGF4 and FGF5 expression are detected in adult skeletal muscle of various species (McGeachie et al., 2001; Mitchell et al., 1999). Consequently, these latter FGFs may be considered as potential candidates to compensate for the absence of FGF2 during ischemic revascularization. FGF4 appears to bind the FGFRs with a similar specificity as FGF2, while FGF5 does not (Table 1.2; Chapter 1). However, *Fgf4* and *Fgf5* mRNA expression were unaltered in various tissues examined from adult FGF2 knockout mice (Zhou et al., 1998). Interestingly, FGF6 is upregulated following skeletal muscle injury in adult mice, but FGF6 was shown to have very little angiogenic activity *in vitro* (Floss et al., 1997; Pizette et al., 1991).

At least one example of partial redundancy between FGF proteins has been documented using knockout mice. Cooperation between FGF8 and FGF17 has been shown during neural development in the mouse (Xu et al., 2000). Compared to *Fgf17*$^{-/-}$ mice, *Fgf17-Fgf8* double knockouts were more severely affected in terms of a decreased cell proliferation in the developing cerebellum and in terms of the size of the mature cerebellum (Xu et al., 2000). This study suggests that FGF8 acts to partially compensate for the absence of FGF17, since loss of FGF8 in the *Fgf17*$^{-/-}$ mice causes a worsening of the FGF17 null phenotype. In this study, *Fgf17*$^{-/-}$ mice had significant tissue loss in the cerebellum, despite the presence of endogenous FGF8. Thus, the presence of FGF8 only partially compensated for the loss of FGF17.

Much of our knowledge of the functions of the FGF proteins is based upon *in vitro* studies, in which exogenous FGF protein is applied to cells out of context of the biological system in which they have evolved. Numerous regulatory steps are likely absent in these *in vitro* systems, such as FGF binding proteins and HSPGs that are important in regulating bioavailability and ligand-receptor binding (Tassi et al., 2001; Whitelock et al., 1996; Yayon et al., 1991). Further, exogenous delivery of FGF protein eliminates transcriptional, translational, and secretory control over its bioavailability. For these reasons, *in vitro* studies that identify FGFs in numerous and sometimes overlapping biological processes need to be interpreted somewhat cautiously. *In vitro* experiments have been perhaps most useful in identifying a broad array of potential functions for FGFs. Recent knockout studies have allowed us to refine the roles of each of the FGFs, identifying the natural processes that are mediated by these growth factors in vivo, while eliminating their requirement in other biological events.

Whether or not compensation is the basis for the lack of vascular growth deficiencies in the *Fgf2*$^{-/-}$ mice is open to debate. Future studies using mice with multiple *Fgf* gene deletions may resolve this issue. Perhaps compensation is so widely accepted because this is the only interpretation of recent results from *Fgf2*$^{-/-}$ mice that does not completely invalidate over 15 years of research establishing the importance of FGF2 in vascular growth.

Differential Gene Expression in the Absence of FGF2

The microarray results presented in Chapter 5 show clear differences in gene expression when comparing the ischemic tissues of *Fgf2*$^{+/+}$ and *Fgf2*$^{-/-}$ mice. These results have the potential of providing information in regard to the action of FGF2 in ischemic tissue, but future studies will be required to identify the function of differentially expressed genes and to determine if structural or functional deficits may have gone undetected in the *Fgf2*$^{-/-}$ mice hindlimb. The altered gene expression in the ischemic muscle tissue of *Fgf2*$^{-/-}$ mice suggests the possibility that endothelial cell and/or smooth muscle cell gene expression could also be affected in the absence of FGF2. Further studies (discussed in the next paragraph) might allow a better evaluation of expression changes in the vessels of the revascularizing hindlimb. It is interesting that those genes that were expressed at different levels in the ischemic *Fgf2*$^{-/-}$ limb as compared to *Fgf2*$^{+/+}$ limb were not necessarily altered in the non-ischemic limb (e.g., cluster 1; Chapter 5). This could be interpreted to mean that FGF2 is affecting the expression of certain genes only in the ischemic condition. This might be related to why the *Fgf2*$^{-/-}$ hyperemia phenotype was only observed in the ischemic limb. Also, FGF2 may regulate different biological events in normal versus ischemic tissue given that different gene groups showed knockout-related differential expression in normal muscle while other gene groups had altered expression in only ischemic tissue.

The goal of identifying differentially expressed genes in the vasculature of the ischemic *Fgf2*$^{-/-}$ limb was not accomplished in the present study. However, future experiments may be able to selectively examine expression levels in the vasculature

rather than the entire hindlimb. Laser capture microdissection allows the isolation of selected cells from tissue sections consisting of a heterogeneous tissue (Emmert-Buck et al., 1996). In fact, a recent study used this technique to capture vessels from brain sections of mice (Ball et al., 2002). Endothelial cells in the brain sections were stained with alkaline phosphatase to allow targeting of vessels with the laser capture system. By comparing expression of an endothelial specific gene to 18S rRNA in laser captured tissue to that in lysate from a whole brain section, the average enrichment of endothelial cells was estimated to be over 90-fold from laser capturing. Importantly, RNA isolated from laser captured cells can be amplified and then used for microarray analysis (Iscove et al., 2002). This may be an experimental approach to discover differentially regulated genes in arteries or microvessels in the ischemic limbs of wildtype versus knockout mice. RNA isolation from targeted cells would eliminate the problem of trying to identify differences in gene expression specific to the vasculature within in a tissue homogenate comprised of predominately skeletal myocytes.

Conclusion

In summary, adult FGF2 knockout mice have similar vascular growth responses when compared to wildtype mice in a variety of situations including tumor growth, arterial injury, and retinal injury. Work from this dissertation extends those findings to include flow-dependent remodeling and ischemic revascularization (Table 6.2).

Table 6.2: Lack of vascular-related phenotypes in studies using *Fgf2* knockout mice. The following papers reported no difference between wildtype and knockout mice in the responses studied.

Observation	Reference
Hyperplastic response following vessel injury	Zhou et al. 1998
Neovascularization related to ischemic retinopathy	Ozaki et al. 1998
Injury-induced choroidal neovascularization	Tobe et al. 1998
Growth and formation of vascularized tumors	Foletti et al. 2002
Flow-dependent carotid artery remodeling	**Sullivan et al. 2002**
Ischemia-induced angiogenesis and arteriogenesis	**Sullivan et al. in press**

Overall, the lack of a detectable deficit in vascular growth, either developmental or pathological, in *Fgf2*$^{-/-}$ mice suggests that we may have to reconsider the importance of endogenous FGF2 in physiological and disease-related vascular adaptation. However, work in this dissertation provides new evidence that endogenous FGF2 has important non-mitogenic actions in the remodeling vasculature during ischemic revascularization. Specifically, endogenous FGF2 appears to modulate vascular reactivity of the collateral

circulation during hindlimb ischemia. Further studies are required to identify the specific mechanism(s) causing altered vascular reactivity in the ischemic limbs of *Fgf2*$^{-/-}$ mice.

APPENDICES

Appendix A: Carotid surgery and histology for flow-dependent remodeling in the mouse

Images before and after placement of ligatures to occlude the occipital (OCC) and internal carotid (IC) arteries, as well as the external carotid (EC) artery. Two total ligations are required to ligate the three branches. A video of this surgery is available on VHS (Titled: Mouse carotid surgery - July 21, 2002).

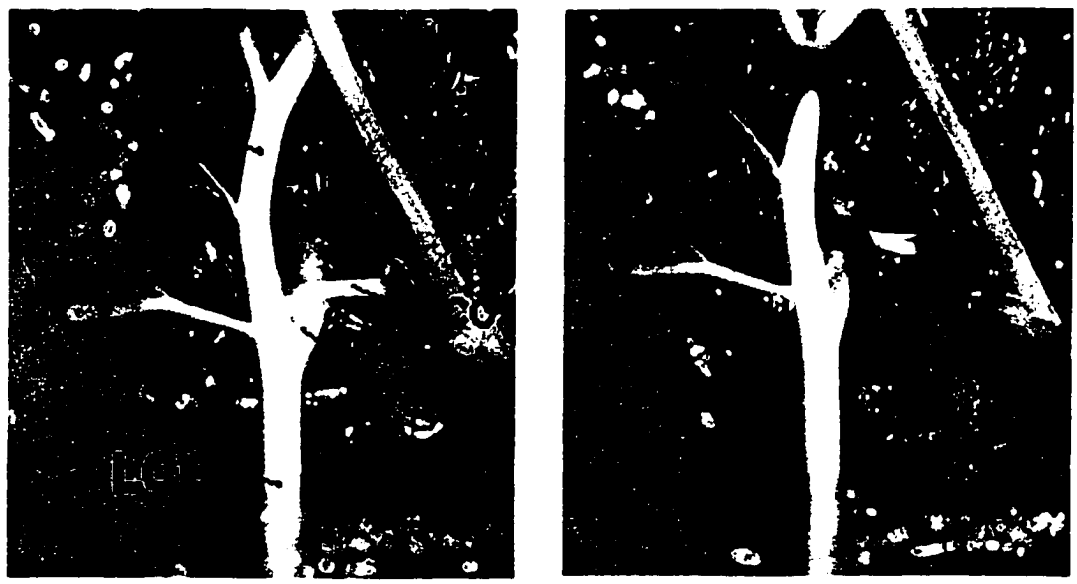

For histology of the neck (described in Chapter 2), cross-sections or transverse sections are cut through the entire neck. Serial sections are cut beginning proximally (closest to

the aorta) and continuing distally until reaching the bifurcation of the common carotid into the internal and external carotid arteries.

Hematoxylin stained cross-section of the neck

Morphometric analysis was carried out on the RCCA and LCCA using digitized images using image analysis software (Scionimage 4.0). The perimeter (length) of the lumen, internal elastic lamina (IEL), and external elastic lamina (EEL) were measured and these values were used to calculate vessel dimensions, assuming the artery was a perfect circle.

Arterial wall histology

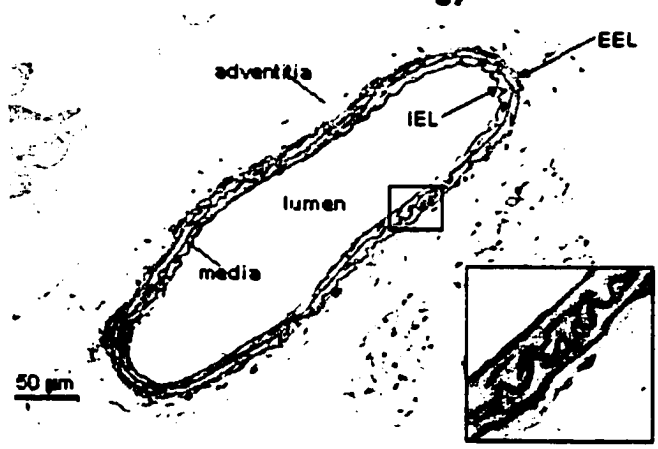

Appendix B: Measurement of carotid artery blood flow in the mouse (see *Tools and Techniques for Hemodynamic Studies in Mice*, Transonic Systems Inc. page 20)

1.) Flow measurements can be made in the common carotid following surgical exposure of approximately 1cm in length of the artery.

2.) The flow probe should be maneuvered into place using a micromanipulator and a dissecting microscope.

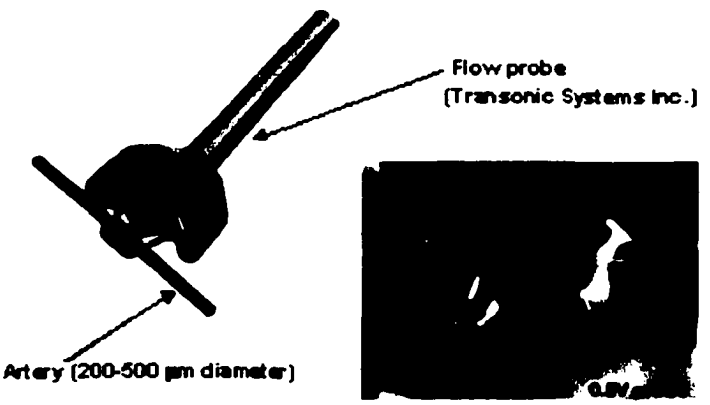

3.) The artery and flow probe need to be submerged in PBS with no air bubbles present in order to record flow. A low signal or acoustic error will occur if the artery or probe is not completely submerged.

4.) To zero the flow probe, place the probe in the PBS solution near the common carotid artery (but not positioned for recording). Use the zero knob to adjust reading to 0 volts.

5.) After zeroing, position the probe so that the vessel lies in the deepest angle of the "V" of the probe head. See the photo above. The following buttons were depressed on the Transonic flow meter: MEA, 0.1 Hz, LOFLO (2.5 ml/min maximum range). The INVERT button should be pushed if the flow values are negative or very low.

6.) Volumetric flow values (ml/min) are displayed on the front of the Transonic flow meter. Also, values can be output to a computer data acquisition system (Notocord) and displayed as raw flow values or average volumetric flow.

Raw Tracing of blood flow through the mouse common carotid artery

Appendix C: TUNEL staining of paraffin embedded sections

(Boehringer Mannheim In Situ Cell Death Detection Kit)

Time	**Reagent**
10 min	Xylene
10 min	Xylene
5 min	100% EtoH
5 min	100% EtoH
5 min	95% EtoH
5 min	95% EtoH
5 min	90% EtoH
5 min	80% EtoH
5 min	70% EtoH
5 min	60% EtoH
5 min	50% EtoH
2 min	PBS

► Microwave Pretreatment: Place slides in microwave slide holder with 200 ml of 0.1M citrate buffer, pH 3.0 and microwave for 1 min at power level 7 (P-70). For rapid cooling, add 80 ml of distilled H_20 and then transfer slides to PBS.

Rinse in PBS

▶30 min milk blocking step (1g / 100 ml PBS)

Rinse in PBS

▶60 min TUNEL reaction (40µl) at 37°C

Rinse in PBS

▶30 min TUNEL POD (40µl) at 37°C

Rinse in PBS

▶2-3 drops of peroxidase substrate; incubation time varies

▶1 dip (15-30 sec) Hematoxylin followed by acid ethanol (1 dip) and ammonia water (5 sec)

▶Distilled H_20 (or multiple rinses for 30 seconds)

▶Mowiol and Coverslip!

Citrate Buffer preparation:

Stock A Citrate Buffer: citric acid 10.5 g / 500 ml distilled H_20

Stock B Citrate Buffer: sodium citrate 14.7 g / 500 ml distilled H_20

Working solution (0.1M citrate Buffer): 36 ml Stock A and 164 ml Stock B, pH to 3.0

Trachea stained using TUNEL kit (Boehringer-Mannhiem)

Appendix D: Protocol for the immunodetection of BrdU

A. DEPARAFFINIZE

Xylene	3-5 min
Xylene	3-5 min
Xylene	3-5 min
100%ETOH	3-5 min
95%ETOH	3-5 min
90%ETOH	3-5 min
80%ETOH	3-5 min
70%ETOH	3-5 min
60%ETOH	3-5 min
PBS	3-5 min

B. STAINING PROCEDURE

1. Prewarm 2N HCl to 37°C in a copeland jar (for 100 ml, 16.7 ml 12N HCl + 83.3 ml H_2O). Prepare Boric Acid/Borate Buffer (for 100 ml, 85 ml boric acid solution + 15 ml sodium borate solution). **Boric Acid**: 12.4 g/L boric acid in distilled H_2O **Sodium Borate**: 19.0 g/L sodium borate in distilled water

2. Incubate deparaffinzed slides in 2 N HCl for **25** min at 37°C. (Timing important)

3. Incubate slides in Boric Acid/Borate Buffer for **1-5** min at room temperature.

5. Wash slides in PBS 3 times for 3 min each at room temperature.

5b. Put in **H_2O_2 for 5 min**, 30ml H_2O_2 added to 270 ml PBS.

6. Incubate slides in Blocking Serum for 20 min at room temperature or 37°C in a humidified chamber or **milk 30 min** at room temp. Blocking serum: 1-5% animal serum in PBS. The animal serum should be chosen to match the species in which the 2° antibody was made. For example: Sigma anti-BrdU Clone BU-33, diluted 1:1000, (1° antibody) is a mouse monoclonal antibody. The biotin labeled anti-mouse IgG antibody from Vectastain (2° antibody) was made in horse. Therefore the blocking serum should be 1-5% horse serum in PBS.

7. Remove the blocking serum and add the anti-BrdU, diluted in Blocking Serum, to each tissue section. In general use the smallest possible volume of antibody that completely covers the tissue sample. The incubation may be done for a **1 hr at 37°C** or overnight at 4°C.

8. Wash slides in PBS 3 times for 3 min each at room temperature.

9. Incubate slides in 2° antibody, diluted in Blocking Serum, for **1 hr at 37°C**

10. Wash slides in PBS 3 times for 3 min each at room temperature.

11. Thirty (30) min before use, prepare Vectastain ABC Reagent. Add Vectastain ABC Reagent to tissue sections and incubate for **30 min at 37°C** or room temperature.

12. Wash slides in PBS 3 times for 3 min each at room temperature.

13. Prepare DAB reagent immediately before use. Add substances according to directions.

14. Wash slides in H20

15. Counterstain with Hematoxylin

16. Coverslip with Mowiol

Small Intestine: No BrdU antibody

Small Intestine: anit-BrdU antibody

Appendix E: Surgery procedure for hindlimb ischemia in mice

1) Sterile surgical instruments and supplies (autoclaved or pre-packaged)

- sterile latex surgical gloves
- sterile PBS or saline, plastic petri dish
- cotton swabs, cotton gauze, 2x2 and 4x4
- 5.0 silk (non-absorbable), 5-6 Michel suture clips
- instruments: fine scissors, precision spring scissors, needle holder, fine forceps

2) Anesthetize mouse with Avertin 2.5 % working solution (0.15ml/ 10g body wt.).

3) Remove hair from left leg with Nair cream depilatory.

4) Spray and wipe mouse (lower half) with 70% EtoH and/or disinfectant.

5) Spray table top and wipe down the surgical scope with paper towel soaked with disinfectant.

6) Make a skin incision over the femoral artery, vein, and nerve. This is the area of the medial thigh between the hip and the knee. Make an initial cut (picture **1**), then extend the

incision along the entire length of the hindlimb from proximal thigh to the ankle (picture **2**).

7) Remove the fat pad that covers the proximal portion of the femoral artery and vein (picture **3**). Be careful not to cut the large artery and vein that extend from the femoral vessels into the fat pad, this will cause bleeding. Removal of the fat tissue should expose two vessels that branch off of the femoral artery and vein (picture **4**). The deep femoral branch is the largest vessel in view as it forms a "V" branch that dives into the thigh muscles. This branch is not always obvious since it extends deep into the muscle tissue.

8) Carefully, expose the femoral artery and vein. Do not damage the nerve that runs along with the artery and vein. It is located on the right side (the surgeon's) of the artery/vein bundle. Gently, using blunt dissection, separate the nerve from the artery and vein. Isolate and expose the artery and vein pair along the entire length of the hindlimb. Next, place a piece of 5.0 silk under the portion of the artery/vein bundle that is just proximal of the two branches depicted in picture 4 (picture **4** and **5**). Tie off the suture around the artery/vein bundle. Repeat this at the distal portion of the artery and vein near the ankle. Once both ends of the artery/vein are ligated, using fine scissors, cut the portion of the artery and vein distal to the ankle/distal ligature. Use the distal ligature to lift the artery and vein away from the muscle of the hindlimb. Using the fine spring scissors cut the artery and vein away from the muscle tissue. Also, use fine forceps to tear all large branching vessels in the thigh and ankle (deep femoral branch etc). Very little cutting will

be required if the vessels are properly exposed. Again, be careful not to damage the nerve. Check for bleeding. Use compression with sterile cotton swabs or gauze to stop and control bleeding. Most bleeding occurs in the thigh after tearing the deep femoral branch.

9) Once bleeding has been stopped, close the skin with Michel suture clips.

10) Place animal on covered heating pad and monitor during recovery (~ 1hour).

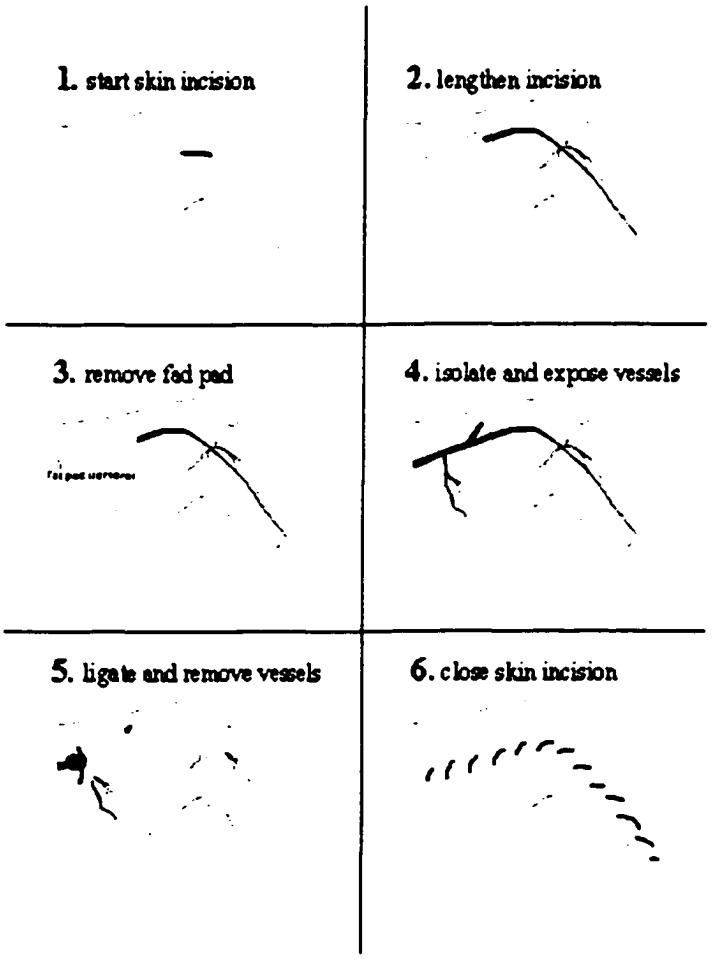

Modified surgery and ligature placement (see below): The distal ligation is placed just below the knee (saphenous artery/vein). This procedure produces a similar decrease in hindlimb flow as the ankle ligation. Also, post-surgery angiograms appear the same as when distal ligation is done near the ankle.

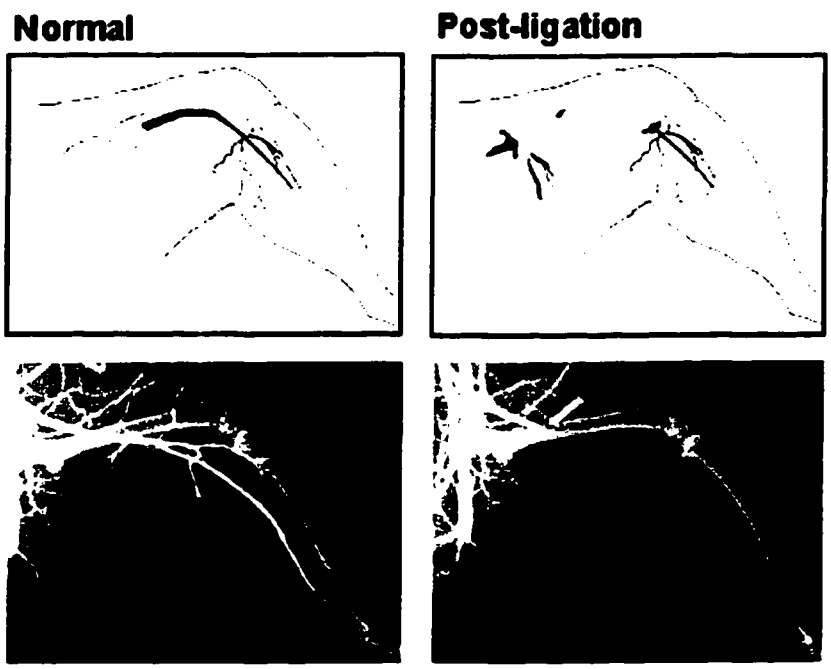

Appendix F: Lisca laser Doppler perfusion imaging (LDPI) procedures for the mouse hindlimb

1.) Turn on water/heat pump connected to circulating heat pad set at 37 degrees C

2.) Anesthetize mouse (Avertin)

3.) Remove excess hair on dorsal skin and ankle (Nair depilatory)

4.) Place mouse on circulating heat pad (dorsal side up)

5.) Cover with 4x4 gauze and blue towel for 10 minutes (use timer) to warm animal prior to scanning. The animal, uncovered, is left on the heat pad during the LDPI scanning to maintain body temperature.

6.) Adjust Scanner head, 14 cm from bottom of the scanner head to top of the heat pad

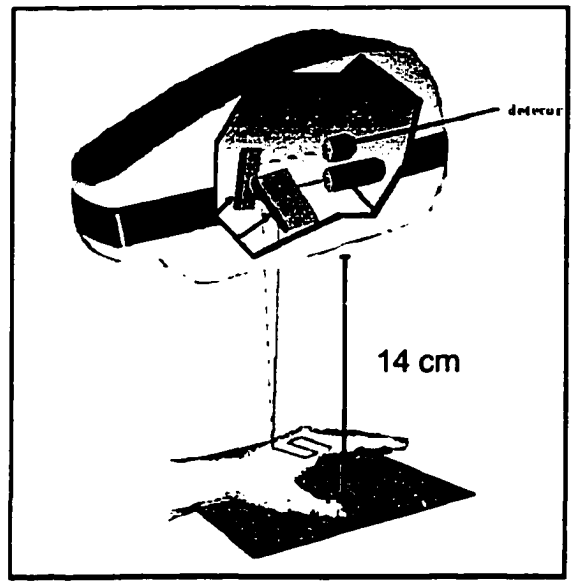

7.) Check level of scanner head (bubble level)

8.) To minimize scan time cover tail with small piece of blue or black material (e.g., small piece of surgery scrubs)

9.) For hindlimb ischemia, the foot and calf regions were contained within the scan area and analyzed for both the right and left hindlimb. The image below shows the tail which was uncovered. This does not interfere with scanning but it will increase the time needed to complete a scan.

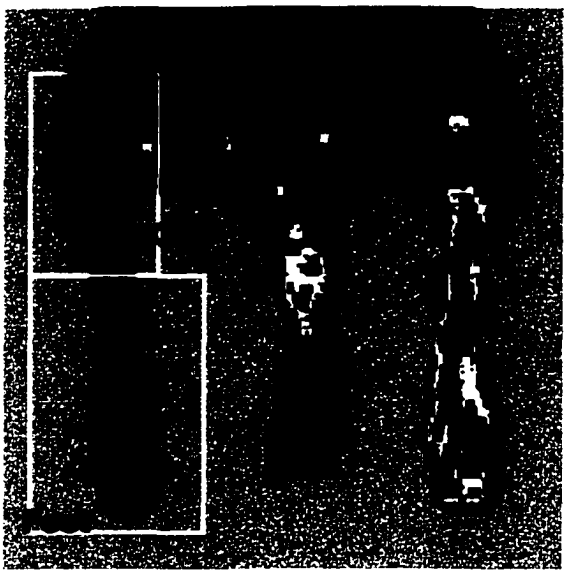

10.) Detailed instructions for the use of the LISCA software (LDPIwin 2.0 & LDISOFT) are available in the LISCA manual (hard copy). PDF versions of these instructions are available on the LISCA computer system in the following location:

C:\Program Files\LISCA\LDIW2\Manuals

Appendix G: Angiograms of hindlimb

Angiograms were taken using an x-ray cabinet system (Faxitron model 43855C). follwing injection of contrast agent (Barium sulfate, 210% w/v; Liqui-Coat HD; Lafayette Pharmaceuticals). Settings for the Faxitron cabinet were as follows: exposure time 6 min; tube voltage 29 kVp. The sample was placed on shelf number 9 and the imaging film (Kodak Ready Pack; X-OMAT XAR-2, 8x10") was placed on shelf number 3 for all hindlimb imaging. Placement of the film closer to the sample and source reduces the magnification of the x-ray image.

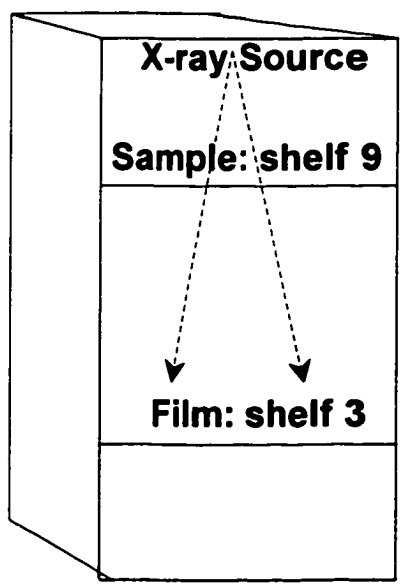

Analysis of images were done using Scion Image. Angiograms were scanned into the computer using a light-box and a HP scanner. Scans were done at 400 dpi resolution and using the "best color photography" scan mode. Using ScionImage, angiograms (A) were inverted (B) and thresholded (C) prior to analysis. An area of interest was drawn around

region below the femur, distal to the femoral ligation site and proximal to tibia (see photos). Scion image will measure the area (unitless) of black pixels within the thresholded region of interest. This process is described in methods section of Chapter 3.

A

B

C

Appendix H: Preparation of Mowiol coverslip solution. Mount slides straight from water. Best following hematoxylin counterstain.

20 ml glycerol

10 g Mowiol 4-88

24 ml dd water

48 ml 0.02 M Tris at pH 8.5

Measure glycerol into 250 ml beaker. Put on stir plate and start to stir before adding Mowiol crystals. Add Mowiol slowly into glycerol. It is VERY thick. Slowly add water and keep stirring. You may need to heat slightly at this step so that the Mowiol dissolves into the solution. Add Tris continue stirring. If you haven't started heating the solution, heat for 30-60 minutes while stirring to dissolve any remaining Mowiol crystals. Spin clarify the solution 5000g for 10 min. Aliquot into small tubes and freeze at –20. Keep in freezer until use. Thawing takes several minutes. Mowiol is thick but warming to room temperature helps reduce this. To coverslip, place 300-500 µl of Mowiol onto slide using micropipette. Slide should still have lots of water on it. Add glass coverlip and allow to dry 1-2 days.

Appendix I: Stain Checklist – Paraffin Embedded Sections – Hematoxylin only

Time	**Reagent**
10 min	Xylene
10 min	Xylene
5 min	100% EtoH
5 min	100% EtoH
5 min	95% EtoH
5 min	95% EtoH
5 min	90% EtoH
5 min	80% EtoH
5 min	70% EtoH
5 min	60% EtoH
5 min	50% EtoH
2 min	Distilled H_20
1 min	Hematoxylin

Use acid-ethanol if staining is too dark or if counterstaining

Distilled H_20 for multiple rinses for 30 seconds

Mowiol (~300 µl) per slide

Coverslip

Appendix J: Microarray hybridization protocol

Materials

Ambion EndoFree RT kit (Cat# 1740)
10-15 mg Total RNA per reaction
dNTP mix
    10 mM dATP
    10 mM dCTP
    10 mM dGTP
    3 mM dTTP
2 mM Amino Allyl dUTP's (Molecular Probes Cat# A-21664)
1M NaOH
1M Hcl
0.5M EDTA pH 8
Qiagen Qiaquick PCR purification spin columns
Sodium bicarbonate (25 mg/ml)
Appropriate dyes
Printed slide(s)
Cot-1 DNA (10 mg/ml)
poly-dA (18-mer)(10mg/ml)

Procedures

1. Reverse transcription reaction:

    Note: The following procedure is done for each sample. In other words, for each hybridization comparing two RNA samples, the steps below will be carried out twice.

Tube 1

    7ml Total RNA
    1ml Oligo dT (in RT kit)

Incubate Tube 1 at 70°C for 5 minutes. While Tube 1 is incubating, proceed to Tube 2.

Tube 2

    6ml Nuclease free H2O (in RT kit)
    2ml RT Buffer (in RT kit)
    2ml Amino Allyl dUTP's

1ml dNTP mix
1ml RNase Inhibitor (in RT kit)

Incubate both Tubes 1 and 2 at 42°C for five minutes.

2. Add Tube 2 to Tube 1.

3. Add 1ml RT enzyme to each tube.

4. Incubate at 42°C for 2 hours.

Base Hydrolysis of RNA

5. Denature samples at 95°C for 5 minutes.

6. Quick chill samples on ice.

7. To each sample add 8.6ml 1M NaOH and 8.6ml 0.5M EDTA.

8. Incubate samples for 15 minutes at 65°C.

9. Add equal volume (8.6ml) 1M HCl to each tube.

Clean-up

10. Bring samples to 100ml with Milli-Q H2O.

11. Add 5x (500 ml) volume of Qiagen Buffer PB.

12. Add solution to spin column.

13. Spin at maximum speed for 1 minute.

14. Dispense flow through. Re-use collection tube.

15. Add 750ml of 75% EtOH to column.

16. Spin at maximum speed for 1 minute.

17. Dispense flow through.

18. Spin empty column to remove residual EtOH.

19. Place spin column in new Eppendorf tube.

20. Add 30ml Milli-Q H20 to column.

21. Spin at maximum speed for 1 minute.

22. Without removing column, again add 30ml to column for final volume of 60ml.

23. Spin at maximum speed for 1 minute.

24. Dry sample to completion in SpeedVac.

Labeling

25. To pellet, add 3ml sodium bicarbonate.

26. Add 5ml of appropriate dye to each tube.
Note: It is important to keep samples separate during this step (i.e. one dye per tube).

27. Wrap tubes in aluminum foil, let stand at room temperature for 1 hour.

Clean-up part II

28. Bring each tube up to 50ml with water.

29. Combine both tubes from each set for final volume of 100ml.

30. Add 500ml of Buffer PB.

31. Carry out the same clean-up procedure as described above, however add one more 75% EtOH wash.

32. To 60ml of labeled sample, add 10mg each of Cot-1 DNA and poly-dA.

33. Add equal volume of 2X Hybridization Buffer.

2X Hybridization Buffer
8X SSC
60% Formamide

0.2% SDS

34. Store in aluminum foil until ready to hybridize.

Slide preparation

35. In beaker, make 0.2% SDS solution.

36. Fill second beaker with Milli-Q H20.
Note: 150 ml beaker works best for rinsing slides.

37. Rinse printed slide in SDS solution for ~1 minute.

38. Rinse in H2O for ~1 minute.

39. Pull slide slowly out of H2O so that slide is dry.

40. Set slide in desicator until ready to use.

Note: The slide preparation step can be done during the hour that the dye is binding.

Hybridization

41. With prepared slide, assemble and position hybridization station cartridge.

42. Select desired hybridization program.

43. Inject sample.

Washing of slides

44. Abort hybridization program, if running.

45. Select desired wash/dry program.

46. Slide is ready to scan.

Appendix K: Various PCR mixes using the PTC-100 (MJ Research, INC) programmable thermal controller. The "MAGIC" program was used at various cycle lengths for cDNA (PCR after reverse transcription). The "H1" program was used for genomic DNA (genotyping).

Date: XX/XX/XX
Samples: SAMPLE PCR MIX FOR cDNA (E.G., GAPDH)
((PCR PORTION OF RT-PCR))

Reagents	volume for 1 reaction	volume for ___ reactions
10x PCR buffer	2 µl	
2.5 mM dNTPs	2 µl	
primer (µM) FORWARD	2 µl	
primer (µM) REVERSE	2 µl	
★ ~~primer µM~~ MgCl2	1 µl	
~~x PCR buffer~~ Q BUFFER	4 µl	
dH2O	6 µl	
~~10x formamide~~	–	
Taq polymerase (.4U/rxn, 5U/µl)	0.2 µl	
DNA substrate	1 µl	
Total	~20 µl	

★ WORKED OUT FOR QIAGEN Taq POLYMERASE KIT (CATALOG # 201203)

Date: XX/XX/XX
Samples: WT (FGF2+/+) GENOTYPE FROM GENOMIC DNA

Reagents	volume for 1 reaction	volume for ___ reactions
10x PCR buffer	2 µl	
2.5 mM dNTPs	2 µl	
primer (µM) FGF2 WT F	1 µl	
primer (µM) FGF2 WT R	1 µl	
~~primer (µM)~~ 25mM MgCl2	1 µl	
~~10x PCR buffer~~ Q BUFFER	4 µl	
dH2O	7.8 µl	
~~H2O (nuclease-free)~~	-	
Taq polymerase (.4U/rxn, 5U/µl)	0.2 µl	
DNA substrate	1 µl	
Total	~20 µl	

★ QIAGEN KIT
(CATALOG # 201203)

Date: XX/XX/XX
Samples: KO (FGF2 -/-) GENOTYPE FROM GENOMIC DNA.

Reagents	volume for 1 reaction	volume for ___ reactions
10x PCR buffer	2 µl	
2.5 mM dNTPs	2 µl	
primer (µM) FGF2 KO F	1 µl	
primer (µM) SERCA3 PRIMER 3	1 µl	
~~primer (µM)~~ 25mM MgCl2	2 µl	
~~5x PCR buffer~~ Q BUFFER	4 µl	
dH2O	7 µl	
~~H2O (nuclease-free)~~	-	
Taq polymerase (.4U/rxn, 5U/µl)	0.2 µl	
DNA substrate	1 µl	
Total	~20 µl	

★ QIAGEN KIT
(#201203)

REFERENCES

Abbruzzese, T A, Guzman, R J, Martin, R L, Yee, C, Zarins, C K, and Dalman, R L. 1998. Matrix metalloproteinase inhibition limits arterial enlargements in a rodent arteriovenous fistula model. Surgery 124:328-334.

Acland, P, Dixon, M, Peters, G, and Dickson, C. 1990. Subcellular fate of the int-2 oncoprotein is determined by choice of initiation codon. Nature 343:662-665.

Aigner, A, Ray, P E, Czubayko, F, and Wellstein, A. 2002. Immunolocalization of an FGF-binding protein reveals a widespread expression pattern during different stages of mouse embryo development. Histochem. Cell Biol. 117:1-11.

Allbrook, D. 1981. Skeletal muscle regeneration. Muscle Nerve 4:234-245.

Anderson, J, Mitchell, C, McGeachie, J, and Grounds, M. 1995. The time course of basic fibroblast growth factor expression in crush-injured skeletal muscles of SJL/J and BALB/c mice. Exp Cell Res 216:325-334.

Ando, A, Yang, A, Mori, K, Yamada, H, Yamada, E, Takahashi, K, Saikia, J, Kim, M, Melia, M, Fishman, M, Huang, P, and Campochiaro, P A. 2002. Nitric oxide is proangiogenic in the retina and choroid. J. Cell Physiol 191:116-124.

Arese, M, Chen, Y, Florkiewicz, R Z, Gualandris, A, Shen, B, and Rifkin, D B. 1999. Nuclear activities of basic fibroblast growth factor: potentiation of low-serum growth mediated by natural or chimeric nuclear localization signals. Mol. Biol. Cell 10:1429-1444.

Arras, M, Ito, W D, Scholz, D, Winkler, B, Schaper, J, and Schaper, W. 1998. Monocyte activation in angiogenesis and collateral growth in the rabbit hindlimb. J. Clin. Invest 101:40-50.

Asahara, T, Chen, D, Tsurumi, Y, Kearney, M, Rossow, S, Passeri, J, Symes, J F, and Isner, J M. 1996. Accelerated restitution of endothelial integrity and endothelium-dependent function after phVEGF165 gene transfer. Circulation 94:3291-3302.

Babaei, S, Teichert-Kuliszewska, K, Monge, J C, Mohamed, F, Bendeck, M P, and Stewart, D J. 1998. Role of nitric oxide in the angiogenic response in vitro to basic fibroblast growth factor. Circ. Res. 82:1007-1015.

Baffour, R, Berman, J, Garb, J L, Rhee, S W, Kaufman, J, and Friedmann, P. 1992. Enhanced angiogenesis and growth of collaterals by in vivo administration of recombinant basic fibroblast growth factor in a rabbit model of acute lower limb ischemia: dose-response effect of basic fibroblast growth factor. J. Vasc. Surg. 16:181-191.

Baldin, V, Roman, A M, Bosc-Bierne, I, Amalric, F, and Bouche, G. 1990. Translocation of bFGF to the nucleus is G1 phase cell cycle specific in bovine aortic endothelial cells. EMBO J. 9:1511-1517.

Ball, H J, McParland, B, Driussi, C, and Hunt, N H. 2002. Isolating vessels from the mouse brain for gene expression analysis using laser capture microdissection. Brain Res. Brain Res. Protoc. 9:206-213.

Bao, X, Lu, C, and Frangos, J A. 1999. Temporal gradient in shear but not steady shear stress induces PDGF-A and MCP-1 expression in endothelial cells: role of NO, NF kappa B, and egr-1. Arterioscler. Thromb. Vasc. Biol. 19:996-1003.

Battler, A, Scheinowitz, M, Bor, A, Hasdai, D, Vered, Z, Di Segni, E, Varda-Bloom, N, Nass, D, Engelberg, S, Eldar, M, and . 1993. Intracoronary injection of basic fibroblast growth factor enhances angiogenesis in infarcted swine myocardium. J. Am. Coll. Cardiol. 22:2001-2006.

Bauters, C. 1997. Growth factors as a potential new treatment for ischemic heart disease. Clin. Cardiol. 20:II-7.

Bauters, C, Asahara, T, Zheng, L P, Takeshita, S, Bunting, S, Ferrara, N, Symes, J F, and Isner, J M. 1995. Recovery of disturbed endothelium-dependent flow in the collateral-perfused rabbit ischemic hindlimb after administration of vascular endothelial growth factor. Circulation 91:2802-2809.

Bayliss, W M. 1902. On the local reactions of the arterial wall to changes of internal pressure. J. Physiol., London 28:220-231.

Ben Driss, A, Benessiano, J, Poitevin, P, Levy, B I, and Michel, J B. 1997. Arterial expansive remodeling induced by high flow rates. Am. J. Physiol 272:H851-H858.

Bikfalvi, A, Klein, S, Pintucci, G, and Rifkin, D. 1997. Biological roles of fibroblast growth factor-2. Endocr Rev 18:26-45.

Bird, I M, Sullivan, J A, Di, T, Cale, J M, Zhang, L, Zheng, J, and Magness, R R. 2000. Pregnancy-dependent changes in cell signaling underlie changes in differential control of vasodilator production in uterine artery endothelial cells. Endocrinology 141:1107-1117.

Bjornberg, J, Albert, U, and Mellander, S. 1990. Resistance responses in proximal arterial vessels, arterioles and veins during reactive hyperaemia in skeletal muscle and their underlying regulatory mechanisms. Acta Physiol Scand. 139:535-550.

Boilly, B, Vercoutter-Edouart, A S, Hondermarck, H, Nurcombe, V, and Le, B, X. 2000. FGF signals for cell proliferation and migration through different pathways. Cytokine Growth Factor Rev. 11:295-302.

Breen, E, Joseph-Silverstein, J, Wagner, H, Tseng, H, Sung, L, and Wagner, P. 1996. Angiogenic growth factor mRNA responses in muscle to a single bout of exercise. J Appl Physiol 81:355-361.

Brevetti, L S, Paek, R, Brady, S E, Hoffman, J I, Sarkar, R, and Messina, L M. 2001. Exercise-induced hyperemia unmasks regional blood flow deficit in experimental hindlimb ischemia. J. Surg. Res. 98:21-26.

Brogi, E, Schatteman, G, Wu, T, Kim, E A, Varticovski, L, Keyt, B, and Isner, J M. . Hypoxia-induced paracrine regulation of vascular endothelial growth factor receptor expression. J. Clin. Invest 97:469-476.

Brown, K J, Hendry, I A, and Parish, C R. 1995. Acidic and basic fibroblast growth factor bind with differing affinity to the same heparan sulfate proteoglycan on BALB/c 3T3 cells: implications for potentiation of growth factor action by heparin. J. Cell Biochem. 58:6-14.

Bryant, S R, Bjercke, R J, Erichsen, D A, Rege, A, and Lindner, V. 1999. Vascular remodeling in response to altered blood flow is mediated by fibroblast growth factor-2. Circ. Res. 84:323-328.

Bugler, B, Amalric, F, and Prats, H. 1991. Alternative initiation of translation determines cytoplasmic or nuclear localization of basic fibroblast growth factor. Mol. Cell Biol. 11:573-577.

Buschmann, I and Schaper, W. 1999. Arteriogenesis Versus Angiogenesis: Two Mechanisms of Vessel Growth. News Physiol Sci. 14:121-125.

Buschmann, I and Schaper, W. 2000. The pathophysiology of the collateral circulation (arteriogenesis). J. Pathol. 190:338-342.

Bush, R, Pevec, W, Ndoye, A, Cheung, A, Sasse, J, and Pearson, D. 1998. Regulation of new blood vessel growth into ischemic skeletal muscle. J Vasc Surg 28:919-928.

Buus, C L, Pourageaud, F, Fazzi, G E, Janssen, G, Mulvany, M J, and De Mey, J G. 2001. Smooth muscle cell changes during flow-related remodeling of rat mesenteric resistance arteries. Circ. Res. 89:180-186.

Cai, W, Vosschulte, R, Afsah-Hedjri, A, Koltai, S, Kocsis, E, Scholz, D, Kostin, S, Schaper, W, and Schaper, J. 2000. Altered balance between extracellular proteolysis and antiproteolysis is associated with adaptive coronary arteriogenesis. J. Mol. Cell Cardiol. 32:997-1011.

Campochiaro, P A. 2000. Retinal and choroidal neovascularization. J. Cell Physiol 184:301-310.

Cao, Y, Ekstrom, M, and Pettersson, R F. 1993. Characterization of the nuclear translocation of acidic fibroblast growth factor. J. Cell Sci. 104 (Pt 1):77-87.

Carmeliet, P. 2000. Mechanisms of angiogenesis and arteriogenesis. Nat. Med. 6:389-395.

Carmeliet, P, Moons, L, Luttun, A, Vincenti, V, Compernolle, V, De Mol, M, Wu, Y, Bono, F, Devy, L, Beck, H, Scholz, D, Acker, T, DiPalma, T, Dewerchin, M, Noel, A, Stalmans, I, Barra, A, Blacher, S, Vandendriessche, T, Ponten, A, Eriksson, U, Plate, K H, Foidart, J M, Schaper, W, Charnock-Jones, D S, Hicklin, D J, Herbert, J M, Collen, D, and Persico, M G. 2001. Synergism between vascular endothelial growth factor and placental growth factor contributes to angiogenesis and plasma extravasation in pathological conditions. Nat. Med. 7:575-583.

Carpenter, S. 1990. Regeneration of skeletal muscle fibers after necrosis. Adv. Exp. Med. Biol. 280:13-15.

Chandrasekharan, S, Qiu, T H, Alkharouf, N, Brantley, K, Mitchell, J B, and Liu, E T. 2002. Characterization of mice deficient in the Src family nonreceptor tyrosine kinase Frk/rak. Mol. Cell Biol. 22:5235-5247.

Chiba, M, Bazoberry, F, Speir, E, Sasse, J, Nesbitt, C, Baird, A, Ferrans, V, Epstein, S, and Casscells, W. 1989. Role of basic fibroblast growth factor in angiogenesis, healing and hypertrophy after rat myocardial infarction. Circulation 80 (Suppl. II):II-452 (Abstract)-

Chleboun, J and Martins, R. 1994. The development and enhancement of the collateral circulation in an animal model of lower limb ischemia. Aust NZ J Surg 64:202-207.

Cohen, M, Vernon, J, Yaghdjian, V, and Hatcher, V. 1994. Longitudinal changes in myocardial basic fibroblast growth factor (FGF-2) activity following coronary artery ligation in the dog. J Mol Cell Cardiol 26:683-690.

Costa, M, Danesi, R, Agen, C, Di Paolo, A, Basolo, F, Del Bianchi, S, and Del Tacca, M. 1994. MCF-10A cells infected with the int-2 oncogene induce angiogenesis in the chick chorioallantoic membrane and in the rat mesentery. Cancer Res. 54:9-11.

Couffinhal, T, Silver, M, Kearney, M, Sullivan, A, Witzenbichler, B, Magner, M, Annex, B, Peters, K, and Isner, J M. 1999. Impaired collateral vessel development associated with reduced expression of vascular endothelial growth factor in ApoE-/- mice. Circulation 99:3188-3198.

Couffinhal, T, Silver, M, Zheng, L P, Kearney, M, Witzenbichler, B, and Isner, J M. 1998. Mouse model of angiogenesis. Am. J. Pathol. 152:1667-1679.

Coulier, F, Pontarotti, P, Roubin, R, Hartung, H, Goldfarb, M, and Birnbaum, D. 1997. Of worms and men: an evolutionary perspective on the fibroblast growth factor (FGF) and FGF receptor families. J. Mol. Evol. 44:43-56.

Cristiani, C, Volpi, D, Landonio, A, and Bertolero, F. 1994. Endothelin-1-selective binding sites are downregulated by transforming growth factor-beta and upregulated by basic fibroblast growth factor in a vascular smooth muscle-derived cell line. J. Cardiovasc. Pharmacol. 23:988-994.

Cuevas, P, Carceller, F, Cuevas, B, Gimenez-Gallego, G, and Martinez-Coso, V. 1997a. A non-mitogenic form of acidic fibroblast growth factor reduces neutrophil infiltration in rat ischemic reperfused heart. Eur. J. Med. Res. 2:139-143.

Cuevas, P, Carceller, F, Lozano, R M, Crespo, A, Zazo, M, and Gimenez-Gallego, G. 1997b. Protection of rat myocardium by mitogenic and non-mitogenic fibroblast growth factor during post-ischemic reperfusion. Growth Factors 15:29-40.

Cuevas, P, Carceller, F, Martinez-Coso, V, Cuevas, B, and Gimenez-Gallego, G. 2002. Role of fobroblast growth factors in the ischemic myocardium. 273-290.

Cuevas, P, Carceller, F, Ortega, S, Zazo, M, Nieto, I, and Gimenez-Gallego, G. 1991. Hypotensive activity of fibroblast growth factor. Science 254:1208-1210.

Cuevas, P, Garcia-Calvo, M, Carceller, F, Reimers, D, Zazo, M, Cuevas, B, Munoz-Willery, I, Martinez-Coso, V, Lamas, S, and Gimenez-Gallego, G. 1996. Correction of hypertension by normalization of endothelial levels of fibroblast growth factor and nitric oxide synthase in spontaneously hypertensive rats. Proc. Natl. Acad. Sci. U. S. A 93:11996-12001.

Cuevas, P, Reimers, D, Carceller, F, Martinez-Coso, V, Redondo-Horcajo, M, Saenz, d T, I, and Gimenez-Gallego, G. 1997c. Fibroblast growth factor-1 prevents myocardial apoptosis triggered by ischemia reperfusion injury. Eur. J. Med. Res. 2:465-468.

Davies, P F. 1995. Flow-mediated endothelial mechanotransduction. Physiol Rev. 75:519-560.

Davis, M G, Zhou, M, Ali, S, Coffin, J D, Doetschman, T, and Dorn, G W. 1997. Intracrine and autocrine effects of basic fibroblast growth factor in vascular smooth muscle cells. J. Mol. Cell Cardiol. 29:1061-1072.

Dawson, J and Hudlicka, O. 1989. The effects of long term administration of prazosin on the microcirculation in skeletal muscles. Cardiovasc Res 23:913-920.

de Kleijn, D P, Sluijter, J P, Smit, J, Velema, E, Richard, W, Schoneveld, A H, Pasterkamp, G, and Borst, C. 2001. Furin and membrane type-1 metalloproteinase

mRNA levels and activation of metalloproteinase-2 are associated with arterial remodeling. FEBS Lett. 501:37-41.

de Smet, B J, de Kleijn, D, Hanemaaijer, R, Verheijen, J H, Robertus, L, Der Helm, Y J, Borst, C, and Post, M J. 2000. Metalloproteinase inhibition reduces constrictive arterial remodeling after balloon angioplasty: a study in the atherosclerotic Yucatan micropig. Circulation 101:2962-2967.

de Wit, C, Jahrbeck, B, Schafer, C, Bolz, S S, and Pohl, U. 1998. Nitric oxide opposes myogenic pressure responses predominantly in large arterioles in vivo. Hypertension 31:787-794.

Deindl, E, Buschmann, I, Hoefer, I E, Podzuweit, T, Boengler, K, Vogel, S, van Royen, N, Fernandez, B, and Schaper, W. 2001. Role of ischemia and of hypoxia-inducible genes in arteriogenesis after femoral artery occlusion in the rabbit. Circ. Res. 89:779-786.

Dinenno, F A, Tanaka, H, Monahan, K D, Clevenger, C M, Eskurza, I, DeSouza, C A, and Seals, D R. 2001. Regular endurance exercise induces expansive arterial remodelling in the trained limbs of healthy men. J. Physiol 534:287-295.

Dono, R, Faulhaber, J, Galli, A, Zuniga, A, Volk, T, Texido, G, Zeller, R, and Ehmke, H. 2002. FGF2 signaling is required for the development of neuronal circuits regulating blood pressure. Circ. Res. 90:E5-E10.

Dono, R, Texido, G, Dussel, R, Ehmke, H, and Zeller, R. 1998. Impaired cerebral cortex development and blood pressure regulation in FGF-2-deficient mice. EMBO J. 17:4213-4225.

Duan, D S, Werner, S, and Williams, L T. 1992. A naturally occurring secreted form of fibroblast growth factor (FGF) receptor 1 binds basic FGF in preference over acidic FGF. J. Biol. Chem. 267:16076-16080.

DuBois, R N, Abramson, S B, Crofford, L, Gupta, R A, Simon, L S, van de Putte, L B, and Lipsky, P E. 1998. Cyclooxygenase in biology and disease. FASEB J. 12:1063-1073.

Duggan, D J, Bittner, M, Chen, Y, Meltzer, P, and Trent, J M. 1999. Expression profiling using cDNA microarrays. Nat. Genet. 21:10-14.

Duling, B R, Hogan, R D, Langille, B L, Lelkes, P, Segal, S S, Vatner, S F, Weigelt, H, and Young, M A. 1987. Vasomotor control: functional hyperemia and beyond. Fed. Proc. 46:251-263.

Egginton, S, Zhou, A L, Brown, M D, and Hudlicka, O. 2001. Unorthodox angiogenesis in skeletal muscle. Cardiovasc. Res. 49:634-646.

Ekelund, U, Bjornberg, J, Grande, P O, Albert, U, and Mellander, S. 1992. Myogenic vascular regulation in skeletal muscle in vivo is not dependent of endothelium-derived nitric oxide. Acta Physiol Scand. 144:199-207.

Emmert-Buck, M R, Bonner, R F, Smith, P D, Chuaqui, R F, Zhuang, Z, Goldstein, S R, Weiss, R A, and Liotta, L A. 1996. Laser capture microdissection. Science 274:998-1001.

Engelson, E T, Skalak, T C, and Schmid-Schonbein, G W. 1985. The microvasculature in skeletal muscle. I. Arteriolar network in rat spinotrapezius muscle. Microvasc. Res. 30:29-44.

Fantl, W J, Johnson, D E, and Williams, L T. 1993. Signalling by receptor tyrosine kinases. Annu. Rev. Biochem. 62:453-481.

Feigl, E O. 1989. The arterial system. 21:849-853.

Fernandez-Patron, C, Stewart, K G, Zhang, Y, Koivunen, E, Radomski, M W, and Davidge, S T. 2000. Vascular matrix metalloproteinase-2-dependent cleavage of calcitonin gene-related peptide promotes vasoconstriction. Circ. Res. 87:670-676.

Fernandez, B, Buehler, A, Wolfram, S, Kostin, S, Espanion, G, Franz, W M, Niemann, H, Doevendans, P A, Schaper, W, and Zimmermann, R. 2000. Transgenic myocardial overexpression of fibroblast growth factor-1 increases coronary artery density and branching. Circ. Res. 87:207-213.

Ferrara, N, Carver-Moore, K, Chen, H, Dowd, M, Lu, L, O'Shea, K, Powell-Braxton, L, Hillan, K, and Moore, M. 1996. Heterozygous embryonic lethality induced by targeted inactivation of the VEGF gene. Nature 380:439-442.

Florkiewicz, R Z and Sommer, A. 1989. Human basic fibroblast growth factor gene encodes four polypeptides: three initiate translation from non-AUG codons. Proc. Natl. Acad. Sci. U. S. A 86:3978-3981.

Floss, T, Arnold, H H, and Braun, T. 1997. A role for FGF-6 in skeletal muscle regeneration. Genes Dev. 11:2040-2051.

Foletti, A, Ackermann, J, Schmidt, A, Hummler, E, and Beermann, F. 2002. Absence of fibroblast growth factor 2 does not prevent tumor formation originating from the RPE. Oncogene 21:1841-1847.

Folkman, J and Klagsbrun, M. 1987. Angiogenic factors. Science 235:442-447.

Fox, J C and Shanley, J R. 1996. Antisense inhibition of basic fibroblast growth factor induces apoptosis in vascular smooth muscle cells. J. Biol. Chem. 271:12578-12584.

Friesel, R E and Maciag, T. 1995. Molecular mechanisms of angiogenesis: fibroblast growth factor signal transduction. FASEB J. 9:919-925.

Galis, Z S and Khatri, J J. 2002. Matrix metalloproteinases in vascular remodeling and atherogenesis: the good, the bad, and the ugly. Circ. Res. 90:251-262.

Gentry, R M and Johnson, P C. 1972. Reactive hyperemia in arterioles and capillaries of frog skeletal muscle following microocclusion. Circ. Res. 31:953-965.

Gibbons, G H and Dzau, V J. 1994. The emerging concept of vascular remodeling. N. Engl. J. Med. 330:1431-1438.

Giordano, F J, Ping, P, McKirnan, M D, Nozaki, S, DeMaria, A N, Dillmann, W H, Mathieu-Costello, O, and Hammond, H K. 1996. Intracoronary gene transfer of fibroblast growth factor-5 increases blood flow and contractile function in an ischemic region of the heart. Nat. Med. 2:534-539.

Glagov, S, Weisenberg, E, Zarins, C K, Stankunavicius, R, and Kolettis, G J. 1987. Compensatory enlargement of human atherosclerotic coronary arteries. N. Engl. J. Med. 316:1371-1375.

Godin, D, Ivan, E, Johnson, C, Magid, R, and Galis, Z S. 2000. Remodeling of carotid artery is associated with increased expression of matrix metalloproteinases in mouse blood flow cessation model. Circulation 102:2861-2866.

Gospodarowicz, D. 1974. Localisation of a fibroblast growth factor and its effect alone and with hydrocortisone on 3T3 cell growth. Nature 249:123-127.

Gospodarowicz, D, Ferrara, N, Haaparanta, T, and Neufeld, G. 1988. Basic fibroblast growth factor: expression in cultured bovine vascular smooth muscle cells. Eur. J. Cell Biol. 46:144-151.

Guyton, J R and Hartley, C J. 1985. Flow restriction of one carotid artery in juvenile rats inhibits growth of arterial diameter. Am. J. Physiol 248:H540-H546.

Guzman, R J, Abe, K, and Zarins, C K. 1997. Flow-induced arterial enlargement is inhibited by suppression of nitric oxide synthase activity in vivo. Surgery 122:273-279.

Haddy, F J and Scott, J B. 1975. Metabolic factors in peripheral circulatory regulation. Fed. Proc. 34:2006-2011.

Hampton, T G, Amende, I, Fong, J, Laubach, V E, Li, J, Metais, C, and Simons, M. 2000. Basic FGF reduces stunning via a NOS2-dependent pathway in coronary- perfused mouse hearts. Am. J. Physiol Heart Circ. Physiol 279:H260-H268.

Hansen-Smith, F, Egginton, S, and Hudlicka, O. 1998. Growth of arterioles in chronically stimulated adult rat skeletal muscle. Microcirculation. 5:49-59.

Hansen-Smith, F, Egginton, S, Zhou, A L, and Hudlicka, O. 2001. Growth of arterioles precedes that of capillaries in stretch-induced angiogenesis in skeletal muscle. Microvasc. Res. 62:1-14.

Hanzlikova, V and Gutmann, E. 1979. Effect of ischemia on contractile and histochemical properties of the rat soleus muscle. Pflugers Arch. 379:209-214.

Harmon, K J, Couper, L L, and Lindner, V. 2000. Strain-dependent vascular remodeling phenotypes in inbred mice. Am. J. Pathol. 156:1741-1748.

Hassid, A, Arabshahi, H, Bourcier, T, Dhaunsi, G S, and Matthews, C. 1994. Nitric oxide selectively amplifies FGF-2-induced mitogenesis in primary rat aortic smooth muscle cells. Am. J. Physiol 267:H1040-H1048.

Hautmann, M B, Adam, P J, and Owens, G K. 1999. Similarities and differences in smooth muscle alpha-actin induction by TGF-beta in smooth muscle versus non-smooth muscle cells. Arterioscler. Thromb. Vasc. Biol. 19:2049-2058.

Hawke, T J and Garry, D J. 2001. Myogenic satellite cells: physiology to molecular biology. J. Appl. Physiol 91:534-551.

Heaps, C L, Sturek, M, Rapps, J A, Laughlin, M H, and Parker, J L. 2000. Exercise training restores adenosine-induced relaxation in coronary arteries distal to chronic occlusion. Am. J. Physiol Heart Circ. Physiol 278:H1984-H1992.

Henriksen, P A and Kotelevtsev, Y. 2002. Application of gene expression profiling to cardiovascular disease. Cardiovasc. Res. 54:16-24.

Hershey, J C, Baskin, E P, Glass, J D, Hartman, H A, Gilberto, D B, Rogers, I T, and Cook, J J. 2001. Revascularization in the rabbit hindlimb: dissociation between capillary sprouting and arteriogenesis. Cardiovasc. Res. 49:618-625.

Hill, M A, Trippe, K M, Li, Q X, and Meininger, G A. 1992. Arteriolar arcades and pressure distribution in cremaster muscle microcirculation. Microvasc. Res. 44:117-124.

Hillier, C, Sayers, R D, Watt, P A, Naylor, R, Bell, P R, and Thurston, H. 1999. Altered small artery morphology and reactivity in critical limb ischaemia. Clin. Sci. (Lond) 96:155-163.

Hoefer, I E, van Royen, N, Buschmann, I R, Piek, J J, and Schaper, W. 2001. Time course of arteriogenesis following femoral artery occlusion in the rabbit. Cardiovasc. Res. 49:609-617.

Hoefer, I E, van Royen, N, Rectenwald, J E, Bray, E J, Abouhamze, Z, Moldawer, L L, Voskuil, M, Piek, J J, Buschmann, I R, and Ozaki, C K. 2002. Direct evidence for tumor necrosis factor-alpha signaling in arteriogenesis. Circulation 105:1639-1641.

Hudlicka, O, Brown, M D, Egginton, S, and Dawson, J M. 1994. Effect of long-term electrical stimulation on vascular supply and fatigue in chronically ischemic muscles. J. Appl. Physiol 77:1317-1324.

Iscove, N N, Barbara, M, Gu, M, Gibson, M, Modi, C, and Winegarden, N. 2002. Representation is faithfully preserved in global cDNA amplified exponentially from sub-picogram quantities of mRNA. Nat. Biotechnol. 20:940-943.

Isner, J M and Takayuki, A. 1998. Therapeutic angiogenesis. Front Biosci. 3:e49-e69.

Ito, W D, Arras, M, Scholz, D, Winkler, B, Htun, P, and Schaper, W. 1997a. Angiogenesis but not collateral growth is associated with ischemia after femoral artery occlusion. Am. J. Physiol 273:H1255-H1265.

Ito, W D, Arras, M, Winkler, B, Scholz, D, Schaper, J, and Schaper, W. 1997b. Monocyte chemotactic protein-1 increases collateral and peripheral conductance after femoral artery occlusion. Circ. Res. 80:829-837.

Itoh, H, Mukoyama, M, Pratt, R E, and Dzau, V J. 1992. Specific blockade of basic fibroblast growth factor gene expression in endothelial cells by antisense oligonucleotide. Biochem. Biophys. Res. Commun. 188:1205-1213.

Jackson, A, Friedman, S, Zhan, X, Engleka, K A, Forough, R, and Maciag, T. 1992. Heat shock induces the release of fibroblast growth factor 1 from NIH 3T3 cells. Proc. Natl. Acad. Sci. U. S. A 89:10691-10695.

Jackson, Z S, Gotlieb, A I, and Langille, B L. 2002. Wall tissue remodeling regulates longitudinal tension in arteries. Circ. Res. 90:918-925.

Jarajapu, Y P, Coats, P, McGrath, J C, MacDonald, A, and Hillier, C. 2001. Increased alpha(1)- and alpha(2)-adrenoceptor-mediated contractile responses of human skeletal muscle resistance arteries in chronic limb ischemia. Cardiovasc. Res. 49:218-225.

Jennische, E. 1986. Rapid regeneration in postischaemic skeletal muscle with undisturbed microcirculation. Acta Physiol Scand. 128:409-414.

Jiang, Z S, Padua, R R, Ju, H, Doble, B W, Jin, Y, Hao, J, Cattini, P A, Dixon, I M, and Kardami, E. 2002. Acute protection of ischemic heart by FGF-2: involvement of FGF-2 receptors and protein kinase C. Am. J. Physiol Heart Circ. Physiol 282:H1071-H1080.

Johnson, J M. 1989. Circulation to skeletal muscle. 21:849-853.

Johnson, P C, Burton, K S, Henrich, H, and Henrich, U. 1976. Effect of occlusion duration on reactive hyperemia in sartorius muscle capillaries. Am. J. Physiol 230:715-719.

Johnson, P C and Henrich, H A. 1975. Metabolic and myogenic factors in local regulation of the microcirculation. Fed. Proc. 34:2020-2024.

Jonca, F, Ortega, N, Gleizes, P, Bertranda, N, and Plouet, J. 1997. Cell release of bioactive fibroblast growth factor-2 by exon 6-encoded sequence of vascular endothelial growth factor. J Biol Chem 272:24203-24209.

Kadota, O, Ohta, S, Kumon, Y, Sakaki, S, Matsuda, S, and Sakanaka, M. 1995. Role of basic fibroblast growth factor in the regulation of rat basilar artery tone in vivo. Neurosci. Lett. 199:99-102.

Kage, K, Fujita, N, Oh-hara, T, Ogata, E, Fujita, T, and Tsuruo, T. 1999. Basic fibroblast growth factor induces cyclooxygenase-2 expression in endothelial cells derived from bone. Biochem. Biophys. Res. Commun. 254:259-263.

Kakuta, T, Currier, J W, Haudenschild, C C, Ryan, T J, and Faxon, D P. 1994. Differences in compensatory vessel enlargement, not intimal formation, account for restenosis after angioplasty in the hypercholesterolemic rabbit model. Circulation 89:2809-2815.

Kakuta, T, Usui, M, Coats, W D, Jr., Currier, J W, Numano, F, and Faxon, D P. 1998. Arterial remodeling at the reference site after angioplasty in the atherosclerotic rabbit model. Arterioscler. Thromb. Vasc. Biol. 18:47-51.

Kamiya, A and Togawa, T. 1980. Adaptive regulation of wall shear stress to flow change in the canine carotid artery. Am. J. Physiol 239:H14-H21.

Kan, M, Wu, X, Wang, F, and McKeehan, W L. 1999. Specificity for fibroblast growth factors determined by heparan sulfate in a binary complex with the receptor kinase. J. Biol. Chem. 274:15947-15952.

Karim, S, Berrou, E, Levy-Toledano, S, Bryckaert, M, and MacLouf, J. 1997. Regulatory role of prostaglandin E2 in induction of cyclo-oxygenase-2 by a thromboxane A2 analogue (U46619) and basic fibroblast growth factor in porcine aortic smooth-muscle cells. Biochem. J. 326 (Pt 2):593-599.

Karsan, A, Yee, E, Poirier, G G, Zhou, P, Craig, R, and Harlan, J M. 1997. Fibroblast growth factor-2 inhibits endothelial cell apoptosis by Bcl-2- dependent and independent mechanisms. Am. J. Pathol. 151:1775-1784.

Kato, M, Wang, H, Kainulainen, V, Fitzgerald, M L, Ledbetter, S, Ornitz, D M, and Bernfield, M. 1998a. Physiological degradation converts the soluble syndecan-1 ectodomain from an inhibitor to a potent activator of FGF-2. Nat. Med. 4:691-697.

Kato, S, Muraishi, A, Miyamoto, T, and Fox, J C. 1998b. Basic fibroblast growth factor regulates extracellular matrix and contractile protein expression independent of proliferation in vascular smooth muscle cells. In Vitro Cell Dev. Biol. Anim 34:341-346.

Kawasaki, T, Dewerchin, M, Lijnen, H R, Vreys, I, Vermylen, J, and Hoylaerts, M F. 2001. Mouse carotid artery ligation induces platelet-leukocyte-dependent luminal fibrin, required for neointima development. Circ. Res. 88:159-166.

Kelsall, C J, Brown, M D, and Hudlicka, O. 2001. Alterations in reactivity of small arterioles in rat skeletal muscle as a result of chronic ischaemia. J. Vasc. Res. 38:212-218.

Kerr, M K and Churchill, G A. 2001a. Experimental design for gene expression microarrays. Biostatistics 2:183-201.

Kerr, M K and Churchill, G A. 2001b. Statistical design and the analysis of gene expression microarray data. Genet. Res. 77:123-128.

Kerr, M K, Martin, M, and Churchill, G A. 2000. Analysis of variance for gene expression microarray data. J. Comput. Biol. 7:819-837.

Klabunde, R E. 1986. Attenuation of reactive and active hyperemia by sympathetic stimulation in dog gracilis muscle. Am. J. Physiol 251:H1183-H1187.

Klabunde, R E and Mayer, S E. 1979. Effects of ischemia on tissue metabolites in red (slow) and white (fast) skeletal muscle of the chicken. Circ. Res. 45:366-373.

Koller, A and Kaley, G. 1990a. Prostaglandins mediate arteriolar dilation to increased blood flow velocity in skeletal muscle microcirculation. Circ. Res. 67:529-534.

Koller, A and Kaley, G. 1990b. Role of endothelium in reactive dilation of skeletal muscle arterioles. Am. J. Physiol 259:H1313-H1316.

Kondo, S, Yin, D, Aoki, T, Takahashi, J A, Morimura, T, and Takeuchi, J. 1994. bcl-2 gene prevents apoptosis of basic fibroblast growth factor- deprived murine aortic endothelial cells. Exp. Cell Res. 213:428-432.

Korsgaard, N, Aalkjaer, C, Heagerty, A M, Izzard, A S, and Mulvany, M J. 1993. Histology of subcutaneous small arteries from patients with essential hypertension. Hypertension 22:523-526.

Kostyk, S K, Kourembanas, S, Wheeler, E L, Medeiros, D, McQuillan, L P, D'Amore, P A, and Braunhut, S J. 1995. Basic fibroblast growth factor increases nitric oxide synthase production in bovine endothelial cells. Am. J. Physiol 269:H1583-H1589.

Krams, R, Wentzel, J J, Oomen, J A, Schuurbiers, J C, Andhyiswara, I, Kloet, J, Post, M, de Smet, B, Borst, C, Slager, C J, and Serruys, P W. 1998. Shear stress in atherosclerosis, and vascular remodelling. Semin. Interv. Cardiol. 3:39-44.

Krishnamurthy, P, Bird, I M, Sheppard, C, and Magness, R R. 1999. Effects of angiogenic growth factors on endothelium-derived prostacyclin production by ovine uterine and placental arteries. Prostaglandins Other Lipid Mediat. 57:1-12.

Kubis, N, Checoury, A, Tedgui, A, and Levy, B I. 2001. Adaptive common carotid arteries remodeling after unilateral internal carotid artery occlusion in adult patients. Cardiovasc. Res. 50:597-602.

Kumar, A, Hoover, J L, Simmons, C A, Lindner, V, and Shebuski, R J. 1997a. Remodeling and neointimal formation in the carotid artery of normal and P-selectin-deficient mice. Circulation 96:4333-4342.

Kumar, A and Lindner, V. 1997b. Remodeling with neointima formation in the mouse carotid artery after cessation of blood flow. Arterioscler. Thromb. Vasc. Biol. 17:2238-2244.

Kuwabara, K, Ogawa, S, Matsumotot, M, Koga, S, Clauss, M, Pinsky, D, Lyn, P, Leavy, J, Witte, L, Joseph-Silverstein, J, Furie, M, Torcia, G, Cozzolino, F, Kamada, T, and Stern, D. 1995. Hypoxia-mediated induction of acidic/basic fibroblast growth factor and platelet-derived growth factor in mononuclear phagocytes stimulates growth of hypoxic endothelial cells. Proc Natl Acad Sci USA 92:4606-4610.

Laham, R J, Rezaee, M, Post, M, Novicki, D, Sellke, F W, Pearlman, J D, Simons, M, and Hung, D. 2000. Intrapericardial delivery of fibroblast growth factor-2 induces neovascularization in a porcine model of chronic myocardial ischemia. J. Pharmacol. Exp. Ther. 292:795-802.

Laham, R J, Simons, M, Tofukuji, M, Hung, D, and Sellke, F W. 1998. Modulation of myocardial perfusion and vascular reactivity by pericardial basic fibroblast growth factor: insight into ischemia- induced reduction in endothelium-dependent vasodilatation. J. Thorac. Cardiovasc. Surg. 116:1022-1028.

Lan, Q, Mercurius, K O, and Davies, P F. 1994. Stimulation of transcription factors NF kappa B and API in endothelial cells subjected to shear stress. Biochem. Biophys. Res. Commun. 201:950-956.

Langille, B L. 1991. Hemodynamic factors and vascular disease. 131-154.

Langille, B L. 1993. Remodeling of developing and mature arteries: endothelium, smooth muscle, and matrix. J. Cardiovasc. Pharmacol. 21 Suppl 1:S11-S17.

Langille, B L, Bendeck, M P, and Keeley, F W. 1989. Adaptations of carotid arteries of young and mature rabbits to reduced carotid blood flow. Am. J. Physiol 256:H931-H939.

Langille, B L and O'Donnell, F. 1986. Reductions in arterial diameter produced by chronic decreases in blood flow are endothelium-dependent. Science 231:405-407.

LaVallee, T M, Prudovsky, I A, McMahon, G A, Hu, X, and Maciag, T. 1998. Activation of the MAP kinase pathway by FGF-1 correlates with cell proliferation induction while activation of the Src pathway correlates with migration. J. Cell Biol. 141:1647-1658.

Lee, P C, Salyapongse, A N, Bragdon, G A, Shears, L L, Watkins, S C, Edington, H D, and Billiar, T R. 1999. Impaired wound healing and angiogenesis in eNOS-deficient mice. Am. J. Physiol 277:H1600-H1608.

Lefaucheur, J, Gjata, B, Lafont, H, and Sebille, A. 1996. Angiogenic and inflammatory responses following skeletal muscle injury are altered by immune neutralization of endogenous basic fibroblast growth factor, insulin-like growth factor-1 and transforming growth factor beta 1. J Neuroimmunol 70:37-44.

Lefaucheur, J and Sebille, A. 1995. Muscle regeneration following injury can be modified in vivo by immune neutralization of basic fibroblast growth factor, transforming growth factor beta 1 or insulin-like growth factor I. J Neuroimmunol 57:85-91.

Lehoux, S, Tronc, F, and Tedgui, A. 2002. Mechanisms of blood flow-induced vascular enlargement. Biorheology 39:319-324.

Leveen, P, Pekny, M, Gebre-Medhin, S, Swolin, B, Larsson, E, and Betsholtz, C. 1994. Mice deficient for PDGF B show renal, cardiovascular, and hematological abnormalities. Genes Dev. 8:1875-1887.

Lindahl, P, Johansson, B R, Leveen, P, and Betsholtz, C. 1997. Pericyte loss and microaneurysm formation in PDGF-B-deficient mice. Science 277:242-245.

Lindner, V, Majack, R A, and Reidy, M A. 1990. Basic fibroblast growth factor stimulates endothelial regrowth and proliferation in denuded arteries. J. Clin. Invest. 85:2004-2008.

Lindner, V and Reidy, M A. 1991. Proliferation of smooth muscle cells after vascular injury is inhibited by an antibody against basic fibroblast growth factor. Proc. Natl. Acad. Sci. U. S. A. 88:3739-3743.

Lloyd, P G, Yang, H T, and Terjung, R L. 2001. Arteriogenesis and angiogenesis in rat ischemic hindlimb: role of nitric oxide. Am. J. Physiol Heart Circ. Physiol 281:H2528-H2538.

Lombard, J H and Duling, B R. 1981. Multiple mechanisms of reactive hyperemia in arterioles of the hamster cheek pouch. Am. J. Physiol 241:H748-H755.

Malek, A M and Izumo, S. 1995. Control of endothelial cell gene expression by flow. J. Biomech. 28:1515-1528.

Malek, A, Gibbons, G, Dzau, V, and Izumo, S. 1993. Fluid shear stress differentially modulates expression of genes encoding basic fibroblast growth factor and platelet-derived growth factor B chain in vascular endothelium. J Clin Invest 92:2013-2021.

Mandriota, S and Pepper, M. 1998. Vascular endothelial growth factor-induced in vitro angiogenesis and plasminogen activator expression are dependent on endogenous basic fibroblast growth factor. J Cell Sci 110:2293-2302.

Margolin, L, Fishbein, I, Banai, S, Golomb, G, Reich, R, Perez, L S, and Gertz, S D. 2002. Metalloproteinase inhibitor attenuates neointima formation and constrictive remodeling after angioplasty in rats: augmentative effect of alpha(v)beta(3) receptor blockade. Atherosclerosis 163:269-277.

Masaki, I, Yonemitsu, Y, Yamashita, A, Sata, S, Tanii, M, Komori, K, Nakagawa, K, Hou, X, Nagai, Y, Hasegawa, M, Sugimachi, K, and Sueishi, K. 2002. Angiogenic gene therapy for experimental critical limb ischemia: acceleration of limb loss by overexpression of vascular endothelial growth factor 165 but not of fibroblast growth factor-2. Circ. Res. 90:966-973.

Masuda, H, Zhuang, Y J, Singh, T M, Kawamura, K, Murakami, M, Zarins, C K, and Glagov, S. 1999. Adaptive remodeling of internal elastic lamina and endothelial lining during flow-induced arterial enlargement. Arterioscler. Thromb. Vasc. Biol. 19:2298-2307.

Mattila, M M, Ruohola, J K, Valve, E M, Tasanen, M J, Seppanen, J A, and Harkonen, P L. 2001. FGF-8b increases angiogenic capacity and tumor growth of androgen-regulated S115 breast cancer cells. Oncogene 20:2791-2804.

McGeachie, A B, Koishi, K, Imamura, T, and McLennan, I S. 2001. Fibroblast growth factor-5 is expressed in Schwann cells and is not essential for motoneurone survival. Neuroscience 104:891-899.

Meininger, G A. 1987. Responses of sequentially branching macro- and microvessels during reactive hyperemia in skeletal muscle. Microvasc. Res. 34:29-45.

Meredith, I T, Currie, K E, Anderson, T J, Roddy, M A, Ganz, P, and Creager, M A. 1996. Postischemic vasodilation in human forearm is dependent on endothelium- derived nitric oxide. Am. J. Physiol 270:H1435-H1440.

Messina, E J, Weiner, R, and Kaley, G. 1977. Arteriolar reactive hyperemia: modification by inhibitors of prostaglandin synthesis. Am. J. Physiol 232:H571-H575.

Meurice, T, Bauters, C, Auffray, J L, Vallet, B, Hamon, M, Valero, F, van Belle, E, Lablanche, J M, and Bertrand, M E. 1996. Basic fibroblast growth factor restores endothelium-dependent responses after balloon injury of rabbit arteries. Circulation 93:18-22.

Meurice, T, Bauters, C, Vallet, B, Corseaux, D, van Belle, E, Hamon, M, Dupuis, B, Lablanche, J M, and Bertrand, M E. 1997. bFGF restores endothelium-dependent responses of hypercholesterolemic rabbit thoracic aorta. Am. J. Physiol 272:H613-H617.

Mignatti, P, Morimoto, T, and Rifkin, D B. 1992. Basic fibroblast growth factor, a protein devoid of secretory signal sequence, is released by cells via a pathway independent of the endoplasmic reticulum-Golgi complex. J. Cell Physiol 151:81-93.

Milkiewicz, M, Brown, M D, Egginton, S, and Hudlicka, O. 2001. Association between shear stress, angiogenesis, and VEGF in skeletal muscles in vivo. Microcirculation. 8:229-241.

Miller, D L, Ortega, S, Bashayan, O, Basch, R, and Basilico, C. 2000. Compensation by fibroblast growth factor 1 (FGF1) does not account for the mild phenotypic defects observed in FGF2 null mice. Mol. Cell Biol. 20:2260-2268.

Mintz, G S, Popma, J J, Pichard, A D, Kent, K M, Satler, L F, Wong, C, Hong, M K, Kovach, J A, and Leon, M B. 1996. Arterial remodeling after coronary angioplasty: a serial intravascular ultrasound study. Circulation 94:35-43.

Mitchell, P, Steenstrup, T, and Hannon, K. 1999. Expression of fibroblast growth factor family during postnatal skeletal muscle hypertrophy. J. Appl. Physiol 86:313-319.

Mitsumata, M, Fishel, R S, Nerem, R M, Alexander, R W, and Berk, B C. 1993. Fluid shear stress stimulates platelet-derived growth factor expression in endothelial cells. Am. J. Physiol 265:H3-H8.

Miyachi, M, Tanaka, H, Yamamoto, K, Yoshioka, A, Takahashi, K, and Onodera, S. 2001. Effects of one-legged endurance training on femoral arterial and venous size in healthy humans. J. Appl. Physiol 90:2439-2444.

Miyashiro, J K, Poppa, V, and Berk, B C. 1997. Flow-induced vascular remodeling in the rat carotid artery diminishes with age. Circ. Res. 81:311-319.

Mondy, J S, Lindner, V, Miyashiro, J K, Berk, B C, Dean, R H, and Geary, R L. 1997. Platelet-derived growth factor ligand and receptor expression in response to altered blood flow in vivo. Circ. Res. 81:320-327.

Montero, A, Okada, Y, Tomita, M, Ito, M, Tsurukami, H, Nakamura, T, Doetschman, T, Coffin, J D, and Hurley, M M. 2000. Disruption of the fibroblast growth factor-2 gene results in decreased bone mass and bone formation. J. Clin. Invest 105:1085-1093.

Monti, J, Gross, V, Luft, F C, Franca, M A, Schulz, H, Dietz, R, Sharma, A M, and Hubner, N. 2001. Expression analysis using oligonucleotide microarrays in mice lacking bradykinin type 2 receptors. Hypertension 38:E1-E3.

Moscatelli, D. 1987. High and low affinity binding sites for basic fibroblast growth factor on cultured cells: absence of a role for low affinity binding in the stimulation of plasminogen activator production by bovine capillary endothelial cells. J. Cell Physiol 131:123-130.

Murohara, T, Asahara, T, Silver, M, Bauters, C, Masuda, H, Kalka, C, Kearney, M, Chen, D, Symes, J F, Fishman, M C, Huang, P L, and Isner, J M. 1998. Nitric oxide synthase modulates angiogenesis in response to tissue ischemia. J. Clin. Invest 101:2567-2578.

Nabel, E G, Yang, Z Y, Plautz, G, Forough, R, Zhan, X, Haudenschild, C C, Maciag, T, and Nabel, G J. 1993. Recombinant fibroblast growth factor-1 promotes intimal hyperplasia and angiogenesis in arteries in vivo. Nature 362:844-846.

Nagel, T, Resnick, N, Dewey, C F, Jr., and Gimbrone, M A, Jr. 1999. Vascular endothelial cells respond to spatial gradients in fluid shear stress by enhanced activation of transcription factors. Arterioscler. Thromb. Vasc. Biol. 19:1825-1834.

Negishi, M, Lu, D, Zhang, Y Q, Sawada, Y, Sasaki, T, Kayo, T, Ando, J, Izumi, T, Kurabayashi, M, Kojima, I, Masuda, H, and Takeuchi, T. 2001. Upregulatory expression of furin and transforming growth factor-beta by fluid shear stress in vascular endothelial cells. Arterioscler. Thromb. Vasc. Biol. 21:785-790.

Nelissen-Vrancken, H J, Leenders, P J, Struijker Boudier, H A, and Smits, J F. 1992. Increased responsiveness of the vascular bed to angiotensin I, angiotensin II and phenylephrine in acute and chronic ischemic hindlimbs in rats. J. Vasc. Res. 29:359-366.

Niebauer, J, Hambrecht, R, Marburger, C, Hauer, K, Velich, T, von Hodenberg, E, Schlierf, G, Kubler, W, and Schuler, G. 1995. Impact of intensive physical exercise and low-fat diet on collateral vessel formation in stable angina pectoris and angiographically confirmed coronary artery disease. Am. J. Cardiol. 76:771-775.

Nugent, M A and Iozzo, R V. 2000. Fibroblast growth factor-2. Int. J. Biochem. Cell Biol. 32:115-120.

Odekon, L E, Sato, Y, and Rifkin, D B. 1992. Urokinase-type plasminogen activator mediates basic fibroblast growth factor-induced bovine endothelial cell migration independent of its proteolytic activity. J. Cell Physiol 150:258-263.

Ohno, M, Cooke, J P, Dzau, V J, and Gibbons, G H. 1995. Fluid shear stress induces endothelial transforming growth factor beta- 1 transcription and production. Modulation by potassium channel blockade. J. Clin. Invest 95:1363-1369.

Orlandi, C, Blackshear, J L, and Hollenberg, N K. 1986. Specific increase in sensitivity to serotonin of the canine hindlimb collateral arterial tree via the 5-hydroxytryptamine-2 receptor. Microvasc. Res. 32:121-130.

Ornitz, D M and Itoh, N. 2001. Fibroblast growth factors. Genome Biol. 2:REVIEWS3005-

Ornitz, D M, Xu, J, Colvin, J S, McEwen, D G, MacArthur, C A, Coulier, F, Gao, G, and Goldfarb, M. 1996. Receptor specificity of the fibroblast growth factor family. J. Biol. Chem. 271:15292-15297.

Orr-Urtreger, A, Bedford, M T, Burakova, T, Arman, E, Zimmer, Y, Yayon, A, Givol, D, and Lonai, P. 1993. Developmental localization of the splicing alternatives of fibroblast growth factor receptor-2 (FGFR2). Dev. Biol. 158:475-486.

Ortega, S, Ittmann, M, Tsang, S H, Ehrlich, M, and Basilico, C. 1998. Neuronal defects and delayed wound healing in mice lacking fibroblast growth factor 2. Proc. Natl. Acad. Sci. U. S. A 95:5672-5677.

Ozaki, H, Okamoto, N, Ortega, S, Chang, M, Ozaki, K, Sadda, S, Vinores, M A, Derevjanik, N, Zack, D J, Basilico, C, and Campochiaro, P A. 1998. Basic fibroblast growth factor is neither necessary nor sufficient for the development of retinal neovascularization [see comments]. Am. J. Pathol. 153:757-765.

Pabon, C, Modrusan, Z, Ruvolo, M V, Coleman, I M, Daniel, S, Yue, H, and Arnold, L J, Jr. 2001. Optimized T7 amplification system for microarray analysis. Biotechniques 31:874-879.

Padua, R R, Merle, P L, Doble, B W, Yu, C H, Zahradka, P, Pierce, G N, Panagia, V, and Kardami, E. 1998. FGF-2-induced negative inotropism and cardioprotection are inhibited by chelerythrine: involvement of sarcolemmal calcium-independent protein kinase C. J. Mol. Cell Cardiol. 30:2695-2709.

Padua, R R, Sethi, R, Dhalla, N S, and Kardami, E. 1995. Basic fibroblast growth factor is cardioprotective in ischemia- reperfusion injury. Mol. Cell Biochem. 143:129-135.

Papetti, M and Herman, I M. 2002. Mechanisms of normal and tumor-derived angiogenesis. Am. J. Physiol Cell Physiol 282:C947-C970.

Parsons-Wingerter, P, Elliott, K E, Clark, J I, and Farr, A G. 2000. Fibroblast growth factor-2 selectively stimulates angiogenesis of small vessels in arterial tree. Arterioscler. Thromb. Vasc. Biol. 20:1250-1256.

Pasterkamp, G, Schoneveld, A H, Hijnen, D J, de Kleijn, D P, Teepen, H, van der Wal, A C, and Borst, C. 2000. Atherosclerotic arterial remodeling and the localization of macrophages and matrix metalloproteases 1, 2 and 9 in the human coronary artery. Atherosclerosis 150:245-253.

Pasterkamp, G, Wensing, P J, Post, M J, Hillen, B, Mali, W P, and Borst, C. 1995. Paradoxical arterial wall shrinkage may contribute to luminal narrowing of human atherosclerotic femoral arteries. Circulation 91:1444-1449.

Pawlik, W W, Hottenstein, O D, and Jacobson, E D. 1991. Adrenergic modulation of reactive hyperemia in rat gut. Am. J. Physiol 261:G392-G400.

Peehl, D M and Sellers, R G. 1998. Basic FGF, EGF, and PDGF modify TGFbeta-induction of smooth muscle cell phenotype in human prostatic stromal cells. Prostate 35:125-134.

Pepper, M S. 1997. Manipulating angiogenesis. From basic science to the bedside. Arterioscler. Thromb. Vasc. Biol. 17:605-619.

Pepper, M and Mandriota, S. 1998. Regulation of vascular endothelial growth factor receptor-2 (Flk-1) expression in vascular endothelial cells. Exp Cell Res 241:414-425.

Peters, K G, Marcus, M L, and Harrison, D G. 1989. Vasopressin and the mature coronary collateral circulation. Circulation 79:1324-1331.

Pickering, J G, Ford, C M, Tang, B, and Chow, L H. 1997. Coordinated effects of fibroblast growth factor-2 on expression of fibrillar collagens, matrix metalloproteinases, and tissue inhibitors of matrix metalloproteinases by human vascular smooth muscle cells. Evidence for repressed collagen production and activated degradative capacity. Arterioscler. Thromb. Vasc. Biol. 17:475-482.

Pizette, S, Batoz, M, Prats, H, Birnbaum, D, and Coulier, F. 1991. Production and functional characterization of human recombinant FGF-6 protein. Cell Growth Differ. 2:561-566.

Pohl, U, de Wit, C, and Gloe, T. 2000. Large arterioles in the control of blood flow: role of endothelium- dependent dilation. Acta Physiol Scand. 168:505-510.

Pohl, U, Herlan, K, Huang, A, and Bassenge, E. 1991. EDRF-mediated shear-induced dilation opposes myogenic vasoconstriction in small rabbit arteries. Am. J. Physiol 261:H2016-H2023.

Pollack, J R, Van de, R M, and Botstein, D. 2002. Challenges in developing a molecular characterization of cancer. Semin. Oncol. 29:280-285.

Powers, C J, McLeskey, S W, and Wellstein, A. 2000. Fibroblast growth factors, their receptors and signaling. Endocr. Relat Cancer 7:165-197.

Prats, H, Kaghad, M, Prats, A C, Klagsbrun, M, Lelias, J M, Liauzun, P, Chalon, P, Tauber, J P, Amalric, F, Smith, J A, and . 1989. High molecular mass forms of basic fibroblast growth factor are initiated by alternative CUG codons. Proc. Natl. Acad. Sci. U. S. A 86:1836-1840.

Price, R J and Skalak, T C. 1998a. Prazosin administration enhances proliferation of arteriolar adventitial fibroblasts. Microvasc. Res. 55:138-145.

Price, R and Skalak, T. 1998b. Arteriolar remodeling in skeletal muscle of rats exposed to chronic hypoxia. J Vasc Res 35:238-244.

Prudovsky, I, Bagala, C, Tarantini, F, Mandinova, A, Soldi, R, Bellum, S, and Maciag, T. 2002. The intracellular translocation of the components of the fibroblast growth factor 1 release complex precedes their assembly prior to export. J. Cell Biol. 158:201-208.

Puskas, L G, Zvara, A, Hackler, L, Jr., and Van Hummelen, P. 2002. RNA amplification results in reproducible microarray data with slight ratio bias. Biotechniques 32:1330-4, 1336, 1338, 1340.

Quarto, N, Finger, F P, and Rifkin, D B. 1991. The NH2-terminal extension of high molecular weight bFGF is a nuclear targeting signal. J. Cell Physiol 147:311-318.

Raballo, R, Rhee, J, Lyn-Cook, R, Leckman, J F, Schwartz, M L, and Vaccarino, F M. 2000. Basic fibroblast growth factor (Fgf2) is necessary for cell proliferation and neurogenesis in the developing cerebral cortex. J. Neurosci. 20:5012-5023.

Rapps, J A, Jones, A W, Sturek, M, Magliola, L, and Parker, J L. 1997a. Mechanisms of altered contractile responses to vasopressin and endothelin in canine coronary collateral arteries. Circulation 95:231-239.

Rapps, J A, Sturek, M, Jones, A W, and Parker, J L. 1997b. Altered reactivity of coronary arteries located distal to a chronic coronary occlusion. Am. J. Physiol 273:H1879-H1887.

Renko, M, Quarto, N, Morimoto, T, and Rifkin, D B. 1990. Nuclear and cytoplasmic localization of different basic fibroblast growth factor species. J. Cell Physiol 144:108-114.

Resnick, N, Collins, T, Atkinson, W, Bonthron, D T, Dewey, C F, Jr., and Gimbrone, M A, Jr. 1993. Platelet-derived growth factor B chain promoter contains a cis-acting fluid shear-stress-responsive element. Proc. Natl. Acad. Sci. U. S. A 90:4591-4595.

Ribatti, D, Vacca, A, and Presta, M. 2000. The discovery of angiogenic factors: a historical review. Gen. Pharmacol. 35:227-231.

Risau, W. 1997. Mechanisms of angiogenesis. Nature 386:671-674.

Rohan, R M, Fernandez, A, Udagawa, T, Yuan, J, and D'Amato, R J. 2000. Genetic heterogeneity of angiogenesis in mice. FASEB J. 14:871-876.

Roy, C S and Brown, J G. 1879. The blood-pressure and its variations in the arterioles, capillaries, and smaller veins. J. Physiol., London 2:323-359.

Rubanyi, G M, Romero, J C, and Vanhoutte, P M. 1986. Flow-induced release of endothelium-derived relaxing factor. Am. J. Physiol 250:H1145-H1149.

Rudic, R D, Bucci, M, Fulton, D, Segal, S S, and Sessa, W C. 2000. Temporal events underlying arterial remodeling after chronic flow reduction in mice: correlation of structural changes with a deficit in basal nitric oxide synthesis. Circ. Res. 86:1160-1166.

Rudic, R D, Shesely, E G, Maeda, N, Smithies, O, Segal, S S, and Sessa, W C. 1998. Direct evidence for the importance of endothelium-derived nitric oxide in vascular remodeling. J. Clin. Invest 101:731-736.

Salani, D, Taraboletti, G, Rosano, L, Di, C, V, Borsotti, P, Giavazzi, R, and Bagnato, A. 2000. Endothelin-1 induces an angiogenic phenotype in cultured endothelial cells and stimulates neovascularization in vivo. Am. J. Pathol. 157:1703-1711.

Sarelius, I H, Maxwell, L C, Gray, S D, and Duling, B R. 1983. Capillarity and fiber types in the cremaster muscle of rat and hamster. Am. J. Physiol 245:H368-H374.

Sasaki, E, Pai, R, Halter, F, Komurasaki, T, Arakawa, T, Kobayashi, K, Kuroki, T, and Tarnawski, A S. 1998. Induction of cyclooxygenase-2 in a rat gastric epithelial cell line by epiregulin and basic fibroblast growth factor. J. Clin. Gastroenterol. 27 Suppl 1:S21-S27.

Sato, Y and Rifkin, D B. 1988. Autocrine activities of basic fibroblast growth factor: regulation of endothelial cell movement, plasminogen activator synthesis, and DNA synthesis. J. Cell Biol. 107:1199-1205.

Schena, M, Shalon, D, Davis, R W, and Brown, P O. 1995. Quantitative monitoring of gene expression patterns with a complementary DNA microarray. Science 270:467-470.

Schiffers, P M, Henrion, D, Boulanger, C M, Colucci-Guyon, E, Langa-Vuves, F, van Essen, H, Fazzi, G E, Levy, B I, and De Mey, J G. 2000. Altered flow-induced arterial remodeling in vimentin-deficient mice. Arterioscler. Thromb. Vasc. Biol. 20:611-616.

Schlake, T and Boehm, T. 2001. Expression domains in the skin of genes affected by the nude mutation and identified by gene expression profiling. Mech. Dev. 109:419-422.

Scholz, D, Cai, W J, and Schaper, W. 2001. Arteriogenesis, a new concept of vascular adaptation in occlusive disease. Angiogenesis. 4:247-257.

Scholz, D, Ziegelhoeffer, T, Helisch, A, Wagner, S, Friedrich, C, Podzuweit, T, and Schaper, W. 2002. Contribution of arteriogenesis and angiogenesis to postocclusive hindlimb perfusion in mice. J. Mol. Cell Cardiol. 34:775-787.

Schultz, J E, Witt, S A, Nieman, M L, Reiser, P J, Engle, S J, Zhou, M, Pawlowski, S A, Lorenz, J N, Kimball, T R, and Doetschman, T. 1999. Fibroblast growth factor-2 mediates pressure-induced hypertrophic response. J. Clin. Invest 104:709-719.

Schultz, J J, Hoying, J B, Sullivan, C J, and Doetschman, T. 2002. FGF and the cardiovascular system. 45-66.

Schwartz, S M, deBlois, D, and O'Brien, E R. 1995. The intima. Soil for atherosclerosis and restenosis. Circ. Res. 77:445-465.

Seghezzi, G, Patel, S, Ren, C, Guanlandris, A, Pintucci, G, Robbins, E, Shapiro, R, Galloway, A, Rifkin, D, and Mignatti, P. 1998. Fibroblast growth factor-2 (FGF-2) induces vascular endothelial growth factor (VEGF) expression in endothelial cells of forming capillaries: An autocrine mechanism contributing to angiogenesis. J Cell Biol 141:1659-1673.

Sellke, F W, Kagaya, Y, Johnson, R G, Shafique, T, Schoen, F J, Grossman, W, and Weintraub, R M. 1992. Endothelial modulation of porcine coronary microcirculation perfused via immature collaterals. Am. J. Physiol 262:H1669-H1675.

Sellke, F W, Li, J, Stamler, A, Lopez, J J, Thomas, K A, and Simons, M. 1996a. Angiogenesis induced by acidic fibroblast growth factor as an alternative method of revascularization for chronic myocardial ischemia. Surgery 120:182-188.

Sellke, F W, Quillen, J E, Brooks, L A, and Harrison, D G. 1990. Endothelial modulation of the coronary vasculature in vessels perfused via mature collaterals. Circulation 81:1938-1947.

Sellke, F W, Wang, S Y, Friedman, M, Harada, K, Edelman, E R, Grossman, W, and Simons, M. 1994. Basic FGF enhances endothelium-dependent relaxation of the collateral- perfused coronary microcirculation. Am. J. Physiol 267:H1303-H1311.

Sellke, F W, Wang, S Y, Stamler, A, Lopez, J J, Li, J, Li, J, and Simons, M. 1996b. Enhanced microvascular relaxations to VEGF and bFGF in chronically ischemic porcine myocardium. Am. J. Physiol 271:H713-H720.

Shankavaram, U T, Lai, W C, Netzel-Arnett, S, Mangan, P R, Ardans, J A, Caterina, N, Stetler-Stevenson, W G, Birkedal-Hansen, H, and Wahl, L M. 2001. Monocyte membrane type 1-matrix metalloproteinase. Prostaglandin- dependent regulation and role in metalloproteinase-2 activation. J. Biol. Chem. 276:19027-19032.

Sheehan, S M and Allen, R E. 1999. Skeletal muscle satellite cell proliferation in response to members of the fibroblast growth factor family and hepatocyte growth factor. J. Cell Physiol 181:499-506.

Shesely, E G, Maeda, N, Kim, H S, Desai, K M, Krege, J H, Laubach, V E, Sherman, P A, Sessa, W C, and Smithies, O. 1996. Elevated blood pressures in mice lacking endothelial nitric oxide synthase. Proc. Natl. Acad. Sci. U. S. A 93:13176-13181.

Shing, Y, Folkman, J, Haudenschild, C, Lund, D, Crum, R, and Klagsbrun, M. 1985. Angiogenesis is stimulated by a tumor-derived endothelial cell growth factor. J. Cell Biochem. 29:275-287.

Shing, Y, Folkman, J, Sullivan, R, Butterfield, C, Murray, J, and Klagsbrun, M. 1984. Heparin affinity: purification of a tumor-derived capillary endothelial cell growth factor. Science 223:1296-1299.

Shircore, A M, Mack, W J, Selzer, R H, Lee, P L, Azen, S P, Alaupovic, P, and Hodis, H N. 1995. Compensatory vascular changes of remote coronary segments in response to lesion progression as observed by sequential angiography from a controlled clinical trial. Circulation 92:2411-2418.

Shyy, J Y, Lin, M C, Han, J, Lu, Y, Petrime, M, and Chien, S. 1995. The cis-acting phorbol ester "12-O-tetradecanoylphorbol 13-acetate"- responsive element is involved in shear stress-induced monocyte chemotactic protein 1 gene expression. Proc. Natl. Acad. Sci. U. S. A 92:8069-8073.

Shyy, Y J, Hsieh, H J, Usami, S, and Chien, S. 1994. Fluid shear stress induces a biphasic response of human monocyte chemotactic protein 1 gene expression in vascular endothelium. Proc. Natl. Acad. Sci. U. S. A 91:4678-4682.

Simons, M, Bonow, R O, Chronos, N A, Cohen, D J, Giordano, F J, Hammond, H K, Laham, R J, Li, W, Pike, M, Sellke, F W, Stegmann, T J, Udelson, J E, and Rosengart, T K. 2000. Clinical trials in coronary angiogenesis: issues, problems, consensus: An expert panel summary. Circulation 102:E73-E86.

Singh, T, Abe, K, Sasaki, T, Zhuang, Y, Masuda, H, and Zarins, C. 1998. Basic fibroblast growth factor expression precedes flow-induced arterial enlargement. J Surg Res 77:165-173.

Skalak, T C and Price, R J. 1996. The role of mechanical stresses in microvascular remodeling. Microcirculation. 3:143-165.

Skalak, T C, Price, R J, and Zeller, P J. 1998. Where do new arterioles come from? Mechanical forces and microvessel adaptation. Microcirculation. 5:91-94.

Sleeman, M, Fraser, J, McDonald, M, Yuan, S, White, D, Grandison, P, Kumble, K, Watson, J D, and Murison, J G. 2001. Identification of a new fibroblast growth factor receptor, FGFR5. Gene 271:171-182.

Smits, P C, Bos, L, Quarles van Ufford, M A, Eefting, F D, Pasterkamp, G, and Borst, C. 1998. Shrinkage of human coronary arteries is an important determinant of de novo atherosclerotic luminal stenosis: an in vivo intravascular ultrasound study. Heart 79:143-147.

Sullivan, C J and Hoying, J B. 2002. Flow-dependent remodeling in the carotid artery of fibroblast growth factor-2 knockout mice. Arterioscler. Thromb. Vasc. Biol. 22:1100-1105.

Sullivan, C J, Doetschman, T, and Hoying, J B. 2002. Targeted Disruption of the Fgf2 Gene Does Not Affect Vascular Growth in the Mouse Ischemic Hindlimb. J. Appl. Physiol

Sunderkotter, C, Goebeler, M, Schulze-Osthoff, K, Bhardwaj, R, and Sorg, C. 1991. Macrophage-derived angiogenesis factors. Pharmacol. Ther. 51:195-216.

Suri, C, Jones, P F, Patan, S, Bartunkova, S, Maisonpierre, P C, Davis, S, Sato, T N, and Yancopoulos, G D. 1996. Requisite role of angiopoietin-1, a ligand for the TIE2 receptor, during embryonic angiogenesis. Cell 87:1171-1180.

Suzuma, K, Takagi, H, Otani, A, Suzuma, I, and Honda, Y. 1998. Increased expression of KDR/Flk-1 (VEGFR-2) in murine model of ischemia-induced retinal neovascularization. Microvasc Res 56:183-191.

Swinscoe, J C and Carlson, E C. 1992. Capillary endothelial cells secrete a heparin-binding mitogen for pericytes. J. Cell Sci. 103 (Pt 2):453-461.

Takeshita, S, Zheng, L, Brogi, E, Kearney, M, Pu, L, Bunting, S, Ferrara, N, Symes, J, and Isner, J. 1994. Threapeutic angiogenesis: A single intraarterial bolus of vascular endothelial growth factor augments revascularization in a rabbit ischemic hind limb model. J Clin Invest 93:662-670.

Takeshita, S, Isshiki, T, Ochiai, M, Eto, K, Mori, H, Tanaka, E, Umetani, K, and Sato, T. 1998. Endothelium-dependent relaxation of collateral microvessels after intramuscular gene transfer of vascular endothelial growth factor in a rat model of hindlimb ischemia. Circulation 98:1261-1263.

Tamarat, R, Silvestre, J S, Kubis, N, Benessiano, J, Duriez, M, deGasparo, M, Henrion, D, and Levy, B I. 2002. Endothelial nitric oxide synthase lies downstream from angiotensin II- induced angiogenesis in ischemic hindlimb. Hypertension 39:830-835.

Tanaka, T S, Jaradat, S A, Lim, M K, Kargul, G J, Wang, X, Grahovac, M J, Pantano, S, Sano, Y, Piao, Y, Nagaraja, R, Doi, H, Wood, W H, III, Becker, K G, and Ko, M S. 2000. Genome-wide expression profiling of mid-gestation placenta and embryo using a 15,000 mouse developmental cDNA microarray. Proc. Natl. Acad. Sci. U. S. A 97:9127-9132.

Tassi, E, Al Attar, A, Aigner, A, Swift, M R, McDonnell, K, Karavanov, A, and Wellstein, A. 2001. Enhancement of fibroblast growth factor (FGF) activity by an FGF-binding protein. J. Biol. Chem. 276:40247-40253.

Thyberg, J, Hedin, U, Sjolund, M, Palmberg, L, and Bottger, B A. 1990. Regulation of differentiated properties and proliferation of arterial smooth muscle cells. Arteriosclerosis 10:966-990.

Tobe, T, Ortega, S, Luna, J D, Ozaki, H, Okamoto, N, Derevjanik, N L, Vinores, S A, Basilico, C, and Campochiaro, P A. 1998. Targeted disruption of the FGF2 gene does not prevent choroidal neovascularization in a murine model. Am. J. Pathol. 153:1641-1646.

Tohda, K, Masuda, H, Kawamura, K, and Shozawa, T. 1992. Difference in dilatation between endothelium-preserved and -desquamated segments in the flow-loaded rat common carotid artery. Arterioscler. Thromb. 12:519-528.

Tronc, F, Mallat, Z, Lehoux, S, Wassef, M, Esposito, B, and Tedgui, A. 2000. Role of matrix metalloproteinases in blood flow-induced arterial enlargement: interaction with NO. Arterioscler. Thromb. Vasc. Biol. 20:E120-E126.

Tronc, F, Wassef, M, Esposito, B, Henrion, D, Glagov, S, and Tedgui, A. 1996. Role of NO in flow-induced remodeling of the rabbit common carotid artery. Arterioscler. Thromb. Vasc. Biol. 16:1256-1262.

Tsurumi, Y, Takeshita, S, Chen, D, Kearney, M, Rossow, S T, Passeri, J, Horowitz, J R, Symes, J F, and Isner, J M. 1996. Direct intramuscular gene transfer of naked DNA encoding vascular endothelial growth factor augments collateral development and tissue perfusion. Circulation 94:3281-3290.

Tuttle, J L, Nachreiner, R D, Bhuller, A S, Condict, K W, Connors, B A, Herring, B P, Dalsing, M C, and Unthank, J L. 2001. Shear level influences resistance artery remodeling: wall dimensions, cell density, and eNOS expression. Am. J. Physiol Heart Circ. Physiol 281:H1380-H1389.

Vainikka, S, Partanen, J, Bellosta, P, Coulier, F, Birnbaum, D, Basilico, C, Jaye, M, and Alitalo, K. 1992. Fibroblast growth factor receptor-4 shows novel features in genomic structure, ligand binding and signal transduction. EMBO J. 11:4273-4280.

Van Nueten, J M, Janssens, W J, and Vanhoutte, P M. 1985. Serotonin and vascular reactivity. Pharmacol. Res. Commun. 17:585-608.

van Royen, N, Hoefer, I, Buschmann, I, Heil, M, Kostin, S, Deindl, E, Vogel, S, Korff, T, Augustin, H, Bode, C, Piek, J J, and Schaper, W. 2002. Exogenous application of transforming growth factor beta 1 stimulates arteriogenesis in the peripheral circulation. FASEB J. 16:432-434.

Verheyen, A, Lauwers, F, Vlaminckx, E, and de Clerck, F. 1989. Differential vasoreactivity to the thromboxane A2 mimic U-46619 of collateral and normal peripheral blood vessels in situ perfused rat hindquarters. Blood Vessels 26:165-176.

Verheyen, A, Lauwers, F, Vlaminckx, E, Wouters, L, and de Clerck, F. 1991. Oversensitivity to serotonin of the collateralized vascular bed in rat hindquarters: mechanisms of increased vasoconstriction. Eur. J. Pharmacol. 194:209-216.

Vernon, S M, Campos, M J, Haystead, T, Thompson, M M, DiCorleto, P E, and Owens, G K. 1997. Endothelial cell-conditioned medium downregulates smooth muscle contractile protein expression. Am. J. Physiol 272:C582-C591.

Walgenbach, K, Gratas, C, Shestak, K, and Becker, D. 1995. Ischaemia-induced expression of bFGF in normal skeletal muscle: A potential paracrine mechanism for mediating angiogenesis in ischemic skeletal muscle. Nature Med 1:453-459.

Waltenberger, J. 1997. Modulation of growth factor action: implications for the treatment of cardiovascular diseases. Circulation 96:4083-4094.

Ward, M R, Jeremias, A, Huegel, H, Fitzgerald, P J, and Yeung, A C. 2000a. Accentuated remodeling on the upstream side of atherosclerotic lesions. Am. J. Cardiol. 85:523-526.

Ward, M R, Pasterkamp, G, Yeung, A C, and Borst, C. 2000b. Arterial remodeling. Mechanisms and clinical implications. Circulation 102:1186-1191.

Ward, M R, Tsao, P S, Agrotis, A, Dilley, R J, Jennings, G L, and Bobik, A. 2001. Low blood flow after angioplasty augments mechanisms of restenosis: inward vessel remodeling, cell migration, and activity of genes regulating migration. Arterioscler. Thromb. Vasc. Biol. 21:208-213.

Wardell, K, Jakobsson, A, and Nilsson, G E. 1993. Laser Doppler perfusion imaging by dynamic light scattering. IEEE Trans. Biomed. Eng 40:309-316.

Weidinger, F F, McLenachan, J M, Cybulsky, M I, Gordon, J B, Rennke, H G, Hollenberg, N K, Fallon, J T, Ganz, P, and Cooke, J P. 1990. Persistent dysfunction of regenerated endothelium after balloon angioplasty of rabbit iliac artery. Circulation 81:1667-1679.

Wentzel, J J, Kloet, J, Andhyiswara, I, Oomen, J A, Schuurbiers, J C, de Smet, B J, Post, M J, de Kleijn, D, Pasterkamp, G, Borst, C, Slager, C J, and Krams, R. 2001. Shear-stress and wall-stress regulation of vascular remodeling after balloon angioplasty: effect of matrix metalloproteinase inhibition. Circulation 104:91-96.

Werner, S, Duan, D S, de Vries, C, Peters, K G, Johnson, D E, and Williams, L T. 1992. Differential splicing in the extracellular region of fibroblast growth factor receptor 1 generates receptor variants with different ligand- binding specificities. Mol. Cell Biol. 12:82-88.

Westall, F C, Lennon, V A, and Gospodarowicz, D. 1978. Brain-derived fibroblast growth factor: identity with a fragment of the basic protein of myelin. Proc. Natl. Acad. Sci. U. S. A 75:4675-4678.

Whitelock, J M, Murdoch, A D, Iozzo, R V, and Underwood, P A. 1996. The degradation of human endothelial cell-derived perlecan and release of bound basic fibroblast growth factor by stromelysin, collagenase, plasmin, and heparanases. J. Biol. Chem. 271:10079-10086.

Winkles, J A, Friesel, R, Burgess, W H, Howk, R, Mehlman, T, Weinstein, R, and Maciag, T. 1987. Human vascular smooth muscle cells both express and respond to heparin- binding growth factor I (endothelial cell growth factor). Proc. Natl. Acad. Sci. U. S. A 84:7124-7128.

Wong, L C and Langille, B L. 1996. Developmental remodeling of the internal elastic lamina of rabbit arteries: effect of blood flow. Circ. Res. 78:799-805.

Xie, Z, Gao, M, Batra, S, and Koyama, T. 1997. The capillarity of left ventricular tissue of rats subjected to coronary artery occlusion. Cardiovasc Res 33:671-676.

Xu, J, Liu, Z, and Ornitz, D M. 2000. Temporal and spatial gradients of Fgf8 and Fgf17 regulate proliferation and differentiation of midline cerebellar structures. Development 127:1833-1843.

Yamashita, T, Yoshioka, M, and Itoh, N. 2000. Identification of a novel fibroblast growth factor, FGF-23, preferentially expressed in the ventrolateral thalamic nucleus of the brain. Biochem. Biophys. Res. Commun. 277:494-498.

Yang, H T, Yan, Z, Abraham, J A, and Terjung, R L. 2001. VEGF(121)- and bFGF-induced increase in collateral blood flow requires normal nitric oxide production. Am. J. Physiol Heart Circ. Physiol 280:H1097-H1104.

Yang, H, Deschenes, M, Ogilive, R, and Terjung, R. 1996. Basic fibroblast growth factor increases collateral blood flow in rats with femoral arterial ligation. Circ Res 79:62-69.

Yayon, A, Klagsbrun, M, Esko, J D, Leder, P, and Ornitz, D M. 1991. Cell surface, heparin-like molecules are required for binding of basic fibroblast growth factor to its high affinity receptor. Cell 64:841-848.

Yoshida, T, Ishimaru, K, Sakamoto, H, Yokota, J, Hirohashi, S, Igarashi, K, Sudo, K, and Terada, M. 1994. Angiogenic activity of the recombinant hst-1 protein. Cancer Lett. 83:261-268.

Yoshimura, S, Takagi, Y, Harada, J, Teramoto, T, Thomas, S S, Waeber, C, Bakowska, J C, Breakefield, X O, and Moskowitz, M A. 2001. FGF-2 regulation of neurogenesis in adult hippocampus after brain injury. Proc. Natl. Acad. Sci. U. S. A 98:5874-5879.

Yu, Z X, Biro, S, Fu, Y M, Sanchez, J, Smale, G, Sasse, J, Ferrans, V J, and Casscells, W. 1993. Localization of basic fibroblast growth factor in bovine endothelial cells: immunohistochemical and biochemical studies. Exp. Cell Res. 204:247-259.

Zhou, M, Sutliff, R L, Paul, R J, Lorenz, J N, Hoying, J B, Haudenschild, C C, Yin, M, Coffin, J D, Kong, L, Kranias, E G, Luo, W, Boivin, G P, Duffy, J J, Pawlowski, S A, and Doetschman, T. 1998. Fibroblast growth factor 2 control of vascular tone. Nat. Med. 4:201-207.

Zhou, Z, Apte, S S, Soininen, R, Cao, R, Baaklini, G Y, Rauser, R W, Wang, J, Cao, Y, and Tryggvason, K. 2000. Impaired endochondral ossification and angiogenesis in mice deficient in membrane-type matrix metalloproteinase I. Proc. Natl. Acad. Sci. U. S. A 97:4052-4057.

Ziche, M, Parenti, A, Ledda, F, Dell'Era, P, Granger, H J, Maggi, C A, and Presta, M. 1997. Nitric oxide promotes proliferation and plasminogen activator production by coronary venular endothelium through endogenous bFGF. Circ. Res. 80:845-852.